WILLIAM ALAN RUNCIMAN

Optical and Structural Properties of Ions in Crystals.

Submitted for the Degree of Doctor of Science in Pure Science at the University of Edinburgh.

March, 1960.

CONTENTS

10. Optical Fluorescence in Non-Destructive Testing.
W. A. Runciman, Brit.J.App.Phys.Supp. No. 6, S34, 1957.

11. Energy levels in Rare-Earth Ions.
J. P. Elliott, B. R. Judd and W. A. Runciman, Proc.Roy. Soc., 240A, 509, 1957.

12. Absorption and Fluorescence Spectra of Ions in Crystals.
W. A. Runciman, Rep.Progr.Phys., 21, 30, 1958.

13. The Absorption Spectrum of Vanadium Corundum.
M.H.L. Pryce and W. A. Runciman, Faraday Soc. Disc. No. 26, 34, 1958.

14. A Neutron-Diffraction Study of Potassium Cobalticyanide.
N. A. Curry and W. A. Runciman, Acta Cryst., 12, 674, 1959.

15. Analysis of the Spectra of Gadolinium Salts.
W. A. Runciman, J.Chem.Phys., 30, 1632, 1959.

16. Spectra of Trivalent Praseodymium and Thulium Salts.
W. A. Runciman and B. G. Wybourne, J.Chem.Phys., 31, 1149, 1959.

Note concerning authorship

The present writer was the originator of all the projects, the results of which comprise this thesis. However, some of the projects depended on skills outside of the writer's competence, and he would like to express his thanks to Dr. Steward and Mr. Curry for their expert collaboration in the field of crystallography, and to the late Professor Hartree, Professor Pryce, Dr. Elliott, Dr. Judd and Mr. Douglas for collaboration in projects involving advanced theoretical physics and numerical methods. Mr. Wybourne is under the supervision of the writer for his Ph.D. studies, and he carried out the detailed calculations in the final communication.

REPRINTED FROM THE
PROCEEDINGS OF THE PHYSICAL SOCIETY, A, VOL. LXVI, p. 484, 1953

The Atomic Position and Size of the Thallium Ions in KCl(Tl) Phosphors

By W. A. RUNCIMAN and E. G. STEWARD
Research Laboratories, The General Electric Company, Wembley, Middx.

MS. received 25*th November* 1952

Abstract. A new x-ray investigation has been made of the KCl(Tl) phosphor in view of the discrepancy between the early theory of Fromherz involving formation of complexes in the KCl(Tl) phosphor and the recent theoretical work of Williams, in which substitutional entry of the thallium ions is assumed. The present study has now shown (*a*) that the expansion of the potassium chloride structure due to the incorporation of thallium is in agreement with Vegard's law and (*b*) that Tl^+ ions enter the structure substitutionally. The present results differ from those obtained by Stasiw and Saur in a less detailed x-ray study.

The intensities of x-ray reflections have also been used to establish the atomic position of the activator atoms in the phosphor and the results fully confirm the interpretation of the observed lattice expansions.

A new value of $1{\cdot}42_7$ Å has been obtained for the ionic radius of the Tl^+ ion in six-fold coordination with Cl^- ions. This is of importance in the detailed calculations of the luminescence of KCl(Tl) which have been made by Williams and others.

§ 1. Introduction

In most impurity activated solid inorganic phosphors the absorption and emission spectra consist of one or more broad bands. Because of their relative simplicity, the alkali halides activated by heavy metals have been studied with a view to gaining insight into the mechanism of this type of luminescence. In particular, potassium chloride activated by thallium and denoted KCl(Tl) has been investigated extensively both experimentally and theoretically.

Following the earlier theory (Seitz 1938) in which a single average configuration coordinate was used to describe the state of a luminescent centre, a detailed theory has been developed to account for the emission and absorption spectra of KCl(Tl) on the assumption that the thallium enters the lattice substitutionally (Williams 1951, Williams and Hebb 1951, Johnson and Williams 1950, 1952). The absorption spectrum of KCl(Tl) has been measured at 4°, 77° and 298°K (Johnson and Studer 1951) and there is good agreement between the experimental and theoretical half-widths of the absorption band.

Others have taken a different view and have proposed that thallium ions or ions of other heavy metallic activators form complex negative ions with the halides and that these complexes are incorporated at points of lattice defects (Fromherz and Menschick 1929, Fromherz 1931, Pringsheim 1942, 1949). In support of this theory it was observed that the absorption band of aqueous solutions of the phosphors is very similar to the long wavelength absorption band of the solid phosphors (Fromherz and Ku-Hu-Li 1929). In contrast, the emission spectra of the aqueous solution (Pringsheim and Vogels 1940) and of the solid phosphor KCl(Tl) do not exhibit close similarity and this seems a

weak feature of the theory, but it has often been used (e.g. Hilsch 1937 and Antonov-Romanovskii 1943) in the discussion of the properties of KCl(Tl) and other phosphors. Furthermore the theory has had support from an x-ray study of the KCl(Tl) phosphor (Stasiw and Saur 1938) where it was claimed that the expansion of the KCl lattice is only about half the amount predicted on the assumption that the thallium enters the lattice substitutionally.

As the KCl(Tl) phosphor represents the only example of a quantitative theoretical interpretation of an impurity activated phosphor, it is of considerable importance to resolve the discrepancy between the above two theories. The crystal structure of the phosphor has therefore been re-studied.

Where a continuous solid solution range exists between two isomorphous compounds it is comparatively easy to prove by x-ray diffraction that substitutional replacement has taken place. For example, both zinc sulphide and cadmium sulphide can have the hexagonal zinc oxide type structure and it is possible to form the complete solid solution range ZnS–CdS (Kröger 1940, Rooksby 1941). The changes in the structure cell dimensions are found to be closely proportional to the replacement of zinc ions by cadmium ions and Vegard's law therefore operates with reasonable accuracy in such instances.

Potassium chloride has a rock salt face-centred cubic crystal structure whilst thallium chloride has a caesium chloride body-centred cubic structure. A complete solid solution range cannot exist therefore between the two since the end members are not structurally isomorphous. If limited solid solubility of thallium chloride in potassium chloride is possible, however, Vegard's law may be applied over that range, by calculating a theoretical structure cell dimension for thallium chloride having a hypothetical face-centred cubic structure.

Preparations of potassium chloride containing 5, 10 and 15% (molecular) of thallium chloride have been prepared and examined by x-ray diffraction in order to test the correlation between composition and structure cell dimension.

In addition to changes in lattice dimensions of the crystal structure, replacement of potassium ions by thallium ions would also modify the intensities of x-ray reflections. This approach has been used to establish the lattice position of the thallium atoms which have entered the potassium chloride structure.

§2. Preparation of Samples

The chemicals used were 'Specpure' potassium and thallous chlorides.

Preliminary experiments were made in which ground mixtures of potassium and thallium chlorides in various proportions were heated in sealed evacuated clear quartz tubes at temperatures in the range 550–750°C. It was considered necessary to seal the tubes to prevent a relative loss of TlCl, which has a melting point of 430°C and a high vapour pressure in the above temperature range. KCl has a melting point of 790°C and a relatively low vapour pressure and the substantial differences in the melting points and vapour pressures are largely responsible for the difficulties in preparing uniform samples.

Regrinding and reheating were included in attempts to produce homogeneous products free from excess thallium chloride. These experiments were not completely successful at higher concentrations of thallium chloride. Entry of the thallium was not fully homogeneous and some free thallium chloride was observed. A sample containing 10% (molecular) TlCl, however, was quite uniform and was included in the x-ray examination described in §3.

Although the solubilities of potassium and thallium chlorides in water are very different an aqueous solution of the two chlorides was evaporated to dryness and the residue ground and subjected to a homogenizing heat treatment. This proved to be successful and solutions of potassium chloride containing 5 and 15% (molecular) TlCl were prepared and evaporated to dryness on a steam bath. The powders obtained were then carefully ground in an agate mortar, sealed in evacuated clear quartz tubes and heated for over 12 hours at 425°C, this temperature being just below the melting point of pure TlCl.

In view of the great difference in vapour pressures of potassium and thallium chlorides, the volume of quartz tube not occupied by the powder sample was reduced to a minimum by inserting a length of solid quartz rod above the powder. Sealing-off under vacuum was then accomplished over the section of the tube containing the quartz rod. This technique also avoided excessive heating of the actual powder sample during the sealing-off operation.

§ 3. X-Ray Examination

A 19 cm diameter Unicam powder camera was used with copper Kα radiation, and reflections were recorded over a Bragg angle range θ 5°–85°; the photographs obtained are shown in fig. 1, Plate.

(i) *Structure Cell Dimensions*

With increasing concentration of thallium chloride, an expansion of the potassium chloride structure was observed. This is revealed by the shift of the x-ray reflections, particularly those at high θ values.

Measurements of the shifts of the 622, 640, 642 and 800 reflections enabled the structure cell dimension to be determined for each sample including the 'Specpure' KCl sample. The values obtained after correction (Nelson and Riley 1945) for various camera factors are given in table 1.

Table 1. Observed and Calculated Structure Cell Dimension for KCl–TlCl

Molecular % TlCl		0	5	10	15
Cell dimension (Å)	Obs.*	6·2922	6·2997	6·3085	6·3164
	Calc.	(6·2922)	6·3007	6·3091	6·3176

* All values ±0·0003.

The value of a_0 obtained for the 'Specpure' KCl is in good agreement with the recorded value of $a_0 = 6{\cdot}291 \pm 0{\cdot}002$ Å* (Strukturbericht 1913–1928).

If thallium ions replace potassium ions substitutionally and at random, a change in the dimensions of the potassium chloride structure will result, and if Vegard's law giving a linear relationship is assumed, the change with composition can be calculated.

Because different values have been reported (Goldschmidt 1929, Pauling 1927) for the ionic radius for Tl^+, it was decided to determine a value from the known lattice parameter of thallium chloride of body-centred cubic structure. Using the value of $a_0 = 3{\cdot}8417$ Å (Wyckoff 1951), the ionic separation denoted Tl–Cl in the caesium chloride structure is given by $\frac{1}{2}\sqrt{3} \times 3{\cdot}8417 = 3{\cdot}327_0$ Å.

* This cell dimension and the various ionic radii given in the literature, though described as ångström units, are really kx units (Bragg 1947). A factor of 1·00202 has been used where necessary to correct to ångström unit.

In deducing the Tl–Cl distance in a rock salt type structure from this, the usual correction for coordination number has to be made (Pauling 1945). This correction is

$$\frac{R_{CsCl}}{R_{NaCl}} = \left[\frac{B_{CsCl}}{B_{NaCl}}\,\frac{A_{NaCl}}{A_{CsCl}}\right]^{1/(n-1)}$$

where B denotes the appropriate repulsive coefficient, A the appropriate Madelung constant and n the Born exponent.

The value of n in this expression is always in the region of 9 but depends upon the ion type. K^+ and Cl^- both have the value of $n=9$ and the value for Tl^+ is approximately 12. In a crystal of mixed ion type, an average value for n is used (Pauling 1945). For TlCl a value of $n=10{\cdot}5$ is therefore indicated, and the above expression gives a co-ordination number correction of $1{\cdot}029_8$.

The Tl–Cl interionic distance in a rock salt structure therefore becomes $3{\cdot}327_0/1{\cdot}029_8=3{\cdot}230_7$ Å. The lattice constant a_0 is therefore $6{\cdot}461_4$ Å.

A theoretical relation can now be calculated using Vegard's law, between the cell dimension and the molecular concentration of thallium chloride. This is shown together with the experimental points in fig. 2, and a comparison between observed and calculated values is given in table 1. The slight deviation of the points from the theoretical line may be partly accounted for by small concentrations of free thallium chloride which are detectable in the original x-ray photographs. For example approximately 0·2% (molecular) was detectable in the 15% preparation.

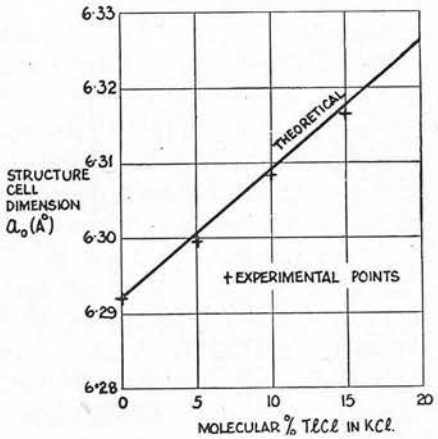

Fig. 2. Structure cell dimensions for KCl–TlCl.

These results show that the observed expansion of the potassium chloride structure is in close agreement with the expansion expected from direct substitutional replacement of K^+ ions by Tl^+ ions. Further confirmation of this is to be expected from an examination of the changes with composition in x-ray line intensities.

(ii) *Intensities of X-Ray Reflections*

In the potassium chloride structure it is well known that those reflections for which h, k and l are all odd, such as 111, 311 and 331 (fig. 1) are very weak on account of the closely similar values of the atomic scattering factors of

potassium and chlorine. The atomic scattering factor for thallium is of course very much greater than that for potassium and if, therefore, thallium ions are situated at the positions normally occupied by potassium ions, the intensities of these reflections are considerably enhanced. This effect is clearly shown by the x-ray photographs in fig. 1.

The intensities of the 111, 311, 331 and 400 reflections have been calculated using a scattering factor which is the appropriate linear combination of the separate scattering factors for K^+ and Tl^+ (International Tables for the Determination of Crystal Structure 1935). Using the 400 reflection as a reference level (unity), the intensities were calculated in the usual way from the expression $I_{calc} = F^2 p(LP)$ where F denotes the crystal structure factor, p denotes the multiplicity of the x-ray reflection concerned, and (LP) denotes the appropriate Lorentz-polarization factor.

Table 2 lists the observed intensities I_{obs} against the calculated values I_{calc} for the various compositions used. The observed intensities of the 311 and 331 reflections were determined from microdensitometer records of the x-ray powder photographs, corrections being made for 'background' and other factors. Only visual estimates are given for the 111 reflections since undiluted x-ray specimens were used to show clearly the line shifts at high θ values, and the consequent absorption at low θ values makes quantitative measurement of the intensity of the 111 reflection unreliable.

Table 2. KCl–TlCl: Calculated and Observed Intensities of x-ray Reflections

Reflection	Composition mol.% TlCl	Intensities*	
		I_{obs}	I_{calc}
331	0	$\ll 0{\cdot}1$	0·01
	5	0·1	0·08
	10	0·2	0·18
	15	0·3	0·29
311	0	$< 0{\cdot}1$	0·04
	5	0·2	0·22
	10	0·5	0·48
	15	0·7	0·75
111†	0	very weak	0·05
	5	weak	0·36
	10	weak–medium	0·80
	15	medium	1·29

* Intensities relative to the 400 reflection.

† The observed intensities given for this reflection are visual estimates, high absorption at low angles making quantitative measurements unreliable.

Within the limits of experimental error, the observed and calculated intensities are in complete agreement, and it should be noted that this proof of the location of the Tl^+ ions is independent of any consideration of either the validity of Vegard's law or the values of the ionic radii.

(iii) *The Size of the Tl^+ Ion*

A value of the size of the Tl^+ ion in sixfold co-ordination in a chloride structure can be calculated from the inter-ionic distance which has received substantial confirmation by the x-ray results.

Using the hypothetical cell dimension of $a_0 = 6{\cdot}461$ Å determined above and an ionic radius of 1·810 Å for Cl^- in sixfold co-ordination (Pauling 1945) the ionic radius for Tl^+ may be calculated, allowance being made for the radius ratio effect (Pauling 1945).

Using a provisional radius for Tl^+ and approximating successively to self-consistency, a value of $1{\cdot}42_7$ Å has been obtained. The final calculation was as follows:

$$\text{Assume } R_{Tl^+} = 1{\cdot}42_7 \text{ Å}$$

$$\text{Radius ratio} = 1{\cdot}42_7/1{\cdot}810 = 0{\cdot}788$$

$$\text{Correction factor } F(\rho) = 0{\cdot}998.$$

Therefore in the rock salt type chloride,

$$R_{Tl^+} + R_{Cl^-} = \frac{6{\cdot}461_4}{2 \times 0{\cdot}998} = 3{\cdot}237_2 \text{ Å}.$$

With $R_{Cl^-} = 1{\cdot}810$ Å, the value of $R_{Tl^+} = 1{\cdot}42_7$ Å.

The size of the thallium ion would vary, of course, with the particular halogen on account of the high polarizability of the thallium ion. The above value, however, would appear to be an accurate assessment for a Tl^+ ion in sixfold co-ordination with Cl^-.

A useful confirmation of the above calculation is provided by determining the value of the ionic radius of K^+ in potassium chloride ($a_0 = 6{\cdot}292$ Å) from the value used above for Cl^-. The result of 1·333 Å is in exact agreement with the size given by Pauling (1945).

§ 4. Discussion

If substitutional entry in KCl(Tl) phosphors is assumed, it is known that there is good agreement between the theoretical and experimental luminescent properties for thallium concentrations of less than 0·1% (Cornell Symposium 1948, p. 14). Since the experiments described here have established that substitutional entry does occur at higher concentrations of thallium, it is reasonable to infer that the thallium ions enter the structure substitutionally over the whole range from very small concentrations of the order of 0·002 (Johnson and Williams 1950, 1952) to 15% (molecular) TlCl. This is supported by the recent theoretical calculations (Brauer 1952) which have shown, by considering the energy changes involved, that substitutional entry of Tl^+ ions is possible.

There is always the possibility that a few thallium atoms will be interstitially incorporated either randomly or at points of lattice irregularities, but the number of such atoms can be only a small fraction of those occupying substitutional positions. It is suggested therefore that upon excitation by ultra-violet radiation the fluorescent emission of samples of KCl containing different concentrations of TlCl is probably capable of explanation on the basis of complete substitutional entry of the Tl^+ ions into the crystal lattice. For instance, it has been proposed that the emission in the band with a peak at 3050 Å is favoured by excitation in the absorption band at 2470 Å and that the blue emission at 4750 Å is favoured by excitation in the absorption band at 1960 Å (Johnson and Williams 1952). These emission bands are attributed to single substitutional Tl^+ ions having $^3P_1 \rightarrow {}^1S_0$ and $^1P_1 \rightarrow {}^1S_0$ transitions respectively. The only electronic transition is believed to be in the thallium ion, the neighbouring ions undergoing an adjustment in position which affects the average equilibrium inter-ionic distances.

When excited by the short ultra-violet radiation from a low vapour pressure mercury discharge in quartz, the three specimens containing 5, 10 and 15% (molecular) of TlCl all have a visible yellow-white fluorescence, which becomes rather deeper with increasing thallium concentration. This yellow emission band (Cornell Symposium 1948, p. 398), the phosphorescence (Seitz 1938) and an emission band at 3775 Å (Johnson and Williams 1952) all occur in samples with high thallium concentration and have all been attributed to pairs of Tl^+ ions which are situated in adjacent positive ion locations.

§ 5. Conclusion

Our results have demonstrated that the lattice expansion of potassium chloride on solid solution with thallium chloride is proportional to the concentration of TlCl and is in very good agreement with a generalized form of Vegard's law. Intensity changes of the x-ray reflections agree with the values predicted on the assumption that Tl^+ ions occupy K^+ positions. Furthermore, it appears very improbable that the intensity results can be explained by any theory other than that of random substitutional replacement by at least a very high percentage of the Tl^+ ions which enter the KCl lattice.

The theory of the formation of negative complexes in solid KCl(Tl) was based (i) on the x-ray evidence (Stasiw and Saur 1938), (ii) on the similarity of the absorption and emission spectra of the solid phosphors and of the aqueous solutions, and (iii) on some indirect evidence of the results obtained in halides activated with silver, antimony, tin or lead. None of these arguments seems convincing in the light of the present more complete x-ray investigation.

Any similarities between the properties of the solid phosphors and of the aqueous solutions can probably be explained by the similarity in the surroundings of a thallium ion in a positive ion location in the crystal lattice and in a concentrated aqueous solution of KCl. The activation by other metallic elements is certainly not completely analogous to the activation by thallium and it is not intended to suggest that the entry is both random and substitutional in these instances without a detailed investigation of each case.

With reference to the size of the thallium ion, a new value of $1{\cdot}42_7$ Å has been obtained for sixfold co-ordination with Cl^-. There has not been general agreement in the literature and a value of 1·49 Å has been used, for example, in a recent calculation of the luminescence of KCl(Tl) (Williams 1951).

Finally, the examination has included the first known application in the study of phosphors, of the intensities of x-ray reflections to the determination of the atomic positions of the activator atoms in the crystal structure of a phosphor. This method is of general applicability and is especially suitable for the many cases where there is activation by a heavy metallic ion.

References

Antonov-Romanovskii, V. V., 1943, *J. Phys. USSR*, **7**, 153.
Bragg, W. L., 1947, *J. Sci. Instrum.*, **24**, 27.
Brauer, P, 1952, *Z. Naturforsch.*, **7a**, 372.
Cornell Symposium, 1948, *Solid Luminescent Materials* (New York : John Wiley).
Fromherz, H, 1931, *Z. Phys.*, **68**, 233.
Fromherz, H., and Ku-Hu-Li, 1929, *Z. Phys. Chem.* A, **153**, 321.
Fromherz, H., and Menschick, W., 1929, *Z. Phys. Chem.* B, **3**, 1.
Goldschmidt, V. M., 1929, *Trans. Faraday Soc.*, **25**, 253.

HILSCH, R., 1937, *Proc. Phys. Soc.*, **49,** 40 (Supplement).
INTERNATIONAL TABLES FOR THE DETERMINATION OF CRYSTAL STRUCTURE, 1935 (Berlin : Borntraeger).
JOHNSON, P. D., and STUDER, F. J., 1951, *Phys. Rev.*, **82,** 976.
JOHNSON, P. D., and WILLIAMS, F. E., 1950, *J. Chem. Phys.*, **18,** 1477; 1952, *Ibid.*, **20,** 124.
KRÖGER, F. A., 1940, *Z. Kristallogr.*, **102,** 132.
NELSON, J. B., and RILEY, D. P., 1945, *Proc. Phys. Soc.*, **57,** 160.
PAULING, L., 1927, *J. Amer. Chem. Soc.*, **49,** 765; 1945, *The Nature of the Chemical Bond* (Cornell : University Press).
PRINGSHEIM, P., 1942, *Rev. Mod. Phys.*, **14,** 133; 1949, *Fluorescence and Phosphorescence* (New York : Interscience), p. 524.
PRINGSHEIM, P., and VOGELS, H., 1940, *Physica*, **7,** 225.
ROOKSBY, H. P., 1941, *J. Sci. Instrum.*, **18,** 89.
SEITZ, F., 1938, *J. Chem. Phys.*, **6,** 150.
STASIW, O., and SAUR, E., 1938, *Verh. Dtsch. Phys. Ges.*, **19,** 4.
Strukturbericht, 1913–1928 (Edited by Ewald, P. P., and Hermann, C.).
WILLIAMS, F. E., 1951, *J. Chem. Phys.*, **19,** 457.
WILLIAMS, F. E., and HEBB, M., 1951, *Phys. Rev.*, **84,** 1181.
WYCKOFF, R. W. G., 1951, *Crystal Structures* (New York : Interscience).

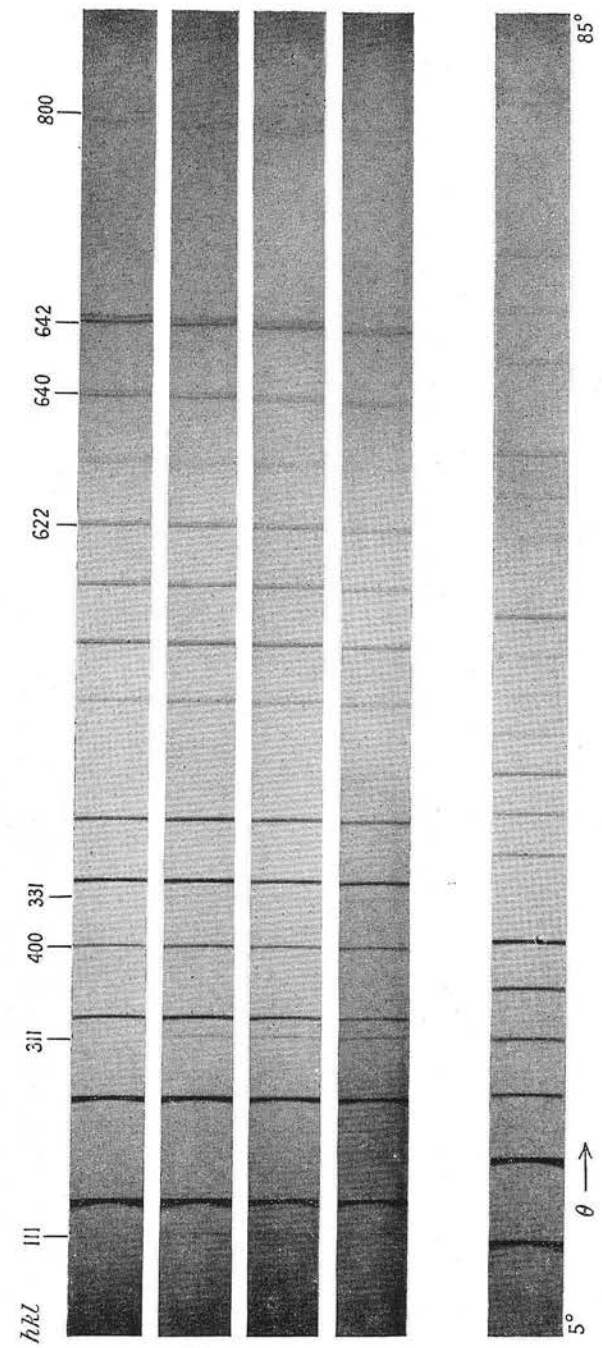

Fig. 1. X-ray powder diffraction photographs of KCl–TlCl preparations, (*a*) KCl, (*b*) KCl–TlCl : 5% (molecular) TlCl, (*c*) KCl–TlCl : 10% (molecular) TlCl, (*d*) KCl–TlCl : 15% (molecular) TlCl, (*e*) TlCl. (19 cm diameter camera : CuKα radiation).

(*Reprinted from Nature, Vol.* 172, *p.* 75, *July* 11, 1953)

Alkaline Earth Uranates of the R_3MX_6 Type

ALKALINE earth uranates of the RMX_4 type are well known and the crystal structures of, for example, the calcium and strontium compounds $CaUO_4$ and $SrUO_4$, respectively, have been investigated in detail[1].

While studying phosphors of the CaO(U) type, it was decided to investigate the formation of other possible uranate compounds. A range of samples containing varying ratios of calcium to uranium was prepared and a transition in fluorescence properties was observed at a 3 : 1 ratio. It was suspected that a calcium compound having the composition $3CaO : 1UO_3$ had been prepared, and an X-ray investigation showed the existence of a new compound. Other similar uranates were prepared and it was found that the new materials possessed the same pseudo-cubic crystal structure as alkaline earth tungstates of the R_3WO_6 type[2], and fluorides of the cryolite, Na_3AlF_6, type[3].

The above tungstates and fluorides approach and attain full cubic symmetry (space group $Fm3m$) when ionic dimensions are favourable. The ideal structure involves cations occupying two different sites with relative abundance of 2 : 1. For this reason, and because ionic radii are favourable, Ba_2CaWO_6 possesses the full symmetry of the $Fm3m$ cubic space group. With this in mind, the further uranate Ba_2CaUO_6 was prepared. The X-ray powder photograph, while revealing slight deformation from the fully cubic arrangement, owing no doubt to the difference in volume between the UO_6 group and the WO_6 group, confirmed that the uranates follow the same general behaviour as the corresponding tungstates.

To check the isomorphism of the tungstate and uranate systems, the intermediate compound $Ca_3(0{\cdot}5W\ 0{\cdot}5U)O_6$ was prepared. The resulting material was found to be a complete solid solution and to possess a pseudo-cubic structure cell dimension of $a_0 = 8{\cdot}1_6$ A., compared with $8{\cdot}0_2$ A. for Ca_3WO_6 and $8{\cdot}2_9$ A. for Ca_3UO_6. X-ray powder photographs of Ca_3UO_6, Ba_2CaUO_6 and, for comparison purposes, $CaUO_4$, Ca_3WO_6 and Ba_2CaWO_6, are reproduced herewith.

Synthesis of the various compounds was accomplished as follows. Using appropriate molecular proportions, alkaline earth carbonate was made into a paste with uranyl nitrate solution ; where necessary,

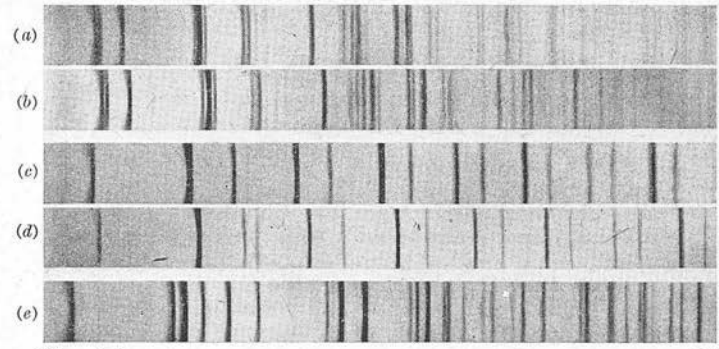

X-ray powder photographs of : (*a*) Ca_3UO_6 ; (*b*) Ca_3WO_6 ; (*c*) Ba_2CaUO_6 ; (*d*) Ba_2CaWO_6 ; (*e*) $CaUO_4$.
19-cm. diameter camera ; copper $K\alpha$ radiation

tungstic oxide was mixed with the carbonate. The resultant paste was dried at 250° C. and fired for one hour at a temperature in the range 1,150–1,350° C., according to which compound was being prepared. The R_3MX_6-type uranates are pale-yellow in appearance.

In common with other uranium compounds, the fluorescence spectra show many interesting features. For example, at liquid-air temperature the fluorescence of Ca_3UO_6 under long wave-length ultraviolet radiation is yellow-green and of medium intensity. The emission consists of a continuous band with a superimposed set of lines or sharp bands, whereas at room temperatures there is a weak diffuse green fluorescence.

Different spectra, but of the same general type, are obtained with the other uranates such as Ba_2CaUO_6. When activated with samarium or europium, these phosphors show, especially at low temperatures, a strong fluorescence exhibiting the characteristic line spectrum of the particular rare-earth activator. With samarium a predominantly orange fluorescence is obtained and with europium the fluorescence is orange-red.

It is hoped to publish a fuller account of the fluorescent properties of these uranates and of related phosphors at a later date.

E. G. Steward
W. A. Runciman

Research Laboratories,
General Electric Co., Ltd.,
Wembley.
April 29.

[1] Zachariasen, W. H., *Acta Cryst.*, **1**, 281 (1948).
[2] Steward, E. G., and Rooksby, H. P., *Acta Cryst.*, **4**, 503 (1951).
[3] Steward, E. G., and Rooksby, H. P., *Acta Cryst.*, **6**, 49 (1953).

Printed in Great Britain by Fisher, Knight & Co., Ltd., St. Albans.

Communication No. 566

ATOMIC CONFIGURATIONS IN LUMINESCENT CENTRES

by

W. A. RUNCIMAN, B.Sc., A.Inst.P.

(Communication from the Staff of the Research Laboratories of The General Electric Company, Limited, Wembley, England)

Reprinted from

Luminescence
Supplement No. 4
pp. S 78–S 85

BRITISH JOURNAL OF APPLIED PHYSICS

Paper 15

Atomic configurations in luminescent centres

By W. A. RUNCIMAN, B.Sc., A.Inst.P., Research Laboratories, The General Electric Company, Ltd., Wembley, Middlesex

When the activator ions in a phosphor have a charge different from that of any ions in the host lattice, it is generally agreed that charge compensation must take place. A new theory of luminescent centres is proposed in which the compensation of charge, by lattice vacancies or by activator ions, is localized in the vicinity of the activator ions. This theory is primarily applicable to ionic crystals, and specific configurations of lowest energy can be deduced. These configurations are described in detail for alkaline-earth oxide, uranate and fluoride phosphors. and the vibrations of these centres are discussed. A number of original phosphors of theoretical interest, including CaO . Bi, Li; CaO . U, Li; CaO . U, Sm; and the uranates, are described and spectra are shown. Finally, necessary modifications of the present theories of sensitized luminescence and multiple-band emission are considered.

There is a good understanding of the nature of the luminescent centres in some of those phosphors in which an activator ion replaces a lattice ion of the same charge. In particular, Williams[1] and others have intensively studied KCl.Tl, which is a phosphor of this type. However, when the activator ions have an ionic charge different from that of the lattice ions, there has been no general agreement as to the specific atomic configurations in the luminescent centres. Kröger[2] and others have stressed that charge compensation must take place, and have applied this idea to the theory of the sulphide phosphors. In the most important examples of this class of phosphor a single ion compensates each activator ion, and the dissociation of the ion pairs has been thought to be considerable[2] due to the high dielectric constant of the sulphides. The results obtained by Kröger and Dikhoff[3] on ZnS.Pr, Cu or Ag indicate otherwise, as they found distinct changes in the line intensities depending on the choice of monovalent ion; but the interpretation of the sulphide phosphors is particularly difficult owing to the partly covalent nature of the interatomic bonds.

The present theory of luminescent centres is an extension of the idea of compensation of charge, and it is now proposed

that in ionic crystals the compensation of charge, taking place either by lattice vacancies or by compensator ions, is localized and occurs without any ions being in interstitial positions. The degree of dissociation of the ions in the centre is expected to be small in most ionic crystals, and especially so in cubic crystals of the RX type, e.g. CaO, where both the shortest distance between positive ions and the dielectric constant are moderately small. Large excess charges and low temperatures will also favour the stability of the centres.

Interesting configurations of the activator ions, and of the compensator ions or vacancies, can be expected to occur when there is an excess charge on the activator ion; and the configuration of lowest energy should provide an adequate description of the centre. Two or more centres may combine and such a group will be called a "cluster," this being in rough conformity to the previous usage.

Although luminescent centres appear to offer the greatest variety of configurations, a few examples have been described in other branches of solid-state physics. Seitz[4] has suggested that in the alkali halides, positive and negative ion vacancies will tend to form neutral pairs, as will also a divalent positive ion and a positive ion vacancy; and he has discussed the formation of groups of such pairs, e.g. the weak aggregation of two pairs of divalent ions with associated vacancies. Reitz and Gammel[5] have calculated that the binding energy of the cadmium ion and a positive ion vacancy in NaCl is 0·44 eV. This is in fairly good agreement with the value of 0·3 eV experimentally determined by Etzel and Maurer,[6] and supports the idea of local charge compensation. Verwey[7] and others have also given examples of charge compensation in their treatment of semiconductors, e.g. the association of a Cu^{2+} ion and a positive ion vacancy in Cu_2O at low temperatures.

The groups of ions in a centre or cluster will have a characteristic set of vibrations, which in favourable cases may have an observable effect on the absorption and emission of the phosphors. The negative ions in the vicinity of the activator must be included in the description of the centre, especially when considering the possible vibrations.

ATOMIC CONFIGURATIONS IN OXIDE PHOSPHORS

The configurations of lowest energy will now be considered for a trivalent, tetravalent or hexavalent activator ion in a face-centred cubic crystal of the RX type, when there is compensation either (*a*) by lattice vacancies due to missing divalent positive ions or (*b*) by the replacement of divalent positive ions by monovalent positive ions. Calculations of the potential energy of possible configurations have been made, to decide in doubtful cases which is the configuration of lowest energy. Only the coulomb energy terms have been included in these rough calculations, but in most cases the configuration of lowest energy is obvious. It would be possible to calculate the energy of dissociation of these configurations by the Mott–Littleton[8] method, which includes displacement and polarization terms, in the same way as Reitz and Gammel,[5] and later Bassani and Fumi,[9] calculated the energy of dissociation of a Cd^{2+} ion and a lattice vacancy in NaCl, but such calculations have not yet been performed.

Case 1. *A trivalent ion.* (*a*) The activator ion, *A*, has one unit of excess positive charge beyond the charge normally present in the crystal lattice, whereas a positive ion lattice vacancy denoted by *D* is equivalent to an excess of two units of negative charge. Hence the simplest way of achieving electrical neutrality is for one lattice vacancy to be associated with two activator ions. The configuration of lowest energy is that of a linear electric quadrupole with the lattice vacancy midway between the two activator ions, i.e. *A D A*, and the orientation will be along the direction for which positive ions are closest together, i.e. the [110] direction for a face-centred cubic crystal. Examples of this type are CaO.Bi and MgO.Cr. It is an interesting feature of the theory of localized charge compensation that a centre may have to contain more than one activator ion in order that electrical neutrality can be achieved. The Bi ions have been shown to be trivalent in CaO.Bi using a chemical test described by Kröger and others.[10]

At liquid-air temperature, the CaO.Bi phosphor has a banded structure on the short wavelength side of 4300 Å, and it has been shown by Ewles[11] that the bands may be numerically represented by an electron vibration band-head formula of the type

$$\nu = \nu_0 + (v' + \tfrac{1}{2})w' - (v'' + \tfrac{1}{2})w''$$

where v' and v'' are small integers or zero, w' and w'' are frequencies of the vibrational order of magnitude $\simeq 500\ \mathrm{cm}^{-1}$ and ν_0 is the frequency of the electronic transition involved. Ewles has suggested that the electron vibration bands are associated with the host lattice; but it is now suggested that the vibrations are those of the two Bi ions in the centre. On this basis, there will be two main normal modes of vibration, the one in which the two Bi ions vibrate symmetrically towards the defect, i.e. $\rightarrow\ \leftarrow$ and a vibration in which the two ions are in phase, i.e. $\rightarrow\ \rightarrow$. A rough calculation can be made of the ratio of the values of the two vibrational frequencies, i.e. w''/w', using a mechanical analogy. If three similar stretched elastic strings are connected end to end between two fixed points *O* and *H*, and masses *m* are attached to the joins at *F* and *G*, thus

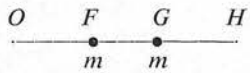

then the frequencies of the normal modes of vibration can be shown, using Lagrange's method for the solution of problems of small oscillations, to be in the ratio $\sqrt{3} : 1$, the symmetric mode having the larger frequency. The values found by Ewles for w' and w'' from an analysis of the CaO.Bi bands yield a ratio of 493 : 298 or 1·65, which is reasonably close to the value of 1·73 for the above simplified model.

Another example of a phosphor containing trivalent ions compensated by defects, is MgO.Cr, which is excited by cathode-rays. Deutschbein[12] has described the spectrum, which consists of broad lines and narrow bands. This spectrum is more complicated than that of CaO.Bi, due to the electronic transition occurring in an incomplete electron shell; but it is being restudied, along with phosphors of the the CaO.Sm type where the shielding is more complete, to determine whether the vibrations of the centre affect the emission.

Case 1(*b*). Compensation by a monovalent positive ion *C* is accomplished when one activator ion and one compensator ion are in neighbouring cation sites, i.e. *C A* along the [110] axis. However, there may be a reduction in energy when a cluster of two such centres is formed, i.e. $\frac{CA}{AC}$. This is the formation of a quadrupole from two dipoles, and is similar to the configuration suggested by Seitz for divalent ions and vacancies in alkali halides. Examples of this type are the new phosphors CaO.Bi, Li, and MgO.Cr, Li.

The CaO.Bi, Li emission spectrum when excited by 3650 Å

radiation includes bands very similar to those for CaO.Bi and also a weak band in the red region in approximately the same position, near 6450 Å, as a band occurring in the CaO.Bi spectrum at high Bi concentrations. This emission is believed to be due to a Bi ion adjacent to another Bi ion. The specific configuration responsible for the emission of red radiation in CaO.Bi is probably a cluster containing two centres, i.e. $\begin{matrix} A\,D\,A \\ A\,D\,A \end{matrix}$, and the emission can be expected to be slightly different from that due to the similar cluster $\begin{matrix} CA \\ AC \end{matrix}$ occurring in the CaO.Bi, Li phosphor.

MgO.Cr, Li has also been investigated, and it is found that the lithium greatly enhances the deep red emission at room temperature under cathode-ray excitation.

valent ions are at the corners of a tetrahedron with the hexavalent ion at the centre, Fig. 2. The tetrahedron is not regular, but can be derived from a regular tetrahedron by stretching along one of the axes of two-fold rotational symmetry. A simple coulomb energy calculation indicates that the tetrahedral formation is very slightly the more stable. It is quite possible that both types of centre can occur in the phosphor. As no previous example of this type was known, it was decided to investigate CaO.U, Li and its liquid-air temperature emission spectrum when excited by 3650 Å radiation is shown, Fig. 1(*b*). This phosphor has a similar spectrum to CaO.U, but the differences in the line intensities are sufficient to suggest that some atoms very near to the U atoms are different. The CaO.U, Li phosphor is much brighter at room temperature than the CaO.U phosphor,

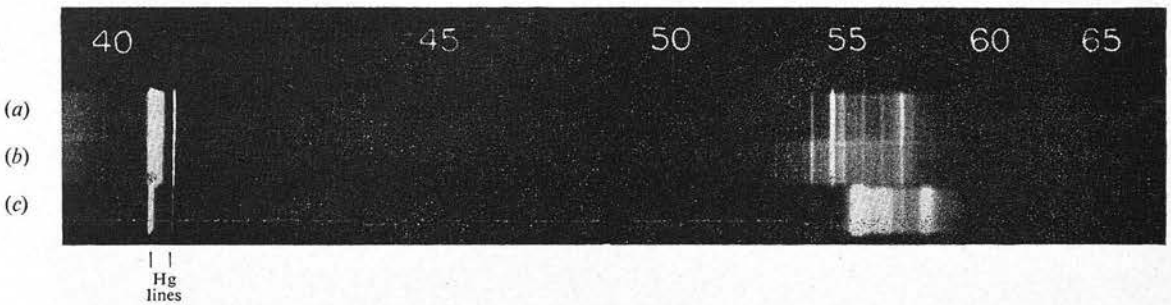

Fig. 1. (*a*) CaO (1% U) (10 min); (*b*) CaO (1% U, 4% Li) (10 min); (*c*) Ba_2CaUO_6 (10 min)

Figs. 1, 4, 6. The spectra were obtained with a Hilger medium quartz spectrograph using the Hartmann diaphragm. The slit width was 0·025 mm and the spectra have been enlarged × 3 (approx.). The exposure times are shown in brackets. Figs. 1 and 6 were obtained from Ilford Rapid Process Panchromatic Plates and Fig. 4 from an Ilford Long Range Spectrum Plate.

Case 2. *A tetravalent ion.* (*a*) Electrical neutrality is maintained by one lattice vacancy being associated with each activator ion, i.e. *DA* along the [110] axis. This type of centre will tend to form clusters, i.e. $\begin{matrix} DA \\ AD \end{matrix}$.

Case 2(*b*). One activator ion is compensated by two monovalent ions instead of by a vacancy, and the linear symmetrical position is the one of lowest energy, i.e. *CAC* along the [110] axis. An example of this class of phosphor is the MgO.Mn, Li phosphor recently described by Prener.[13] When excited by 3650 Å radiation at liquid-air temperature, it has a complex emission spectrum containing narrow bands which may be at least partly due to the vibrations of the centre.

Case 3. *A hexavalent ion.* (*a*) The centre consists of a linear arrangement of one activator ion and two lattice vacancies, i.e. *D A D* along the [110] axis. CaO.U is of this type, and it has been found to have a complex emission spectrum at liquid-air temperature when excited by 3650 Å radiation, Fig. 1(*a*). This sample was prepared from calcium carbonate and uranyl nitrate, and fired at 1250° C in air. The main unit which contributes to the vibrational fine structure is believed to be a UO_6 group, rather than a UO_2 group, and in this respect it is similar to the recently discovered uranates[14] which also have UO_6 groups. For comparison, the $Ba_2Ca\,UO_6$ spectrum, when excited by 3650 Å radiation at liquid-air temperature, is also shown, Fig. 1(*c*). Both spectra have a repetition frequency interval $\simeq 730\ cm^{-1}$, but the two spectra are relatively displaced.

Case 3(*b*). One hexavalent ion combines with four monovalent compensator ions to form a centre. There are two possible configurations which might occur, either a formation in which the monovalent ions form a square with the hexavalent ion at the centre, or a formation in which the monovalent ions are at the corners of a tetrahedron with the hexavalent ion at the centre, Fig. 2. The tetrahedron is not regular, but can be derived from a regular tetrahedron by stretching along one of the axes of two-fold rotational symmetry. A simple coulomb energy calculation indicates that the tetrahedral formation is very slightly the more stable. It is quite possible that both types of centre can occur in the phosphor. As no previous example of this type was known, it was decided to investigate CaO.U, Li and its liquid-air temperature emission spectrum when excited by 3650 Å radiation is shown, Fig. 1(*b*). This phosphor has a similar spectrum to CaO.U, but the differences in the line intensities are sufficient to suggest that some atoms very near to the U atoms are different. The CaO.U, Li phosphor is much brighter at room temperature than the CaO.U phosphor, though they are of comparable brightness at liquid-air temperature, and these two phosphors are considered strong evidence in favour of the localization of charge compensation.

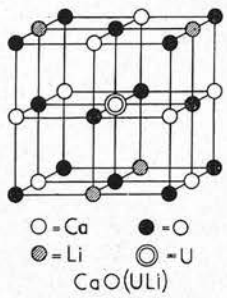

Fig. 2. The atomic configuration of CaO.U, Li

THE EMISSION SPECTRA OF SOME URANATE PHOSPHORS

In the course of an investigation of CaO.U it was found possible to make a uranate of composition Ca_3UO_6. It was shown[14] that the structure was similar to that of Ca_3WO_6 and, as expected from knowledge of the tungstates,[15] that it was possible to form a compound Ba_2CaUO_6 having a nearly cubic crystal structure. The idealized unit cell is shown in Fig. 3. Because of the greater simplicity in this structure, attention has been concentrated on these Ba_2CaUO_6 phosphors. Ba_2CaUO_6 is itself luminescent, see Fig. 1(*c*). The uranates can be activated by some of the rare earths, samarium and europium emitting their characteristic line spectra in the orange-red and red regions respectively; whereas

gadolinium, lanthanum and ytterbium act as intensifiers of the uranium emission. Of all these cases, the samarium

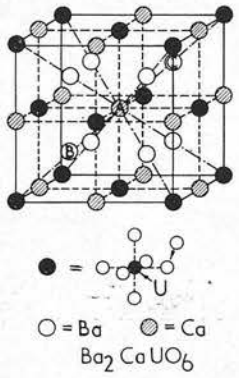

Fig. 3. The idealized unit cell of Ba_2CaUO_6

activation has been most studied. For Ba_2CaUO_6.Sm the configuration of lowest energy is probably obtained by replacing the Ba atoms B and C (Fig. 3) by Sm atoms, and removing the Ca atom at position A; whereas for the case of Sm, Li activation the Li and Sm ions probably occupy positions A and B respectively. However, an alternative possibility is that the Sm ions, and also the associated defects or monovalent ions, are all situated at Ca ion sites, the configurations being directed along the [110] axis. The emission spectra at liquid-air temperature when excited by 3650 Å radiation are shown in Fig. 4(*a*), (*b*). The energy transfer from the uranium ions is very good and no uranium emission is observable. The differences between the spectra are of the same type as those between CaO.U and CaO.U, Li, but are not so large, the line intensities still being markedly different, although the line positions are extremely similar. The emission spectrum of CaO.U, Sm is also included for comparison, Fig. 4(*c*), and it is obvious that the details of the emission spectrum of a rare earth ion can be greatly changed by the ionic surroundings.

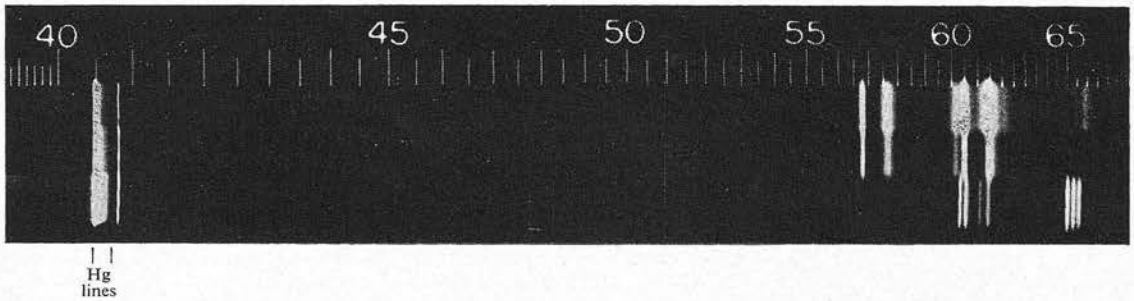

Fig. 4. (*a*) Ba_2CaUO_6 (1% Sm) (10 min); (*b*) Ba_2CaUO_6 (1% Sm, 1% Li) (20 min); (*c*) CaO (1% U, 0·2% Sm) (10 min)

It is known that the absorption and emission spectra of phosphors activated by rare earths contain too many lines to be explained on Bethe's theory of Stark splitting of the energy levels, when the rare earth ions are considered to be in positive ion sites, the neighbouring ions being normal. The present account explains the extra lines by the fact that each rare earth ion is in a field of much lower symmetry, due to the near proximity of a lattice defect or compensator ion. Furthermore, the vibrations of the centre may be expected to interact with the electronic energy levels, causing further splitting of the spectral lines.

FLUORITE

Toorks[16] has claimed that CaF_2.U is intensified by the addition of CaO, and Kröger[17] has briefly discussed this result assuming charge compensation. Excluding the possibility of the entry of ions interstitially, there are still three possible methods of charge compensation. These are (*a*) compensation by lattice vacancies, (*b*) compensation by monovalent positive ions, and (*c*) compensation by divalent negative ions.

(*a*) The U ion replaces one Ca ion and is compensated by two lattice vacancies, i.e. *D A D*. This formation will be directed along the [110] axis, since the calcium ions form a face-centred cubic lattice.

(*b*) Four monovalent ions compensate one U ion, so that the positive ion configurations are exactly the same as for CaO.U, Li. Hence the stretched tetrahedral formation is the most likely configuration of lowest energy.

(*c*) Four oxygen ions replace four fluorine ions to compensate the excess charge, and Kröger[17] has stated that the U ion will be surrounded by four oxygen and four fluorine atoms. It is now suggested that these ions will be arranged in a specific configuration, i.e. that the groups of oxygen and fluorine ions will each form a regular tetrahedron, as shown in Fig. 5. The spectra of CaF_2.U, CaF_2.U, O and CaF_2.U, Li, excited by 3650 Å radiation at liquid-air temperature are shown in Fig. 6. It is not claimed that the first and third of these phosphors are free from oxygen, as the uranium was introduced as a uranyl salt.

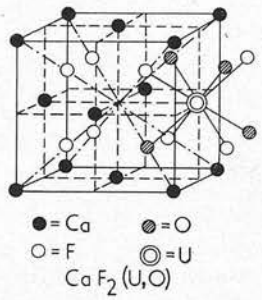

Fig. 5. The atomic configuration of CaF_2.U, O

There are also many interesting examples of fluoride phosphors activated by rare earths, and work is in progress on these phosphors. It will be interesting to note any systematic differences between the group of phosphors containing

vacancies and the groups containing different compensator ions.

It is also instructive to examine the implications of localized charge compensation in the general theories of sensitized luminescence and multiple band emission.

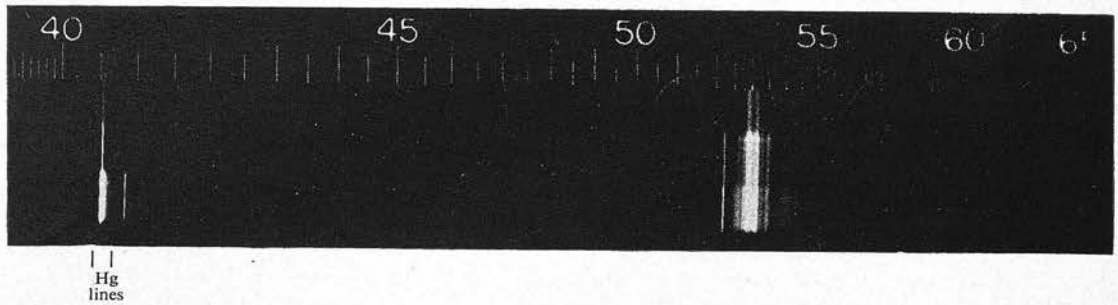

Fig. 6. (*a*) CaF_2 (0·1% U) (5 sec); (*b*) CaF_2 (0·1% U, 10% O) (5 sec); (*c*) CaF_2 (0·1% U, 1% Li) (30 min)

SENSITIZED LUMINESCENCE

In the many known cases of sensitized luminescence it is generally accepted that the sensitizer atoms absorb the incident radiation and then transfer the energy, directly or indirectly, to the activator ions which emit the fluorescent radiation. Botden[18] has recently summarized the existing theories in addition to presenting his own conclusions. He concluded that transport of energy from the sensitizer to the activator *via* the conduction band is very improbable because the quantum efficiency does not depend quadratically on the exciting radiation intensity. A similar objection holds for transport of vibration energy which could modify the activator potential energy curve in such a way that the activator could now be excited by another quantum of incident radiation. A more hopeful approach is that of supposing that direct transfer can take place from the sensitizer ions to the activator ions, or to other sensitizer ions, by a resonance process. Botden,[18] and Schulman and others[19] have performed calculations on the distance over which such transfer can take place, on the assumption of the random distribution of the sensitizer and activator ions. It is now suggested that this assumption is not valid and that the centres which have been already described will tend to pair. In this way, the present account is an extension of Kröger's[20] theory of associated-pairs and Murata and Smith's[21] idea of co-activators. It is to be noted, however, that it is centres and not ions which pair or tend to pair. For instance, a stable configuration can be obtained when a hexavalent centre in an oxide lattice is paired with one or two trivalent centres, i.e. $\begin{matrix} D\,A_6\,D \\ A_3D\,A_3 \end{matrix}$ or $\begin{matrix} A_3D\,A_3 \\ D\,A_6D \\ A_3D\,A_3 \end{matrix}$. CaO.U, Sm is believed to be an example of this, Fig. 4(*c*), which would account for the remarkable energy transfer at liquid-air temperature. On the other hand, without localized charge compensation the U and Sm ions would have tended to repel each other. No strong evidence has been put forward against the formation of pairs, and certainly one cannot draw a clear conclusion from the fact that some sensitized phosphors have optical characteristics which are independent of the rate of cooling after firing,[18] as the configuration containing two or more centres may be formed and be reasonably stable even at the firing temperature. The mathematical analysis of the results is not unique and is in itself no proof of random distribution of the sensitizer and activator ions. The exact nature of the clusters is not always very clear as it will depend not only on the charge of the ions, but also on the size and on the magnetic and other properties of the ions. However, the coulomb forces can often be expected to be predominant, e.g. in NaCl.Pb, Mn or KCl.Pb, Mn the Pb and Mn centres will tend to pair with each other and amongst themselves, i.e. $\begin{matrix} D\,\mathrm{Pb} \\ \mathrm{Mn}\,D \end{matrix}$ or $\begin{matrix} D\,\mathrm{Pb} \\ \mathrm{Pb}\,D \end{matrix}$ or $\begin{matrix} D\,\mathrm{Mn} \\ \mathrm{Mn}\,D \end{matrix}$, and clusters of the first type will be responsible for the sensitization.

A great advantage of this theory of specific configuration is that it is not necessary to postulate long range resonance processes between unlike ions. It is still expected that resonance transfer between like atoms can take place over considerable distances of the order of 50 Å, and this is reasonable on Förster's[22] theory of resonance transfer between equivalent molecules. Dexter[23] has extended this theory to include the forbidden transitions occurring in the luminescence of inorganic materials.

THE THEORY OF MULTIPLE-BAND EMISSION

In a similar way, the theory of localized charge compensation tends to support the cluster theory of multiple-band emission. When the ion has a different co-ordination number (C.N.) in different substances there may be a change in the colour of the emission, e.g. $CdWO_4$.U is red, C.N. = 4; Ca_2MgWO_6.U is green, C.N. = 6. In a specific crystal structure, however, it would appear that clustering is the most likely mechanism by which changes in the environment of the activator ion may occur. For instance, trivalent, tetravalent and hexavalent ions in a face-centred cubic oxide crystal, will tend to pair when electrical neutrality is achieved by the presence of defects. Trivalent and tetravalent ions will tend to pair when compensated by monovalent ions.

There may even be a tendency for the hexavalent ions, when compensated by monovalent ions, to pair; but this is expected to be very slight, owing to the screening of the hexavalent ion by the symmetrically arranged monovalent ions. Even when no charge compensation is necessary, there will still be ionic properties which will tend to reduce the randomness of the distribution of the activator. There will be least disturbance of randomness in the case of an activator ion where no charge compensation is necessary, and where the electronic configuration in the ground state consists of complete shells or sub-shells of electrons. An example of this is KCl.Tl, and the Tl^+ ions are believed to be nearly randomly distributed in K^+ sites. A detailed X-ray investigation of the KCl.Tl system, carried out by Runciman and Steward,[24] showed that the Tl^+ ions substituted for

K^+ ions. Both the line positions and intensities were in agreement with the values predicted from a random distribution of Tl^+ ions.

Where the sub-shell is incomplete as in Mn^{2+}, then there is likely to be a strong deviation from randomness, and Larach and Turkevich[25] have obtained results which may be interpreted in this way.

Evidence was presented earlier to show that the centres in CaO.Bi cause a new band to appear when pairing occurs, in a similar fashion to the emission bands at 3755 and 5800 Å due to Tl^+ ion pairs in KCl[26]. Pb^{2+} ion pairs in CaO also are the likely cause of the red emission band in the CaO.Pb phosphor, and this similarity is not surprising, since Bi^{3+}, Pb^{2+} and Tl^+ are all iso-electronic with the neutral Hg atom. Some weak vibrational lines have been found superimposed on the red emission band of CaO.Pb, when excited by 3650 Å radiation at liquid-air temperatures, and these are of a very similar type to those reported by Randall[27] for CaO.Mn. They occur at approximately 6060, 6150, 6230, 6300 and 6360 Å.

CONCLUSION

It has been shown that a theory of localized charge compensation provides a framework capable of synthesizing many of the previously puzzling results in the luminescence of ionic crystals. In consequence of this theory calculations which have been based on the assumption of a random distribution of activator ions, must be considered as requiring revision in many cases. It will be possible to calculate the binding energies of the centres, the absorption and emission of phosphors, etc., on the new theory using the established methods of solid-state physics. However, when a detailed knowledge of the vibrations of the ions in the centre is required, these calculations will be rather formidable, owing to possible anharmonicity of the vibrations.

The spectra of CaO.U, Li, CaO.U, Sm and of various uranate phosphors have been described, and it appears that alkaline earth oxide, uranate and fluoride phosphors form an ideal system for the study of the effects caused by changes in the surroundings of the luminescent ions. It is fortunate that both the uranium and the rare earth emission spectra consist of lines and narrow bands, enabling a detailed analysis to be made of the effects of slight changes in the luminescent centres.

REFERENCES

(1) Williams, F. E. *J. Chem. Phys.*, **19**, p. 457 (1951) and other papers.
(2) Kröger, F. A., and Hellingman, J. E. *J. Electrochem. Soc.*, **93**, p. 156 (1948) and other papers.
(3) Kröger, F. A., and Dikhoff, J. A. M. *Physica*, **16**, p. 297 (1950).
(4) Seitz, F. *Phys. Rev.*, **83**, p. 134 (1951).
(5) Reitz, J. R., and Gammel, J. L. *J. Chem. Phys.*, **19**, p. 894 (1951).
(6) Etzel, H. W., and Maurer, R. J. *J. Chem. Phys.*, **18**, p. 1003 (1950).
(7) Verwey, E. J. W., and Kröger, F. A. *Philips Tech. Rev.*, **13**, p. 90 (1951).
(8) Mott, N. F., and Littleton, M. J. *Trans Faraday Soc.*, **34**, (1), p. 485 (1938).
(9) Bassani, F., and Fumi, F. G. *Phil. Mag.*, **45**, p. 228 (1954).
(10) Kröger, F. A., Overbeek, J. T. G., Goorissen, J., and Boomgaard, J. van den. *J. Electrochem. Soc.*, **96**, p. 132 (1949).
(11) Ewles, J. *Proc. Roy. Soc. A*, **167**, p. 34 (1938).
(12) Deutschbein, O. *Ann. Phys.* [*Leipzig*], **5**, p. 712 (1932).
(13) Prener, J. S. *J. Chem. Phys.*, **21**, p. 160 (1953).
(14) Steward, E. G., and Runciman, W. A. *Nature* [*London*], **172**, p. 75 (1953).
(15) Steward, E. G., and Rooksby, H. P. *Acta Cryst.*, **4**, p. 503 (1951).
(16) Toorks, W. P. U.S. Patent 2323284.
(17) Kröger, F. A. *Physica*, **14**, p. 488 (1948).
(18) Botden, T. P. J. *Philips Res. Rep.*, **7**, p. 197 (1952).
(19) Schulman, J. H., Ginther, R. J., and Klick, C. C. *J. Electrochem. Soc.*, **97**, p. 123 (1950).
(20) Kröger, F. A. *Physica*, **15**, p. 801 (1949).
(21) Murata, K. J., and Smith, R. L. *Amer. Mineral.*, **31**, p. 527 (1946).
(22) Förster, V. T. *Ann. Phys.* [*Leipzig*], **2**, p. 55 (1948).
(23) Dexter, D. L. *J. Chem. Phys.*, **21**, p. 836 (1953).
(24) Runciman, W. A., and Steward, E. G. *Proc. Phys. Soc.* [*London*] *A*, **66**, p. 484 (1953).
(25) Larach, S., and Turkevich, J. *Phys. Rev.*, **89**, p. 1060 (1953).
(26) Johnson, P. D., and Williams, F. E. *J. Chem. Phys.*, **20**, p. 124 (1952).
(27) Randall, J. T. *Proc. Roy. Soc. A*, **170**, p. 272 (1939).

DISCUSSION

Dr. P. Brauer: I am impressed by Mr. Runciman's success in calculating the ratio of the vibration frequencies for CaO.Bi, for we tried in vain to calculate similar vibration frequencies, found by Tomaschek for Sm^{3+} and Pr^{3+} in alkaline earth oxides and sulphides. We did not know how to calculate the reduced mass of the vibrating system.

When an activator ion of different valency or charge is introduced into an ionic lattice, the valency of the activator may have other values than those in ordinary chemical compounds. For Tl and the alkaline halides it is probable that Tl is monovalent. Nevertheless we did not consider it correct to exclude other possibilities and therefore used the complete Mott–Littleton theory[1] to estimate how many foreign ions will enter the lattice at a given temperature and a given concentration of these ions in another phase; and, in addition, to explain the very great differences in the preference of a foreign ion for different host lattices.[2]

The charge of the foreign ion may be completely uncertain. For Eu in the alkaline earth oxides and sulphides we have shown by calculation that it has to be trivalent in the oxides but divalent in the sulphides, selenides and tellurides, when the pressure of the gaseous phase during preparation is considerable. Thus we explained the different emission spectra of the phosphors.[3] However, the valency of Eu may change if the pressure of the gaseous phase is changed. Thus mixed crystals of SrO and EuO (divalent Eu) were made using reducing conditions,[4] in spite of the fact that pure EuO is unknown. This agrees with our calculation, according to which the chemical affinity of the reaction

$$\underset{\text{(in SrO)}}{2Eu^{3+} + |Sr^{2+}|} + SrO \rightleftharpoons \underset{\text{(in SrO)}}{2Eu^{2+}} + \tfrac{1}{2}O_2,$$

where $|Sr^{2+}|$ is a Sr^{2+} vacancy in the lattice, is at least 3 eV greater than the affinity of

$$Eu_2O_3 \rightleftharpoons 2EuO + \tfrac{1}{2}O_2$$

In this manner it is possible to prepare quite different samples of SrO.Eu: white ones containing Eu^{3+}, charge compensated probably by Schottky holes, and pink to deep violet ones, containing Eu^{2+} without charge compensation.

Charge compensation should, therefore, be discussed only in connexion with changes of charge, and we must calculate the free energy or the affinity of the chemical reaction as a whole.

Dr. F. A. Kröger: When ions of opposite effective charge are present in a solid, energy conditions favour a clustering into pairs or even larger agglomerations while entropy conditions tend to keep them apart. At the high temperature of preparation a fraction of the ions is present in the "associated" form and another fraction in the "dissociated" form. During cooling association is favoured, but below a critical temperature for ionic migration, further association is impossible.

In general both "free" ions and associated pairs may be responsible for luminescence, trapping, etc., and, as has been shown for ZnS.Ag^+, Pr^{3+}, it is probable that while the blue luminescence originates in Ag^+ at sites far from Pr^{3+}, characteristic Pr^{3+} emission originates both from Pr^{3+} ions and from Ag^+–Pr^{3+} pairs. I do not agree with Mr. Runciman's preference for the pairs.

(*b*) It is stated that the position of spectral lines is independent of the symmetry and the strength of the electric field in which the activator atom is situated, but that the intensity of the lines is dependent on them. This seems to be in conflict with Bethe's theory.[5]

Runciman mentions that often oxides or sulphides activated by rare earth ions do not show the simple fluorescence pattern predicted by the Bethe theory for cubic lattices. Deutschbein[6] and Brauer[7] have shown, however, that MgO, CaO, SrO and BaO activated by Eu^{3+} emit a strong line in the red predicted by the Bethe theory for pure cubic symmetry, all other lines present being at least ten times weaker.

(*c*) The proposed return to the pair theory of sensitization which I once advocated is impossible, for Botden[8] has proved that this theory cannot explain, in particular, the increase of the ratio of manganese to sensitizer emission with increasing concentration of sensitizer.

The centres proposed by Runciman may well exist, but in general they do not play the predominant role he assigns to them.

Dr. F. E. Williams: I support the remarks of Dr. Brauer and of Dr. Kröger regarding the importance of the entropy, in addition to the potential energy, in determining the relative concentration of the associated and unassociated centres.

The emission spectrum of CaO.Bi, Li can be adequately accounted for on the basis of isolated Bi^{3+} at cation sites. Bi^{3+} is isoelectronic with Tl^+ and would be expected to exhibit similar luminescence properties. The two emission bands can be attributed to the $^3P_1^0 \rightarrow {}^1S_0$ and the $^1P_1^0 \rightarrow {}^1S_0$ transitions; the fine structure, to the vibrational levels of the activator system consisting of Bi^{3+} and its six nearest neighbour O^{2-} ions. From the coulomb interaction alone the force constant K for the activator system of CaO.Bi should be six times that for KCl.Tl. The effective mass M should be approximately one-half. Since the separation ΔE of the vibrational levels is $\hbar\sqrt{(K/M)}$ an emission fine structure separation of 0·05 eV is calculated, in good agreement with the experimental value of 0·06 eV.

Dr. B. V. Thosar: While considering the atomic configurations of luminescence centres it would be of interest to examine the structure of luminescence in the deep red due to Cr^{3+}, in relation to the crystal structure of the various natural oxides and silicates in which it becomes luminescent by replacing the Al^{3+} ion. From Deutschbein's results the following conclusions may be drawn:

(*a*) The red luminescence, normally a doublet, is characteristic of a Cr^{3+} ion at the centre of an octahedron, the corners of which are occupied by six oxygen ions or other anions.

(*b*) This octahedron shares corners, edges or faces with other polyhedra and may become distorted. The amount of this distortion can be correlated with the separation of the two lines of the doublet. In MgO, a regular cubic crystal, there is a single line emitted instead of a doublet.

(*c*) The case of disthene, Al_2SiO_5, is of special interest. In this, octahedra with Al at the centre and O at the corners form chains along the *c*-axis by sharing edges. Similar octahedra, structurally non-equivalent with the former, occur in the crystal and link the chains laterally. Cr^{3+} replacing Al^{3+} ions at the centre of these two different kinds of octahedra should give luminescence lines not identical in wavelength, and this is indeed the case. There are in disthene two emission doublets and not one.

Mr. J. Ewles: The suggestion that the vibrational frequencies which I reported in the resolved CaO.Bi spectrum are attributable to two modes of vibration of a linear quadrupole is ingenious but can hardly be sustained in its present form.

(*a*) The ratio $\sqrt{3} : 1$ of the two vibration frequencies, deduced from the model, does not hold for SrO.Bi (2·05), CaS.Bi (1·93), MgO.Bi (2·21) and CaO.Pb (1·92).

(*b*) The two frequencies involved in the electron vibration band formula must refer to the vibration frequencies of the luminescence centre in the upper and lower states, and not to two different lower state frequencies.

(*c*) It is tempting to accept the charge compensation idea to explain the effect of a flux, but the addition to a divalent host lattice of a flux containing a monovalent ion (e.g. CaO.Bi, NaCl) does not alter the luminescence spectrum as would be expected if the monovalent ion forms part of the centre, unless it is assumed that an ineradicable trace of flux is always present in the purest ionic crystal. It is certainly true that luminescence effects can be produced by a concentration of 10^{-7} of activator.

Author's reply: Dr. Brauer has shown how the charge on an impurity ion may vary with the conditions of preparation. In the cases I have considered the ionic charge is fairly certain and it is possible to consider how charge compensation may take place without considering all the chemical reactions involved.

Dr. Kröger has clearly indicated the importance of entropy in considering the degree of clustering which takes place. Experimental results to date indicate that there is a preference for clustering in many cases, but further experimental and theoretical work should clarify this point. I have nowhere made the statement given in Dr. Kröger's point (*b*), but have quoted the spectra of CaO.U, Sm and Ba_2CaUO_6.Sm to prove the contrary. However, the changes in the field caused by differences between the nearest positive ions in Ba_2CaUO_6.Sm and Ba_2CaUO_6.Sm, Li produce only slight modifications in the line positions. This seems reasonable as the nearest negative ions make the largest contributions to the field.

Kröger's point (*c*) is also not valid, since I do not make the assumption, involved in Botden's deduction, that only absorption in a sensitizer ion adjacent to an activator ion will give rise to activator fluorescence. On the contrary I have stated that it is still expected that resonance transfer

between like atoms can take place over considerable distances. Transfer between unlike ions over large distances is not considered necessary to explain the experimental results and in this respect I disagree with Botden's conclusions, which were based on a random distribution of both activator and sensitizer ions.

I now agree with Dr. Williams that the fine structure in the CaO.Bi spectrum can be attributed to vibrations of the six oxygen ions surrounding the Bi^{3+} activator ions. The Bi^{3+} ions need not be isolated, and the difference in relative intensities of the red and blue bands for CaO.Bi and CaO.Bi, Li can be satisfactorily ascribed to the association of the positive ions. The spectrum seems too complex for all the lines to be due to radial symmetric oscillations of the oxygen ions. The change in charge distribution when the Bi^{3+} ion goes from a dumb-bell 6p state oriented along the [110] axis to a spherical 6S state will cause the oxygen ions to rearrange their equilibrium positions in a way which can be described by three independent parameters. Hence we may expect three normal modes of vibration rather similar to the three Raman vibrations of an octahedral molecule such as SF_6. The transition is similar to that of Tl^+ in the KCl.Tl phosphor,[9] and the existence of three degrees of freedom demonstrates the limitations of the configuration co-ordinate model used by Williams. This new model may explain some extra lines recently observed in both the absorption and emission spectra of a CaO.Bi phosphor at liquid nitrogen temperature: these lines were not easily explicable in terms of the previous model. Yet the objections raised by Mr. Ewles are not conclusive and I still maintain that the two vibrational frequencies observable in the fluorescence spectrum refer to the ground state. This necessitates a modification of the vibration formula used by Ewles to represent the line positions. The absorption spectrum is almost a "mirror image" of the fluorescence spectrum, but the vibrational frequencies are considerably smaller. Useful confirmation comes from the results of Ewles and Lee[10] which show that both sets of lines in the emission spectrum still exist at 20° K; at this temperature with a Boltzmann distribution almost all the excited ions should reach the lowest vibrational state before emission takes place.

There is definite evidence that the addition of Li_2CO_3 to the CaO.Bi phosphor before firing alters the emission spectrum as described above. Compensation by monovalent ions will not take place if it is energetically unfavourable, e.g. because of an unsuitable ionic radius, and it may not be possible for the Na^+ ions to enter the CaO lattice in the case quoted by Ewles, where only a normal flux action appears to occur.

REFERENCES

(1) Brauer, P. *Z. Naturforsch.*, **7a**, p. 372 (1952).
(2) Brauer, P. *Z. Naturforsch.*, **7a**, p. 741 (1952); **8a**, p. 273 (1953); *Z. Elektrochem.*, **57**, p. 744 (1953).
(3) Brauer, P. *Z. Naturforsch.*, **6a**, p. 561 (1951).
(4) Brauer, G. *Angew. Chem.*, **65**, p. 261 (1953).
(5) Bethe, H. *Ann. Phys.*, **3**, p. 133 (1929).
(6) Deutschbein, O. *Leuchten und Struktur fester Stoffen*, p. 179 (München, 1943).
(7) Brauer, P. *Z. Naturforsch.*, **6a**, p. 561 (1951).
(8) Botden, T. P. J. *Philips Res. Rep.*, **7**, p. 197 (1952).
(9) Williams, F. E. *J. Phys. Chem.*, **57**, p. 780 (1953), and this Supplement: Paper 19.
(10) Ewles, J., and Lee, N. *J. Electrochem. Soc.*, **100**, p. 399 (1953).

UNWIN BROTHERS LIMITED, WOKING AND LONDON

REPRINTED FROM THE
PROCEEDINGS OF THE PHYSICAL SOCIETY, A, VOL. LXVIII, p. 647, 1955

PRINTED IN GREAT BRITAIN

Absorption and Emission Spectra of Bismuth-Activated Phosphors

BY W. A. RUNCIMAN
Atomic Energy Research Establishment, Harwell, Didcot, Berks.

MS. received 14*th February* 1955

SOME phosphors show fine structure in their low-temperature absorption and emission spectra, and an investigation of this is likely to help our understanding of the nature of luminescent centres. Bismuth-activated oxide phosphors have a particularly well-defined vibrational fine structure and in consequence have been the subject of several investigations (Ewles 1938, Ewles and Curry 1950, Ewles and Lee 1953).

The frequencies of the maxima of the low-temperature emission bands have been represented (Ewles 1938) by the equation

$$\nu = \nu_e + (v' + \tfrac{1}{2})w' - (v'' + \tfrac{1}{2})w'', \qquad \ldots\ldots(1)$$

where v' and v'' are small integers or zero, w' and w'' are vibrational frequencies and ν_e is the frequency of the electronic transition. The plus sign indicates that the frequency w' refers to the excited state, and the minus sign that the frequency w'' belongs to the ground state.

Exactly the same bands can equally well be described by the equation

$$\nu = \nu_0 - v_1 w_1 - v_2 w_2 \qquad \ldots\ldots(2)$$

which has previously been applied to other fluorescent systems (e.g. Hausser, Kuhn and Kuhn 1935). The relations between the constants in equation (1) and (2) are:

$$v_1 = v'' \qquad w_1 = w''$$
$$v_2 = v' \qquad w_2 = w'' - w'$$
$$\nu_0 = \nu_e - \tfrac{1}{2}(w'' - w').$$

It is convenient to describe the bands by the number of vibrational quanta present (v_1, v_2) and the (0, 0) band will be called the fundamental band. For bismuth-activated phosphors v_1 ranges from 0 to 7 or 8, whereas v_2 is usually 0 or 1. The number of vibrational quanta excited by the electronic transition can only be integral, so the halves of equation (1) have been omitted. Any term due to the zero-point energy is effectively included in ν_0.

In equation (2) both frequencies w_1 and w_2 now belong to the ground state and hence at least two modes of vibration must be involved, whereas in (1) it was only necessary to postulate one normal mode whose frequencies were different in the ground and excited states.

The equation corresponding to (2) for absorption is

$$\nu_0 = \nu_0^* + v_1 w_1^* + v_2 w_2^* \qquad \ldots\ldots (3)$$

where w_1^* and w_2^* are vibrational frequencies of the excited state corresponding to w_1 and w_2 in the ground state.

The difference $\nu_0^* - \nu_0$ represents the energy difference between the electronic transitions for absorption and emission. If $\nu_0^* - \nu_0 = 0$ then the fundamental line is a resonance line. It has been maintained (Pringsheim 1949) that if $\nu_0^* - \nu_0 \neq 0$ then the first observed absorption and emission lines cannot be (0, 0) lines. Selection rules in solids are not very rigid and this explanation seems unlikely. An alternative explanation is that the surroundings of the activator ion are different in the ground and excited states. The neighbouring atoms do not readjust their positions during the electronic transitions by the Franck–Condon principle and hence the frequencies ν_0 and ν_0^* may be unequal.

For CaO (Bi) the frequencies, measured as wave numbers in cm^{-1}, of the emission bands have been represented (Ewles and Lee 1953) by

$$\nu = 25815 + 298(v' + \tfrac{1}{2}) - 493(v'' + \tfrac{1}{2}).$$

When this is rewritten in form (2) it becomes

$$\nu = 25717 - 493 v_1 - 195 v_2, \qquad \ldots\ldots (4)$$

and this is in agreement within the limits of experimental error, $\sim 10\ cm^{-1}$, with recent observations.

Furthermore, the absorption bands in CaO(Bi) have been obtained (figure, (*a*), Plate) by a reflection technique in which a 36w 6v tungsten lamp was focused through two pieces of Chance OX7 filter, each 2 mm thick, on to the phosphor in a Dewar flask.

In form (3) these bands are expressed by

$$\nu = 27230 + 430 v_1 + 215 v_2. \qquad \ldots\ldots (5)$$

Since different vibrational frequencies occur in (4) and (5), there are at least two modes of vibration active in both electronic states and equation (1) is not applicable. With a Boltzmann distribution of energy these vibrations will not be appreciably thermally excited at 77°K or lower temperatures. Hence the absorption bands only show vibrational levels of the upper state and the emission bands

levels of the ground state. It might be argued that the centre retains some vibrational energy after excitation, but this is most improbable as the vibrational frequency is of the order of 10^{13} sec^{-1} and the excited state has usually a half-life of the order of 10^{-8} second.

There is no theoretical reason for there to be only two vibrational terms in (2) and (3), and weak bands due to a third term with a frequency of the order of 360 cm^{-1} have been observed in both the absorption and emission spectra of CaO(Bi). In the case of uranium activated phosphors many more vibrational terms are necessary in (2) and (3), although (1) has been used (Ewles and Lee 1953).

The electronic transmission ($^1S_0 \rightarrow {}^3P_1{}^0$) responsible for the absorption spectrum is that of Bi^{3+} ion going from a $6s^2$ to a 6s 6p state. In contrast with the earlier view (Ewles and Curry 1950) that the vibrations were those of the host lattice, it has been suggested (Williams 1955) that the main vibrational frequency w_1 is that of a radially symmetric oscillation of the six oxygen ions surrounding the bismuth ion. Extending this idea it appears (Runciman 1955) that the change in charge distribution during the electronic transition from a spherical 6s to a dumb-bell 6p state oriented along the [110] axis will cause the equilibrium position of the six oxygen ions to be changed in a way determined by three independent parameters, e.g. two to fix the radial and deformation motions of the four oxygen ions in the xy plane and one to fix the radial motion of the two oxygen ions on the z axis. Hence in addition to the radially symmetric mode two more modes of vibration are especially likely to occur. The three active normal modes may correspond roughly to the three Raman active modes of an octahedral molecule, e.g. UF_6.

Emission bands for SrO(Bi) have been expressed (Ewles and Curry 1950) by

$$\nu = 24180 + 190(v' + \tfrac{1}{2}) - 390\,(v'' + \tfrac{1}{2}),$$

and in form (2) this becomes

$$\nu = 24080 - 390\,v_1 - 200\,v_2. \qquad \ldots\ldots(6)$$

The present results for SrO(Bi), figure 1 (*b*) lead to the equation

$$\nu = 24320 - 400\,v_1 - 200\,v_2. \qquad \ldots\ldots(7)$$

The vibrational frequencies in (6) and (7) are in good agreement though it was with difficulty that the lines due to the second vibrational term were observed and measured. On the other hand the difference in the fundamental band is well outside the limits of experimental error and is probably due to the detection of a weak band at 4107Å not previously reported.

The reason for some discrepancies with earlier results may be partly due to the higher firing temperature, 1300°c, which has been used in the preparation of phosphors, as compared with temperatures as low as 650°c previously used (Ewles and Lee 1953).

References

Ewles, J., 1938, *Proc. Roy. Soc.* A, **167,** 34.

Ewles, J., and Curry, C., 1950, *Proc. Phys. Soc.* A, **63,** 708.

Ewles, J., and Lee, N., 1953, *J. Electrochem. Soc.*, **100,** 392, 399, 402.

Hausser, K. W., Kuhn, R., and Kuhn, E., 1935, *Z. Phys. Chem.* B, **29,** 417.

Pringsheim, P., 1949, *Fluorescence and Phosphorescence* (New York: Interscience), pp. 304, 431.

Runciman, W. A., 1955, Cambridge Conference on Luminescence, *Brit. J. Appl. Phys.*, Suppl. No. 4, pp. 78, 84.

Williams, F. E., 1955, Cambridge Conference on Luminescence, *Brit. J. Appl. Phys.*, Suppl. No. 4, pp. 84, 97.

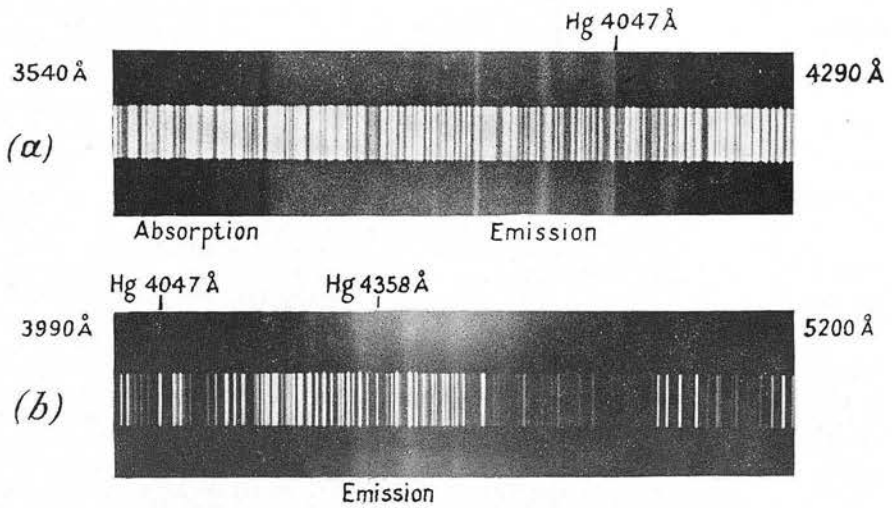

(*a*) Absorption and emission spectra of CaO(Bi) at 77°K (2 min exposure Zenith plate).
(*b*) Emission spectrum of SrO(Bi) at 77°K with 3650 Å excitation (1 min exposure. Thin film half tone plate).
The spectra were obtained on a Hilger medium Quartz Spectrograph, and the wavelength limits are as shown.

(*Reprinted from Nature, Vol.* 175, *p.* 1082, *June* 18, 1955)

Fluorescent Centres in Uranium-activated Sodium Fluoride

THE sodium fluoride fusion method is commonly used for the determination of minute amounts of uranium[1]. The sample to be tested is fused in a platinum crucible with sodium fluoride, and the fluorescence is measured in a fluorimeter. By this method, amounts of uranium down to 10^{-10} gm. can be determined in 0·2 gm. of fluoride.

Sodium fluoride containing uranium has a bright yellow-green fluorescence when excited by long-wave ultra-violet radiation. Even at room temperature the emission consists of broad bands partially resolved into lines, and at 77° K. the spectrum consists of more than twenty lines (see Fig. 1). This emission has been described by Slattery[2], who concluded that the uranium is in solid solution with the fluoride. The fluorescence would then be attributed to a UF_6 group. Solid UF_6, however, has a bright violet fluorescence bearing little resemblance to the sodium fluoride (uranium) emission.

Another possibility which has been considered in the past is that the fluorescence belongs to a uranyl group. The fluorescence exhibits the right colour, but does not show the characteristic unresolved bands at room temperature or the repetition frequency of about 860 cm.$^{-1}$.

A consideration of the principle of localized charge compensation[3] has suggested another solution to this problem. Supposing a uranium ion in the hexavalent state replaces a sodium ion, then there will be an excess of five units of charge. This can be compensated either by positive ion vacancies or by divalent negative ions. As the samples are melted in air, and since the uranium is often present as a uranyl group, it is

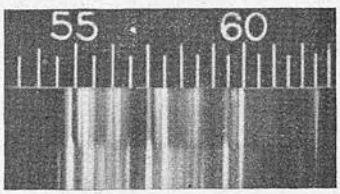

Fig. 1. Fluorescence at 77° K. with 3650 A. excitation. (*a*) sodium fluoride (0·1 per cent uranium); (*b*) sodium fluoride (0·1 per cent uranium, 0·1 per cent calcium chloride). The spectra were obtained on an Astra III plate using a medium quartz spectrograph

quite probable that charge compensation can occur by the entry of oxygen ions, five being necessary to give perfect compensation. The relative simplicity of the emission spectrum indicates a highly symmetrical arrangement, and in view of the known stability of octahedral UO_6 groups in alkaline-earth oxide[3] and uranate[4] phosphors, it is concluded that the six fluorines surrounding the uranium ion are replaced by oxygens. This hypothesis explains both the colour of the emission, which is characteristic of U—O bonding, and the repetition frequency of about 740 cm.$^{-1}$ characteristic of the UO_6 group[3].

The centre has now a net charge of minus one and can attract ions with an excess positive charge. In particular, a divalent ion in the nearest positive ion site will cause complete charge neutrality. This is especially significant, as it has been shown[5] that small quantities of divalent ions, for example, calcium or magnesium, can cause an anomalous enhancement of the fluorescence of uranium in alkali-metal carbonate fluxes containing sodium fluoride.

In the present investigation it has been found that there is a marked change in the line intensities of the spectra, when calcium, in this case as chloride, is added to sodium fluoride (uranium) (see Fig. 1). This occurs when the atomic percentage of both the uranium and calcium is less than 0·1; and it is difficult to see how the relative intensities of the principal lines can change, as shown, unless pairing of the uranium and calcium ions occurs.

This conclusion is in disagreement with that of previous authors[6], who based their argument on the observation that the percentage quenching of an impurity is independent of the concentration of uranium. This independence has not been fully verified by other workers[7], although the variation with uranium concentration is not great.

It is hoped to extend these preliminary observations and to publish a fuller account at a later date.

W. A. Runciman

Atomic Energy Research Establishment,
Harwell, Didcot, Berks.
March 3.

[1] Price, G. R., Ferretti, B. J., and Schwarz, S., *Anal. Chem.*, 25, 322 (1953).

[2] Slattery, M. K., *J. Opt. Soc. Amer.*, 19, 175 (1929).

[3] Runciman, W. A., Cambridge Conference on Luminescence, *Brit. J. App. Phys.*, Supp. No. 4, *S*78 (1955).

[4] Steward, E. G., and Runciman, W. A., *Nature*, 172, 75 (1953).

[5] Jacobs, S., *CRL/A.E.*, 54 (1950).

[6] Price, G. R., Ferretti, B. J., and Schwarz, S., *A.E.C.D.*, 2282 (1945).

[7] Walton, G. N., Hutton, G., and Dalziel, J. A. W., *A.E.R.E. C/R* 966 (1952).

Printed in Great Britain by Fisher, Knight & Co., Ltd., St. Albans.

Reprinted from the *Proceedings of the Cambridge Philosophical Society*,
Volume 51, Part 3, pp. 486–503, 1955.
PRINTED IN GREAT BRITAIN

ATOMIC WAVE FUNCTIONS FOR GOLD AND THALLIUM

BY A. S. DOUGLAS, D. R. HARTREE AND W. A. RUNCIMAN

Received 1 September 1954

1. *Introduction.* Before the war, self-consistent field calculations for the Au^+ ion had been carried out by W. Hartree but were left still unpublished at his death (see prefatory note in (5)). These results have been used by Brenner and Brown (1) in a relativistic calculation of the K-absorption edge for gold, and they were also used in obtaining initial estimates for the partial self-consistent field calculations for thallium of which results are given in §§3–5 of the present paper. In the meantime an independent calculation for Au^+ has been carried out by Henry (6), and his results agree closely with those of W. Hartree. However, it still seems desirable to publish the latter, since they give directly the radial wave function $P(nl; r)$ at exact values of r, whereas Henry used $\log r$ as independent variable, as had been done for similar calculations for Hg (4), and has tabulated $r^{\frac{1}{2}}P(nl; r)$ which is the natural dependent variable to use with $\log r$ as independent variable (2); in some applications it is more convenient to have the radial wave functions themselves.

The calculations for thallium were carried out in order to provide data for a refinement of the work of Williams (10) on the theory of luminescence of solids and its application to the luminescence of KCl activated by Tl. Williams used a Thomas-Fermi approximation to the field of the Tl^{+3} ion for calculating the radial wave functions for the valence electrons in the normal and first excited state of Tl^+, and obtained results in encouraging agreement with observation. Results of self-consistent field calculations for other atoms suggest that the Thomas–Fermi field may be rather inaccurate in the outer regions of an atom, and this may appreciably affect the wave functions for the valence electrons. It seemed worth while examining whether the quantitative agreement of Williams's theory with experiment would be improved by the use of wave functions for the Tl^+ ion derived from a self-consistent field calculation. It is hoped that the results for thallium may also be of value in other contexts.

Both for gold and for thallium the non-relativistic Schrödinger equation has been used. It is realized that relativistic effects are appreciable in atoms as heavy as these, but to include these would increase considerably the amount of calculation required; and in any case, if relativistic calculations were ever contemplated, it would probably be advisable to carry out a non-relativistic calculation first, to provide a good approximation to the field from which to start the relativistic calculation.

2. *Gold* (Au^+). In calculations for mercury (4), $\log r$ was used as independent variable and, correspondingly, $Pr^{-\frac{1}{2}}$ as dependent variable, partly because these variables had been used in earlier work (2) using a differential analyser for which they were convenient, and partly because this choice of independent variable reduces the number of changes of interval length required in the course of the integrations. It has

also been used in some other work (8, 9). However, from the experience of the work for mercury, it was considered that for a hand calculation the advantage of a small number of changes of interval is more than offset by the disadvantage of not obtaining the radial wave functions $P(nl; r)$ directly, and by some minor inconveniences in the numerical work. So in the calculations for gold, a return was made to the use of r as independent variable.

The work was done for the Au^+ ion, with a configuration of complete groups up to and including $(5d)^{10}$. In the calculation of a self-consistent field without exchange, it is most convenient to start from estimates of 'contributions to Z' from the different (nl) groups; for a configuration of complete groups these are (see (3), §5)

$$2(2l+1)\,[1-Z_0(nl, nl; r)] = 2(2l+1)\int_r^\infty P^2(nl; r)\,dr.$$

Initial estimates of these contributions to Z for Au^+ were made by a process of scaling from the corresponding results for mercury, and the process of successive approximation to the self-consistent field was continued until the greatest difference between estimated and calculated contributions to Z from any group was less than 0·02.

The radial wave functions $P(nl; r)$ are given in Table 1 and the contributions to Z in Table 2.

3. *Thallium* (Tl^{+3}). The results required for application in luminescence theory are for the normal and first excited states of Tl^+. It seemed likely that the contributions to Z from all groups up to and including $(5p)^6$ could be estimated closely enough from the corresponding results for gold and mercury, but unlikely that this could be done for $(5d)^{10}$. So calculations for Tl^{+3} were carried out first to obtain a good approximation to the contribution to Z from the $(5d)^{10}$ group, which would be a good first approximation to use in calculation for Tl^+. The results for mercury suggested that the perturbation of the $(5d)^{10}$ group by the electrons of the $(6s)^2$ group of Tl^+ would be small but not negligible.

The estimates of the contributions to Z were made by a modified scaling procedure as follows. Let R be some characteristic length defining the radial scale of the wave function $P(nl; r)$ (for example, the radius of the main maximum of $P(nl; r)$, or the radius for which $Z_0(nl, nl; r) = \frac{1}{2}$). If, for different atoms and given values of nl, the normalized radial wave functions $P(nl; r)$ can be derived from one another simply by a change of scale, then

$$R^{\frac{1}{2}}P(nl; r) \text{ is a function of } r/R \text{ only,} \tag{1}$$

independent of the atomic number N (the $R^{\frac{1}{2}}$ factor here arises from the condition that the functions $P(nl; r)$ are normalized). Let $P(N; nl; r)$ be written for the (nl) radial wave function for an atom of atomic number N, and similarly $Z_0(N; nl, nl; r)$ for the function $Z_0(nl, nl; r)$ for such an atom (for a particular atom or ion, N may be replaced by the chemical symbol for the element with, if necessary, an index indicating the degree of ionization). Then if the relation (1) holds, the wave functions and contributions for Z for two atoms of atomic number N_0 and N are related by

$$P(N; nl; r) = (R_0/R)^{\frac{1}{2}}P(N_0; nl; R_0 r/R) \tag{2}$$

and

$$Z_0(N; nl, nl; r) = Z_0(N_0; nl, nl; R_0 r/R). \tag{3}$$

Further, if $R_{(H)}$ is the value of R for the (nl) wave function of the hydrogen atom, then in the Coulomb field of a point charge N'

$$R = R_{(H)}/N', \tag{4}$$

so that $N' = R_{(H)}/R$ can be considered as the 'effective nuclear charge' for R, and

$$\sigma = N - R_{(H)}/R$$

expresses the effect on the value of R, for the wave function considered, of the screening of the nucleus by the electrons in other occupied wave functions of the atom. It will of course depend on (nl), and will be written σ_{nl} when it is necessary to specify the values of (nl).

For each complete (nl) group this screening number σ_{nl} is likely to vary only slowly with the atomic number N, so that for atoms of neighbouring atomic numbers N_0 and N we have

$$R/R_0 = (N_0 - \sigma)/(N - \sigma),$$

so that (2) and (3) become

$$P(N; nl; r) = \left(\frac{N_0-\sigma}{N-\sigma}\right)^{\frac{1}{2}} P\left(N_0; nl; \frac{N_0-\sigma}{N-\sigma} r\right) \tag{5}$$

and

$$Z_0(N; nl, nl; r) = Z_0\left(N_0; nl, nl; \frac{N_0-\sigma}{N-\sigma} r\right). \tag{6}$$

For neighbouring values of N the scaling ratio $(N_0-\sigma)/(N-\sigma)$ is not sensitive to the value taken for σ.

For Tl^{+3} $(N = 81)$, formula (6) was used both with $N_0 = 79\,(Au^+)$ and with $N_0 = 80\,(Hg^{+2})$, with the following values of σ_{nl}:

(nl)	$1s$	$2s$	$2p$	$3s$	$3p$	$3d$	$4s$	$4p$	$4d$	$4f$	$5s$	$5p$
σ_{nl}	0·3	3·6	4·2	10·3	11·6	16·2	21	25	31	47	40	46

(7)

For the inner groups, up to $(4d)$, there were no systematic differences, to two decimals, between the values of $2(2l+1)\,[1 - Z_0(nl, nl; r)]$ for Tl^{+3} derived in this way from Au^+ and from Hg^{+2}, and the agreement between the values obtained from these two sources provided a valuable check. For the $(4f)^{14}$ to $(5p)^6$ groups there were systematic, though small, differences between the contributions to Z for Tl^{+3} estimated by this scaling procedure from Au^+ and Hg^{+2}; these differences indicate a departure from the similarity on which (6) is based, and enable estimates for Tl^{+3} to be made allowing for these departures from similarity. For the $(5d)^{10}$ group the difference between the results of applying formula (6) with $N_0 = 79$ and with $N_0 = 80$ were considerably larger than for the inner groups, and only rather rough estimates could be made of the contribution to Z from this group.

It is hoped that the estimates for the $(1s)^2$ to $(5p)^6$ groups, which are given in Table 3, are not in error by more than 0·03 for any (nl) group except perhaps for $(4f)^{14}$, and for this group the greatest uncertainty occurs in a range of r (0·3 to 0·6) where the total Z is large, and is not more than $\frac{1}{500}$ of the whole. These estimates were taken as given, and only the $(5d)$ wave function and the contribution of the $(5d)^{10}$ group to Z have been determined by further calculation.

As for Au^+ and Hg^{+2}, the $(5d)$ wave function is rather sensitive to the estimate of the field, and several steps of successive approximation were required in order to make

it self-consistent. The greater part of the numerical work of this calculation was carried out on the EDSAC, the automatic digital calculating machine at the University Mathematical Laboratory, Cambridge. The final $(5d)$ wave function is given in Table 4, and contribution to Z from the $(5d)^{10}$ group is included in Table 3.

If further work on this ion is contemplated, attention should first be given to the $(4f)$ and $(5p)$ groups, for which the estimated contributions to Z in Table 3 are least certain (though the uncertainties are probably no greater than the exchange and relativistic effects which have been neglected).

Approximate wave functions $P(1s)$ to $P(5p)$ for Tl^+ were obtained by the scaling procedure expressed by formula (6), using the values (7) for the screening numbers σ_{nl}, and have been used to calculate the radial charge distribution (see §5); the normalized wave functions are tabulated in Table 5, as they may be useful in other applications also.

4. *Thallium* (Tl^+). For application to the theory of luminescence, wave functions are required for the $(6s)^2$ and $(6s)(6p)$ states of Tl^+. The EDSAC was used to obtain these, using the contributions to Z from the $(1s)^2$ to $(5d)^{10}$ groups for Tl^{+3} given in Table 3. From the results for Hg and Hg^{+2}, it is to be expected that for Tl^+ the $(5d)^{10}$ group will be slightly but appreciably perturbed by the addition of the valence electrons to the Tl^{+3} ion, but that the other groups of the Tl^{+3} core will not be appreciably affected. A further calculation was carried out to make the $(5d)^{10}$ and $(6s)^2$ groups of the normal state of Tl^+ self-consistent in the field of the $(1s)^2$ to $(5p)^6$ groups regarded as given; the contribution to Z from the $(5d)^{10}$ group obtained in this way was also used in a calculation for the $(6s)(6p)$ state. Radial wave functions are given in Table 4 and contributions to Z in Table 3. It will be seen that the perturbation of the $(5d)^{10}$ group by the $(6s)^2$ group is appreciable.

5. *Thallium. Charge distribution.* If $q(nl)$ is the number of electrons in the (nl) group, the radial charge distribution function $U(r)$ is

$$U(r) = \Sigma_{nl} q(nl)\, P^2(nl; r), \tag{8}$$

the radial wave functions $P(nl; r)$ being normalized. The radial charge distribution function $U(r)$ given by (8) was evaluated for Tl^{+3} and Tl^+ from these estimated wave functions for the inner groups given in Table 5 and from the $(5d)$, $(6d)$ and $(6p)$ wave functions given in Table 4. The results are given in Table 6.

The integral $\int_0^\infty r^2 U(r)\, dr$, which occurs both in the diamagnetic susceptibility and in Kirkwood's (7) approximate theory of the electrical polarizability, has the values (in atomic units):

	$\int_0^\infty r^2 U(r)\, dr$
Tl^{+3}	42·8
$Tl^+(6s)^2$	64·7
$(6s)(6p)$	69·6

The field of the core used in this work should be a considerable improvement on the Thomas–Fermi field, especially in the outer regions of the core which particularly

affect the wave functions of the valence electrons. These wave functions, and hence the radial charge distributions, would be still further improved by the use of the relativistic equations, and by the inclusion of exchange and correlation effects at least among the outer electrons of the core and the wave functions of the valence electrons. Inclusion of exchange between the (6*s*) and the (6*p*) wave functions of the (6*s*) (6*p*) configuration would be interesting, as it would enable separate radial wave functions and charge distributions to be calculated for the ^3P and ^1P states, which are both of interest for the luminescence applications.

REFERENCES

(1) BRENNER, S. and BROWN, G. E. *Proc. roy. Soc.* A, 218 (1953), 422.
(2) HARTREE, D. R. *Phys. Rev.* (2), 46 (1934), 738.
(3) HARTREE, D. R. *Rep. Progr. Phys.* 11 (1948), 113.
(4) HARTREE, D. R. and HARTREE, W. *Proc. roy. Soc.* A, 149 (1935), 210.
(5) HARTREE, D. R. and HARTREE, W. *Proc. roy. Soc.* A, 193 (1948), 299.
(6) HENRY, W. G. *Proc. phys. Soc. Lond.* A, 67 (1954), 789.
(7) KIRKWOOD, J. G. *Phys. Z.* 33 (1932), 57.
(8) MANNING, M. F. and GOLDBERG, L. *Phys. Rev.* (2), 53 (1938), 662.
(9) MANNING, M. F. and MILLMAN, J. *Phys.* (2), 49 (1936), 848.
(10) WILLIAMS, F. E. *J. chem. Phys.* 19 (1951), 457.

UNIVERSITY MATHEMATICAL LABORATORY
CAMBRIDGE

CAVENDISH LABORATORY
CAMBRIDGE

G.E.C. RESEARCH LABORATORIES
WEMBLEY, MIDDLESEX†

† Present address: Atomic Energy Research Establishment, Harwell.

Table 1. Au^+. *Radial wave functions (unnormalized)*

(nl)	$(1s)$	$(2s)$	$(2p)$	$(3s)$	$(3p)$	$(3d)$	$(4f)$
ϵ_{nl}	5405	898	865	209·8	193·6	164·3	7·69
$\int_0^\infty P^2 dr$	0·003296	0·03002	0·03919	0·1353	0·1576	0·1748	0·8287
r			Table of $P(nl; r)/r^{l+1}$				
0·000	80·00	80·00	2000	80·00	2000	10000	12000
0·001	73·92	73·87	1922	73·86	1922	9741	11765
0·002	68·31	68·10	1848	68·07	1848	9489	11536
0·003	63·13	62·69	1777	62·61	1776	9244	11312
0·004	58·34	57·58	1708	57·46	1707	9006	11094
0·005	53·91	52·79	1643	52·62	1641	8775	10881
r			Table of $P(nl; r)$				
0·000	0·000	0·000	0·000	0·000	0·000	0·000	—
0·001	0·074	0·074	0·002	0·074	0·002	0·000	—
0·002	0·137	0·136	0·007	0·136	0·007	0·000	—
0·003	0·189	0·188	0·016	0·188	0·016	0·000	—
0·004	0·233	0·230	0·027	0·230	0·027	0·000	—
0·005	0·270	0·264	0·041	0·263	0·041	0·001	—
0·006	0·299	0·290	0·057	0·288	0·057	0·002	—
0·007	0·322	0·308	0·074	0·306	0·074	0·003	—
0·008	0·341	0·321	0·094	0·318	0·093	0·004	—
0·009	0·354	0·328	0·114	0·323	0·113	0·006	—
0·010	0·364	0·329	0·135	0·324	0·134	0·008	—
0·015	0·368	0·277	0·251	0·264	0·247	0·023	—
0·020	0·332	0·163	0·368	0·141	0·357	0·048	—
0·025	0·280	0·023	0·475	−0·007	0·451	0·083	—
0·030	0·227	−0·120	0·565	−0·155	0·522	0·126	—
0·04	0·139	−0·369	0·689	−0·394	0·587	0·234	—
0·05	0·080	−0·537	0·741	−0·522	0·552	0·360	—
0·06	0·044	−0·624	0·736	−0·537	0·439	0·492	—
0·07	0·024	−0·647	0·692	−0·460	0·275	0·619	—
0·08	0·013	−0·625	0·627	−0·320	0·083	0·735	—
0·09	0·007	−0·575	0·551	−0·144	−0·115	0·834	—
0·10	0·004	−0·512	0·474	+0·045	−0·307	0·915	—
0·12	0·001	−0·376	0·332	0·404	−0·631	1·017	—
0·14	—	−0·258	0·222	0·679	−0·851	1·050	—
0·16	—	−0·169	0·143	0·850	−0·968	1·026	—
0·18	—	−0·108	0·090	0·926	−1·000	0·963	—
0·20	—	−0·067	0·056	0·929	−0·971	0·878	—
0·22	—	−0·041	0·034	0·881	−0·901	0·780	—
0·24	—	−0·024	0·020	0·802	−0·809	0·681	—
0·26	—	−0·014	0·012	0·708	−0·709	0·584	—
0·28	—	−0·008	0·007	0·611	−0·608	0·495	—
0·30	—	−0·005	0·004	0·517	−0·513	0·414	—
0·32	—	−0·003	0·002	0·431	−0·427	0·344	—
0·34	—	−0·002	0·001	0·354	−0·352	0·283	—
0·36	—	−0·001	0·001	0·288	−0·287	0·231	—
0·38	—	—	—	0·232	−0·232	0·188	—
0·40	—	—	—	0·185	−0·186	0·152	—
0·45	—	—	—	0·103	−0·105	0·088	—
0·50	—	—	—	0·056	−0·058	0·050	—
0·55	—	—	—	0·029	−0·031	0·028	—
0·60	—	—	—	0·015	−0·016	0·015	—
0·65	—	—	—	0·008	−0·009	0·008	—
0·70	—	—	—	0·004	−0·004	0·004	—
0·8	—	—	—	0·001	−0·001	0·001	—

Table 1 (cont.). Au^+. *Radial wave functions (unnormalized)*

(nl)	$(4s)$	$(4p)$	$(4d)$	$(4f)$	$(5s)$	$(5p)$	$(5d)$
ϵ_{nl}	44·24	37·32	24·60	7·69	6·89	4·635	1·171
$\int_0^\infty P^2 dr$	0·5508	0·6561	0·6889	0·8287	2·825	3·925	8·65
r			Table of $P(nl;r)$				
0·000	0·000	0·000	0·000	0·000	0·000	0·000	0·000
0·005	0·263	0·041	0·001	0·000	0·263	0·041	0·001
0·010	0·323	0·134	0·008	0·000	0·322	0·134	0·008
0·015	0·261	0·245	0·023	0·000	0·260	0·245	0·023
0·020	0·136	0·354	0·048	0·001	0·134	0·353	0·048
0·025	−0·014	0·445	0·082	0·003	−0·016	0·444	0·082
0·030	−0·162	0·512	0·125	0·006	−0·165	0·510	0·125
0·04	−0·399	0·564	0·230	0·015	−0·401	0·559	0·230
0·05	−0·516	0·511	0·350	0·030	−0·516	0·504	0·348
0·06	−0·514	0·379	0·470	0·053	−0·510	0·368	0·467
0·07	−0·416	0·197	0·580	0·083	−0·405	0·183	0·575
0·08	−0·254	−0·008	0·672	0·120	−0·239	−0·024	0·663
0·09	−0·060	−0·212	0·740	0·165	−0·041	−0·229	0·727
0·10	0·142	−0·400	0·782	0·215	+0·162	−0·415	0·764
0·12	0·493	−0·681	0·785	0·329	0·509	−0·685	0·754
0·14	0·710	−0·809	0·692	0·456	0·711	−0·795	0·646
0·16	0·774	−0·792	0·526	0·587	0·750	−0·751	0·465
0·18	0·702	−0·658	0·312	0·716	0·647	−0·588	0·237
0·20	0·528	−0·442	0·073	0·838	0·441	−0·345	−0·011
0·22	0·292	−0·182	−0·171	0·948	0·177	−0·063	−0·259
0·24	0·026	+0·095	−0·406	1·045	−0·108	+0·226	−0·490
0·26	−0·242	0·365	−0·621	1·126	−0·383	0·497	−0·694
0·28	−0·495	0·614	−0·810	1·193	−0·627	0·732	−0·863
0·30	−0·719	0·831	−0·970	1·244	−0·826	0·920	−0·993
0·32	−0·907	1·012	−1·100	1·281	−0·972	1·058	−1·085
0·34	−1·057	1·155	−1·200	1·305	−1·063	1·143	−1·138
0·36	−1·169	1·262	−1·272	1·319	−1·102	1·179	−1·157
0·38	−1·247	1·336	−1·321	1·322	−1·092	1·169	−1·144
0·40	−1·293	1·380	−1·348	1·316	−1·040	1·119	−1·102
0·45	−1·300	1·386	−1·340	1·273	−0·764	0·856	−0·901
0·50	−1·204	1·291	−1·259	1·203	−0·358	0·464	−0·603
0·55	−1·055	1·145	−1·139	1·116	+0·096	0·017	−0·253
0·60	−0·891	0·981	−1·002	1·023	0·543	−0·434	+0·114
0·65	−0·731	0·819	−0·863	0·927	0·945	−0·853	0·476
0·70	−0·587	0·670	−0·732	0·834	1·283	−1·220	0·817
0·8	−0·361	0·429	−0·508	0·662	1·746	−1·767	1·400
0·9	−0·212	0·264	−0·340	0·515	1·951	−2·069	1·836
1·0	−0·121	0·157	−0·222	0·396	1·961	−2·174	2·132
1·1	−0·067	0·092	−0·143	0·301	1·847	−2·139	2·310
1·2	−0·037	0·053	−0·091	0·228	1·667	−2·015	2·398
1·3	−0·020	0·030	−0·057	0·172	1·459	−1·842	2·419
1·4	−0·011	0·017	−0·036	0·130	1·250	−1·648	2·392
1·5	−0·006	0·010	−0·022	0·098	1·053	−1·450	2·333
1·6	−0·003	0·006	−0·014	0·074	0·876	−1·262	2·252
1·8	−0·001	0·002	−0·005	0·042	0·589	−0·931	2·055
2·0	—	0·001	−0·002	0·024	0·386	−0·670	1·841
2·2	—	—	−0·001	0·014	0·249	−0·475	1·632
2·4	—	—	—	0·008	0·159	−0·333	1·435
2·6	—	—	—	0·005	0·101	−0·231	1·256
2·8	—	—	—	0·003	0·063	−0·160	1·096

Table 1 (*cont.*). Au^+. *Radial wave functions* (*unnormalized*)

(nl)	$(4s)$	$(4p)$	$(4d)$	$(4f)$	$(5s)$	$(5p)$	$(5d)$
r			Table of $P(nl; r)$				
3·0	—	—	—	0·002	0·039	−0·110	0·951
3·2	—	—	—	0·001	0·025	−0·075	0·824
3·4	—	—	—	—	0·015	−0·051	0·713
3·6	—	—	—	—	0·009	−0·035	0·615
3·8	—	—	—	—	0·006	−0·024	0·529
4·0	—	—	—	—	0·004	−0·016	0·455
4·5	—	—	—	—	0·001	−0·006	0·309
5·0	—	—	—	—	—	−0·002	0·208
5·5	—	—	—	—	—	−0·001	0·138
6·0	—	—	—	—	—	—	0·091
6·5	—	—	—	—	—	—	0·060
7·0	—	—	—	—	—	—	0·039
8	—	—	—	—	—	—	0·016
9	—	—	—	—	—	—	0·007
10	—	—	—	—	—	—	0·003
11	—	—	—	—	—	—	0·001

Table 2. Au^+. *Contributions to Z. Table of* $2(2l+1)[1-Z_0(nl, nl; r)]$

r	$(1s)$	$(2s)$	$(2p)$	$(3s)$	$(3p)$	$(3d)$
0·000	2·00	2·00	6·00	2·00	6·00	10·00
0·002	1·99	2·00	6·00	2·00	6·00	10·00
0·004	1·95	1·99	6·00	2·00	6·00	10·00
0·006	1·86	1·98	6·00	2·00	6·00	10·00
0·008	1·73	1·97	6·00	1·99	6·00	10·00
0·010	1·58	1·96	5·99	1·99	6·00	10·00
0·015	1·16	1·93	5·96	1·98	5·99	10·00
0·020	0·79	1·91	5·89	1·98	5·97	10·00
0·025	0·50	1·90	5·75	1·98	5·94	10·00
0·030	0·30	1·90	5·54	1·98	5·89	9·99
0·04	0·10	1·86	4·93	1·97	5·77	9·98
0·05	0·03	1·71	4·13	1·93	5·65	9·93
0·06	0·01	1·48	3·29	1·89	5·55	9·82
0·07	—	1·21	2·50	1·85	5·51	9·64
0·08	—	0·94	1·83	1·83	5·49	9·38
0·09	—	0·70	1·30	1·82	5·49	9·03
0·10	—	0·50	0·90	1·82	5·47	8·59
0·12	—	0·24	0·40	1·80	5·29	7·50
0·14	—	0·10	0·17	1·71	4·86	6·27
0·16	—	0·04	0·07	1·54	4·22	5·03
0·18	—	0·02	0·03	1·30	3·47	3·89
0·20	—	0·01	0·01	1·04	2·73	2·92
0·22	—	—	—	0·80	2·06	2·13
0·24	—	—	—	0·59	1·50	1·52
0·26	—	—	—	0·42	1·06	1·06
0·28	—	—	—	0·29	0·73	0·73
0·30	—	—	—	0·19	0·49	0·49
0·32	—	—	—	0·13	0·33	0·33
0·34	—	—	—	0·09	0·22	0·22
0·36	—	—	—	0·05	0·14	0·14
0·38	—	—	—	0·03	0·09	0·09
0·40	—	—	—	0·02	0·06	0·06
0·45	—	—	—	—	0·02	0·02

Table 2 (cont.). Au^+. *Contributions to Z.*

r	(4s)	(4p)	(4d)	(4f)	(5s)	(5p)	(5d)
0·00	2·00	6·00	10·00	14·00	2·00	6·00	10·00
0·02	2·00	5·99	10·00	14·00	2·00	6·00	10·00
0·04	1·99	5·95	9·99	14·00	2·00	5·99	10·00
0·06	1·97	5·90	9·96	14·00	2·00	5·99	10·00
0·08	1·96	5·89	9·86	14·00	1·99	5·98	9·99
0·10	1·96	5·88	9·70	13·99	1·99	5·98	9·98
0·12	1·95	5·83	9·52	13·96	1·99	5·97	9·96
0·14	1·92	5·72	9·36	13·91	1·99	5·96	9·95
0·16	1·88	5·60	9·25	13·82	1·98	5·94	9·94
0·18	1·84	5·50	9·20	13·67	1·97	5·92	9·94
0·20	1·81	5·44	9·18	13·47	1·97	5·92	9·94
0·22	1·80	5·42	9·18	13·20	1·96	5·91	9·94
0·24	1·80	5·42	9·16	12·86	1·96	5·91	9·94
0·26	1·80	5·41	9·08	12·46	1·96	5·91	9·93
0·28	1·79	5·37	8·93	12·01	1·96	5·90	9·91
0·30	1·76	5·27	8·70	11·51	1·95	5·88	9·89
0·32	1·71	5·11	8·38	10·97	1·94	5·85	9·87
0·34	1·64	4·90	8·00	10·40	1·93	5·81	9·84
0·36	1·55	4·63	7·55	9·82	1·91	5·76	9·81
0·38	1·44	4·32	7·06	9·23	1·89	5·72	9·78
0·40	1·33	3·98	6·54	8·64	1·88	5·68	9·75
0·45	1·01	3·09	5·22	7·22	1·85	5·61	9·69
0·50	0·73	2·27	3·98	5·92	1·83	5·57	9·66
0·55	0·49	1·58	2·93	4·78	1·83	5·56	9·65
0·60	0·32	1·06	2·10	3·81	1·83	5·56	9·65
0·65	0·20	0·69	1·46	3·01	1·81	5·53	9·64
0·70	0·12	0·44	1·00	2·35	1·76	5·45	9·61
0·8	0·05	0·17	0·45	1·41	1·59	5·09	9·47
0·9	0·02	0·06	0·19	0·83	1·35	4·52	9·16
1·0	0·01	0·02	0·08	0·48	1·08	3·82	8·70
1·1	—	—	0·03	0·27	0·82	3·10	8·12
1·2	—	—	0·01	0·15	0·60	2·44	7·48
1·3	—	—	—	0·09	0·42	1·87	6·80
1·4	—	—	—	0·05	0·29	1·41	6·13
1·5	—	—	—	0·03	0·20	1·04	5·49
1·6	—	—	—	0·02	0·13	0·75	4·88
1·8	—	—	—	—	0·06	0·39	3·80
2·0	—	—	—	—	0·02	0·20	2·92
2·2	—	—	—	—	0·01	0·10	2·23
2·4	—	—	—	—	—	0·04	1·68
2·6	—	—	—	—	—	0·02	1·26
2·8	—	—	—	—	—	0·01	0·94
3·0	—	—	—	—	—	—	0·70
3·2	—	—	—	—	—	—	0·52
3·4	—	—	—	—	—	—	0·38
3·6	—	—	—	—	—	—	0·28
3·8	—	—	—	—	—	—	0·21
4·0	—	—	—	—	—	—	0·15
4·5	—	—	—	—	—	—	0·07
5·0	—	—	—	—	—	—	0·03
5·5	—	—	—	—	—	—	0·01

Table 3. *Contributions to Z for* Tl^{+3} *and* Tl^{+}

r	$1s$	$2s$	$2p$	$3s$	$3p$	$3d$
0·000	2·00	2·00	6·00	2·00	6·00	10·00
0·001	2·00	2·00	6·00	2·00	6·00	10·00
0·002	1·99	2·00	6·00	2·00	6·00	10·00
0·003	$1·97_5$	$1·99_5$	6·00	2·00	6·00	10·00
0·004	$1·94_5$	$1·99_5$	6·00	2·00	6·00	10·00
0·005	1·90	1·99	6·00	$1·99_5$	6·00	10·00
0·006	1·85	$1·98_5$	6·00	$1·99_5$	6·00	10·00
0·007	1·79	1·98	6·00	$1·99_5$	6·00	10·00
0·008	1·72	1·97	$5·99_5$	$1·99_5$	6·00	10·00
0·009	1·64	1·96	$5·99_5$	$1·99_5$	6·00	10·00
0·010	1·56	$1·95_5$	5·99	1·99	6·00	10·00
0·015	1·13	$1·92_5$	5·96	$1·98_5$	5·99	10·00
0·020	$0·75_5$	1·91	$5·87_5$	1·98	5·97	10·00
0·025	0·47	$1·90_5$	$5·72_5$	1·98	$5·93_5$	10·00
0·030	0·28	1·90	5·50	1·98	$5·88_5$	$9·99_5$
0·035	0·16	1·88	5·20	$1·97_5$	$5·82_5$	$9·98_5$
0·040	$0·09_5$	$1·84_5$	$4·84_5$	$1·96_5$	5·76	9·97
0·05	$0·02_5$	$1·68_5$	$4·01_5$	$1·92_5$	5·63	9·91
0·06	0·01	1·44	3·15	$1·88_5$	5·54	9·79
0·07	—	$1·15_5$	$2·36_5$	1·85	5·50	$9·58_5$
0·08	—	$0·88_5$	1·70	$1·82_5$	5·49	$9·29_5$
0·09	—	$0·64_5$	1·19	1·82	$5·48_5$	8·91
0·10	—	$0·45_5$	0·81	1·82	$5·45_5$	8·44
0·11	—	$0·30_5$	0·54	$1·81_5$	$5·37_5$	$7·88_5$
0·12	—	$0·19_5$	$0·35_5$	$1·79_5$	$5·23_5$	$7·27_5$
0·14	—	0·09	0·14	$1·68_5$	$4·73_5$	5·99
0·16	—	$0·03_5$	$0·05_5$	$1·48_5$	$4·04_5$	$4·72_5$
0·18	—	$0·01_5$	0·02	1·23	3·27	3·60
0·20	—	$0·00_5$	0·01	0·97	2·52	2·65
0·22	—	—	—	0·73	$1·86_5$	1·90
0·24	—	—	—	$0·52_5$	1·33	$1·32_5$
0·26	—	—	—	$0·36_5$	0·92	$0·91_5$
0·28	—	—	—	0·25	0·62	$0·61_5$
0·30	—	—	—	0·16	$0·41_5$	0·41
0·32	—	—	—	$0·10_5$	$0·27_5$	0·27
0·34	—	—	—	0·07	$0·17_5$	$0·17_5$
0·36	—	—	—	0·04	0·11	0·11
0·38	—	—	—	$0·02_5$	$0·07_5$	$0·07_5$
0·40	—	—	—	$0·01_5$	$0·04_5$	$0·04_5$
0·45	—	—	—	—	0·01	$0·01_5$
0·50	—	—	—	—	—	$0·00_5$

Table 3 (cont.). *Contributions to Z for* Tl^{+3} *and* Tl^{+}

r	$4s$	$4p$	$4d$	$4f$	$5s$	$5p$
0·00	2·00	6·00	10·00	14·00	2·00	6·00
0·02	$1·99_5$	$5·99_5$	10·00	14·00	2·00	6·00
0·04	1·99	$5·94_5$	9·99	14·00	2·00	5·99
0·06	$1·97_5$	5·90	9·95	14·00	$1·99_5$	$5·98_5$
0·08	1·96	$5·89_5$	9·84	$13·99_5$	$1·99_5$	$5·98_5$
0·10	1·96	$5·87_5$	$9·66_5$	13·98	1·99	5·98
0·12	1·95	$5·80_5$	9·48	13·95	1·99	$5·96_5$
0·14	$1·91_5$	5·69	9·32	13·88	1·98	$5·94_5$
0·16	1·87	5·57	$9·22_5$	13·76	$1·97_5$	$5·92_5$
0·18	1·83	5·48	$9·18_5$	13·59	$1·96_5$	$5·91_5$
0·20	$1·80_5$	$5·43_5$	9·18	13·33	$1·96_5$	5·91
0·22	1·80	5·42	9·17	13·00	$1·96_5$	5·91
0·24	1·80	5·42	9·12	12·60	$1·96_5$	5·91
0·26	$1·79_5$	$5·39_5$	$9·00_5$	12·13	1·96	5·90
0·28	$1·77_5$	$5·32_5$	8·80	11·61	$1·95_5$	$5·87_5$
0·30	$1·73_5$	$5·19_5$	8·51	11·04	$1·94_5$	$5·84_5$
0·32	$1·67_5$	5·00	8·14	10·43	1·93	5·81
0·34	$1·59_5$	4·74	7·69	9·79	$1·91_5$	$5·76_5$
0·36	$1·49_5$	$4·43_5$	$7·19_5$	$9·16_5$	1·89	5·72
0·38	1·37	4·09	$6·66_5$	8·53	$1·87_5$	$5·67_5$
0·40	1·24	$3·72_5$	6·11	7·91	1·86	$5·63_5$
0·45	0·92	$2·81_5$	$4·74_5$	6·43	$1·83_5$	5·57
0·50	0·64	2·00	$3·52_5$	5·14	1·83	5·54
0·55	0·42	1·35	$2·52_5$	4·02	1·83	5·54
0·60	$0·26_5$	$0·88_5$	$1·75_5$	3·11	$1·81_5$	5·52
0·65	$0·16_5$	$0·56_5$	$1·19_5$	2·40	1·78	5·45
0·70	$0·09_5$	$0·34_5$	$0·79_5$	1·82	$1·71_5$	5·32
0·75	$0·05_5$	$0·20_5$	0·52	1·37	1·62	5·11
0·80	$0·03_5$	$0·12_5$	$0·33_5$	1·02	$1·50_5$	4·84
0·9	0·01	0·04	$0·13_5$	0·56	1·23	4·15
1·0	$0·00_5$	$0·01_5$	$0·05_5$	0·31	$0·93_5$	3·38
1·1	—	$0·00_5$	0·02	0·16	$0·68_5$	2·65
1·2	—	—	0·01	0·08	0·48	1·99
1·3	—	—	$0·00_5$	0·04	0·33	1·47
1·4	—	—	—	0·02	0·22	1·05
1·5	—	—	—	0·01	$0·14_5$	0·75
1·6	—	—	—	$0·00_5$	$0·09_5$	0·53
1·8	—	—	—	—	$0·03_5$	$0·26_5$
2·0	—	—	—	—	$0·01_5$	0·12
2·2	—	—	—	—	$0·00_5$	$0·05_5$
2·4	—	—	—	—	—	$0·02_5$
2·6	—	—	—	—	—	0·01
2·8	—	—	—	—	—	$0·00_5$

Table 3 (cont.). *Contributions to Z for* Tl^{+3} *and* Tl^{+}

			Tl^{+}	Tl^{+} (excited state)	
	Tl^{+3}	Tl^{+}	(ground state)		
r	$5d$	$5d$	$6s$	$6s$	$6p$
0·00	10·00	10·00	2·00	1·00	1·00
0·02	10·00	10·00	2·00	1·00	1·00
0·04	10·00	10·00	2·00	1·00	1·00
0·06	10·00	10·00	2·00	1·00	1·00
0·08	$9·98_5$	$9·98_5$	2·00	1·00	1·00
0·10	9·97	9·97	2·00	1·00	1·00
0·12	9·95	9·95	2·00	1·00	1·00
0·14	$9·93_5$	$9·93_5$	2·00	1·00	1·00
0·16	$9·92_5$	$9·92_5$	2·00	1·00	1·00
0·18	$9·92_5$	$9·92_5$	2·00	1·00	1·00
0·20	$9·92_5$	$9·92_5$	2·00	1·00	1·00
0·22	9·92	9·92	2·00	1·00	1·00
0·24	$9·91_5$	$9·91_5$	2·00	1·00	1·00
0·26	9·90	9·90	2·00	1·00	1·00
0·28	$9·87_5$	$9·87_5$	2·00	1·00	1·00
0·30	$9·84_5$	$9·84_5$	2·00	1·00	1·00
0·32	$9·80_5$	$9·80_5$	$1·99_5$	1·00	1·00
0·34	$9·76_5$	$9·76_5$	$1·99_5$	1·00	1·00
0·36	9·72	$9·72_5$	$1·99_5$	1·00	1·00
0·38	9·68	$9·68_5$	$1·99_5$	1·00	1·00
0·40	9·64	$9·64_5$	$1·99_5$	$0·99_5$	1·00
0·45	$9·57_5$	9·58	1·99	$0·99_5$	$0·99_5$
0·50	9·54	9·55	1·99	$0·99_5$	$0·99_5$
0·55	$9·53_5$	9·54	1·99	$0·99_5$	$0·99_5$
0·60	9·53	9·54	1·99	$0·99_5$	$0·99_5$
0·65	9·51	$9·51_5$	$1·98_5$	$0·99_5$	$0·99_5$
0·70	$9·44_5$	$9·45_5$	1·98	0·99	$0·99_5$
0·75	9·33	9·34	$1·97_5$	$0·98_5$	$0·99_5$
0·80	$9·15_5$	9·17	$1·96_5$	0·98	0·99
0·9	$8·63_5$	$8·66_5$	1·95	$0·97_5$	$0·98_5$
1·0	7·93	$7·97_5$	1·94	$0·96_5$	0·98
1·1	7·12	$7·18_5$	1·93	$0·96_5$	$0·97_5$
1·2	$6·26_5$	6·35	1·93	0·96	$0·97_5$
1·3	5·43	5·53	1·93	0·96	0·97
1·4	4·64	$4·75_5$	1·93	0·96	0·97
1·5	$3·92_5$	$4·04_5$	1·92	$0·95_5$	0·97
1·6	$3·28_5$	$3·41_5$	1·90	$0·94_5$	0·97
1·8	$2·25_5$	2·39	$1·83_5$	0·91	0·96
2·0	$1·50_5$	1·64	1·73	$0·85_5$	0·94
2·2	0·99	1·11	1·59	0·78	$0·90_5$
2·4	$0·63_5$	0·74	1·43	$0·69_5$	0·86
2·6	$0·40_5$	$0·49_5$	1·26	0·61	$0·80_5$
2·8	$0·25_5$	$0·32_5$	1·09	0·52	$0·74_5$
3·0	$0·15_5$	$0·21_5$	0·93	0·44	0·68
3·2	$0·09_5$	0·14	0·78	$0·36_5$	$0·61_5$
3·4	0·06	0·09	$0·64_5$	0·30	$0·54_5$
3·6	$0·03_5$	0·06	0·53	0·24	$0·48_5$
3·8	0·02	$0·03_5$	$0·42_5$	$0·19_5$	$0·42_5$
4·0	0·01	$0·02_5$	0·34	$0·15_5$	$0·36_5$
4·5	—	0·01	0·19	0·08	0·25
5·0	—	$0·00_5$	0·10	0·04	0·16
5·5	—	—	0·05	0·02	0·10
6·0	—	—	$0·02_5$	0·01	0·06
6·5	—	—	$0·01_5$	$0·00_5$	$0·03_5$
7·0	—	—	$0·00_5$	—	0·02
7·5	—	—	$0·00_5$	—	0·01
8·0	—	—	—	—	$0·00_5$
8·5	—	—	—	—	$0·00_5$

Table 4. *Normalized radial wave functions $P_N(nl; r)$ for* Tl^{+3} *and* Tl^{+}

	Tl^{+3}	Tl^{+}	Tl^{+} (ground state)	Tl^{+} (excited state)	
r	$5d$	$5d$	$6s$	$6s$	$6p$
0·000	0·000	0·000	0·000	0·000	0·000
0·001	0·000	0·000	0·013	0·014	0·001
0·002	0·000	0·000	0·024	0·025	0·002
0·003	0·000	0·000	0·034	0·035	0·003
0·004	0·000	0·000	0·041	0·043	0·004
0·005	0·001	0·000	0·047	0·048	0·006
0·006	0·001	0·001	0·051	0·053	0·008
0·007	0·001	0·001	0·054	0·056	0·010
0·008	0·002	0·002	0·056	0·057	0·013
0·009	0·003	0·002	0·057	0·058	0·016
0·010	0·003	0·003	0·056	0·058	0·018
0·015	0·010	0·010	0·046	0·047	0·032
0·020	0·021	0·020	0·022	0·022	0·047
0·025	0·036	0·035	−0·005	−0·005	0·059
0·030	0·054	0·053	−0·032	−0·033	0·067
0·035	0·075	0·074	−0·054	−0·056	0·071
0·040	0·098	0·097	−0·072	−0·074	0·072
0·05	0·148	0·146	−0·090	−0·093	0·063
0·06	0·197	0·194	−0·087	−0·090	0·044
0·07	0·240	0·237	−0·066	−0·068	0·018
0·08	0·275	0·271	−0·034	−0·036	−0·010
0·09	0·298	0·295	0·001	0·001	−0·037
0·10	0·310	0·306	0·037	0·038	−0·060
0·11	0·309	0·306	0·069	0·071	−0·079
0·12	0·298	0·294	0·095	0·098	−0·093
0·14	0·245	0·242	0·126	0·130	−0·102
0·16	0·163	0·161	0·126	0·130	−0·092
0·18	0·064	0·064	0·102	0·106	−0·066
0·20	−0·041	−0·040	0·062	0·064	−0·032
0·22	−0·142	−0·140	0·013	0·014	0·007
0·24	−0·235	−0·231	−0·038	−0·040	0·045
0·26	−0·313	−0·309	−0·086	−0·088	0·079
0·28	−0·375	−0·371	−0·126	−0·130	0·107
0·30	−0·421	−0·416	−0·156	−0·161	0·129
0·32	−0·449	−0·444	−0·176	−0·182	0·143
0·34	−0·461	−0·456	−0·185	−0·190	0·149
0·36	−0·459	−0·454	−0·185	−0·191	0·149
0·38	−0·444	−0·439	−0·177	−0·182	0·142
0·40	−0·417	−0·413	−0·162	−0·166	0·131
0·45	−0·314	−0·311	−0·098	−0·101	0·085
0·50	−0·175	−0·174	−0·016	−0·017	0·026
0·55	−0·020	−0·021	0·068	0·070	−0·037
0·60	0·136	0·133	0·145	0·150	−0·096
0·65	0·285	0·280	0·208	0·215	−0·148
0·70	0·420	0·414	0·254	0·262	−0·188
0·75	0·538	0·531	0·282	0·290	−0·217
0·80	0·640	0·631	0·293	0·302	−0·236
0·9	0·790	0·780	0·274	0·282	−0·243
1·0	0·878	0·868	0·212	0·218	−0·218
1·1	0·918	0·908	0·126	0·129	−0·172
1·2	0·923	0·914	0·029	0·028	−0·112
1·3	0·904	0·896	−0·071	−0·075	−0·047
1·4	0·869	0·862	−0·167	−0·174	0·022
1·5	0·823	0·818	−0·256	−0·266	0·089
1·6	0·772	0·768	−0·335	−0·348	0·154

Table 4 (cont.). *Normalized radial wave functions* $P_N(nl;r)$ *for* Tl^{+3} *and* Tl^+

	Tl^{+3}	Tl^+	Tl^+ (ground state)	Tl^+ (excited state)	
r	$5d$	$5d$	$6s$	$6s$	$6p$
1·8	0·663	0·663	−0·465	−0·482	0·274
2·0	0·558	0·561	−0·558	−0·575	0·371
2·2	0·461	0·469	−0·616	−0·631	0·446
2·4	0·377	0·388	−0·646	−0·660	0·501
2·6	0·305	0·319	−0·655	−0·664	0·539
2·8	0·245	0·261	−0·646	−0·652	0·563
3·0	0·195	0·213	−0·626	−0·628	0·575
3·2	0·154	0·173	−0·596	−0·594	0·577
3·4	0·121	0·140	−0·561	−0·555	0·570
3·6	0·095	0·113	−0·522	−0·512	0·557
3·8	0·074	0·091	−0·480	−0·469	0·539
4·0	0·057	0·073	−0·439	−0·425	0·517
4·5	0·030	0·042	−0·340	−0·325	0·452
5·0	0·015	0·024	−0·255	−0·240	0·381
5·5	0·008	0·014	−0·186	−0·173	0·313
6·0	0·004	0·008	−0·134	−0·122	0·251
6·5	0·002	0·004	−0·095	−0·086	0·198
7·0	0·001	0·002	−0·066	−0·060	0·154
7·5	—	0·001	−0·046	−0·041	0·118
8·0	—	0·001	−0·032	−0·028	0·089
8·5	—	—	−0·022	−0·019	0·067
9·0	—	—	−0·015	−0·012	0·050
9·5	—	—	−0·010	−0·008	0·037
10·0	—	—	−0·006	−0·005	0·027
11·0	—	—	−0·003	−0·002	0·014
12·0	—	—	−0·001	−0·001	0·007
13·0	—	—	−0·001	—	0·004
14·0	—	—	—	—	0·002
15·0	—	—	—	—	0·001
16·0	—	—	—	—	0·001
ϵ	3·181	1·799	1·054	1·100	0·749

Table 5. *Normalized radial wave functions* $P_N(nl; r)$ *for* Tl^{+3} *and* Tl^{+}

r	$1s$	$2s$	$2p$	$3s$	$3p$	$3d$
0·000	0·000	0·000	0·000	0·000	0·000	0·000
0·001	1·341	0·444	0·010	0·210	0·005	0·000
0·002	2·470	0·813	0·036	0·383	0·020	0·000
0·003	3·388	1·118	0·087	0·530	0·043	0·000
0·004	4·182	1·370	0·143	0·645	0·074	0·001
0·005	4·835	1·569	0·220	0·736	0·110	0·002
0·006	5·347	1·715	0·307	0·803	0·153	0·005
0·007	5·735	1·820	0·399	0·852	0·199	0·007
0·008	6·070	1·885	0·502	0·883	0·250	0·010
0·009	6·282	1·919	0·609	0·894	0·304	0·015
0·010	6·459	1·919	0·722	0·891	0·359	0·022
0·015	6·459	1·580	1·331	0·703	0·656	0·061
0·020	5·771	0·872	1·925	0·345	0·942	0·126
0·025	4·817	0·035	2·498	−0·080	1·181	0·219
0·030	3·882	−0·831	2·958	−0·494	1·358	0·328
0·035	3·052	−1·606	3·317	−0·852	1·470	0·459
0·040	2·329	−2·288	3·574	−1·144	1·501	0·605
0·05	1·306	−3·236	3·804	−1·461	1·376	0·926
0·06	0·706	−3·699	3·743	−1·458	1·054	1·256
0·07	0·370	−3·781	3·487	−1·201	0·602	1·564
0·08	0·212	−3·605	3·134	−0·775	0·092	1·851
0·09	0·106	−3·283	2·723	−0·262	−0·428	2·087
0·10	0·071	−2·892	2·324	0·276	−0·919	2·274
0·11	0·040	−2·482	1·939	0·791	−1·355	2·409
0·12	0·018	−2·078	1·597	1·265	−1·730	2·497
0·14	—	−1·399	1·049	1·990	−2·254	2·548
0·16	—	−0·902	0·665	2·412	−2·509	2·461
0·18	—	−0·562	0·415	2·572	−2·544	2·286
0·20	—	−0·345	0·251	2·534	−2·432	2·060
0·22	—	−0·205	0·148	2·365	−2·228	1·810
0·24	—	−0·117	0·087	2·123	−1·975	1·562
0·26	—	−0·071	0·051	1·850	−1·710	1·326
0·28	—	−0·041	0·031	1·577	−1·450	1·113
0·30	—	−0·024	0·015	1·320	−1·210	0·923
0·32	—	−0·015	0·010	1·086	−0·996	0·758
0·34	—	−0·009	0·005	0·883	−0·812	0·617
0·36	—	−0·006	0·003	0·712	−0·653	0·498
0·38	—	—	—	0·565	−0·523	0·401
0·40	—	—	—	0·447	−0·416	0·323
0·45	—	—	—	0·243	−0·230	0·182
0·50	—	—	—	0·127	−0·123	0·102
0·55	—	—	—	0·061	−0·064	0·056
0·60	—	—	—	0·033	−0·033	0·029
0·65	—	—	—	0·017	−0·018	0·015
0·70	—	—	—	0·008	−0·008	0·007
0·75	—	—	—	0·004	−0·004	0·003
0·80	—	—	—	0·003	−0·003	0·002
0·90	—	—	—	—	—	0·001

Table 5 (cont.). *Normalized radial wave functions* $P_N(nl; r)$ *for* Tl^{+3} *and* Tl^{+}

r	$4s$	$4p$	$4d$	$4f$	$5s$	$5p$
0·000	0·000	0·000	0·000	0·000	0·000	0·000
0·001	0·104	0·003	0·000	0·000	0·047	0·001
0·002	0·192	0·010	0·000	0·000	0·086	0·004
0·003	0·263	0·021	0·000	0·000	0·119	0·009
0·004	0·321	0·036	0·000	0·000	0·145	0·016
0·005	0·367	0·055	0·001	0·000	0·165	0·024
0·006	0·402	0·077	0·002	0·000	0·180	0·033
0·007	0·425	0·099	0·004	0·000	0·190	0·043
0·008	0·437	0·124	0·006	0·000	0·195	0·054
0·009	0·443	0·151	0·008	0·000	0·197	0·064
0·010	0·440	0·179	0·011	0·000	0·195	0·076
0·015	0·341	0·326	0·031	0·001	0·149	0·138
0·020	0·164	0·463	0·065	0·002	0·064	0·196
0·025	−0·055	0·577	0·111	0·005	−0·034	0·243
0·030	−0·262	0·652	0·168	0·008	−0·126	0·274
0·035	−0·438	0·697	0·234	0·013	−0·204	0·289
0·040	−0·578	0·707	0·306	0·020	−0·265	0·289
0·05	−0·718	0·619	0·461	0·041	−0·320	0·244
0·06	−0·687	0·430	0·614	0·071	−0·296	0·159
0·07	−0·522	0·182	0·749	0·111	−0·214	0·050
0·08	−0·277	−0·087	0·858	0·161	−0·098	−0·064
0·09	0·004	−0·350	0·933	0·217	0·032	−0·174
0·10	0·285	−0·581	0·973	0·282	0·159	−0·266
0·11	0·539	−0·768	0·976	0·352	0·269	−0·337
0·12	0·754	−0·908	0·947	0·426	0·358	−0·386
0·14	1·009	−1·028	0·799	0·581	0·453	−0·412
0·16	1·050	−0·958	0·564	0·738	0·441	−0·356
0·18	0·903	−0·744	0·275	0·890	0·343	−0·241
0·20	0·619	−0·440	−0·036	1·028	0·189	−0·092
0·22	0·265	−0·088	−0·346	1·152	0·010	0·007
0·24	−0·118	0·273	−0·636	1·254	−0·170	0·221
0·26	−0·491	0·614	−0·894	1·337	−0·336	0·356
0·28	−0·832	0·918	−1·115	1·403	−0·473	0·465
0·30	−1·125	1·177	−1·296	1·448	−0·574	0·543
0·32	−1·364	1·384	−1·439	1·479	−0·640	0·592
0·34	−1·545	1·541	−1·543	1·494	−0·670	0·612
0·36	−1·673	1·652	−1·612	1·496	−0·667	0·605
0·38	−1·754	1·722	−1·653	1·488	−0·634	0·575
0·40	−1·794	1·755	−1·666	1·471	−0·577	0·526
0·45	−1·751	1·712	−1·619	1·401	−0·420	0·339
0·50	−1·586	1·560	−1·492	1·302	−0·080	0·102
0·55	−1·362	1·357	−1·324	1·191	0·213	−0·148
0·60	−1·129	1·142	−1·147	1·077	0·487	−0·386
0·65	−0·910	0·937	−0·973	0·964	0·717	−0·595
0·70	−0·721	0·756	−0·814	0·856	0·902	−0·769
0·75	−0·561	0·600	−0·672	0·755	1·039	−0·905
0·80	−0·429	0·469	−0·548	0·662	1·132	−1·007

Table 5 (cont.). *Normalized radial wave functions* $P_N(nl; r)$ *for* Tl^{+3} *and* Tl^{+}

r	$4s$	$4p$	$4d$	$4f$	$5s$	$5p$
0·9	−0·245	0·280	−0·358	0·504	1·204	−1·115
1·0	−0·136	0·162	−0·227	0·378	1·167	−1·125
1·1	−0·074	0·092	−0·143	0·282	1·067	−1·072
1·2	−0·040	0·052	−0·089	0·209	0·939	−0·983
1·3	−0·021	0·029	−0·055	0·155	0·804	−0·878
1·4	−0·012	0·015	−0·033	0·116	0·674	−0·768
1·5	−0·005	0·009	−0·021	0·085	0·557	−0·663
1·6	−0·003	0·005	−0·012	0·063	0·456	−0·568
1·8	−0·001	0·001	−0·005	0·035	0·296	−0·406
2·0	—	—	−0·002	0·018	0·188	−0·283
2·2	—	—	−0·001	0·011	0·118	−0·195
2·4	—	—	—	0·006	0·073	−0·133
2·6	—	—	—	0·003	0·045	−0·090
2·8	—	—	—	0·002	0·027	−0·061
3·0	—	—	—	0·001	0·016	−0·040
3·2	—	—	—	—	0·010	−0·027
3·4	—	—	—	—	0·006	−0·018
3·6	—	—	—	—	0·004	−0·012
3·8	—	—	—	—	0·002	−0·008
4·0	—	—	—	—	0·001	−0·005
4·5	—	—	—	—	—	−0·002
5·0	—	—	—	—	—	−0·001

Table 6. *Radial charge density $U(r)$ for* Tl^{+3} *and* Tl^{+}

r	$U(r)$ (all states)	r	Tl^{+3}	Tl^{+} (ground state) $(6s)^2$	Tl^{+} (excited state) $(6s)(6p)$
0·000	0·0	0·45	80·19	80·19	80·19
0·001	4·1	0·50	66·20	66·19	66·19
0·002	13·9	0·55	52·40	52·41	52·41
0·003	26·2	0·60	41·31	41·37	41·36
0·004	40·0	0·65	33·37	33·43	33·41
0·005	53·5	0·70	28·29	28·37	28·34
0·006	65·5	0·75	25·26	25·35	25·32
0·007	75·6	0·80	23·58	23·63	23·61
0·008	84·8				
0·009	91·3	0·9	22·02	22·01	22·00
0·010	97·0	1·0	20·74	20·65	20·66
		1·1	18·99	18·83	18·85
0·015	103·7	1·2	16·81	16·64	16·65
0·020	97·7	1·3	14·48	14·35	14·35
0·025	95·2	1·4	12·19	12·13	12·10
0·030	100·2	1·5	10·13	10·18	10·13
0·035	110·8	1·6	8·371	8·531	8·452
0·040	123·1				
		1·8	5·579	6·007	5·882
0·05	141·6	2·0	3·663	4·324	4·170
0·06	145·7	2·2	2·386	3·216	3·054
0·07	138·5	2·4	1·540	2·457	2·309
0·08	129·2	2·6	0·985	1·929	1·803
0·09	122·0	2·8	0·623	1·539	1·446
0·10	120·3	3·0	0·392	1·249	1·190
0·11	122·4	3·2	0·242	1·013	0·989
0·12	127·1	3·4	0·149	0·827	0·831
		3·6	0·091	0·674	0·701
0·14	135·4	3·8	0·055	0·544	0·594
0·16	134·2	4·0	0·0326	0·4387	0·5012
0·18	123·4				
0·20	108·3	4·5	0·0088	0·2488	0·3275
0·22	94·1	5·0	0·0023	0·1359	0·2086
0·24	84·3	5·5	0·0006	0·0712	0·1299
0·26	79·7	6·0	0·0001	0·0365	0·0785
0·28	79·6	6·5	—	0·0183	0·0468
0·30	82·0	7·0	—	0·0087	0·0273
0·32	85·5	7·5	—	0·0042	0·0156
0·34	88·7	8·0	—	0·0020	0·0087
0·36	90·5	8·5	—	0·0010	0·0049
0·38	90·9	9·0	—	0·0005	0·0026
0·40	89·5	9·5	—	0·0002	0·0015
		10·0	—	0·0001	0·0007
		11·0	—	—	0·0002

CENTRES LUMINOGÈNS DANS LES FLUORURES ACTIVÉS A L'URANIUM

Par W. A. RUNCIMAN,
Atomic Energy Research Establishment, Harwell.

Summary. — The idea of localised charge compensation is introduced, and used to obtain probable atomic configurations in uranium-activated fluorides, particular attention being given to uranium-activated sodium fluoride. High- dispersion fluorescence and absorption spectra of various sodium fluoride phosphors are shown and discussed. There are large effects due to other impurities present and also to cooling down from 77 °K to 4,2 °K.

1. Introduction. — Pour faire une étude détaillée d'un centre luminogène, il faut connaître la configuration atomique près de l'ion fluorescent. Lorsque la charge ionique de l'ion fluorescent n'est pas la même que celle des ions du réseau, on a admis [1] que la compensation de la charge s'effectue localement, soit par des lacunes dans le réseau, soit par l'occupation des positions normales par des ions compensateurs. Cette idée d'une compensation localisée de charge a conduit à proposer des configurations probables dans les oxydes, uranates et fluorures phosphorescents. Par exemple selon cette hypothèse l'ion U^{6+} dans un fluorure de calcium activé à l'uranium, $CaF_2(U)$ est entouré de quatre ions oxygène et quatre ions fluor. Dans cette configuration, qui résulte du travail précédent de Krôger [2] sur la compensation de charge, chaque groupe de quatre ions constitue un tétraèdre régulier. Pourtant il n'est pas toujours possible de trouver une telle disposition symétrique pour le centre.

A cause de l'importance de la méthode de fusion du fluorure de sodium pour la microanalyse de l'uranium [3], en quantités qui peuvent ne pas dépasser 10^{-10} gramme, on a examiné les fluorures alcalins activés à l'uranium, et particulièrement le fluorure de sodium, NaF(U). Une étude détaillée de cette substance semblait intéressante, car on sait depuis longtemps [4] que NaF(U) a une brillante fluorescence jaune-verte quand on l'excite aux rayons ultra-violets, et que le spectre se résout bien en raies à la température de l'azote liquide.

2. Configurations atomiques dans les « phosphores » NaF(U). — On a suggéré antérieurement que le centre dans NaF(U) est un groupe uranyle $(UO_2)^{2+}$ ou un groupe UF_6 ; cependant aucune de ces deux hypothèses ne semble expliquer d'une manière satisfaisante à la fois la couleur et la répétition des groupes de raies avec une fréquence de 720 cm^{-1} environ. En utilisant le principe de la compensation localisée de charge, on a proposé une nouvelle solution de ce problème [5]. Si un ion hexavalent d'uranium remplace un ion sodium, *il y a un grand écart à la neutralité électrique* qui pourrait être compensé soit par cinq lacunes d'ions positifs, soit par le remplacement de cinq ions fluor par des ions oxygène.

Comme on ne peut former NaF(U) fluorescent si l'oxygène est absent, la compensation par des lacunes d'ions positifs ne paraît pas à envisager dans le centre luminogène. En raison de la simplicité du spectre de fluorescence, il est probable que le voisinage de l'ion uranium a un haut degré de symétrie, et *on suggère que les six ions fluor voisins soient tous remplacés par des ions oxygène.* De semblables groupes octaèdre se rencontrent dans les oxydes [1] et uranates [6] luminescents des alcalino-terreux, et en ces cas la fluorescence a la même couleur et approximativement la même fréquence de répétition. Les centres de ce type se formeront plus facilement dans les fluorures que dans les autres halogénures, car l'ion O^{--} ($r = 1{,}40$ Å) et l'ion F^- ($r = 1{,}36$ Å) ont des rayons presque égaux [7]. Ainsi s'explique le fait que les fluorures donnent les spectres les plus intenses et les mieux résolus parmi les halogénures alcalins et alcalino-terreux [4].

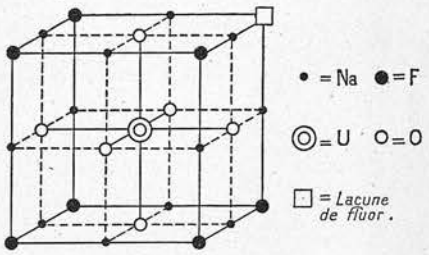

FIG. 1. — Le centre NaF(U).

Le centre postulé a une charge négative — 1, qui peut être compensée soit par une lacune d'ion négatif dans une position (111) (*fig.* 1), soit par un ion divalent dans une position (110) (*fig.* 2). La compensation par des ions trivalents ou tétravalents peut aussi se rencontrer, et l'on peut facilement suggérer des modèles de centres où les ions d'impuretés se trouvent dans les positions voisines des ions positifs.

Avec une concentration élevée en uranium, il semble qu'on rencontrera la paire symétrique de centres $NaF(U_2)$ (*fig.* 3). Dans ce centre, les deux ions uranium sont exactement compensés par dix ions oxygène, qui occupent toutes les positions les plus voisines d'ions négatifs. On ne pourra observer de tels centres dans le spectre de fluorescence s'ils éteignent tout le rayonnement qu'ils absorbent.

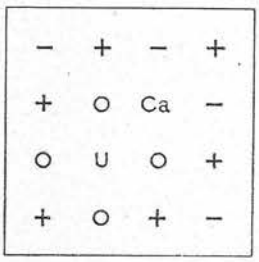

FIG. 2.
Le centre NaF(U, Ca).

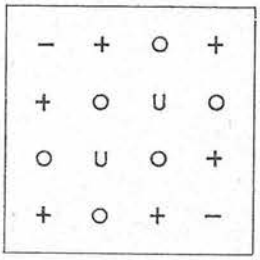

FIG. 3.
Le centre $NaF(U_2)$.

Dans les figures 2 et 3, des ions oxygène se trouvent aussi au-dessus et au-dessous du plan du diagramme, aux positions des ions uranium.

3. **Spectres des phosphores NaF(U) à basse température.** — On a obtenu les spectres de fluorescence et d'absorption avec un spectrographe de Littrow, ayant une dispersion de 8 Å/mm environ à 5 500 Å. Les échantillons étaient scellés dans des tubes de verre ; ceux-ci contenaient de l'hélium à une pression de quelques mm de mercure ; l'hélium servait à égaliser la température du tube et de l'échantillon. Les tubes étaient immergés soit dans de l'azote liquide (77 °K) soit dans de l'hélium liquide (4,2 °K) pendant les observations. Pour le travail avec l'hélium liquide, on a employé un vase Dewar double, dont l'extérieur contenait de l'azote liquide. On utilisait une lampe à vapeur de mercure à haute pression (80 watts), avec une ampoule en verre noir, pour exciter les spectres de fluorescence. Pour les mesures d'absorption, la source était une lampe à ruban (108 watts, 6 volts) ; on a trouvé que les spectres d'absorption pouvaient s'obtenir, soit par réflexion, soit par transmission à travers la poudre ; cette seconde méthode donne les meilleurs résultats, mais il faut exposer les plaques plus longtemps.

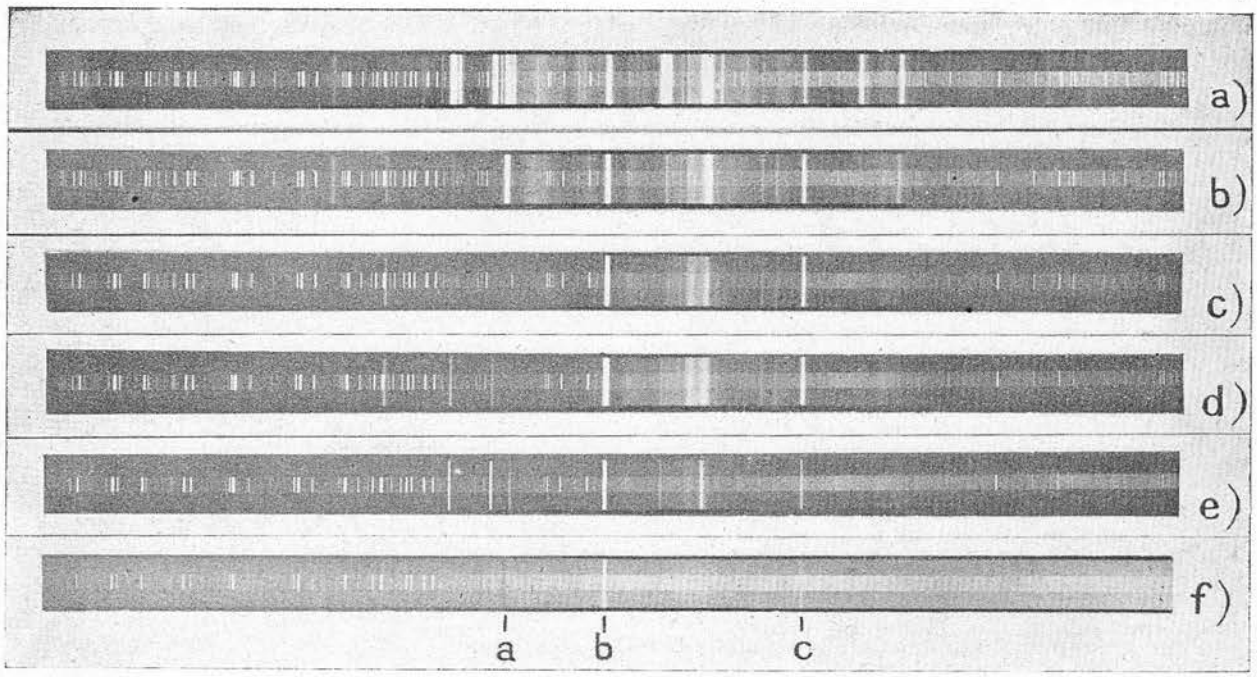

PLANCHE 1. — Spectres de fluorescence et d'absorption à température basse. Les concentrations des ions, activateur et d'impureté, et les temps d'exposition, sont donnés entre parenthèses. Des plaques Ilford Astra III ont été employées ; des spectres de comparaison, donnés par un arc au fer, ont été superposés aux spectres de fluorescence, en utilisant un diaphragme de Hartmann.

a) Émission de NaF(U) impur à 77 °K (0,1 % U ; 60 min).
b) Émission de NaF(U) pur à 77 °K (0,01 % U ; 6 min.)
c) Émission de NaF(U) pur à 4,2 °K (0,01 % U ; 8 min).
d) Émission de NaF(U, Ca) à 4,2 °K (0,01 % U, 0,2 % Ca ; 8 min).
e) Émission de NaF(U, Si) à 4,2 °K (0,01 % U, 0,75 % Si ; 32 min).
f) Absorption de NaF(U) pur à 4,2 °K (0,01 % U ; 30 min).

a = 18 091 cm^{-1} b = 17 748 cm^{-1} c = 17 037 cm^{-1}.

Tous les phosphores ont été préparés en chauffant les mélanges à l'air en creuset de platine pendant une heure à 900° C. Les premiers échantillons ont été faits avec NaF impur, et les spectres de fluorescence obtenus à 77 °K sont assez complexes ; la fréquence de répétition est 720 cm^{-1} environ (pl. 1*a*). Plus tard, on a obtenu du NaF pur, et les spectres de fluorescence observés étaient bien plus simples (pl. 1*b*). A 4,2 °K, le spectre est encore simplifié ; en particulier, une raie intense sur deux disparaît du spectre. Les autres raies intenses forment une série unique dont la fréquence de répétition est 710 cm^{-1} environ, et cette fréquence est probablement celle de la vibration entièrement symétrique du groupe UO_6.

L'explication la plus simple de la disparition de la moitié des raies intenses à 4,2 °K est qu'elles seraient dues à des transitions depuis un niveau vibrationnel excité. Les fréquences des raies principales en cm^{-1} peuvent alors être exprimées par :

$$\nu = 17748 - 709\,\nu_1 + 343\,\nu_2$$

où $\nu_1 = 0,1$ ou 2 et $\nu_2 = 0$ ou 1.

Cette situation contraste avec celle pour CaO(Bi) [8, 9] où le spectre à 77 °K est constitué par une semblable double série de raies, mais qui subsistent toutes à 4,2 °K. Pour CaO(Bi), par conséquent, il faut représenter les raies par une équation où les deux signes sont négatifs, à savoir :

$$\nu = 25717 - 493\,\nu_1 - 195\,\nu_2.$$

Nous avons préparé des phosphores à fluorure de sodium contenant Ca, Si et d'autres éléments, pour trouver l'origine des raies additionnelles dans le spectre du NaF(U) impur. Les planches 1*d*, 1*e* montrent les émissions de NaF(U,Ca) et NaF(U,Si) à 4,2 °K ; on voit que les positions des raies additionnelles qui apparaissent avec l'impureté ne dépendent pas de celle-ci, quoique leur intensité relative dépende de la nature et de la concentration d'impureté. On peut admettre que les raies additionnelles caractérisent le groupe UO_6 non perturbé, mais qu'elles n'apparaissent avec une intensité appréciable que lorsque le centre est déformé par l'ion d'impureté voisin. Dans le cas où la compensation est produite par une lacune dans NaF(U) pur, il se peut que la déformation du groupe UO_6 produite par la lacune soit peu importante puisqu'aucun des ions du groupe UO_6 n'est son voisin immédiat (*fig.* 1).

Les spectres d'absorption de ces phosphores ont été étudiés par les méthodes de réflexion et de transmission. Le spectre d'absorption de NaF(U) pur à 4,2 °K (pl. 1*f*) a été obtenu par transmission. Il y a une forte raie d'absorption à 18 091 cm^{-1}, qui correspond à la première des raies d'émission disparaissant à 4,2 °K. Cependant on ne sait pas encore si la raie à 17 748 cm^{-1} est une raie de résonance. Aucune absorption n'a été remarquée, mais l'absorption pourrait bien être supprimée par l'émission à la même longueur d'onde. On constate que les raies d'absorption se présentent à des énergies plus basses que certaines des raies de fluorescence additionnelles, associées à la présence d'impuretés ; ce fait pourrait impliquer l'existence de plus d'une transition électronique contribuant à l'émission dans cette région du spectre. Comme dans les composés d'uranyle, des groupes nouveaux de raies d'absorption se présentent à des énergies bien plus élevées et sont certainement dus à des états électroniques hautement excités.

4. **Discussion.** — Les spectres pourraient s'interpréter par l'interaction des ions d'activateurs et d'impuretés. L'énergie d'interaction peut être assez petite ; en ce cas, il faut ajouter une assez grande quantité d'impureté. Il est fort improbable que ces résultats puissent s'expliquer par une répartition de hasard des ions activateurs et d'impureté. Cette conclusion est à rapprocher des théories récentes sur la sensibilisation et l'extinction des phosphores.

A températures très basses, on réduit la largeur des bandes d'émission, ou on élimine les ions qui sont dans des états vibrationnels excités avant la transition électronique. Ce deuxième effet se produit nettement dans NaF(U) .On peut voir sur les spectres que la réduction de la largeur des bandes entre 77 °K et 4,2 °K est petite. Cependant, dans d'autres phosphores, on a trouvé une réduction considérable de la largeur des bandes, par exemple, dans les cas où il y a activation par Eu^{++}.

On a trouvé récemment que les impuretés peuvent entraîner l'apparition de raies additionnelles à une longueur d'onde encore plus courte que celle d'aucune des raies de fluorescence figurant dans les spectres ci-joints. Cela explique sans doute le renforcement anormal qu'on a trouvé en utilisant la méthode fluorométrique pour mesurer l'uranium [10], parce que les photomultiplicateurs employés sont plus sensibles aux longueurs d'ondes plus courtes.

Les spectres de NaF(U) montrent une grande diversité, qui pourrait s'expliquer par l'absence d'une compensation complète de la charge du groupe UO_6, tandis que dans le système $CaF_2(U)$, où le groupe symétrique UO_4 produit une compensation complète de la charge, les impuretés semblent produire des effets moins grands sur les spectres. Des investigations préliminaires indiquent que les « phosphores » KF(U) et LiF(U) ont des spectres semblables à ceux de NaF(U) ; pourtant nous effectuons actuellement une investigation approfondie de tous les fluorures activés à l'uranium.

DISCUSSION

1. *Prof. P. Pringsheim.* — Avez-vous une idée de la raison pour laquelle les bandes de fluorescence de NaF(U) subissent une translation vers les grandes longueurs d'onde par rapport aux bandes de fluorescence de la plupart des sels d'uranyle ? Dans le premier cas la couleur est jaune ($\lambda > 5\,300$ Å), dans le second elle est verte ($\lambda = 4\,500$ à $5\,700$ Å). La fluorescence de U dans LiF est également verte, tandis qu'elle est jaune dans le tungstate de magnésium.

Dr W. A. Runciman. — Bien que les traits généraux de la luminescence ne soient pas changés, il y a des déplacements nets de longueur d'onde lorsqu'on passe de NaF(U) à LiF(U) : Ce sont les ions positifs du réseau qui sont les plus proches voisins du groupement UO_6, et la transition électronique responsable de la luminescence est attribuée à une modification de la distribution des électrons de liaison. Contrairement à un travail antérieur, je trouve que le déplacement pour LiF est vers le bleu : en conséquence de ce glissement vers les courtes longueurs d'onde, ce phosphore n'est pas aussi bien excité par la radiation 3 650 Å. Du fait de la coordination différente dans les sels d'uranyle, $MgWO_4$(U) et NaF(U), il n'y a pas de raison pour que les solides activés à l'uranium aient la même couleur que les sels d'uranyle, qui ont eux-mêmes une couleur variable.

2. *Dr E. Grillot* (Paris). — Par application du principe de « compensation de charge », Runciman envisage lapossibilité de formation dans son luminophore de grosses agglomérations constituées par un atome d'uranium et six atomes d'oxygène ou par deux atomes d'uranium et dix atomes d'oxygène. Ces groupements, qui rappellent un peu les centres de Lenard, devraient conduire à des distorsions du réseau, décelables par la diffraction X.

Le principe de « compensation de charge », souvent évoqué au cours de ce Colloque, a été proposé par Kröger et Hellingman à partir de dosages chimiques, par exemple sur ZnS(Cu, Cl) et il a été ensuite étendu par Kröger et Dikhoff au cas des co-activateurs trivalents. La compensation de charge par deux sortes d'ions étrangers doit donc conserver un caractère arithmétique, un peu comme les lois stoechiométriques de la Chimie.

Or, de nombreuses exceptions ont été relevées. Pour l'activation du sulfure de cadmium (poudre ou microcristaux), avec Ag comme avec Cu l'addition d'un coactivateur est inutile. Pour ZnS le traitement par un fondant est généralement nécessaire (mais n'est pas indispensable comme N. Riehl et H. Ortmann nous l'ont montré hier). Mais, à l'aide de microdosages radiochimiques qui seuls donnent la précision nécessaire à ces mesures, M^me^ M. Grillot a montré que le traitement par le fondant pouvait être préalable et qu'ensuite, dans un produit contenant $3{,}8.10^{-5}$ ion-g Cl par mole ZnS, on pouvait faire pénétrer dans le réseau cristallin, à 500° seulement, jusqu'à 21.10^{-5} ion-g Cu par mole ZnS, soit plus de cinq fois plus. Tcherepniev et Dobroloubskaia ont utilisé comme fondant du borax, de l'acide borique, du sulfate de sodium, du phosphate disodique pour lesquels la compensation de charge par deux sortes d'ions étrangers n'apparaît pas clairement. Enfin, Kröger et Dikhoff d'une part ont constaté qu'avec 2 % de ZnO l'activation au cuivre se faisait sans fondant et d'autre part ont préparé des ZnS activés à Cu, Ag ou Au avec des preportions très variables de co-activateur trivalent (allant par exemple jusqu'à 10 fois plus d'Al que d'Ag).

Il apparaît donc que le principe de compensation locale de charge par deux sortes d'ions étrangers au réseau ne présente pas, comme une loi chimique de combinaison stoechiométrique, un caractère aussi général qu'on l'admet souvent. Quant à la compensation locale de charge par des lacunes du réseau, bien moins aisément susceptible de vérification, son mécanisme paraît moins compliqué et elle semble plus vraisemblable. D'autres considérations d'ordre cristallo-chimique, par exemple concernant la disposition des nuages électroniques selon la nature plus ou moins ionique ou covalente des liaisons chimiques de l'activateur, peuvent cependant lui être opposées.

BIBLIOGRAPHIE

[1] Runciman (W. A.), Conférence sur la Luminescence, Cambridge, *British J. App. Physics*, 1955, supp. n° 4, 78.

[2] Krôger (F. A.), *Physica*, 1948, **14**, 488.

[3] Price (T. R.), Ferretti (B. J.) et Schwarz (S.), *Ann. Chem.*, 1953, **25**, 322.

[4] Slattery (M. K.), *J. Opt. Soc. Amer.*, 1929, **19**, 175.

[5] Runciman (W. A.), *Nature*, 1955, **175**, 1082.

[6] Steward (E. G.) et Runciman (W. A.), *Nature*, 1953, **172**, 75.

[7] Pauling (L.), *The Nature of Chemical Bond*, 1945, p. 346.

[8] Ewles (J.) et Lee (N. J.), *J. Electrochem. Soc.*, 1953, **100**, 392. 399, 402.

[9] Runciman (W. A.), *Proc. Phys. Soc.*, 1955, **68** A, 647.

[10] Jacobs (S.), CRL/AE, 1950, 54.

Reprinted without change of pagination from the
Proceedings of the Royal Society, A, *volume* 237, pp. 39–47, 1956

The luminescence of uranium-activated sodium fluoride

By W. A. Runciman
Atomic Energy Research Establishment, Harwell, Berks

(*Communicated by M. H. L. Pryce, F.R.S.—Received* 13 *March* 1956)

[Plate 1]

The fluorescence and absorption spectra of various uranium-activated sodium fluoride phosphors have been studied at liquid-nitrogen and liquid-helium temperatures. These results are interpreted in terms of a model in which the uranium ion is surrounded octahedrally by six oxygen ions. Experiments with ^{18}O have provided support for this atomic configuration, several lines in the fluorescence spectrum having an isotope shift. These isotope shifts are in agreement with the predictions of a general theory of the vibrational fine structure in luminescence spectra.

1. Introduction

Many impurity-activated solids, and some pure solids, are luminescent upon excitation with ultra-violet radiation. A quantum of the incident ultra-violet radiation is absorbed by an activator ion and some time later, 10^{-9} s or longer, a quantum of visible radiation is emitted. A complete theory of luminescence in any particular case should account for all the major absorption and emission bands, including any fine structure in these bands due to vibrational interaction or to Stark splitting of the electronic levels.

Before such a detailed theoretical investigation of a luminescent centre can be undertaken it is necessary to have a knowledge of the atomic configuration in the vicinity of the fluorescent ion. If possible the activator ion will replace an ion with the same charge in the host lattice. In cases where the ionic charge of the activator ion is different from that of any of the lattice ions, it has been suggested (Runciman 1955*a*) that compensation of charge takes place locally either by lattice vacancies or by compensator ions occupying normal lattice sites. This idea of localized charge compensation has led to the proposal of probable configurations in oxide, uranate and fluoride phosphors. For instance, on this hypothesis, the U^{6+} ion in uranium-activated calcium fluoride $CaF_2(U)$ is surrounded by four oxygen and four fluorine ions. In this configuration, which is a development of earlier work on charge compensation (Kröger 1948), each group of four ions forms a perfect tetrahedron, but it is not always possible to find such a symmetric arrangement for a centre. The question of the stability of a postulated centre is not easy to decide, and will depend on the properties such as radii and polarizabilities of the foreign ions introduced into the lattice.

In view of the importance of the sodium fluoride fusion method for the micro-determination of uranium (Price, Ferretti & Schwarz 1953) in amounts which may be as small as 10^{-10} g, it was decided to investigate the uranium-activated alkali fluorides with special reference to uranium-activated sodium fluoride, NaF(U).

This seemed a promising substance for a detailed study, as it has long been known (Slattery 1929) that NaF(U) has a brilliant yellow-green fluorescence when excited with ultra-violet radiation, and that the spectrum is well resolved into many lines at liquid-nitrogen temperature.

2. Atomic configurations in NaF(U) phosphors

Suggestions which have been made previously for the atomic configuration in NaF(U) are that the centre is either a uranyl $(UO_2)^{2+}$ or a UF_6 group, but neither suggestion seems to account satisfactorily for both the colour and the repetition frequency of the line groups of about 720 cm^{-1}. Using the principle of localized charge compensation, another solution has been proposed for this problem (Runciman 1955*b*). If a hexavalent ion replaces a sodium ion there is a large departure

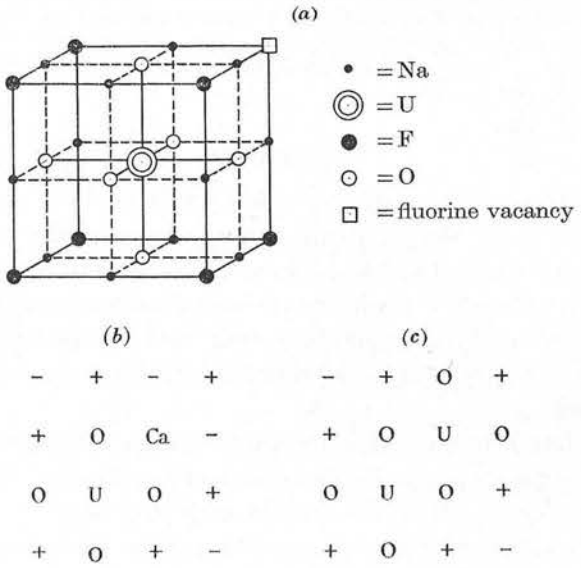

Figure 1. (*a*) The NaF(U) centre. (*b*) The NaF(U,Ca) centre. (*c*) The $NaF(U_2)$ centre. In (*b*) and (*c*) there are also oxygen ions above and below the plane of the diagram at the uranium ion positions.

from electrical neutrality which could be balanced by five positive-ion vacancies or by the replacement of five fluorine ions with oxygen ions. In fact, it is not found possible to form fluorescent NaF(U) in the absence of oxygen, so that complete compensation by positive-ion vacancies does not occur in the luminescent centre. In view of the simplicity of the fluorescence spectrum it is probable that the uranium ion is in surroundings of high symmetry, and it is suggested that all six of the neighbouring fluorine ions are replaced by oxygen ions. Similar octahedral UO_6 groups occur in alkaline earth oxide (Runciman 1955*a*) and uranate (Steward & Runciman 1953) phosphors, and the fluorescence in these cases shows the same colour and approximately the same repetition frequency. It will be easier to form centres of this type in the fluorides than in the other halides, since the O^{2-} ion ($r = 1{\cdot}40$ Å) and the F^- ion ($r = 1{\cdot}36$ Å) have similar radii (Pauling 1945). This

accounts for the fact that the fluorides give the most intense and well-resolved spectra of all the alkali and alkaline-earth halides (Slattery 1929). The postulated centre has a net charge of -1, and this can be compensated either by a negative-ion vacancy at a corner site (figure 1*a*) or by a divalent ion on a nearest positive-ion site (figure 1*b*). Compensation by trivalent and tetravalent ions can also occur, and it is easy to suggest possible centres in which impurity ions are in nearest neighbour positive-ion sites.

At high uranium concentrations it is likely that the symmetrical $NaF(U_2)$ centre (figure 1*c*) will occur. In this centre the two uranium ions are exactly compensated by ten oxygen ions which fill all the nearest negative-ion sites. Centres such as this will not be detected in the fluorescence spectrum if they quench all the absorbed incident radiation.

3. Vibrations in luminescent centres

Some phosphors, e.g. CaO(Bi) and NaF(U), show a considerable amount of fine structure due to vibrational effects. It is therefore important to find out which vibrations can cause frequency shifts in the absorption and emission spectra. It is not yet possible to treat complicated centres in the rigorous manner which has been developed for a few simple cases (Montroll & Potts 1955). However, a model which is adequate for a qualitative discussion is to treat the activator ion and its nearest neighbours as a molecular group, and to consider the normal modes of vibration of this group. This approximation may be expected to apply where the activator ion has an ionic charge greater than that of any of the host lattice ions, e.g. Bi^{3+} in CaO, and it is precisely in these cases that considerable vibrational fine structure is observed.

Table 1. Vibrations of an octahedral group

	UF_6 (cm^{-1})	O_h	C_{4v}
ν_1	668	A_{1g}	A_1
ν_2	532	E_g	A_1+B_1
ν_3	626	F_{1u}	A_1+E
ν_4	189	F_{1u}	A_1+E
ν_5	202	F_{2g}	B_2+E
ν_6	144	F_{2u}	B_1+E

The case of an octahedral MX_6 group will be considered in detail, as it applies to many substances including CaO(Bi) and NaF(U). Comparison with the molecule UF_6 is useful, and it has octahedral symmetry, point group O_h, $m3m$. In table 1, the frequencies of the vibrations of UF_6 are listed (Gaunt 1953), and under the heading O_h, the symmetries of the vibrations are written in the usual notation. The symbols A and B are used for singly degenerate, E for doubly degenerate, and F for triply degenerate vibrations. Vibrations symmetric or anti-symmetric with respect to inversion through the centre of the group have subscripts 'g' and 'u' respectively.

In CaO(Bi) the electronic transition is an allowed transition, $^1S \leftrightarrow {}^3P_1$, and applying group-theoretical considerations similar to those developed for free molecules (Sponer & Teller 1941) it is found that the g or Raman vibrations ν_1, ν_2 and ν_5 can appear in any number of quanta, and the u vibrations with only an even number of

quanta. This confirms the view expressed earlier (Runciman 1955*c*) that the Raman-active modes are the most likely to appear in the fluorescence and absorption spectra.

The fundamental absorption and emission lines do not appear to coincide in the CaO(Bi) spectra, and this may be due to the neighbouring ions being in a different state of polarization during the two transitions. An effect of this type has been noted in organic solutions (Sambursky & Wolfsohn 1942). The configuration co-ordinate model, which has been used in a detailed calculation of the luminescence of thallium-activated potassium chloride (Williams 1951), can be easily extended in principle to include any number of co-ordinates representing atomic positions, but it is not so obvious what the effect will be of introducing co-ordinates for the degrees of polarization of the ions. Another factor which can cause an apparent displacement of the fundamental lines occurs if the electronic transition is forbidden, as in the case of benzene (Sponer, Nordheim, Sklar & Teller 1939), and this situation while not likely for CaO(Bi) might well occur in uranium-activated phosphors.

4. Low-temperature spectra

Fluorescence and absorption spectra have been obtained using a Littrow-type spectrograph having a dispersion of 8 Å/mm at 5500 Å. The samples were sealed in glass tubes containing helium at a pressure of a few millimetres of mercury, the gaseous helium being to aid heat conduction from the sample. The tubes were totally immersed in either liquid nitrogen (77° K) or liquid helium (4·2° K) during observation. For liquid-helium work a double Dewar was used, the outer Dewar containing liquid nitrogen. An 80 W high-pressure mercury-vapour lamp with a black glass bulb was used for exciting the fluorescence spectra. For absorption the source was a 108 W 6 V strip-filament lamp, and it was found that absorption spectra could either be obtained by reflexion or by transmission through the powder, the latter method giving better results but needing longer exposure times.

All the phosphors were made by heating the mixtures in platinum crucibles for 1 h at 900° C in air. The first samples were made with impure sodium fluoride and the fluorescence spectrum at 77° K consists of a fairly complex pattern with a repetition frequency of about 725 cm^{-1} (figure 2*a*, plate 1). Later pure sodium fluoride was obtained and the fluorescence spectrum of a phosphor made with this material is very much simpler (figure 2*b*). At 4·2° K the spectrum shows further simplification, and in particular every alternate strong line disappears from the spectrum in a striking manner (figure 2*c*). The remaining strong lines form a single series with a repetition frequency of 709 cm^{-1}, and this frequency is probably that of the totally symmetric vibration, ν_1 of the UO_6 group.

The simplest explanation of the disappearance of half the strong lines at 4·2° K is that they are due to transitions from an excited vibrational level of the upper electronic state. The wave-numbers of the main lines, in cm^{-1}, may then be expressed by the equation

$$\nu = 17\,748 - 709v_1 + 343v_2,$$

where $v_1 = 0$, 1 or 2, and $v_2 = 0$ or 1.

This is unlike the situation in CaO(Bi) (Ewles & Lee 1953; Runciman 1955*b*), where at 77° K the spectrum consists of a similar double series of lines, which, however, all persist at 4·2° K. For CaO(Bi) therefore, the lines have to be represented by an equation where both signs are negative

$$\nu = 25\,717 - 493v_1 - 195v_2.$$

Sodium fluoride phosphors containing calcium, silicon and other elements were made up to find the cause of the extra 'impurity' lines in the spectrum of the impure sodium fluoride phosphor. The emission spectra of NaF(U,Ca) and NaF(U,Si) at 4·2° K (figure 2*d*, *e*) demonstrate that the extra lines which appear are independent in position of the particular impurity, although the amount of quenching and the relative intensity of the lines are dependent on the nature and amount of the added impurity ions. This can be explained if the extra lines are characteristic of the unperturbed UO_6 group, but only appear with appreciable intensity when the centre is deformed owing to a neighbouring impurity ion. In the case of compensation by a vacancy in pure sodium fluoride (figure 1*a*), the deformation of the UO_6 group may be very slight, as none of the ions of the UO_6 group is immediately adjacent to the vacancy.

The absorption spectra of these phosphors have also been studied by both reflexion and transmission methods. The absorption spectrum of pure NaF(U) at 4·2° K (figure 2*f*) was obtained by transmission. There is a strong absorption line at 18 091 cm^{-1} corresponding to the first of the emission lines which disappears at 4·2° K. It is not yet clear whether the line at 17 748 cm^{-1} is a resonance line. No sign of absorption has been observed there, but this could have been obscured by emission at the same wavelength.

One of the puzzling features of these spectra is that absorption lines occur at lower energies than some of the extra 'impurity' lines, and this may indicate that there is more than one electronic transition contributing to the spectra in this region. This is reasonable, though, if the electronic structure of the UO_6 group is similar to that of the uranyl group (Eisenstein & Pryce 1955), but possesses a greater degree of degeneracy due to the increased number of oxygen ions. As in uranyl compounds (Dieke & Duncan 1949), further groups of absorption lines occur at considerably higher energies, and these are due to higher excited electronic states.

5. Oxygen-isotope results

The idea of a UO_6 group being responsible for the fluorescence in NaF(U) appears reasonable, but it is difficult from the results so far discussed to show that it is the only possible configuration for the centre. Oxygen-isotope experiments were started to decide this issue.

The symmetry of the UO_6 group is reduced by substituting a heavier isotope for one of the oxygen ions to that of point group C_{4v}, $4mm$, and all vibrations become allowed with any number of quanta. The degeneracy of the vibrations is partly removed and the component vibrations are listed in the final column of table 1. All the vibrations, except the totally symmetric mode ν_1, split into two components, and this should prove helpful in assigning the frequencies to the different vibrations.

The magnitude of the isotope shift can be approximately calculated for the symmetric frequency ν_1. If all the ^{16}O ions were replaced by ^{18}O ions, the isotope shift would be about 6 %, since the frequency is inversely proportional to the square root of the mass of the oxygen ions. For a substitution of a single ^{16}O ion by ^{18}O, it can be shown that the shift is one-sixth as great, or 1 %. The perturbation theory necessary for this calculation was originally developed for a tetrahedral molecule, and applies for small mass difference (Wilson 1934). Thus, the calculation predicts a reduction of 7 cm^{-1} in the symmetric vibration if it is right to assign a value of 709 cm^{-1} to that mode. This may be compared with shifts of 30 cm^{-1} found for ^{18}O substitution in uranyl groups (Dieke & Duncan 1949).

The preparation of the enriched samples was made in two stages, the starting material being water containing 9·7 % ^{18}O. First, clean uranium metal turnings were oxidized to U_3O_8 in a stream of oxygen previously obtained by electrolysis from the enriched water. The reaction was started by heating the uranium and was thereafter self-sustaining, control being effected by altering the flow of the oxygen, which was mixed with argon to reduce the rate of reaction.

Secondly, the U_3O_8 was added to the sodium fluoride and a phosphor was prepared by heating the mixture for 1 h at 900° C, in a closed platinum capsule, which had been filled with an atmosphere of enriched oxygen. In this way even though there was exchange between the mixture and the atmosphere the enrichment remained constant at about 9·7 %.

The platinum capsule was made by pressing the ends of a tube in a vice, and running an oxygen/coal-gas flame along the cut end of the tube to melt the edge of the platinum. The original platinum tubing was 7 mm in diameter, with a wall thickness of 0·01 in., the lengths of the capsules being from 3 to 6 in.

At first, the spectra obtained from these samples showed the impurity spectrum, and many of the lines had neighbouring isotope lines (figure 3*a*, plate 1). If the samples were refired in air at 800° C, both the impurity and isotope lines vanished, but if refired at 600° C in air the pure spectrum with isotope lines was obtained (figure 3*a*). For comparison the spectra without isotopic enrichment are also shown (figure 3*b*, *d*).

The main isotope lines are listed with all the other principal lines in the NaF(U) spectrum in table 2. The wavelengths in air were determined using the Hartmann dispersion formula, and the wave numbers are calculated to the nearest cm^{-1}, this being about the limit of accuracy of the stronger lines. For convenience, letters are assigned to the lines to show the repetitive nature of the spectrum, and intensities are roughly indicated. However, the intensities of the impurity lines vary in different specimens in an obscure manner.

The troublesome impurity in the isotope experiments is believed to have been water, it being difficult to keep the sodium fluoride completely dry. With water present total charge compensation can be achieved if one of the oxygens gains a hydrogen ion to form an $(OH)^-$ group. An H^+ ion, i.e. a proton, having negligible size can readily remain interstitially near an oxygen ion. This centre forms an understandable exception to the general rule that impurity ions enter the lattice substitutionally.

The line at 17 037 cm^{-1} has an isotope shift of 6 cm^{-1} and remains single. This is within the limits of experimental error in agreement with theory, assuming that the vibrational frequency ν_1, A_{1g}, is 709 cm^{-1}. The lines in the impurity spectrum with a repetition frequency of 725 cm^{-1} split into two components with shifts of 8 and 17 cm^{-1}, and multiples thereof for lines due to more than one quantum of this vibration. The most probable assignment for this frequency of 725 cm^{-1} is ν_2, E_g. The increase of the isotope shift with the number of vibrational quanta in the way expected gives full confidence that the lines are due to ^{18}O rather than to some other cause.

TABLE 2. FLUORESCENCE LINES IN NaF(U)

designation	strength	λ (Å)	ν (cm^{-1})	comments
N_1	*m*	5356·6	18669	at 77°K only
N_2	*w*	5442·3	18375	at 77°K only
A_1	*s*	5471·8	18276	
D_1	*s*	5478·4	18254	
B_1	*s*	5513·9	18136	
E_1	*m*	5520·6	18114	
K_1	*s*	5527·5	18091	at 77°K only
F_1	*s*	5533·7	18071	
C_1	*s*	5635·4	17748	
A_2''	*w*	5692·2	17568	^{18}O
A_2'	*w*	5695·5	17558	^{18}O
A_2	*s*	5698·0	17550	
D_2	*m*	5705·3	17527	
B_2''	*w*	5740·5	17420	^{18}O
B_2'	*w*	5743·6	17411	^{18}O
B_2	*s*	5746·2	17403	
E_2+K_2	*m*	5753·4	17381	
F_2	*m*	5767·2	17339	
C_2'	*w*	5867·0	17044	^{18}O
C_2	*s*	5869·4	17037	
A_3	*s*	5943·5	16825	
D_3	*w*	5951·7	16802	
B_3''	*w*	5986·1	16705	^{18}O
B_3'	*w*	5992·9	16686	^{18}O
B_3+K_3	*s*	5997·8	16673	
C_3	*w*	6124·5	16328	
A_4	*w*	6209·7	16104	
B_4	*w*	6271·0	15946	

s = strong; *m* = medium; *w* = weak.

6. DISCUSSION

The spectra provide support for the idea that pairing the activator and impurity ions can occur in phosphors. In particular, the existence of a UO_6 group in NaF(U) appears essential for the interpretation of the oxygen isotope experiments. The binding energy of a UO_6 group with the charge-compensating defect, e.g. a divalent ion, may be fairly small, in which case a fair amount of impurity may need to be added, but it is unlikely that these results could be explained on a purely random distribution of the activator and impurity ions. This conclusion is important in connexion with theories of sensitization and quenching of phosphors, where an assumption of randomness is often made.

Measurements at very low temperatures may be made either to reduce the band width of the spectrum lines or to eliminate ions in excited vibrational states prior to the electronic transition. In the present investigation, although the reduction in band width was slight on reducing the temperature from 77 to 4·2° K, liquid-helium experiments were essential for a successful interpretation of the NaF(U) spectrum owing to the importance of excited vibrational states.

It has recently been found that impurities can cause extra lines to appear at even shorter wavelengths than any fluorescent lines shown in the accompanying spectra. This no doubt accounts for the anomalous enhancement which has been found (Jacobs 1950) using a fluorimetric method for the determination of uranium, since photomultipliers are more sensitive at these shorter wavelengths. This effect and others involving changes in line intensities due to impurities are in need of further study, and illustrate the great complexity of the NaF(U) system.

I wish to thank the many people who have helped in the course of this investigation, and in particular Mr E. Furby of the Preparative Group at Harwell for the preparation of the enriched U_3O_8, Dr A. R. Meetham of the National Physical Laboratory, Teddington, for the helium liquefaction, and Drs H. London and F. J. Webb of Harwell for help with the handling of the helium. Also I should like to acknowledge the stimulus and encouragement derived from discussions with Professor M. H. L. Pryce, F.R.S.

References

Dieke, G. H. & Duncan, A. B. F. 1949 *Spectroscopic properties of uranium compounds* (National Nuclear Energy Series III, 2). New York: McGraw Hill.
Eisenstein, J. C. & Pryce, M. H. L. 1955 *Proc. Roy. Soc.* A, **229**, 20.
Ewles, J. & Lee, N. 1953 *J. Electrochem. Soc.* **100**, 392, 399, 402.
Gaunt, J. 1953 *Trans. Faraday Soc.* **49**, 1122.
Jacobs, S. 1950 CRL/AE 54.
Kröger, F. A. 1948 *Physica*, **14**, 488.
Montroll, E. W. & Potts, R. B. 1955 *Phys. Rev.* **100**, 525.
Pauling, L. 1945 *Nature of the chemical bond.* Cornell: University Press.
Price, G. R., Ferretti, B. J. & Schwarz, S. 1953 *Analyt. Chem.* **25**, 322.
Runciman, W. A. 1955*a* Cambridge Conference on Luminescence. *Brit. J. Appl. Phys. Suppl.* no. 4, S 78.
Runciman, W. A. 1955*b* *Nature, Lond.*, **175**, 1082.
Runciman, W. A. 1955*c* *Proc. Phys. Soc.* A, **68**, 647.
Sambursky, S. & Wolfsohn, G. 1942 *Phys. Rev.* **62**, 357.
Slattery, M. K. 1929 *J. Opt. Soc. Amer.* **19**, 175.
Sponer, H., Nordheim, G., Sklar, A. L. & Teller, E. 1939 *J. Chem. Phys.* **7**, 207.
Sponer, H. & Teller, E. 1941 *Rev. Mod. Phys.* **13**, 75.
Steward, E. G. & Runciman, W. A. 1953 *Nature, Lond.*, **172**, 75.
Williams, F. E. 1951 *J. Chem. Phys.* **19**, 457.
Wilson, E. B. 1934 *Phys. Rev.* **45**, 427.

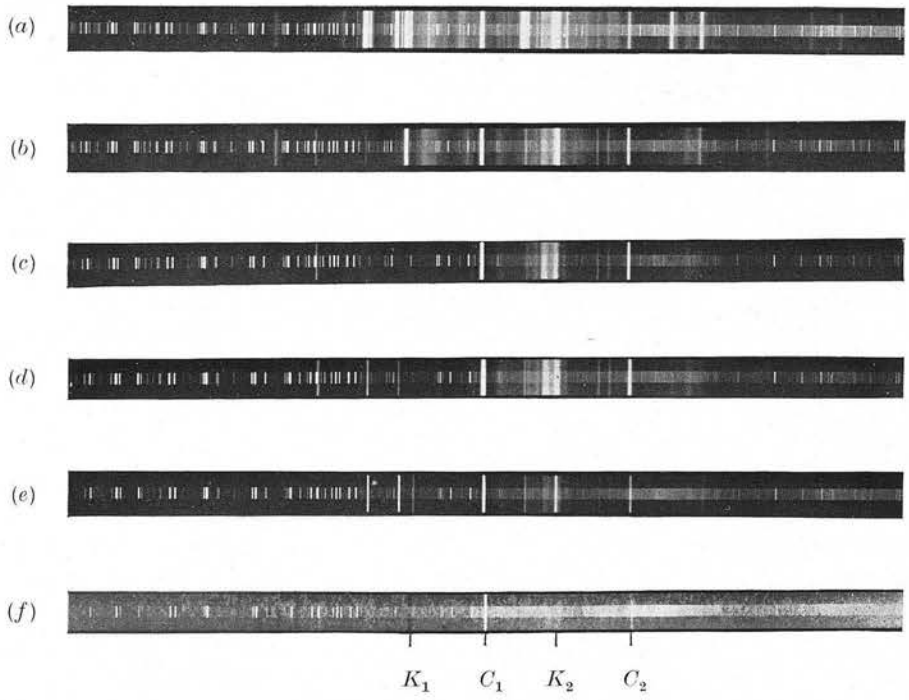

FIGURE 2

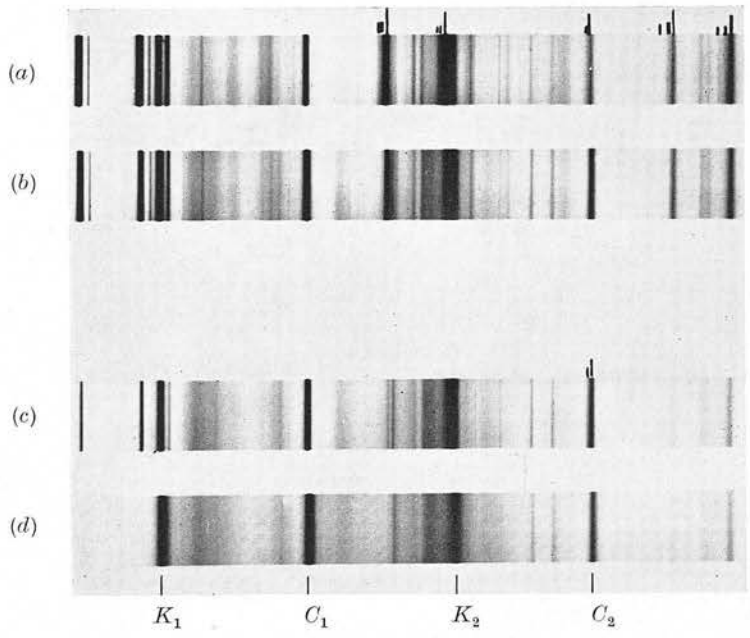

FIGURE 3

(*Facing p.* 47)

Description of plate 1

Figures 2 and 3. Fluorescence and absorption spectra at low temperatures. Concentrations of activator and impurity ions and exposure times are noted in brackets. Ilford Astra III plates were used, and iron-arc comparison spectra were superimposed on the fluorescence spectra (figure 2) using a Hartmann diaphragm. The fluorescence emission lines in figure 2 are white, but in figure 3 are reproduced black in the hope that the faint isotope lines, indicated by shorter marks above the spectra, would be more visible.

Figure 2. (*a*) Impure NaF(U) emission at 77°K (0·1 % U; 60 min).
(*b*) Pure NaF(U) emission at 77°K (0·01 % U; 6 min).
(*c*) Pure NaF(U) emission at 4·2°K (0·01 % U; 8 min).
(*d*) NaF(U,Ca) emission at 4·2°K (0·01 % U; 0·2 % Ca; 8 min).
(*e*) NaF(U,Si) emission at 4·2°K (0·01 % U; 0·75 % Si; 32 min).
(*f*) Pure NaF(U) absorption and emission at 4·2°K (0·01 % U; 30 min).

Figure 3. (*a*) Impure NaF(U,^{18}O) emission at 77°K (0·1 % U; 36 min).
(*b*) Impure NaF(U) emission at 77°K (0·1 % U; 12 min).
(*c*) Pure NaF(U,^{18}O) emission at 77°K (0·1 % U; 16 min).
(*d*) Pure NaF(U) emission at 77°K (0·1 % U; 4 min).

PRINTED IN GREAT BRITAIN AT THE UNIVERSITY PRESS, CAMBRIDGE
(BROOKE CRUTCHLEY, UNIVERSITY PRINTER)

Preprint of a paper to appear in
THE PHILOSOPHICAL MAGAZINE, November 1956

Stark-Splitting in Crystals

By W. A. RUNCIMAN
Atomic Energy Research Establishment, Harwell

[Received May 18, 1956]

RARE-EARTH ions in crystals have absorption and fluoresence spectra consisting of line multiplets separated by a wave number difference $\sim$1000 cm^{-1}. The lines within a group may have separations $\sim$100 cm^{-1} and are all due to transitions to a multiplet of levels with the same total angular momentum (J). The splitting of the levels within a multiplet has been examined by Bethe (1929) using the methods of group theory, and his treatment of the crystallographic double-groups needed to deal with half integral values of J has been extended by Opechowski (1940) to include tetrahedral and rhombohedral symmetries. Using a slightly different approach Hellwege (1948) has considered in detail the wave functions involved in a discussion of the levels in fields having the symmetry of any of the 32 crystallographic point groups. These theoretical papers do not express the results in a condensed form suitable for comparison with experiment ; but Gobrecht (1937) compiled a table of the number of levels for a given J in fields of different symmetry, and this table has been frequently reproduced (Freed 1942 ; Yost *et al.* 1947 ; Pringsheim 1949). Unfortunately all these tabulations are in error in their treatment of fields of tetragonal symmetry which are asserted to produce as many distinct levels as the lowest symmetry groups. It is now intended to rectify this error which is not present in the original work, and to discuss the splitting of the levels in nearly cubic fields, which frequently occur both in pure salts, e.g. alums, and when impurity ions requiring charge compensation enter cubic crystals (Runciman 1955).

The 32 crystallographic point groups can be classified into seven systems and for the present purpose these will be grouped under four headings (*a*) cubic, (*b*) hexagonal, containing the hexagonal and rhombohedral systems, (*c*) tetragonal, and (*d*) lower symmetry including orthorhombic, monoclinic and triclinic. The point groups in Schoenflies notation under these four headings are as follows :

(*a*) Cubic :—O_h, O, T_d, T_h, T.

(*b*) Hexagonal :—D_{6h}, D_6, C_{6v}, C_{6h}, C_6, D_{3h}, C_{3h}, D_{3d}, D_3, C_{3v}, S_6, C_3.

(*c*) Tetragonal :—D_{4h}, D_4, C_{4v}, C_{4h}, C_4, D_{2d}, S_4.

(*d*) Lower symmetry :—D_{2h}, D_2, C_{2v}, C_{2h}, C_2, C_s, S_2, C_i.

A recalculation of the splitting for integral J has shown that all point groups within one of these four categories produce the same splitting,

and the number of lines for given J is listed in table 1. The number of triply, doubly and singly degenerate levels (n_3, n_2, n_1) are written below the total number of levels for cubic symmetry. An inspection of correlation tables for the species of a group and its subgroups (Wilson, Decius and Cross 1955) shows that for a cubic field with slight hexagonal distortion the triply degenerate levels will split into a doublet and a singlet, and the doublet levels will remain doublet ; whereas for a tetragonal distortion the triplet levels will again split into a doublet and a singlet, and doublet levels will split into two singlets.

Levels are counted as doublets, even though the characters for the representations are distinct, so long as the characters are complex conjugates of each other, as in this case there is no frequency separation of the levels. For orthorhombic and lower symmetry there is complete splitting into $2J+1$ levels for integral J.

For half-integral J, i.e. for an odd number of electrons, the calculation of the splitting involves the double-groups. Bethe's results have been confirmed and table 2 lists the number of levels, either quadruplets or doublets, for any of the five cubic point groups. For all other groups there is total splitting into $J+\frac{1}{2}$ doublets, all levels remaining doubly-degenerate in any electric field (Kramers 1930). It therefore appears as if ions with an even number of electrons are better suited to determine the site-symmetry of salts or impurity-activated solids containing rare-earth ions. The application of a magnetic field, which in general removes all degeneracy, may also help in finding the terms responsible for an emission or absorption line.

Table 1. Term-splitting for Integral J

J	0	1	2	3	4	5	6	7	8	General rule
Cubic	1	1	2	3	4	4	6	6	7	add 5 every 6
($n_3\, n_2\, n_1$)	(001)	(100)	(110)	(201)	(211)	(301)	(312)	(411)	(421)	add (311) every 6
Hexagonal	1	2	3	5	6	7	9	10	11	add 4 every 3
Tetragonal	1	2	4	5	7	8	10	11	13	add 3 every 2
Lower symmetry	1	3	5	7	9	11	13	15	17	$2J+1$

Table 2. Term-splitting for Half-integral J

J	1/2	3/2	5/2	7/2	9/2	11/2	13/2	15/2	17/2	General rule
Cubic	1	1	2	3	3	4	5	5	6	add 2 every 3
All other groups	1	2	3	4	5	6	7	8	9	$J+\frac{1}{2}$

ACKNOWLEDGMENT

I wish to thank Dr. D. F. Johnston of the Theoretical Physics Division at Harwell for many invaluable discussions.

References

Bethe, H., 1929, *Ann. Phys.*, **3**, 133.

Freed, S., 1942, *Rev. Mod. Phys.*, **14**, 105.

Gobrecht, H., 1937, *Ann. Phys.*, **28**, 673.

Hellwege, K. H., 1948, *Ann. Phys.*, **4**, 95, 127, 136, 143 and 150.

Kramers, H. A., 1930, *Proc. Amst. Acad. Sci.*, **33**, 959.

Opechowski, W., 1940, *Physica*, **7**, 552.

Pringsheim, P., 1949, *Fluorescence and Phosphorescence* (New York: Interscience).

Runciman, W. A., 1955, *Brit. J. App. Phys., Supp. No.* 4, S 78.

Wilson, E. B., Decius, J. C., and Cross, P. C., 1955, *Molecular Vibrations* (New York: McGraw-Hill).

Yost, D. M., Russell, H., and Garner, C. S., 1947, *The Rare-earth Elements and Their Compounds* (New York: John Wiley).

Reprinted from the *British Journal of Applied Physics*, SUPPLEMENT No. 6, pp. S 34–S 36, 1957

Optical fluorescence in non-destructive testing

By W. A. RUNCIMAN, B.Sc., A.Inst.P., Atomic Energy Research Establishment, Harwell, Berks.

Fluorescence techniques have a wide range of applicability. In non-destructive testing they are used for the detection of X-rays, and also in the examination of metals. Magnetic materials can be tested by the fluorescent magnetic particle method, and the surface of any metal can be inspected for cracks using the fluorescent penetrant method. The main properties of the luminescent centre are outlined with a view to obtaining a deeper understanding of the processes involved, and to applying them to further types of problem. Examples of fluorescent substances include pure and impurity-activated solids, both organic and inorganic. Metals are non-fluorescent, but materials which can be directly studied by fluorescence include some glasses, ceramics and textiles.

INTRODUCTION

Fluorescence must be a phenomenon known to all in the field of non-destructive testing as it has long been used in intensifying and fluoroscopic screens for the detection of X-rays. Intensifying screens are usually made with calcium tungstate, and for fluoroscopic screens the most commonly used material is silver-activated zinc cadmium sulphide.(1) The fluorescent screen may be directly observed, or as in the case of mass radiography it may be photographed to provide a permanent record.

Another familiar application of fluorescence concerns the examination of metals. Magnetic materials can be tested for irregularities on or near the surface by the fluorescent magnetic particle method, and the surfaces of any metal, and of some non-metals, can be inspected for cracks by the fluorescent penetrant method.(2) In this method the specimen is dipped into a fluorescent penetrant, the surface is cleaned and dried, and then dusted with a developing powder which draws the penetrant out of any cracks. The cracks are then easily visible under an ultra-violet "black" lamp. The method has been made more sensitive recently by the use of the post-emulsification technique,(3) in which the emulsifier is applied after the penetration of the organic fluorescent dye. Owing to the tendency of emulsifiers to reduce the depth of penetration, this new technique can be applied to find finer cracks.

The physical processes involved in luminescence will now be outlined to provide a basis for the discussion of new possibilities.

THE NATURE OF LUMINESCENCE

Luminescence occurs when a substance emits light with a wavelength characteristic of the substance. Such a luminescent material is often called a phosphor—even when it is not phosphorescent! The phosphor first has to absorb incident energy, which may consist of atomic particles or X-rays (in scintillation counters), electrons (in cathode-ray tubes or television screens), X-rays (in fluoroscopy), or ultra-violet radiation (in fluorescent lighting). In the case of ultra-violet or visible radiation, the absorbed light has usually a greater quantum energy than the emitted light, but when there is equality in energy, and hence in wavelength, the emitted light is called resonance radiation.

Fluorescence describes the process of light emission in cases where there is a simple de-excitation of the luminescent centres; phosphorescence relates to the case where the light is emitted only after the energy is released from trapping states in the solid. A phosphorescent decay may range from a fraction of a second to several hours, whereas the half-lives of the simple exponential decay in fluorescence are usually in the range 10^{-9} to 10^{-3} s.

Fluorescent light is emitted from centres in the solid, and these centres may be either single ions or groups of ions. Some pure substances, e.g. anthracene or uranyl nitrate, are luminescent, but very often the fluorescence is characteristic of a small amount of impurity added to the base material, e.g. thallium activated potassium iodide [KI(Tl)]. In more complex cases more than one impurity ion may have to be present in the lattice, either because the emitting ion does not absorb the incident radiation or because charge compensation is necessary for the ion to be incorporated in the lattice in the proper valency state.(4)

Let us consider in more detail a simple fluorescent system in which an impurity ion replaces an ion of the base lattice and acts as a luminescent centre. Thallium activated potassium chloride [KCl(Tl)] is a system of this type which has been extensively studied both experimentally and theoretically.(5) The configuration co-ordinate diagram shown in the figure is a convenient aid to the understanding of this system.

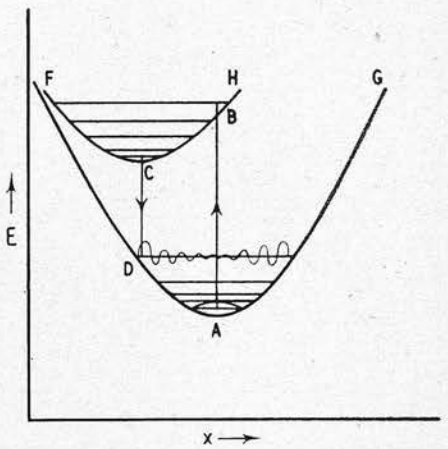

Configuration co-ordinate diagram

In this diagram one spatial co-ordinate x, perhaps the distance of nearest neighbours from the activator ion, is picked out as representative of all the atomic co-ordinates necessary to specify the system. The luminescent centre in its ground state is represented by the potential energy curve *FG*, which is nearly parabolic. The ordinate E is the energy of the luminescent centre, and at low temperatures the energy level will be near the bottom of the parabola. It can never quite be at the lowest point because of the zero point energy. The approximate shape of the lowest wave function is shown, it being a maximum above the minimum of the parabola. In contrast the wave function of one of the vibrationally excited states is oscillatory with maximum amplitude near the parabola. When ultra-violet light is absorbed the transition

AB takes place to a point near the upper parabola *FH*, which represents the electronically excited state of the luminescent centre. The configuration co-ordinate x cannot alter during the transition if the Franck–Condon principle is to hold. (The Franck–Condon principle asserts that during an electronic transition the positions and momenta of atomic nuclei are substantially unchanged.) The luminescent centre then relaxes to a point near the minimum of the upper parabola before the emission of a visible quantum of fluorescent radiation in the transition *CD*. The centre again dissipates energy as heat in reverting from *D* to the initial position *A*.

Unfortunately this picture is oversimplified for any real system, because of the reduction in symmetry of the excited state which occurs as a result of the Jahn–Teller effect, and because of the changes in polarization of the ions in the vicinity of the activator ion. (The Jahn–Teller effect states that a crystal lattice will distort if this will remove the degeneracy of the electronic state of an ion in the crystal.) Normally the vibrational fine structure of the energy levels within either the ground or excited state of the luminescent centre is so complex that the absorption and emission spectra consist of broad bands. However, in some instances the vibrational fine structure is resolved, e.g. in CaO(Bi); and in other phosphors, especially those activated by rare-earth or transuranic ions, the electric crystalline field produces an easily detectable Stark splitting of the levels. In brief, the phenomenon of fluorescence is one of the electronic excitation of an atom or group of atoms with perturbations due to the surrounding ions in the solid.

MORE COMPLEX SYSTEMS

Many phosphor systems—if not all—have a more complicated behaviour than would be expected on the above model, and a brief résumé follows of some of the phenomena which occur.

Sensitized luminescence. In many phosphor systems the energy is absorbed by one set of impurity ions and is then transferred to the other set of impurity ions. Thus although the luminescence is characteristic in its emission band of one impurity, the system is not fluorescent if only that impurity is added to the base material. There is still uncertainty about the way the two sets of ions are distributed in the lattice and about the nature of the energy transfer process.

Photoconductivity. Sulphides are examples of phosphors which are photoconducting on the absorption of ultra-violet radiation capable of producing fluorescence. This means that an electron in the excited state is not localized as in the figure, and it is necessary to consider the energy band scheme of the whole solid.

Phosphorescence. An electron in the conduction band may get trapped at a defect, and as the traps gradually get emptied by thermal agitation the luminescent centres can return to the ground state accompanied by light emission. This process may go on for hours after the excitation of the phosphor. The analysis of the process is complicated by possible retrapping of the electron, and by the existence of many trapping levels.[6]

Thermoluminescence. The deepest traps in a phosphor can only be emptied at an appreciable rate by heating the phosphor to several hundred degrees Centigrade. A glow curve is obtained by plotting the light output as a function of temperature in an experiment where the rate of temperature increase is kept constant. It is unfortunately not possible to get a complete picture of the trapping states by this type of experiment due to the occurrence of radiationless transitions to the ground state.

Infra-red stimulability. Yet another way of releasing stored energy in phosphors is by infra-red irradiation. As in the case of sensitized luminescence two activators are present. Calcium or strontium sulphide activated by europium and samarium show the effect, the stimulation spectrum being characteristic of the samarium and the emission being characteristic of the europium. In other instances infra-red irradiation causes a quenching of the phosphorescence.

EXCITATION OF LUMINESCENCE

When a phosphor is excited by highly energetic radiation, e.g. X-rays, the incident radiation has to be subdivided by secondary electron formation until the luminescent centre can absorb the few electron volts necessary for excitation. The efficiency of this process can be expected to be low and may be of the order of one-tenth. On the other hand with ultra-violet excitation the process may be of the type illustrated in the figure, and the quantum efficiency may be very close to unity. There is, of course, some energy loss due to the degradation in energy from ultra-violet to visible radiation.

The commonest sources of ultra-violet radiation are the low-pressure mercury vapour lamp for 2537 Å, and the high-pressure mercury vapour lamp for 3650 Å. Both these lamps can have undesirable visible radiation removed by solid or liquid filters. In the case of the high-pressure lamp filter material can be incorporated into the outer glass bulb. This "black" lamp emits a considerable amount of continuum in the near-ultra violet in addition to the strong triplet at 3650 Å; whereas the low pressure lamp concentrates most of its light in the resonance line at 2537 Å.

For geological survey work it has been found possible to make battery-operated models of these lamps, and the lamps have been incorporated into many types of fluorimeter developed for specific applications. For instance, fluorimeters designed for the microfluorimetric determination of uranium measure quantities down to 10^{-10} g using the sodium fluoride fusion method, and even smaller quantities of uranium may be detected.

APPLICATIONS OF FLUORESCENCE

There have been many applications of fluorescence techniques to analysis, and one book lists 3500 references,[7] some of which may have a bearing on non-destructive testing. It is noteworthy that fluorescence methods are essentially non-destructive, although there may be a few cases of photodecomposition or fading if ultra-violet irradiation is prolonged. Fluorescent materials include organic and inorganic compounds, minerals, gemstones, glass, paper, textiles, ceramics, food and drugs.

Even if the material under investigation is not fluorescent it may still be possible to use fluorescence techniques by adding a fluorescent tracer in a similar way to the use of radioactive tracers. This might be useful in a study of mixing techniques. Metals may be tested by the use of fluorescent penetrants for the detection of surface flaws, and the porosity of materials can be tested in a similar way. Luminescent substances have efficiencies which are dependent on temperature, and this or thermoluminescent effects may provide a basis for checking the temperature over large surface areas. The efficiency of luminescence may also be affected by the amount of high-energy irradiation received. Because of this fluorescent glasses can be used in dosimeters, and there are other possibilities in the study of radiation damage in solids.

Many substances fluoresce most strongly at low temperatures, and there is scope for the microscopic investigation of fluorescent minerals at liquid air temperature. This would be especially valuable in spotting traces of secondary uranium minerals. In general, it is advisable to test for fluorescence with more than one type of excitation and, if possible, at liquid air temperature as well as at room temperature. Another way in which fluorescence studies can be extended is by the spectrographic examination of the fluorescent light. Here especially the use of low temperatures is important as there is sometimes a striking resolution of the fluorescence bands into lines at liquid air or liquid helium temperatures. With this fine resolution it is possible to study the effects of impurities and the effect of isotopic substitution of the constituents.

In conclusion, while it is not possible over the wide field of non-destructive testing to give fully adequate illustrations, it appears that there may well be scope for the ingenious application of fluorescence methods in the field of non-destructive testing.

ACKNOWLEDGEMENTS

I wish to thank Mr. R. T. P. Derbyshire of the Metallurgy Division at Harwell for a most helpful discussion on the fluorescent penetrant method.

REFERENCES

(1) LEVY, L. A., WEST, D. W., and HILL, C. G. A. *Brit. J. Radiol.*, **28**, p. 206 (1955).

(2) GLOVER, K. E. *Industrial Radiography*, **5**, p. 41 (1947).

(3) ROHDE, F. W. *Non-Destructive Testing*, **13**, p. 27 (1955).

(4) RUNCIMAN, W. A. *Brit. J. Appl. Phys. Supp. No.* 4, p. S 78 (1955).

(5) WILLIAMS, F. E. *J. Chem. Phys.*, **19**, p. 457 (1951).

(6) GARLICK, G. F. J. *Luminescent Materials* (Oxford: Clarendon Press, 1949).

(7) RADLEY, J. A., and GRANT, J. *Fluorescence Analysis in Ultra-violet Light*, 4*th Edn.* (London: Chapman and Hall, 1954).

UNWIN BROTHERS LIMITED, WOKING AND LONDON

Reprinted without change of pagination from the
Proceedings of the Royal Society, A, *volume* 240, pp. 509–523, 1957

Energy levels in rare-earth ions

By J. P. Elliott,* B. R. Judd† and W. A. Runciman*

(*Communicated by M. H. L. Pryce, F.R.S.—Received* 20 *January* 1957)

The tensor-operator and group-theoretical methods of Racah are used to examine the following contributions to the Hamiltonian of a rare-earth ion: (*a*) the Coulomb interaction between the electrons, (*b*) the spin-orbit coupling of the electrons, and (*c*) the term arising from the influence of an external electrostatic field such as occurs when the rare-earth ion is situated in a crystal lattice. With regard to (*a*), the positions of all the terms of the configurations f^2, f^3 and f^4, as well as all the terms of other configurations f^n whose multiplicities are the highest or the highest but one, are tabulated on the basis of a hydrogenic $4f$ wave function. The theory of (*b*) is developed, and the parameter λ defining the spin-orbit splitting of a term is given for all terms whose energies have been found. (*c*) is treated by similar techniques and the theory is related to the one at present in use. All the general methods are illustrated by examples.

1. Introduction

The absorption spectra of rare-earth salts, or of transparent solids containing a small percentage of rare-earth ions exhibit well-resolved groups of lines. Each group of lines corresponds to transitions to a level characterized by a value of J, the quantum number corresponding to the total angular momentum. The crystalline electric field splits the level into a group of not more than $2J+1$ components covering a frequency range of the order of 100 cm^{-1}. These groups are often arranged in accordance with Russell–Saunders (LS) coupling, although considerable departures from the Landé interval rule occur. Such deviations are ascribed to intermediate coupling effects (Judd 1956). In general, for rare-earth salts the crystal field splitting is much less than the spin-orbit splitting, which in turn is much less than the Coulomb splitting.

It is difficult to interpret the spectra without any theoretical guidance about the positions of the levels. This is because the selection rules for polarization combined with a knowledge of the number of components that any level breaks up into under the influence of a specific field do not, in general, lead to an unambiguous assignment of the groups (Sayre & Freed 1956). Our present knowledge is, therefore, restricted almost exclusively to the ground states of ions, or to ions with three or less f electrons, where detailed calculations of the energy levels and the spin-orbit splittings are available. The present paper provides this information in the Russell–Saunders approximation for all f^n configurations.

The calculation of the energies of terms of configurations with four or more f electrons by the methods described by Condon & Shortley (1935) is very laborious. However, the tensor-operator and group-theoretical methods that Racah has developed greatly simplify the problem (Racah 1942, 1943 and 1949, hereafter referred to as II, III and IV). In order to calculate the energies of the terms and in some cases their properties, one has to make an assumption about the radial wave function. In the absence of better information, it has been assumed to be hydrogenic.

* Atomic Energy Research Establishment, Harwell, Berks.
† The Clarendon Laboratory, University of Oxford.

Such a wave function is a good approximation and leads to reasonable results (Judd 1955*b*, 1956). Similar calculations for the term energies have been made by Jørgensen (1955*a*) on the basis of different assumptions, but these calculations neglect some states which will be shown to be of considerable importance.

Since the energies of the terms of f^{14-n} are the same as for f^n, only configurations up to f^7 will be considered in detail here. It is hoped that the prediction of the positions of levels made in this paper, combined with the general method for the calculation of their crystal splittings, will facilitate the interpretation of the spectra of rare-earth salts.

2. The classification of the many-electron wave functions

In the p shell the energy may be obtained quite simply by the diagonal sum method. The d shell is more complex, as several terms with the same L and S occur twice or more and Racah (III) has shown that the concept of fractional parentage is of great assistance here. The basic idea is as follows. Any state of the configuration l^n may be expanded in terms of products of states of the first $(n-1)$ particles with those of the nth particle as follows:

$$\psi(l^n\tau SLS_zL_z) = \sum_{\bar{\tau}\bar{S}\bar{L}} (l^n(\tau SL)\{\,|\,l^{n-1}(\bar{\tau}\bar{S}\bar{L})) \sum_{\bar{S}_z\bar{L}_zs_zl_z} (\bar{S}\tfrac{1}{2}SS_z\,|\,\bar{S}\tfrac{1}{2}\bar{S}_zs_z) \times (\bar{L}lLL_z\,|\,\bar{L}l\bar{L}_zl_z)\,\overline{\psi}(l^{n-1}\bar{\tau}\bar{S}\bar{L}\bar{S}_z\bar{L}_z)\,\phi(ls_zl_z). \tag{1}$$

In this expansion the second sum merely performs the vector coupling of the total S and L values while the first coefficients $(l^n(\tau SL)\{\,|\,l^{n-1}(\bar{\tau}\bar{S}\bar{L}))$ are the coefficients of fractional parentage (c.f.p.). An example will illustrate the concept. The antisymmetric states of the p^2 configuration are ^3P, ^1S, ^1D. By adding a third p particle, the only antisymmetric states which may be formed are ^4S, ^2P, ^2D of p^3. The quartet state can only be formed from the ^3P and so this antisymmetric state must be the simple vector-coupled product,

$$\psi(p^3_{123}\tfrac{3}{2}0S_zL_z) = \sum_{\bar{S}_z\bar{L}_zs_zl_z} (1\,\tfrac{1}{2}\,\tfrac{3}{2}S_z\,|\,1\,\tfrac{1}{2}\bar{S}_zs_z)\,(1\,10L_z\,|\,1\,1\bar{L}_zl_z)\,\overline{\psi}(p^2_{12}11\bar{S}_z\bar{L}_z)\phi(p_3s_zl_z).$$

A ^2P state on the other hand may be formed by vector coupling from any of the three parent p^2 states. Only one combination of these ^2P states will be antisymmetric however, and the coefficients occurring in that combination are called the coefficients of fractional parentage. They are shown in table 1.

Table 1

p^3 \ p^2	^3P	^1S	^1D
^4S	1	0	0
^2P	$-\sqrt{\frac{1}{2}}$	$\sqrt{\frac{4}{15}}$	$-\sqrt{\frac{5}{15}}$
^2D	$-\sqrt{\frac{1}{2}}$	0	$\sqrt{\frac{1}{2}}$

For the more complicated f shell, where the straightforward c.f.p. method becomes laborious, Racah (IV) devised a further simplification by using the theory of groups of transformations.

In simple terms his method consists first of classifying the complete set of states of the configuration l^n by their properties under certain groups of transformations, and then making use of these properties in deriving the energy matrix. For example, it is well known that if the states are constructed with definite total orbital angular momentum L, then the electrostatic energy matrix is diagonal in L. In group-theoretical language this is the same as saying that if the states are constructed to transform according to definite irreducible representations of the group of rotations

TABLE 2. CLASSIFICATION OF STATES

n	v	W	U	SL	n	v	W	U	SL
2	2	(110)	(10)	^3F	5	5	(110)	(10)	^6F
			(11)	^3PH				(11)	^6PH
	2	(200)	(20)	^1DGI		5	(211)	(10)	^4F
	0	(000)	(00)	^1S				(11)	^4PH
								(20)	^4DGI
3	3	(111)	(00)	^4S				(21)	^4DFGHKL
			(10)	^4F				(30)	$^4PFGHIKM$
			(20)	^4DGI		3	(111)	(00)	^4S
	3	(210)	(11)	^2PH				(10)	^4F
			(20)	^2DGI				(20)	^4DGI
			(21)	^2DFGHKL					
	1	(100)	(10)	^2F	6	6	(100)	(10)	^7F
						6	(210)	(11)	^5PH
4	4	(111)	(00)	^5S				(20)	^5DGI
			(10)	^5F				(21)	^5DFGHKL
			(20)	^5DGI		4	(111)	(00)	^5S
	4	(211)	(10)	^3F				(10)	^5F
			(11)	^3PH				(20)	^5DGI
			(20)	^3DGI					
			(21)	^3DFGHKL	7	7	(000)	(00)	^8S
			(30)	$^3PFGHIKM$		7	(200)	(20)	^6DGI
	2	(110)	(10)	^3F		5	(110)	(10)	^6F
			(11)	^3PH				(11)	^6PH
	4	(220)	(20)	^1DGI					
			(21)	^1DFGHKL					
			(22)	$^1SDGHILN$					
	2	(200)	(20)	^1DGI					
	0	(000)	(00)	^1S					

in three dimensions, then the fact that we know the interaction to be invariant with respect to such rotations enables us to say that its matrix is diagonal in L. Racah's method is essentially a generalization of this idea to more general groups of transformations in the $(2l+1)$-dimensional function space spanned by the orbital wave functions $\phi(lm)$ of a single electron. To each new group used there will be new quantum numbers, generalizations of L, which specify the properties of the many electron wave functions and serve to classify them. These new quantum numbers will not necessarily be 'good' quantum numbers, i.e. the energy matrix will not be diagonal in them; but this does not matter, since they are primarily introduced as a mathematical convenience and one may evaluate the coupling terms between them and diagonalize the matrix numerically.

In the particular case of the f shell, Racah (IV) introduced two groups providing two sets of quantum numbers W and U. The first is a set of three integral numbers $W \equiv (w_1 w_2 w_3)$ with $w_1 \geqslant w_2 \geqslant w_3 \geqslant 0$ and all $w \leqslant 2$, while the second is a set of two integral numbers $U \equiv (u_1 u_2)$. With a few exceptions these labels distinguish all states of the f shell and, using the symbol τ to separate these exceptions, the wave functions are denoted by

$$\psi(f^n \tau W U S L S_z L_z). \tag{2}$$

In earlier work Racah used a 'seniority number' v, which is essentially equivalent to W, to label the states. If we define a and b such that

$$w_1 = \ldots = w_a = 2, \quad w_{a+1} = \ldots = w_{a+b} = 1, \quad w_{a+b+1} = \ldots = w_3 = 0,$$

then the relation between W and v is given by

$$a = \tfrac{1}{2}v - S, \quad b = \min(2S, 2l+1-v).$$

The corresponding notation alternative to (2) is

$$\psi(f^n \tau U v S L S_z L_z). \tag{3}$$

In table 2 we list, from IV, all the states of f^2, f^3 and f^4 and the states of highest and next highest multiplicity of f^5, f^6 and f^7 classified by the group theoretical quantum numbers introduced above.

3. The energy matrix

By expanding the interaction between electrons in Legendre polynomials of the cosine of the angle between them, the electrostatic energy $\mathscr{E}$ may be written as a linear combination of Slater radial integrals

$$\mathscr{E} = \sum_{k=0}^{2l} f^k F_k, \quad k \text{ even}. \tag{4}$$

For the two-electron configuration the coefficients f^k are simply angular integrals over spherical harmonics. Using the calculated c.f.p. together with equation (1) of IV to derive the coefficients of the F_k in the configuration l^n from those in the configuration l^{n-1}, we may build up a chain process from the known l^2 coefficients; but in the f shell such a process is tedious.

To simplify the calculation, Racah observed that, in the two-electron problem, the coefficient f^k is essentially the expectation value of the scalar product operator $(Y_k(1).Y_k(2))$ of two spherical harmonics. Although this operator is a scalar with respect to rotations in three dimensions it is neither scalar nor has simple properties with respect to the more general groups of transformations used to classify the wave functions. However, by taking certain linear combinations of these operators one may construct new operators which have simple transformation properties under the groups employed. The energy becomes

$$\mathscr{E} = \sum_{k=0}^{l} e_k E^k, \tag{5}$$

where the e_k are the expectation values of the new operators and the E^k are linear combinations of the F_k.

In the f shell

$$\left.\begin{aligned} E^0 &= F_0 - 10F_2 - 33F_4 - 286F_6, \\ E^1 &= \tfrac{1}{9}(70F_2 + 231F_4 + 2002F_6), \\ E^2 &= \tfrac{1}{9}(F_2 - 3F_4 + 7F_6), \\ E^3 &= \tfrac{1}{3}(5F_2 + 6F_4 - 91F_6). \end{aligned}\right\} \tag{6}$$

For configurations f^n Racah (IV) has shown that both e_0 and e_1 are diagonal in the $UvSL$ scheme with values,

$$\left.\begin{aligned} e_0 &= \tfrac{1}{2}n(n-1), \\ e_1 &= \tfrac{9}{2}(n-v) + \tfrac{1}{4}v(v+2) - S(S+1). \end{aligned}\right\} \tag{7}$$

The remaining coefficients are more difficult to derive and necessitate the use of the c.f.p. derived in IV. Using these, Racah has prepared subsidiary tables from which the values of e_2 and e_3 may be derived in any configuration f^n.

Apart from a sign, e_2 is the product of quantities χ and x. With the exception of the following values,

$$x[(200),(20)(20)] = 2,$$

and

$$x[(111),(20)(20)] = 0,$$

which are deducible from known results for f^2 and f^3, these are given in tables VI to XI of IV. The calculation of e_3 is similar but more complicated. The tabulation is complete apart from a table containing one element for f^2, which because of recurrence relations, is also needed for f^4. In Racah's notation it is

$$y[f^2, \tfrac{1}{2}(20), \tfrac{1}{2}(20)] = 2.$$

4. The energy levels

By the method of the preceding section the energy matrix can be calculated for any group of states with the same values of S and L. As an example consider the ^5D terms of f^6. Judd (1955*b*) has previously examined the properties of these terms by writing down the total wave function as a linear combination of determinantal product states, and the same terms have been chosen to illustrate the methods used here so that a comparison between the two approaches is always possible. The possible states are found to be

$$\begin{aligned} &(a)\quad f_6^6(210)(20)\,{}^5D, \\ &(b)\quad f_6^6(210)(21)\,{}^5D, \\ &(c)\quad f_4^6(111)(20)\,{}^5D, \end{aligned}$$

where the 'seniority number' v is written as a suffix.

The energy matrix $[E]$ is as follows:

$$\begin{array}{c} \\ (a) \\ (b) \\ (c) \end{array} \begin{array}{c} \begin{array}{ccc} (a) & (b) & (c) \end{array} \\ \begin{bmatrix} 15E^0 + 6E^1 + \frac{858}{7}E^2 + 11E^3 & \frac{468}{7}\sqrt{33}E^2 & \frac{22}{7}\sqrt{(14)}E^3 \\ \frac{468}{7}\sqrt{(33)}\,E^2 & 15E^0 + 6E^1 - \frac{1131}{7}E^2 + 18E^3 & \frac{12}{7}\sqrt{(462)}\,E^3 \\ \frac{22}{7}\sqrt{(14)}\,E^3 & \frac{12}{7}\sqrt{(462)}\,E^3 & 15E^0 + 9E^1 - 11E^3 \end{bmatrix} \end{array}. \tag{8}$$

Values of the parameters E^k are now required. Assuming that the $4f$ radial wave function is hydrogenic, the following relations between F_k are obtained (Judd 1955*b*):

$$F_4/F_2 = 41/297 = 0{\cdot}138, \qquad (9)$$
$$F_3/F_2 = 7.25/81.143 = 0{\cdot}0151.$$

Using equations (6) values of the E^k may be found, and the following have been used in the calculations:

$$E^0 = -18{\cdot}87\,F_2, \quad E^2 = 0{\cdot}077\,F_2, \qquad (10)$$
$$E^1 = 14{\cdot}68\,F_2, \quad E^3 = 1{\cdot}49\,F_2.$$

In view of intermediate coupling effects, which often displace levels by about $3F_2$, and also the inherent uncertainty in the ratios of the F_k, these values are considered sufficiently accurate.

Substituting for the E^k, the secular equation $|E-\epsilon I| = 0$ can be solved, giving for the ^5D states,

$$\epsilon = -231{\cdot}3\,F_2, \quad -183{\cdot}3\,F_2 \quad \text{and} \quad -102{\cdot}4\,F_2. \qquad (11)$$

The ground state of f^6 is ^7F with an energy of $15E^0$. The energies relative to this level are

$$\epsilon_0 = 51{\cdot}8F_2, \quad 99{\cdot}8F_2 \quad \text{and} \quad 180{\cdot}7F_2. \qquad (12)$$

For f^5 and f^6, Jørgensen ignored states whose seniority number was smaller than the maximum value. In the above example this amounts to neglecting the pure state (*c*), which will be seen (24) to make an important contribution to the ground state. This leads in our approximation to values of $78{\cdot}1F_2$ and $138{\cdot}3F_2$ for the two lowest ^5D terms. It is at once obvious that seniority is not a 'good' quantum number, and states of all seniorities must be included in the diagonalization. A mistake was originally made by Jørgensen in his calculation of the diagonal term for the ^5D state (*c*) with seniority 4, but this has been corrected to the value given in (8) (Jørgensen 1955*a*, *b*).

In the present work all the energy matrices have been calculated using IV. They have been found to agree with previous calculations where these were available, with the exception of the diagonal term for $f_5^5(211)(11)^4H$. This has an energy of $10E^0+5E^1-4E^3$, whereas $10E^0+5E^1-2E^3$ is given by Jørgensen (1955*a*). There was full agreement with the complete energy matrices for all states of f^4 (Reilly 1953).

Some of the cubic equations and all the quartic secular equations were solved on an electronic digital computer, although this was from convenience rather than from necessity. The results for all levels of f^2, f^3 and f^4, and the levels of highest and second highest multiplicity of f^5, f^6 and f^7 are listed in table 3. To convert these energies into wave numbers, it is only necessary to find a value of F_2. For the $4f$ shell it is possible to make a good estimate of F_2 using a formula of the type (Judd 1956)

$$F_2 = 12{\cdot}4(Z-34)\,\text{cm}^{-1}, \qquad (13)$$

where Z is the atomic number of the rare-earth ion. In table 3 the energies of the terms are expressed as multiples of F_2, and it is to be noted that a table for f^n applies equally for f^{14-n}.

TABLE 3. ENERGY LEVELS (IN UNITS OF F_2) AND SPIN-ORBIT SPLITTING FACTORS

f^2	ϵ_0	λ
^3H	0·0	0·500
^3F	13·4	0·500
^1G	16·8	—
^1D	48·4	—
^1I	58·6	—
^3P	62·6	0·500
^1S	145·5	—

f^3	ϵ_0	λ
^4I	0·0	0·333
^4S	31·3	—
^4F	31·3	0·333
^2H	32·9	0·510
^2G	43·2	0·351
^2K	48·5	0·321
^4G	49·2	0·333
^2P	58·9	0·000
^2D	58·9	0·080
^2I	77·5	0·095
^2L	78·9	0·250
^4D	80·5	0·333
$^2H'$	88·1	0·091
$^2D'$	90·3	0·920
^2F	107·9	0·783
$^2G'$	134·8	−0·285
$^2F'$	195·1	−0·450

f^4	ϵ_0	λ
^5I	0·0	0·250
^5F	31·3	0·250
^5S	31·3	—
^3K	40·0	0·248
^5G	49·2	0·250
^3H	50·9	0·340
^3G	54·4	0·147
^3L	55·1	0·208
^1G	57·0	—
^3P	61·3	0·279
^1L	64·3	—
^3M	65·5	0·167
^3F	68·1	−0·175
^3I	71·0	0·101
^1D	71·2	—
^3D	77·0	0·105
^1H	78·0	—
^5D	80·5	0·250
$^3F'$	81·9	0·957
^1I	90·5	—
^1K	93·0	—
$^3H'$	93·0	−0·004
$^1D'$	94·6	—
$^3G'$	104·0	−0·058
^1N	107·6	—
$^3F''$	109·0	−0·158
$^3K'$	114·0	0·092
$^1G'$	114·1	—
$^3H''$	117·9	0·164
$^1L'$	122·3	—
$^1H'$	128·2	—
$^3I'$	133·6	0·102
$^3P'$	137·5	1·666
$^3D'$	141·8	−0·188
$^3G''$	143·3	0·463
$^1I'$	143·6	—
^1F	153·5	—
$^1D''$	155·8	—
$^1G''$	175·6	—
^1S	184·4	—
$^3F'''$	189·7	−0·039
$^3H'''$	201·2	0·032
$^1I''$	201·8	—
$^3P''$	206·6	−1·445
$^1G'''$	236·6	—
$^1D'''$	304·8	—
$^1S'$	358·8	—

f^5	ϵ_0	λ
^6H	0·0	0·200
^6F	13·4	0·200
^4I	48·4	0·152
^4M	48·7	0·111
^4F	49·0	0·622
^4G	51·1	0·338
^4K	56·6	0·156
^4L	59·1	0·139
^6P	62·6	0·200
^4D	63·0	0·021
^4H	65·4	0·088
^4P	71·1	−0·256
$^4G'$	71·7	0·070
$^4F'$	81·9	−0·251
$^4I'$	84·8	0·065
$^4H'$	107·2	0·059
$^4G''$	107·4	0·249
$^4K'$	116·0	0·070
$^4P'$	125·3	0·389
$^4D'$	136·2	0·256
$^4H''$	143·1	0·008
^4S	145·5	—
$^4F''$	147·4	0·140
$^4D''$	160·6	−0·165
$^4I''$	165·9	0·084
$^4F'''$	183·8	−0·155
$^4G'''$	197·6	−0·125

f^6	ϵ_0	λ
^7F	0·0	0·167
^5D	51·8	0·737
^5L	57·7	0·063
^5G	60·7	0·045
^5H	68·9	0·054
^5I	73·3	0·055
^5F	78·9	0·074
^5K	88·1	0·080
$^5G'$	96·8	0·160
$^5D'$	99·8	0·004
^5P	104·5	0·000
$^5H'$	110·1	0·096
^5S	132·2	—
$^5F'$	148·7	−0·073
$^5I'$	149·3	0·052
$^5G''$	177·5	−0·103
$^5D''$	180·7	−0·409

f^7	ϵ_0	λ
^8S	0·0	—
^6P	82·9	0·000
^6I	86·9	0·000
^6D	97·1	0·000
^6G	128·7	0·000
^6F	132·1	0·000
^6H	145·5	0·000

It is hoped that table 3 will also be useful as a first guide to $5f$ spectra, although not enough progress has yet been made to write an equation similar to (13). Strictly speaking the relations (9) and (10) hold only for $4f$ wave functions, but it may be mentioned that the results for a hydrogenic $5f$ wave function are not so very dissimilar. They are

$$F_4/F_2 = 0{\cdot}145, \qquad F_6/F_2 = 0{\cdot}0164 \tag{14}$$

and

$$\left.\begin{aligned} E^0 &= -19{\cdot}48F_2, & E^2 &= 0{\cdot}076F_2 \\ E^1 &= 15{\cdot}15F_2, & E^3 &= 1{\cdot}459F_2. \end{aligned}\right\} \tag{15}$$

5. The spin-orbit interaction

Using the tensor operator methods of Racah (II) together with the fractional parentage coefficients, the matrix elements of the spin-orbit operator $\zeta \sum_i (\mathbf{s}_i.\mathbf{l}_i)$ between two general states ψ_{JM}, ψ'_{JM} of the configuration l^n is given by

$$(\psi_{JM} \,|\, \zeta \textstyle\sum_i (\mathbf{s}_i.\mathbf{l}_i) \,|\, \psi'_{JM}) = -n\zeta\{3l(l+1)(2l+1)(2L+1)(2L'+1)(2S+1)(2S'+1)/2\}^{\frac{1}{2}}$$
$$\times W(JLS'1; SL') \sum_{\overline{\psi}} (\psi\{\,|\,\overline{\psi})\,(\psi'\{\,|\,\overline{\psi})\, W(\bar{S}S\tfrac{1}{2}1; \tfrac{1}{2}S')\, W(\bar{L}Ll1; lL'), \tag{16}$$

where W is a Racah function. Many of these have been tabulated (Biedenharn 1952; Simon, Vander Sluis & Biedenharn 1954). In (16) we have used the symbol ψ to represent the set of quantum numbers by which the state is defined, and similarly with the parent state $\overline{\psi}$. The symbols $(\psi\{\,|\,\overline{\psi})$ are, in the same vein, an abbreviation for the c.f.p. of (1), while the summation over $\overline{\psi}$ represents a summation over all the parent states $\overline{\psi}$. For the f shell, Racah (IV) shows that the c.f.p. may be factorized into three parts,

$$(f^n(\tau U v SL)\{\,|\,f^{n-1}(\bar{\tau}\bar{U}\bar{v}\bar{S}\bar{L})) = (f^n v S\{\,|\,f^{n-1}\bar{v}\bar{S}+f)\,(WU\,|\,\bar{W}\bar{U}+f)\,(U\tau L\,|\,\bar{U}\bar{\tau}\bar{L}+f). \tag{17}$$

The first factor may be calculated from equations (IV), (52), (56), while the second and third are given in tables III and IV of IV.

The complete generality of (16) is necessary only when considering the mixing of different S and L values, i.e. for intermediate coupling. In this paper we are concerned only with the splitting of the J values for each given S and L, i.e. with the splitting in Russell–Saunders coupling. For such a specialization it is possible to simplify (16).

In the first place we notice that the parental spin $\bar{S}$ may take only two possible values $\bar{S} = S \pm \frac{1}{2}$, so that the sum over $\overline{\psi}$ may be written as

$$W(S-\tfrac{1}{2}S\tfrac{1}{2}1; \tfrac{1}{2}S') \sum_{\overline{\psi}} (\psi\{\,|\,\overline{\psi})\,(\psi'\{\,|\,\overline{\psi})\, W(\bar{L}Ll1; lL')$$
$$+\{W(S+\tfrac{1}{2}S\tfrac{1}{2}1; \tfrac{1}{2}S') - W(S-\tfrac{1}{2}S\tfrac{1}{2}1; \tfrac{1}{2}S')\} \sum_{\overline{\psi}}{}' (\psi\{\,|\,\overline{\psi})\,(\psi'\{\,|\,\overline{\psi})\, W(\bar{L}Ll1; lL'), \tag{18}$$

where Σ' is a restricted sum over those $\overline{\psi}$ for which $\bar{S} = S + \frac{1}{2}$. If we now confine our attention to states ψ, ψ' belonging to the same multiplicity $S = S'$, the first sum in

(18) may be carried out. Substituting back into (16) and putting in the explicit form of the simple Racah functions, we obtain

$$(\psi \mid \zeta \sum_i (\mathbf{s}_i . \mathbf{l}_i) \mid \psi') = \frac{\zeta}{4S} \delta(\psi, \psi') \{J(J+1) - L(L+1) - S(S+1)\}$$
$$+ \frac{n\zeta}{2} \left\{ \frac{l(l+1)(2l+1)(2L+1)(2L'+1)(2S+1)^3}{S(S+1)} \right\}^{\frac{1}{2}} W(JLS1; SL')$$
$$\times \sum_{\bar{\psi}}' (\psi\{ \mid \bar{\psi}) (\psi'\{ \mid \bar{\psi}) W(\bar{L}Ll1; lL'). \tag{19}$$

The value of (19) lies in the fact that the summation over $\bar{\psi}$, which can be laborious, is restricted. Although (19) is a special case of (16) in that it applies only to states of the same multiplicity $S = S'$, it may be used to calculate the intermediate coupling matrix elements between different L values of that multiplicity.

If we put $L = L'$ in (19) restricting ourselves to Russell–Saunders coupling, we have the further simplification to

$$(\psi \mid \zeta \sum_i (\mathbf{s}_i . \mathbf{l}_i) \mid \psi') = \frac{\zeta\{J(J+1) - L(L+1) - S(S+1)\}}{8SL(L+1)}$$
$$\times \Big[\{(2S+2-n) L(L+1) - (n-2S) l(l+1)\} \delta(\psi, \psi')$$
$$+ n\left(\frac{2S+1}{S+1}\right) \sum_{\bar{\psi}}' (\psi\{ \mid \bar{\psi}) (\psi'\{ \mid \bar{\psi}) \bar{L}(\bar{L}+1) \Big]. \tag{20}$$

The spin-orbit splitting factor λ in Russell–Saunders approximation is defined by

$$(\psi \mid \zeta \sum_i (\mathbf{s}_i . \mathbf{l}_i) \mid \psi') = \frac{\lambda\zeta}{2} \{J(J+1) - L(L+1) - S(S+1)\}. \tag{21}$$

For the states of highest multiplicity, $n = 2S$ (in the first half shell), and there are no parents with $\bar{S} = S + \frac{1}{2}$ so that the summation in (20) disappears. This leads to the familiar result,

$$\lambda = \pm \frac{1}{2S},$$

where the plus sign applies in the first half of the shell. For states of next highest multiplicity $n = 2S + 2$, and λ follows from (20) putting $l = 3$,

$$\lambda = \frac{\pm 1}{(n-2) L(L+1)} [-12\delta(\psi, \psi') + (n-1) \sum_{\bar{\psi}}' (\psi\{ \mid \bar{\psi}) (\psi'\{ \mid \bar{\psi}) \bar{L}(\bar{L}+1)]. \tag{22}$$

This is a simple formula to use as the summation is only over the few states of highest multiplicity of the parent configuration.

The spin-orbit matrices for all states in table 2 have been evaluated using (22) and the known values of the c.f.p. (17). As an example the matrix for the ^5D states of f^6 is

$$\begin{array}{c} \\ (a) \\ (b) \\ (c) \end{array} \begin{array}{c} \begin{array}{ccc} (a) & (b) & (c) \end{array} \\ \begin{bmatrix} \frac{1}{42} & -\frac{1}{21}\sqrt{(33)} & \frac{1}{84}\sqrt{(14)} \\ -\frac{1}{21}\sqrt{(33)} & \frac{19}{84} & -\frac{1}{42}\sqrt{(462)} \\ \frac{1}{84}\sqrt{(14)} & -\frac{1}{42}\sqrt{(462)} & \frac{1}{12} \end{bmatrix} \end{array}. \tag{23}$$

The values of λ for the actual states are found by taking the expectation value of the spin-orbit interaction. For the lowest ^5D state the coefficients in the linear combination $X|a\rangle+Y|b\rangle+Z|c\rangle$ are

$$X=-0{\cdot}196, \quad Y=0{\cdot}770, \quad Z=-0{\cdot}607. \tag{24}$$

Using (23), we obtain $\lambda=0{\cdot}737$.

Calculations of this type have been performed for all the SL states capable of spin-orbit splitting, and the results are shown in table 3.

The diagonal sums of the spin-orbit matrices have fairly simple fractional values which are independent of the Slater integrals F^k, and which may be used as a check for the validity of the Russell–Saunders approximation. These diagonal sums are listed for all states of second highest multiplicity in table 4, where N is the number of states contributing to a sum. Results for $\Sigma\lambda/N$ previously obtained for f^3 (Satten 1953) and f^4 (Rao 1950) are in complete agreement with those given in table 4.

TABLE 4. SUM OF SPIN-ORBIT SPLITTING FACTORS

f^3	N	$\Sigma\lambda$	f^4	N	$\Sigma\lambda$	f^5	N	$\Sigma\lambda$	f^6	N	$\Sigma\lambda$
^2P	1	0	^3P	3	$\frac{1}{2}$	^4P	2	$\frac{2}{15}$	^5P	1	0
^2D	2	1	^3D	2	$-\frac{1}{12}$	^4D	3	$\frac{1}{9}$	^5D	3	$\frac{1}{3}$
^2F	2	$\frac{1}{3}$	^3F	4	$\frac{7}{12}$	^4F	4	$\frac{16}{45}$	^5F	2	0
^2G	2	$\frac{1}{15}$	^3G	3	$\frac{11}{20}$	^4G	4	$\frac{8}{15}$	^5G	3	$\frac{1}{10}$
^2H	2	$\frac{3}{5}$	^3H	4	$\frac{8}{15}$	^4H	3	$\frac{7}{45}$	^5H	2	$\frac{3}{20}$
^2I	1	$\frac{2}{21}$	^3I	2	$\frac{17}{84}$	^4I	3	$\frac{19}{63}$	^5I	2	$\frac{3}{28}$
^2K	1	$\frac{9}{28}$	^3K	2	$\frac{19}{56}$	^4K	2	$\frac{19}{84}$	^5K	1	$\frac{9}{112}$
^2L	1	$\frac{1}{4}$	^3L	1	$\frac{5}{24}$	^4L	1	$\frac{5}{36}$	^5L	1	$\frac{1}{16}$
			^3M	1	$\frac{1}{6}$	^4M	1	$\frac{1}{9}$			

For states with the same $WUSL$ classification the matrix elements are inversely proportional to $n-2$, owing to a cancellation of the $(n-1)$ in (22). This leads to a considerable reduction in the labour involved in calculations for all the configurations f^n. In particular, the (210) states of f^3 and f^6 are in the ratio 4:1 illustrated in table 4 for P, H, K and L states; and the (211) states of f^4 and f^5 are in the ratio 3:2 as can be seen for K, L and M states.

In order to calculate the energy levels within an SL multiplet one also needs to know ζ, and values for this have been derived from experiment (Bleaney 1955; Judd 1956).

6. THE CRYSTAL FIELD

The first step in calculating the influence of the crystal lattice on the energy-level system of the free ion is to expand the crystalline electric potential in a series of spherical harmonics, taking the centre of the ion as the origin (Bleaney & Stevens 1953). The contribution to the Hamiltonian is the sum of the potential energies of the electrons, and thus can be written as

$$\sum_{k,q} A_k^q V_k^q,$$

where the coefficients A_k^q depend on the lattice, and each V_k^q is the sum over the electrons of functions that transform like the spherical harmonics Y_k^q. A correspondence can then be made between the V_k^q and the tensor operators U_q^k of II. For rare-earth ions, the effect of the crystal field is generally smaller than that of the Coulomb and spin-orbit interactions of the electrons, and it may therefore be estimated by conventional perturbation theory.

The fundamental problem is therefore to calculate matrix elements of the form

$$(f^n\tau UvSLJJ_z \,|\, U_q^k \,|\, f^n\tau' U'v'S'L'J'J_z').$$

Since V_k^q does not contain spin variables, $S' = S$. From equation (29) of II, it follows that the dependence of this matrix element on q, J_z, J_z' is contained in a Wigner coefficient, i.e.

$$\begin{aligned}(f^n\tau UvSLJJ_z \,|\, U_q^k \,|\, f^n\tau' U'v'SL'J'J_z') \\ = (-1)^{J+J_z+k+q}(2k+1)^{-\frac{1}{2}}(f^n\tau UvSLJ \,\|\, U^k \,\|\, f^n\tau' U'v'SL'J')\,(JJ'-J_zJ_z' \,|\, JJ'k-q).\end{aligned} \tag{25}$$

Explicit forms for the Wigner coefficients are given by Condon & Shortley (1935).

Using (44*b*) of II,

$$\begin{aligned}(f^n\tau UvSLJ \,\|\, U^k \,\|\, f^n\tau' U'v'SL'J') = (-1)^{S+k-L-J'}\{(2J+1)\,(2J'+1)\}^{\frac{1}{2}} \\ \times W(LJL'J';\,Sk)\,(f^n\tau UvSL \,\|\, U^k \,\|\, f^n\tau' U'v'SL').\end{aligned} \tag{26}$$

Adopting the abbreviated notation of § 5,

$$\begin{aligned}(f^n\tau UvSL \,\|\, U^k \,\|\, f^n\tau' U'v'SL') &= (\psi \,\|\, U^k \,\|\, \psi') \\ &= n\sum_{\bar\psi}(\psi\{\,|\,\bar\psi)\,(\psi'\{\,|\,\bar\psi)\,(f^{n-1}\bar\psi, f, \psi \,\|\, U^k(n) \,\|\, f^{n-1}\bar\psi, f, \psi') \\ &= n\sum_{\bar\psi}(\psi\{\,|\,\bar\psi)\,(\psi'\{\,|\,\bar\psi)\,(-1)^{\bar L+k-3-L'}\{(2L+1)\,(2L'+1)\}^{\frac{1}{2}}W(3L3L';\,\bar Lk).\end{aligned} \tag{27}$$

In obtaining this result (44*b*) of II is used again, and also the convention that

$$(f \,\|\, U^k \,\|\, f) = 1.$$

The fractional parentage coefficients are given by (17) and the evaluation of $(f^n\tau UvSL \,\|\, U^k \,\|\, f^n\tau' U'v'SL')$ is completed.

We shall now show how this theory is related to the one that is at present in use. Stevens (1952) has used operator equivalences to find the matrix elements of V_k^q between states with the same value of J. The so-called operator equivalent factors α, β and γ are defined by

$$(\psi_{JJ_z} \,|\, \Sigma\,(3z^2-r^2) \,|\, \psi'_{JJ_z}) = \alpha\langle r^2\rangle[3J_z^2-J(J+1)], \tag{28a}$$

$$\begin{aligned}(\psi_{JJ_z} \,|\, \Sigma\,(35z^4-30r^2z^2+3r^4) \,|\, \psi'_{JJ_z}) \\ = \beta\langle r^4\rangle[35J_z^4-30J(J+1)J_z^2+25J_z^2-6J(J+1)+3J^2(J+1)^2],\end{aligned} \tag{28b}$$

$$\begin{aligned}(\psi_{JJ_z} \,|\, \Sigma\,(231z^6-315r^2z^4+105r^4z^2-5r^6) \,|\, \psi'_{JJ_z}) \\ = \gamma\langle r^6\rangle[231J_z^6-315J(J+1)J_z^4+735J_z^4+105J^2(J+1)^2J_z^2 \\ -525J(J+1)J_z^2+294J_z^2-5J^3(J+1)^3+40J^2(J+1)^2-60J(J+1)],\end{aligned} \tag{28c}$$

where $\langle r^n \rangle$ is the mean value of r^n for a single $4f$ electron. As before, ψ represents the set of quantum numbers $f^n \tau U v S L$. It is sometimes convenient to specify the operator equivalent factors completely by writing $(\psi_J \| \alpha \| \psi'_J)$ for α etc. Now if the expressions

$$2(-1)^{J+J_z}\sqrt{\frac{(2J-2)!}{(2J+3)!}}, \quad 2(-1)^{J+J_z}\sqrt{\frac{(2J-4)!}{(2J+5)!}} \quad \text{and} \quad 4(-1)^{J+J_z}\sqrt{\frac{(2J-6)!}{(2J+7)!}},$$

are included in the right-hand sides of equations (28a), (28b) and (28c) respectively, they become

$$\frac{1}{\sqrt{5}}\alpha\langle r^2\rangle (JJ-J_zJ_z;\, JJ20), \quad \tfrac{1}{3}\beta\langle r^4\rangle (JJ-J_zJ_z;\, JJ40)$$

and

$$\frac{1}{\sqrt{13}}\gamma\langle r^6\rangle (JJ-J_zJ_z;\, JJ60).$$

Comparing these expressions with (25), and using the relations

$$(f,l_z \mid 3z^2-r^2 \mid f,l_z) = -\tfrac{4}{5}\langle r^2\rangle \sqrt{\tfrac{7}{3}}(-1)^{3+l_z}(33-l_zl_z;\, 3320),$$

$$(f,l_z \mid 35z^4-30r^2z^2+3r^4 \mid f,l_z) = \tfrac{8}{3}\langle r^4\rangle \sqrt{\tfrac{14}{11}}(-1)^{3+l_z}(33-l_zl_z;\, 3340),$$

$$(f,l_z \mid 231z^6-315r^2z^4+105r^4z^2-5r^6 \mid f,l_z) = -\tfrac{160}{13}\langle r^6\rangle \sqrt{\tfrac{7}{33}}(-1)^{3+l_z}(33-l_zl_z;\, 3360),$$

whereas $(f,l_z \mid U^k_0 \mid f,l_z) = (-1)^{3+l_z}(2k+1)^{-\frac{1}{2}}(33-l_zl_z,\, 33k0)$,

one obtains

$$(\psi_J \| \alpha \| \psi'_J) = -8\sqrt{\left(\frac{7(2J-2)!}{15(2J+3)!}\right)}(\psi_J \| U^2 \| \psi'_J), \tag{29a}$$

$$(\psi_J \| \beta \| \psi'_J) = 16\sqrt{\left(\frac{14(2J-4)!}{11(2J+5)!}\right)}(\psi_J \| U^4 \| \psi'_J), \tag{29b}$$

$$(\psi_J \| \gamma \| \psi'_J) = -640\sqrt{\left(\frac{7(2J-6)!}{429(2J+7)!}\right)}(\psi_J \| U^6 \| \psi'_J). \tag{29c}$$

The factors $(\psi_J \| \theta_k \| \psi'_{J'})$ introduced by Judd (1955a) are related to the corresponding reduced matrix elements $(\psi_J \| U^k \| \psi'_{J'})$ by similar expressions.

In view of equation (26) it is clear that simple relations exist between the operator equivalent factors of the various levels of a particular multiplet. For instance,

$$(\psi_J \| \alpha \| \psi_J) = (-1)^{J-J'}\frac{2J+1}{2J'+1}\sqrt{\frac{(2J-2)!\,(2J'+3)!}{(2J'-2)!\,(2J+3)!}}(\psi_{J'} \| \alpha \| \psi_{J'})\frac{W(LJLJ;\, S2)}{W(LJ'LJ';\, S2)}$$

and analogous results may be obtained for β and γ.

As an example of the above theory, the operator equivalent factor α for the $^2P_{\frac{3}{2}}$ level in f^3 will be calculated. The parents of (210) (11) ^2P are (100) (10) ^3F, (200) (20) ^1D and (200) (20) ^1G. Equation (27) becomes

$$((210)(11)^2P \| U^2 \| (210)(11)^2P)$$
$$= 9\{-\tfrac{1}{2}W(3131;\, 32)+\tfrac{1}{2}.\tfrac{10}{21}W(3131;\, 22)+\tfrac{1}{2}.\tfrac{11}{21}W(3131;\, 42)\} = -1/\sqrt{14}$$

From (26) and (29a),

$$(^2P_{\frac{3}{2}} \| \alpha \| {}^2P_{\frac{3}{2}}) = \frac{8}{15\sqrt{6}}W(1\tfrac{3}{2}\,1\tfrac{3}{2};\, \tfrac{1}{2}2) = \tfrac{2}{45}.$$

In cases such as this where the value of L is small, the method is extremely powerful. This is because the alternative procedure of Judd (1955*a*) requires the transition from SLS_zL_z to sls_zl_z quantization, and the number of determinantal product states that have to be examined increases rapidly as L decreases.

When two or more terms possessing the same S and L occur in a configuration, all the reduced matrix elements of the form $(f^n\tau UvSL \| U^k \| f^n\tau' U'v'SL)$ must be calculated. The results are conveniently tabulated in a square matrix. For the three ^5D states of f^6, for example, the values for $k = 2$ are given by

$$\begin{array}{c} \\ (a) \\ (b) \\ (c) \end{array} \begin{array}{c} \begin{array}{ccc} (a) & (b) & (c) \end{array} \\ \begin{bmatrix} \frac{52}{441}\sqrt{(6)} & \frac{5}{49}\sqrt{(22)} & \frac{67}{441}\sqrt{(21)} \\ \frac{5}{49}\sqrt{(22)} & \frac{11}{98}\sqrt{(6)} & \frac{2}{49}\sqrt{(77)} \\ \frac{67}{441}\sqrt{(21)} & \frac{2}{49}\sqrt{(77)} & -\frac{17}{126}\sqrt{(6)} \end{bmatrix}. \end{array}$$

It is interesting to note that if the coefficients X, Y, Z that define a particular ^5D state are put in the form

$$X = \sqrt{(\tfrac{1}{5})}\,(7x-6y)n, \quad Y = -2\sqrt{(\tfrac{33}{5})}\,yn \quad \text{and} \quad Z = -\sqrt{(\tfrac{7}{10})}\,(2x+6y+3)n,$$

then the parameters x, y, and n are identical to those used by Judd (1955*b*) to express the coefficients of the determinantal product states in the expansion of $|\,^5D, L_z = 2, S_z = 2\rangle$. Using (26) and (29*a*), and taking the value of the reduced matrix elements of U^2 tabulated above, one obtains

$$-7n^2(44x^2+288xy-420y^2+112x-84y+17)/250$$

for the operator equivalent factor α of an arbitrary mixture of $^5D_1$ states, in complete agreement with the expression previously derived by Judd (1955*b*). The values of x and y given in that paper for the lowest ^5D term lead to

$$X = -0{\cdot}196, \quad Y = 0{\cdot}771, \quad Z = -0{\cdot}606,$$

results in good agreement with those previously obtained (see equation (24)).

Having found the values of α, β and γ for a particular level, one can now express the crystal splitting in terms of the parameters A_k^q. Each A_k^q always occurs in the analysis with the corresponding $\langle r^k\rangle$ and the usual procedure is to treat the products $A_k^q\langle r^k\rangle$ as variable parameters (see, for example, Elliott & Stevens (1953) and Judd (1955*c*)). The values that these parameters can assume must be consistent with the point symmetry at a rare-earth ion in the lattice, and by choosing suitable axes, several of them can often be made to vanish. To demonstrate the general procedure the splitting of a $J = 2$ level will be calculated for a crystal field corresponding to point symmetry of the type C_{3v}. Taking the z axis along the axis of the crystal, the only non-zero parameters are $A_2^0\langle r^2\rangle$, $A_4^0\langle r^4\rangle$, $A_4^3\langle r^4\rangle$, $A_6^0\langle r^6\rangle$, $A_6^3\langle r^6\rangle$ and $A_6^6\langle r^6\rangle$. A 5×5 matrix is constructed, each row and column corresponding to a particular value of J_z. The matrix elements of the crystal field potential are now calculated. Equation (25) can be used for this purpose, though it is usually easier to find the operator equivalent factors and make use of the tables given by Stevens

(1952), Elliott & Stevens (1953) and Judd (1955*a*). The secular determinant of the 5×5 matrix breaks up into two identical 2×2 determinants,

$$\begin{vmatrix} 6\alpha A_2^0\langle r^2\rangle + 12\beta A_4^0\langle r^4\rangle - \epsilon & 3\beta A_4^3\langle r^4\rangle \\ 3\beta A_4^3\langle r^4\rangle & -3\alpha A_2^0\langle r^2\rangle - 48\beta A_4^0\langle r^4\rangle - \epsilon \end{vmatrix},$$

corresponding to J_z admixtures of the type $(2, -1)$ and $(-2, 1)$, and the linear form

$$-6\alpha A_2^0\langle r^2\rangle + 72\beta A_4^0\langle r^4\rangle - \epsilon,$$

corresponding to $J_z = 0$. The crystal splitting of the level is given by setting these expressions equal to zero and solving for the roots ϵ. No parameter of the type $A_6^m\langle r^6\rangle$ is involved since γ is zero for a $J = 2$ level; this can be seen by examining the Racah coefficient in equation (26).

It is sometimes convenient to introduce 'crystal quantum numbers' to indicate the nature of the various components of a level. All the roots that derive from the same determinant will correspond to the same crystal quantum number, and it is clear that this classification is equivalent to labelling the components of the level by the irreducible representations of the group corresponding to the point symmetry at the rare-earth ion (Bethe 1929).

7. Conclusion

The methods of Racah have been used to treat the general problem of a rare-earth ion in a crystal field. The great advantage is the avoidance of the explicit mention of determinantal product states. The number of such states that must be included in the linear combination, which is necessary to specify the state of a given LS term is often quite high, particularly when L and S are not near their maximum values. In such cases the previous methods of analysing these terms are extremely tedious. Moreover, the group theoretical methods give a greater insight into the properties of complex configurations.

It is intended that the positions of the levels that have been tabulated should be used to suggest assignments to observed groups of lines, and any tentative identifications can be checked by calculations of the crystal field splittings. A few such calculations have been performed (Judd) and will be published separately.

Owing to departures from Russell–Saunders coupling, there will be discrepancies between this theory and experiment. Estimates indicate an order of magnitude for this departure to be $3F_2$ or $1000\,\mathrm{cm}^{-1}$, although in unfavourable cases this figure will be considerably exceeded in the second half of the shell. An improvement on this would involve both the use of the intermediate coupling formulae of §5, and revised estimates of the Slater integrals F_k, which should be based on a calculated wave function for the ion in question.

The calculation of f^4 is of special interest as table 3 lists levels of three multiplicities, and it is evident that in an intermediate coupling calculation it would be inadequate to discuss only the two highest multiplicities. For this reason accurate calculations for configurations with more than four f electrons will require extensive computation.

We wish to thank Mr P. D. Preston of the Theoretical Physics Division at Harwell for the machine computation of cubic and quartic secular equations.

References

Bethe, H. 1929 *Ann. Phys., Lpz.*, (5) **3**, 133.
Biedenharn, L. C. 1952 *Tables of the Racah coefficients*, ORNL 1098.
Bleaney, B. 1955 *Proc. Phys. Soc.* A, **68**, 937.
Bleaney, B. & Stevens, K. W. H. 1953 *Rep. Progr. Phys.* **16**, 108.
Condon, E. U. & Shortley, G. H. 1935 *The theory of atomic spectra*. Cambridge University Press.
Elliott, R. J. & Stevens, K. W. H. 1953 *Proc. Roy. Soc.* A, **219**, 387.
Jørgensen, C. K. 1955*a* *K. danske vidensk. Selsk. Mat. Fys. Medd.* **29**, no. 11.
Jørgensen, C. K. 1955*b* *Acta chem. scand.* **9**, 540.
Judd, B. R. 1955*a* *Proc. Roy. Soc.* A, **227**, 552.
Judd, B. R. 1955*b* *Proc. Roy. Soc.* A, **228**, 120.
Judd, B. R. 1955*c* *Proc. Roy. Soc.* A, **232**, 458.
Judd, B. R. 1956 *Proc. Phys. Soc.* A, **69**, 157.
Racah, G. 1942 *Phys. Rev.* **62**, 438 (referred to as II).
Racah, G. 1943 *Phys. Rev.* **63**, 367 (referred to as III).
Racah, G. 1949 *Phys. Rev.* **76**, 1352 (referred to as IV).
Rao, K. S. 1950 *Indian J. Phys.* **24**, 296.
Reilly, E. 1953 *Phys. Rev.* **91**, 876.
Satten, R. A. 1953 *J. Chem. Phys.* **21**, 637.
Sayre, E. V. & Freed, S. 1956 *J. Chem. Phys.* **24**, 1213.
Simon, A., Vander Sluis, J. H. & Biedenharn, L. C. 1954 *Tables of the Racah coefficients*, ORNL 1679.
Stevens, K. W. H. 1952 *Proc. Phys. Soc.* A, **65**, 209.

PRINTED IN GREAT BRITAIN AT THE UNIVERSITY PRESS, CAMBRIDGE
(BROOKE CRUTCHLEY, UNIVERSITY PRINTER)

THE PHYSICAL SOCIETY
REPRINTED FROM THE
REPORTS ON PROGRESS IN PHYSICS, VOL. XXI, p. 30, 1958

ABSORPTION AND FLUORESCENCE SPECTRA OF IONS IN CRYSTALS

BY

W. A. RUNCIMAN
Atomic Energy Research Establishment, Harwell, Berks.

ABSORPTION AND FLUORESCENCE SPECTRA OF IONS IN CRYSTALS

By W. A. RUNCIMAN

Atomic Energy Research Establishment, Harwell, Berks.

CONTENTS

Abstract. The absorption and fluorescence spectra provide direct information about the energy levels of the ions in a crystal. Alternatively, the ions may be regarded as probes measuring the crystalline field. The introduction deals with the influence of the crystal on the energy levels of the free ions. After a brief description of the experimental techniques, which include measurements down to 1°K, the various ion groups are considered in some detail. Ions of the 3d group are often in approximately octahedral surroundings, and the spectra of such complex ions are described. Then the 4d and 5d groups are discussed. The theory of the spectra of rare-earth salts is reviewed with special reference to polarization and Zeeman effects, and the individual ions are considered. Lastly there are two sections devoted to the heavy metal ions, including thallium, and to uranium and the transuranics, which are of interest because of the importance of the 5f electrons in the interpretation of the spectra.

§ 1. Introduction

The study of the optical spectra of crystals is one of the oldest branches of spectroscopy, and some of the substances found to be of interest in the late nineteenth century, e.g. ruby and the uranyl salts, are still actively investigated today. Since optical absorption is essentially a process in which a *quantum* of light is absorbed, it is not surprising that theoretical understanding was delayed

until quantum mechanics was established in the nineteen-twenties. However, physicists were being attracted to new fields (neutrons have a lot to answer for!), and most of the investigations into luminescent materials of the next twenty years were largely empirical, often stimulated by the growing needs of industry for fluorescent materials. The vast body of experimental material available has been most ably collected and presented by Pringsheim (1949). The luminescence of solids has attracted a lot of attention, and books by Kröger (1948) and Garlick (1949) are also recommended, the latter being particularly useful as a guide to the wider topic of the physical properties, e.g. photoconductivity, of luminescent materials.

This report will attempt to cover the years since the above-mentioned volumes appeared. This is a most significant period, as the results of paramagnetic resonance experiments provided a great stimulus to the understanding of the effects of crystalline and magnetic fields on the energy levels of ions. Many of the same substances are of interest for optical and paramagnetic resonance research, as ions with incomplete electronic shells have a large number of energy levels in the optical region. Paramagnetic resonance techniques can only find low-lying energy levels ($\sim 0{\cdot}1$ cm^{-1}); whereas for optical absorption and fluorescence both low and high energy levels are involved (0 to 50 000 cm^{-1}). Nevertheless the two techniques yield inter-related results as the splitting of the lowest energy levels is often related to the nature and spacing of the excited states. For an account of paramagnetic resonance techniques and results, reference may be made to two earlier reports in this series (Bleaney and Stevens 1953, Bowers and Owen 1955). The corresponding optical data have been tabulated by Hellwege (1955). However, certain substances containing heavy metal ions, e.g. thallium-activated potassium chloride KCl(Tl), and also some compounds containing complex ions, e.g. tungstates, have non-degenerate ground states, and therefore no paramagnetic resonance spectrum, but they can still be studied optically.

The interest in the absorption and fluorescence spectra in solids is two-fold. First it can give information about the energy levels in the ions, and secondly the ions may be considered as probes which can be used to study the crystalline field. Attention will be focused in this review on the former method of approach, as the use of ions as probes depends not only on a knowledge of the energy levels of the ions, but also on their wave functions which have in many cases not yet been calculated. The problem of the interpretation of fluorescence and absorption spectra is a dynamic one as the crystal is vibrating, even if low temperatures are employed to minimize this. Furthermore there may be interaction between absorption centres which will affect the spectra. These effects complicate the analysis of results, but increase the possible scope of optical methods in solid-state research. In order to place the individual problems in perspective, the properties of free ions will be briefly outlined, followed by a discussion of the effects due to the crystal field.

Unfortunately it will not be possible to include an account of irradiation effects. The irradiation colours and luminescence in minerals have been recently described by Przibram (1956). Many interesting problems are raised by the fluorescence of minerals, an example being the origin of the vibrational structure in the sulphur-containing aluminosilicates of the sodalite type (Kirk 1954).

1.1. *Free Ion Spectra*

The energy levels of a free ion, i.e. an ion not embedded in a crystal, are dependent on the Coulomb interaction between electrons, and also on the electronic spin–orbit interaction. If the spin–orbit interaction is small, the Russell–Saunders (LS) scheme is applicable in which energy levels are labelled by the total orbital angular momentum L and the total spin S, in addition to the total angular momentum J, where $\mathbf{J} \equiv \mathbf{L} + \mathbf{S}$. J is always a *good* quantum number for the free ion, since the interactions within the ion only mix states with the same J value.

The total orbital angular momentum is denoted by a letter according to the convention :

$L =$	0	1	2	3	4	5	6	7	8	9	10
	S	P	D	F	G	H	I	K	L	M	N

The spin multiplicity, which is equal to $2S+1$, is written as a prefix and the total angular momentum J as a suffix, e.g. $^3P_2$ stands for a state with $L = 1, S = 1$, $J = 2$. We will not need to be concerned with cases where the spin–orbit interaction dominates and the j–j coupling scheme applies ; but for all the heavier elements there is appreciable spin–orbit interaction. Therefore, although LS labels are useful, detailed calculations have to include spin–orbit interaction in the intermediate coupling approximation. These energy levels schemes are fully described by Condon and Shortley (1935), who give methods for calculating the energy levels.

The ground state of an ion can be rapidly determined by Hund's rules if the electronic configuration is known. These rules state that of all the terms allowed by the Pauli principle, the lowest term will be one of maximum multiplicity. Of those terms with maximum multiplicity, that one with the greatest L value will be lowest. Furthermore for configurations consisting of electrons in a less than half-filled subgroup the spin–orbit splitting is usually normal, i.e. smallest J lowest ; and for configurations with more than a half-filled subgroup the multiplets are usually inverted. As an example, the Pauli principle allows ^{1}SDGI and ^{3}PFH for the configuration f^2, neglecting as always any completely filled subgroups. The ground state in accordance with Hund's rule is $^3H_4$. (Warning : Hund's rules are *not* to be applied to excited states.)

Electric dipole transitions either in absorption or emission can occur for the free ions when the selection rules permit. These are $\Delta J = 0, \pm 1$ (*not* $0 \longleftrightarrow 0$) ; and in addition if LS coupling holds, $\Delta S = 0$, $\Delta L = 0, \pm 1$ (*not* $0 \longleftrightarrow 0$). Laporte's rule states that the parity of the ionic state must also be changed for an allowed transition. The parity is even if the arithmetic sum of the angular momenta of the individual electrons, Σl, is even, and odd if this sum is odd. The half-life of an excited state is about 10^{-8} sec for a free ion if it is capable of an allowed transition to a lower state, the energy difference between states being assumed such that the emitted radiation will be in the visible or near visible spectral range. In inorganic fluorescent materials the half-lives are usually longer than this ($\sim 10^{-7}$–10^{-2} sec), and it is to be expected that the transitions will often be forbidden on the basis of the above selection rules for free ions.

Transitions which are forbidden by the electric dipole selection rules are sometimes observed in free ion spectra. Weak electric quadrupole and magnetic

dipole transitions can occur between states with the same parity. For electric quadrupole transitions, the selection rules are

$$\Delta J \leqslant 2, \quad (not\ 0 \rightarrow 0,\ 1)$$
$$\Delta L \leqslant 2, \quad (not\ 0 \rightarrow 0,\ 1).$$

The corresponding selection rules for magnetic dipole transitions are

$$\Delta J \leqslant 1 \quad (not\ 0 \rightarrow 0)$$
$$\Delta L \leqslant 1 \quad (not\ 0 \rightarrow 0).$$

The selection rules on L only apply for Russell–Saunders coupling.

1.2. *The Static Lattice*

Luminescent solids may consist either of pure compounds or of impurity-activated materials. As there are many new features when an ion is embedded in a crystal, first consider the simplified model of a static lattice, in which all vibrational effects are neglected.

The energy levels of the ion will have their $(2J+1)$-fold degeneracy either partially or completely removed by Stark splitting in the electric crystalline field. Now all the energy levels will have new crystal quantum numbers which can be used to label the states. These crystal quantum numbers will be associated with the irreducible representations belonging to the point group of the ion site in the crystal. For instance, if the crystal field is strong, the orbital angular momentum L will be *quenched*, and hence will cease to be a good quantum number for labelling states. Nevertheless, the total spin S may still be a good quantum number, as the spin–lattice interaction (Bleaney and Stevens 1953) is usually small.

The transitions observed in the solid state are often between states of the same parity. These could be, but very rarely are, transitions of the magnetic dipole or electric quadrupole type. Instead, in a crystal field which has no centre of symmetry the state of an electronic configuration will get mixed with states of different parity, and this will enable electric dipole transitions to take place even between two states of the same nominal configuration. Such transitions are sometimes called forced electric dipole. For ions at a centre of symmetry, asymmetric vibrations can enable electric dipole transitions to occur (Van Vleck 1937).

The site symmetry of the ion may be reduced from that in the pure crystal if the ion is present as an impurity. Firstly, if the ion has a degenerate ground state in the crystal field, then the Jahn–Teller theorem asserts that the lattice configuration is unstable and the lattice will distort, thus lowering the symmetry in the neighbourhood of the ion. Secondly, if an impurity ion is of different valency from the ion which it replaces in the pure crystal, then the symmetry may be lowered by associated defects locally compensating the excess charge.

When an ion in a pure crystal is highly excited it may lose an electron to another ion. This is the cause of the charge transfer spectra which lead to strong absorption in the ultra-violet. If all the ions in the crystal have an inert gas configuration in the ground state, then the solid will have no visible absorption and this fundamental absorption will occur at wavelengths shorter than the absorption edge, $\sim$2000Å. Such materials are obviously good base materials for incorporating impurity ions which do have a detailed absorption in the visible range, 4000–7000Å.

Owing to the high density of solids as compared with gases, even forbidden transitions can cause appreciable absorption when impurity ions are incorporated in solids.

When an electron is excited to such an extent that it is freed from its ion, it is normally in a conducting state ; but in some compounds it is possible for the electron to travel through the lattice bound to a compensating *hole*. This combination is called an *exciton*. The absorption and fluorescence spectra of excitons have much in common with those of ions, but always occur just to the long wavelength side of the absorption edge. Cu_2O and HgI_2 have well-defined exciton spectra, but it is still not clearly demonstrated that the spectra are independent of impurities in the crystal.

1.3. *The Adiabatic Approximation*

The above model of an ion embedded in a static lattice is useful if the electronic transition to be considered does not change the surroundings of the ion. This is especially true for the rare-earth ions, where the 4f electrons responsible for the absorption and emission spectra are shielded from the neighbouring ions by 5s and 5p electrons. In these circumstances the absorption energy which raises the ion to its lowest excited states is the same as the fluorescence energy from these states. This leads to well-defined lines in the absorption and fluorescence spectra.

On the other hand, when the outer electrons are involved in an electronic transition, there will usually be a change in the effective radius of the ion. The transition will induce lattice vibrations which will result either in a vibrational structure being observable in the spectra or else in the appearance of very broad bands. The dissipation of some of the absorbed energy thermally accounts for Stokes' law which states that fluorescent emission occurs at wavelengths equal to or longer than the absorption wavelength.

A full treatment of the optical excitation of an impurity ion in a crystal is so complex that it is fortunate that approximations can often be usefully employed. The adiabatic or Born–Oppenheimer approximation depends on the small ratio of the electronic to nuclear mass, and uses this to separate out the calculation of electronic and nuclear motions. In this approximation the nuclei can be considered as vibrating in the averaged potential of the electrons. The adiabatic approximation is valid so long as the spacing between the electronic energy levels is large compared with the vibrational energies, since otherwise the vibrations cause a mixing of the electronic states. Hence if an electronic energy level is degenerate, the adiabatic approximation will break down. This will be the case if an ion which is a constituent in a pure solid is excited, since the energy is the same as that obtained if any of the other ions were excited. This may lead to an increase in the number of lines in the absorption spectrum. The splittings (Davydov splitting) so produced, though large in some organic crystals, are usually negligible in inorganic crystals due to the forbidden nature of the electronic transitions involved. Unresolved splittings can however contribute to the line widths of absorption and fluorescent lines.

The adiabatic approximation is the basis for the configuration coordinate model. The positions of the nuclei are represented by a single variable x, e.g. the distance of the nearest neighbours from the impurity ion. The potential energy of the nuclei in the ground electronic state is shown as a function of x by

curve FAG in figure 1. Similarly in the excited state the nuclei move in a potential well FCH. In the harmonic approximation the potential energy curves are parabolic. The energy levels of the centre are represented by horizontal lines the lowest of which is a little above the minimum of the parabola on account of the zero-point energy. The higher lines refer to states in which some vibrational quanta are present. The wave function of the nuclear motion is approximately Gaussian for the lowest state, and has the largest values near the parabola for a highly excited state as shown in figure 1.

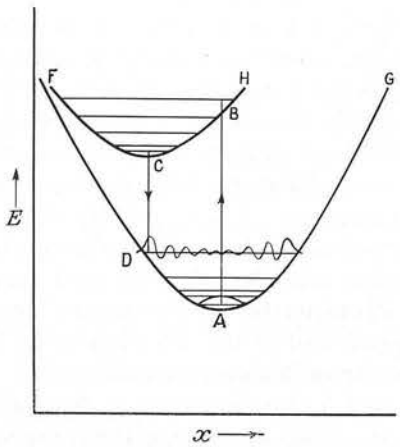

Figure 1. Configuration coordinate diagram.

The Franck–Condon principle states that during an electronic transition the positions and momenta of the ions will be substantially unchanged, owing to the large ratio of ionic masses to the electronic mass. Hence on figure 1 electronic transitions are shown as vertical lines, AB for absorption and CD for emission. After the absorption of light AB, the centre will relax BC to the new equilibrium position C, some of the vibrational energy being dissipated thermally to the rest of the lattice. Similarly heat is dissipated after fluorescence CD, while the centre relaxes to its original state. It follows that the fluorescence is normally at longer wavelengths than the absorption.

This configuration coordinate diagram has been used by Dexter, Klick and Russell (1955) to formulate a criterion for luminescence. If the intersection of the parabolae at F is lower than the point B reached on the upper parabola when energy is absorbed, then they suggest that the vibrations are sufficiently undamped for the configuration to cross to the other side of the parabola near F. It will then transfer to the lower parabola without emitting radiation before equilibrium at C can be reached.

This suggestion seems valid provided restrictions due to spin or spatial symmetry do not prevent the radiationless cross-over at F. The situation is obscure near F due to the breakdown of the adiabatic approximation whenever electronic levels are near-degenerate.

In general, fluorescence is more probable for a large energy gap between the upper and lower states, as the transition probability for radiation is proportional

to the cube of the radiation frequency, whereas radiationless transitions decrease in probability, as more vibrational quanta are needed to dissipate the energy. A spin change may only be effected by lattice vibrations through the spin–orbit interaction, hence there may be a rule for inorganic materials that the fluorescent state, if one exists for the system in question, is the lowest state with spin differing from the ground state. Fluorescence may be absent if this excited state is heavily mixed with a state whose spin is the same as that of the ground state.

§ 2. Experimental Methods

The absorption spectrum of a single crystal is obtained by analysing a light beam, originating from a source with a continuous energy spectrum, after it has traversed the crystal. Black body radiation is useful in the visible and infra-red, and the source most commonly used is the 6 volt, 18 amp, ribbon-filament lamp. For wavelengths below 3400 Å a hydrogen lamp with a quartz window is necessary. Xenon arcs and zirconia lamps have also been used to obtain continuous spectra, but are more difficult to operate.

The spectra are either recorded photographically or photoelectrically. As the sources are of only moderate intensity, all high-resolution work has so far been done photographically. Photoelectric measurements have been obtained in the visible using photomultipliers and in the infra-red using lead-sulphide cells, and are to be preferred if intensity measurements are required. Glass or quartz prism spectrographs have been used for low or moderate dispersion,† and grating instruments for high dispersion, e.g. Dieke and Singh (1956) obtain a first-order dispersion of 1·2 Å mm^{-1} using a 21 ft concave grating spectrograph. Wavelength measurements are made by comparison with a standard source, e.g. an iron arc.

If crystals have less than cubic symmetry, further information can be gained by inserting a polarizer into the light path. A Nicol calcite polarizer can be used, or a quartz double prism of the Wollaston type if both polarization spectra are to be photographed simultaneously. For wavelengths below 3000Å, the components are usually joined with glycerin or castor oil rather than Canada balsam ; but gedamine provides an adhesive useful to 2500Å (Bouriau and Lenoble 1957). Cubic crystals can be studied using polarized light if the intensity of the radiation is measured in different directions (Feofilov 1956 a).

For Zeeman work, a magnetic field of 25–40 kilogauss is necessary, as, owing to the natural line width, it is not possible to resolve the components with smaller fields. A pole gap of about 1 inch is needed to accommodate the crystal and cryostat. A typical iron-core magnet satisfying these requirements weighs over two tons, and dissipates 18 kw of power (Bowen 1957).

Most of the apparatus is the same for fluorescence, except that instead of irradiating with a continuous source, one irradiates preferentially in a wavelength region where there is a high excitation probability. Low pressure and high pressure mercury vapour lamps produce short wavelength (2537Å) and long wavelength (3650Å) ultra-violet radiation respectively. The high pressure lamp can be obtained with a coloured glass outer bulb, then known as a *black* lamp, to filter

† Quartz optics can give absorption bands a spurious banded structure, due to the optical rotation of the quartz (Ellis and Kaplan 1935, 1937). This appears if the incident light is polarized either by the dichroism of a crystal or by the use of a conventional polarizer.

out the visible radiation. If required, the residual near infra-red radiation it emits can be filtered out with a copper sulphate solution (125g $CuSO_4.5H_2O$ per litre of water) as recommended by Bowen (1946).

The crystal under investigation is often cooled to liquid oxygen (90°K), nitrogen (77°K), hydrogen (20°K) or helium (4·2°K) temperatures. In the case of liquid helium, a double Dewar is used, the outer containing liquid nitrogen or oxygen. Temperatures down to 1°K may be obtained by keeping the helium at reduced pressure.

If single crystals are not available the spectra from powder samples can yield valuable information, the fluorescence spectrum being obtained normally, and the absorption spectrum being replaced by a similar reflection spectrum. However, it is not usually possible to obtain polarization or Zeeman spectra from powders. For work at low temperatures, the powders can be inserted in glass or quartz tubes, containing helium at a few millimetres of mercury pressure to remove heat from the powder. Single crystals are grown from the melt or from solution, whereas activators are often incorporated in powders by heating in a furnace, sometimes in a controlled atmosphere.

§ 3. Ions with an Incomplete d-shell

3.1. *The Octahedral Complex*

Ions of the 3d, 4d and 5d groups often occupy sites of six-fold coordination, the surrounding ions being arranged in nearly octahedral symmetry. The crystal field is strong enough to perturb and sometimes to dominate the effect of the Coulomb forces in the ion. In a strong field the five magnetic substates of a d-electron, each double because of spin, are split into a triplet capable of accommodating six t_{2g} electrons and a doublet for four e_g electrons. The separation between the possible energy levels will be denoted by Δ (Owen 1955) and replaces the older $10Dq$. In octahedral surroundings the triplet is lower than the doublet, whereas the reverse is true for a tetrahedral arrangement of negative ions around the central ion. These t_{2g} and e_g orbitals are described by Bowers and Owen (1955), who also give a brief description of the crystallography of many transition metal salts. Hush and Pryce (1957) have shown that irregularities in the ionic radii of iron group ions are due to the different occupation of the two types of orbital.

Tanabe and Sugano (1954 a, b) and Orgel (1952, 1955 a, b, c, d) have calculated the effect of a cubic field on the energy levels of ions with an electronic configuration d^n. The results are best shown graphically, and as an example the energy level diagram for d^3 is shown in figure 2. The energy ordinate E and the strength of the crystal field Δ are both in units of B, a linear combination of Slater integrals introduced by Racah. At the left-hand side are the Russell–Saunders levels and at the right are the values for a strong field. Irrespective of the crystal field strength, the spin and the symmetry are good quantum numbers. The symmetries are labelled by the irreducible representations of the cubic group A_1, A_2, E, T_1 and T_2, where A is singly, E doubly and T triply degenerate.

A strong crystal field will sometimes alter the spin and spatial symmetry of the ground state, but not for d^3, figure 2, which always has a $^4A_2$ ground state

independent of field strength. Since energies are measured relative to the ground state this change in the character of the ground state, when it occurs, causes a discontinuity in the slope of the energy levels in the diagram. In weak or medium fields the spin of the ground state is the maximum possible in accordance with Hund's rules ; but in strong fields the spin is only the maximum consistent with first filling all the t_{2g} states before any e_g states.

The octahedral surroundings of the ion will be distorted by the Jahn–Teller effect if the ground state of the ion in a cubic field is degenerate. This effect has been studied recently by Öpik and Pryce (1957) and by Orgel and Dunitz (1957), and has been shown to be large in some cases, especially for cupric salts.

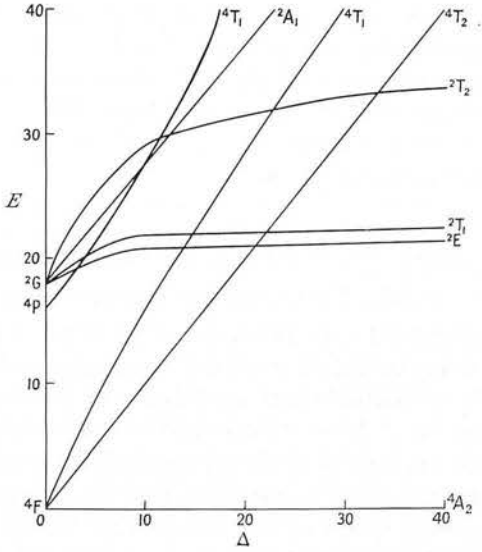

Figure 2. Energy diagram for d^3 in a cubic field.

However, there may also be considerable distortions of the octahedral surroundings due to more general crystallographic considerations. These distortions and also spin–orbit interaction will split the levels which are degenerate in the cubic field. The spin–orbit splitting will have a first-order effect on levels of symmetry types T_{1g} and T_{2g}. Second-order effects will usually remove all degeneracy, except that for ions with an odd number of electrons the levels will consist of Kramer's doublets even in fields of lowest symmetry. Some aspects of ions containing d-electrons in fields of less than cubic symmetry have been theoretically investigated by Ballhausen and Jørgensen (1955). For a more general account of crystal field theory applied to d-electrons reference may be made to the review of Moffitt and Ballhausen (1956).

The line-width of an absorption line will be small if the energy level of the excited state is parallel or near parallel to the energy level of the ground state in the energy level diagram. This condition obtains for sufficiently strong crystal fields when the number of t_{2g} and e_g electrons is the same for both the ground and excited state. For example, in figure 2 this is true for the states ^2E, $^2T_1$ and $^2T_2$ which have the same configuration t_{2g}^3 as the ground state $^4A_2$. The ionic radius

is not then appreciably affected by the transition, and hence the transition will not excite many vibrations in the lattice. Furthermore the thermal and zero point energy of the lattice will cause a variation in the effective crystal field strength when the electronic transition takes place, and, if the lines in the energy level diagram are not parallel, this will lead to a broadening of the absorption line. It follows from this criterion that transitions from the ground state which involve no spin change are always broad. They are also the strongest transitions, since they are the least forbidden, and may obscure any narrow lines due to intersystem transitions. Ballhausen (1955) and Liehr and Ballhausen (1957) have considered the effect of symmetry on the intensities of the absorption bands of octahedral complexes.

When detailed calculations are made of the splitting of energy levels in the crystal, the parameters have to be modified from those of the free ion to include the effects of covalent bonding. Owen (1955) has given a detailed discussion for some hydrated salts. This generalized type of crystal field theory is now usually termed ' ligand field theory '.

3.2. *The* 3d *Group*

The various ions will now be discussed in order of the number of d-electrons which they contain. The hydrated ions have been especially studied, and most recently by Holmes and McClure (1957). After each ion will be listed the ground state, of the ion in an octahedral complex, appropriate to the weak field approximation, which applies moderately well for the hydrated salts. The splitting of the lowest *LS* state is inverted in the d^{10-n} configuration from that of d^n, and hence the ground states have the same spin, but different spatial symmetry.

d^1 : Ti^{3+}, *ground state* $^2T_2$

In a cubic field the only *LS* state ^2D splits into the ground state $^2T_2$ and an excited state ^2E. Hartmann and Schläfer (1951 a) report a single broad band peaked at 20 300 cm^{-1} which can be attributed to the transition $^2T_2 \rightarrow {}^2E$.

d^2 : V^{3+}, *ground state* $^3T_1$

Hartmann and Schläfer (1951 b) report bands at 17 800 and 25 600 cm^{-1}, which can be assigned to the transitions $^3T_1 \rightarrow {}^3T_2$ and $^3T_1 \rightarrow {}^3T_1$, as these are the transitions most likely to give rise to strong absorption bands.†

d^3 : V^{2+}, Cr^{3+}, Mn^{4+}, *ground state* $^4A_2$

The absorption spectrum can be interpreted in terms of the energy level diagram, figure 2. The main absorption bands of hydrated chromium salts are at 17 500 and 24 500 cm^{-1} and are due to transitions to $^4T_2$ and $^4T_1$ states respectively, transitions to the doublet states being weak as discussed above. Holmes and McClure (1957) have found similar bands for vanadous solutions at 11 800 and 17 500 cm^{-1}. A further band in the chromium salts at 36 600 cm^{-1} is probably due to a transition to a higher $^4T_1$ state. There are also sharp lines in the absorption

† Low (1957 a) has described a vibrational structure in the absorption band due to the transition $^3T_1 \rightarrow {}^3T_2$ and found an absorption line at 21 000 cm^{-1} in Al_2O_3(v). The author (unpublished) has resolved the line $^3T_1 \rightarrow {}^1A_1$ into two components, differently polarized, and found two further lines in the near infra-red, $^3T_1 \rightarrow {}^1E$, $^1T_2$.

spectra of chromium salts caused by transitions to the doublet states ^2E, $^2T_1$ and $^2T_2$. Spedding and Nutting (1934, 1935) found that in a magnetic field each of the three strong absorption lines of potassium chrome alum, $KCr(SO_4)_2.12H_2O$, splits into three elliptically polarized components with a separation close to the 'spin only' value, i.e. $g = 2$. The theoretical interpretation is not complete, but

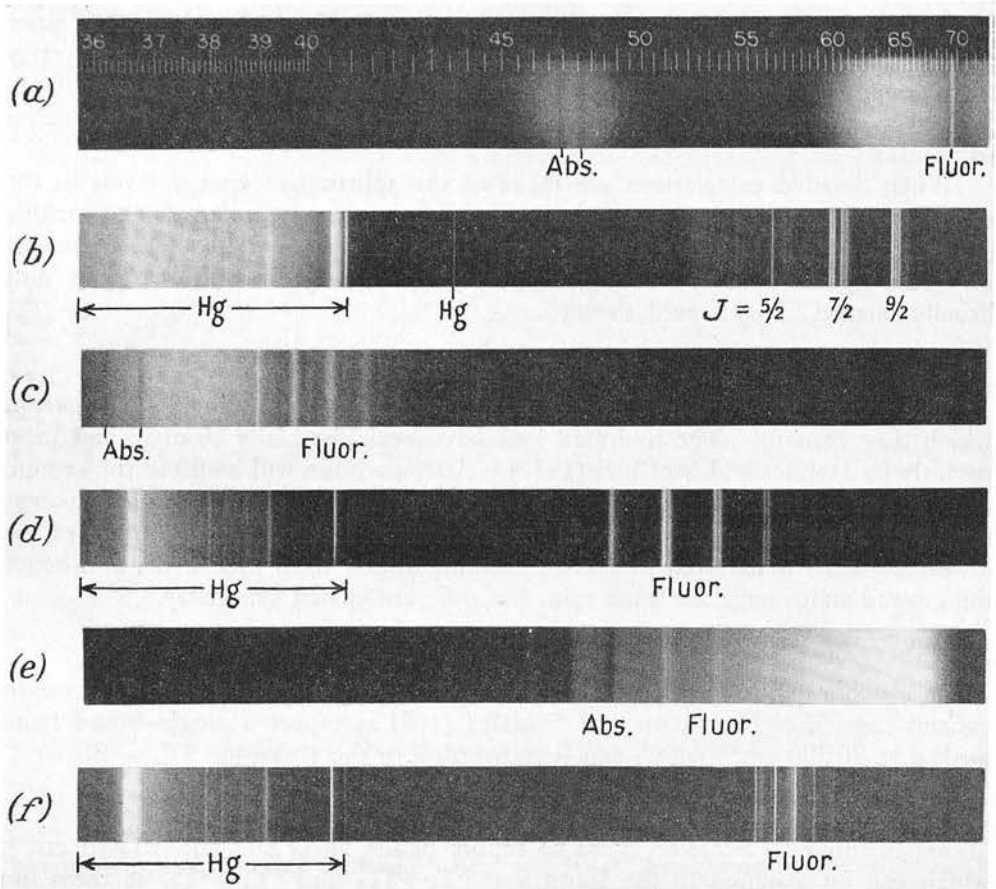

Figure 3. Crystal spectra obtained using a medium quartz spectrograph. The scale is in units of 100Å. (*a*) Absorption spectrum of ruby at room temperature. (*b*) Fluorescence spectrum of CaO(U, Sm) at 77°K. (*c*) Absorption spectrum of CaO(Bi) at 77°K. (*d*) Fluorescence spectrum of uranyl nitrate hexahydrate at 77°K. (*e*) Absorption spectrum of uranyl nitrate hexahydrate at 77°K. (*f*) Fluorescence spectrum of NaF(U, O) at 77°K.

calculations by Van Vleck (1940) and by Finkelstein and Van Vleck (1940) demonstrate that the upper state is a doublet. Couture, Jacquinot and Tsujikawa (1956) have found complicated changes in the absorption spectrum of ammonium chrome alum at the transition temperature, *c.* 80°K, and Couture (1957) finds similar effects in potassium chrome alum at 60°K. Low (1957 b) has described the paramagnetic resonance and optical spectra of Cr^{3+} in MgO.

There have been many investigations of the absorption and fluorescence spectra of ruby, $Al_2O_3(Cr)$. Two lines at 14 450 and 14 420 cm^{-1} appear in both

fluorescence and absorption. The upper energy levels in these transitions are two components of the ^2E state, split by the combined effect of spin–orbit interaction and a trigonal component of the crystal field (Tanabe and Sugano 1957). Krishnan (1947) has compared the frequency shifts of vibrational satellites to the above lines with infra-red and Raman frequencies. Deutschbein (1939) has studied the fluorescence of chromium-activated solids down to 1·6°K and has shown that the levels are populated in accordance with a Boltzmann distribution. Slight shifts ($\sim 0{\cdot}1$ cm^{-1}) have been detected by Deutschbein, Joos and Teltow (1942) between the centres of the absorption and emission lines.

The absorption lines between 4600 and 4800Å (figure 3 (*a*)) in ruby are attributable to transitions to $^2T_2$ levels. The polarization of these and the other absorption and fluorescence lines has been studied by Mani (1942). Grechushnikov and Feofilov (1955) have observed a vibrational fine structure in the main absorption band between 5500 and 6000Å when ruby is cooled to liquid nitrogen temperatures.

Prener (1953) has reported a low temperature fluorescence of MgO (Mn, Li). The fluorescence of the tetravalent manganese is analogous to that in chromium-activated solids.

d^4 : Mn^{3+}, Cr^{2+}, *ground state* ^5E

Hartmann and Schläfer (1951 b) find a single absorption band at 21 000 cm^{-1} in $CsMn(SO_4)_2.12H_2O$. Similarly there is an absorption band at 13 900 in $CrSO_4.7H_2O$. Both these may be assigned to the transition $^5E \rightarrow {}^5T_2$.

d^5 : Mn^{2+}, Fe^{3+}, *ground state* $^6A_1$

The ground state is the only sextet state, d^5 being a half-filled shell, and hence it is to be expected that all absorption bands will be weak. Because of this weakness, Holmes and McClure (1957) investigated the spectra of the ions in solution, finding bands at 18 900 and 23 000 cm^{-1} for Mn^{2+} solutions and bands at 12 500 and 18 200 cm^{-1} for Fe^{3+} solutions. These correspond to transitions to the $^4T_1$ and $^4T_2$ states respectively for each ion. Gielessen (1935) observed line spectra in solid $MnCl_2.4H_2O$, and Pappalardo (1957 b) has attributed line groups in manganese salts to transitions to the upper states as follows: 25 000 (^4A, and ^4E_a), 27 000 ($^4T_2$) and 29 000 cm^{-1} (^4E_b).

Divalent manganese is an extremely efficient luminescent activator in a wide variety of chemical systems. In cubic surroundings the upper state for fluorescent transitions belongs to the $^4T_1$ representation. The fluorescence spectrum consists of a single band, often in the green or orange, which is appreciably asymmetric. As has been pointed out by Klick and Schulman (1952), this asymmetry can arise if the parabolae of figure 1 are only slightly displaced from each other in the horizontal direction.

The configuration d^5 consisting of a half-filled shell has a ground state which is only split because of high-order perturbations. The resultant small splittings have been investigated by paramagnetic resonance (Bleaney and Stevens 1953, Bowers and Owen 1955).

d^6 : Fe^{2+}, *ground state* $^5T_2$

Holmes and McClure (1957) report a band at 10 000 cm^{-1} in $FeSO_4.7H_2O$ which is just resolved into a double peak. Dreisch and Kallscheuer (1944) had

earlier obtained similar results from ferrous chloride solutions, and in each case the bands are probably due to $^5T_2 \rightarrow {}^5E$ transitions.

$d^7 : Co^{2+}$, *ground state* $^4T_1$

Holmes and McClure (1957) find an absorption band at 8350 cm^{-1} due to the transition $^4T_1 \rightarrow {}^4T_2$, and also another band at 19 800 cm^{-1}, resolvable into four components at liquid nitrogen temperature, which they attribute to a superposition of the transitions $^4T_1 \rightarrow {}^4A_2$ and $^4T_1 \rightarrow {}^4T_1$. Gielessen (1935) has studied a wide variety of cobaltous salts at 84°K and found a detailed line spectrum which varies appreciably from salt to salt, and is possibly due to transitions to the doublet states $^2T_1$ and $^2T_2$. Low (to be published) has reported optical and paramagnetic resonance spectra of divalent cobalt in single crystals of MgO and has found no appreciable Jahn–Teller distortions from octahedral symmetry.

$d^8 : Ni^{2+}$, *ground state* $^3A_2$

$NiSO_4.7H_2O$ has three absorption bands at 8600, 14 700 and 25 500 cm^{-1} which are attributed to transitions to the upper states $^3T_2$, $^3T_{1a}$ and $^3T_{1b}$ respectively by Holmes and McClure (1957), in accordance with an earlier analysis of the experimental results by Tanabe and Sugano (1954 b). Gielessen (1935) found a detailed line spectrum in $NiCl_2.6H_2O$ at 84°K in the frequency range 17 000–21 000 cm^{-1}. Pappalardo (1957 a) has observed that the spectra of nickel salts change on cooling from 77°K to either 4°K or 20°K. He attributes line groups near 16 000 and 24 000 cm^{-1} to transitions to ^1E and $^1A_1$ levels respectively. Low (to be published) has obtained and analysed the spectrum of divalent nickel in single cystals of MgO.

$d^9 : Cu^{2+}$, *ground state* ^2E

The single absorption band at 12 200 cm^{-1} in $CuSO_4.5H_2O$ is due to the only transition within the d^9 configuration, $^2E \rightarrow {}^2T_2$. The two-fold degenerate ground state leads to a complicated Jahn–Teller distortion which has been discussed by Öpik and Pryce (1957) and by Orgel and Dunitz (1957). The optical spectra of the deformed complexes have been described by Bjerrum, Ballhausen and Jørgensen (1954), and the theory further developed by Ballhausen (1954).

3.3. *The* 4d *Group*

This group has not been so extensively studied as the 3d group ; but two main classes have received considerable attention.

(*a*) *Molybdates.*

There is a full discussion of the absorption and fluorescence of the molybdates in Kröger (1948). For example, $CaMoO_4$ at 180°c has a broad absorption band whose low energy edge is about 34 000 cm^{-1} and has a fluorescent band at 18 700 cm^{-1}.

(*b*) *Palladium salts.*

Yamada (1951) has shown that the absorption of the planar complexes in K_2PdCl_4 and other salts has a marked dichroism, which he uses in a discussion of the origin of the absorption bands.

3.4. *The* 5d *Group*

This group is in many ways similar to the 4d group, and discussion will be restricted to two main classes as before.

(*a*) *Tungstates.*

The tungstates are also described in detail by Kröger (1948). $CaWO_4$ at $-180°$C has an absorption edge at 41 000 cm^{-1} and an emission peak at 23 800 cm^{-1}. Hameka and Vlam (1953) have derived the configuration coordinate diagram suitable for calcium tungstate.

(*b*) *Platinum salts.*

Yamada (1951) has investigated the dichroism of small crystals of K_2PtCl_4 and other salts with planar complexes.

3.5. *Covalent Complexes*

Some salts, especially the cyanides, have ground states with spins in accordance with the strong field approximation. The t_{2g} orbitals fill first, and with six d-electrons this sub-group is complete. Hence for the configuration d^6 the ground state is $^1A_1$ and the salt is diamagnetic, e.g. $K_3Co(CN)_6$. No salts of this strong field type are known for ions with more than six d-electrons. Owen (1955) has found it necessary to postulate a covalent character in the cyanides to explain the experimental results quantitatively.

The manganate $(MnO_4)^{2-}$, permanganate $(MnO_4)^-$ and chromate $(CrO_4)^{2-}$ ions have complex spectra (Teltow 1938, 1939), especially when present in mixed crystals, e.g. $K_2(S, Mn)O_4$ and $K(Cl, Mn)O_4$. The electronic structure and spectra of the tetrahedral permanganate and chromate ions have been theoretically studied by Wolfsberg and Helmholz (1952).

§ 4. Rare-earth Ions

4.1. *Outline of Theory*

The trivalent rare-earth ions have long been known to have absorption spectra, and in some cases fluorescence spectra, consisting of groups of lines. References to the earlier literature will be found in the books by Pringsheim (1949) and by Yost, Russell and Garner (1947). A single level in the free ion, characterized by total angular momentum J, is split by the crystal field (Stark effect) to produce a group of levels. Each group of lines corresponds to transitions to such a group of levels. The number of levels into which a given level of the free ion is split by the crystal field can be derived by the group-theoretical methods of Bethe (1929). The results for the 32 crystallographic groups have been summarized (Runciman 1956 a). The point groups are classified under four headings : (*a*) cubic groups, (*b*) hexagonal and rhombohedral, (*c*) tetragonal, and (*d*) orthorhombic and lower symmetry groups. The levels are then split as shown in table 1.

Judd (1957 a) has found it helpful in some cases to consider the splitting which would occur in icosahedral symmetry and then to find the effects of the deviations from this idealization. From a detailed consideration of the wave functions, Hellwege (1948) has derived selection rules for absorption by polarized light. Unfortunately these selection rules are often apparently violated because of effects

due to the lattice vibrations. The vibration–electronic interaction has been considered by Satten (1957), with special reference to the spectra of neodymium salts. Because of this difficulty in interpreting the crystal spectra, Elliott, Judd and Runciman (1957) have calculated the energy levels of the multiplets in the Russell–Saunders approximation using the tensor-operator and group-theoretical methods of Racah (1949). Assignments of levels to the various line groups can be made, and tested by detailed calculations of the crystal splittings.

Table 1. Number of Levels produced by Stark Splitting of an Ion Level with Angular Momentum J in Crystal Fields of Different Symmetries

J	0	1	2	3	4	5	6	1/2	3/2	5/2	7/2	9/2	11/2
cubic	1	1	2	3	4	4	6	1	1	2	3	3	4
hexagonal	1	2	3	5	6	7	9	1	2	3	4	5	6
tetragonal	1	2	4	5	7	8	10	1	2	3	4	5	6
orthorhombic	1	3	5	7	9	11	13	1	2	3	4	5	6

The Coulomb energy of the free ion is evaluated in terms of the Slater integrals F_2, F_4 and F_6 as defined in Condon and Shortley (1935). A hydrogenic type wave function has sometimes been used (Judd 1955 b) to determine the ratios of the Slater integrals for a 4f electron, i.e.

$$F_4/F_2 = 0{\cdot}138, \quad F_6/F_2 = 0{\cdot}0151.$$

Then the Coulomb energy levels can be expressed in terms of the single parameter F_2, which in turn can be expressed as a function of the atomic number Z of the rare-earth ion by the equation (Judd 1956)

$$F_2 = 12{\cdot}4(Z-34)\ \mathrm{cm}^{-1}.$$

When the Coulomb energies are expressed in terms of F_2, the same energy level diagram holds for f^n and f^{14-n}. The lowest levels determined by Elliott, Judd and Runciman (1957) are shown in figure 4. These values are in some cases different from those found earlier by Jørgensen (1955 a), who incorporated fewer states in his calculations and used different ratios for the Slater integrals. It must be emphasized that figure 4 only gives a general indication of the energy levels, and it will be necessary to introduce appreciable spin–orbit coupling in order to get good agreement with experiment. Also it is to be hoped that calculated wave functions for the rare-earth ions will become available to avoid the necessity of a rather arbitrary choice for the Slater integrals.†

A weak spin-orbit interaction splits each of the Coulomb levels into a multiplet. The shift of a component of a multiplet from the centre of the multiplet is given by

$$\Delta\nu = \tfrac{1}{2}\lambda\xi[J(J+1)-L(L+1)-S(S+1)],$$

where λ is the spin–orbit splitting factor and ξ is the spin–orbit interaction for a single 4f electron. Bleaney (1955) has derived semi-empirical values of ξ for all rare-earth ions. The spin–orbit splitting factors are listed in Elliott, Judd and Runciman (1957) for all levels for which the Coulomb energies have been calculated,

† Dr. E. C. Ridley (unpublished) has just completed her calculations of the wave functions for Pr^{3+} and Tm^{3+} using the method of self-consistent fields, without exchange.

i.e. all levels of f^2, f^3 and f^4 and the two highest multiplicities of f^5, f^6 and f^7. The spin–orbit splitting factors for f^{14-n} are the same as those for f^n, but with reversed sign. This paper also describes how to calculate the matrix elements of the spin–orbit matrices, if it is found necessary to use intermediate coupling calculations which allow mixing of LS states.

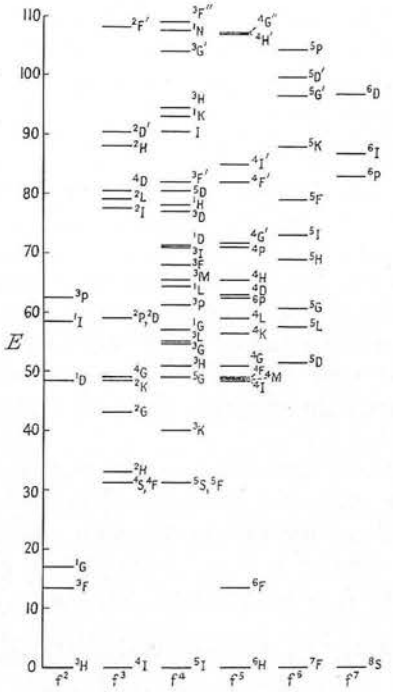

Figure 4. Energy levels of means of multiplets for f^n.

Owing to the screening of the 4f electrons by the outer electron of the rare-earth ion, the effect of the crystal field can be considered to be small so that normally we may keep J as a quantum number and calculate crystal field splittings by the methods of perturbation theory. Most of the salts which have been extensively studied have trigonal symmetry. In the ethylsulphates the rare-earth ion is on a site of C_{3h} symmetry for which the potential energy of an electron may be written

$$V = A_2^0 V_2^0 + A_4^0 V_4^0 + A_6^0 V_6^0 + A_6^6 V_6^6,$$

where the V_k^q transform like spherical harmonics Y_{kq}. The axial terms V_k^0 cause a splitting of levels with differing $|M|$, where M is the z-component of J, whereas V_k^q mixes states for which $M - M' = q$. Hence it is convenient to define a crystal quantum number μ, where $M \equiv \mu \pmod{q}$.

4.2. *Polarization Spectra*

The only transitions which are likely to occur in rare-earth spectra are electric dipole, electric quadrupole or magnetic dipole. These can be partially resolved as follows. The absorption spectrum of a uniaxial crystal is measured with the

light path parallel to the crystallographic axis for the ' axial ' spectrum, and with the light perpendicular to the axis for the transverse spectrum. The transverse spectrum is split into π and σ spectra depending on whether the axis of polarization, i.e. the direction of the electric vector, is parallel to or perpendicular to the crystal axis. If a line in the axial and σ spectra coincide the transition is electric dipole, and if the axial and π spectra coincide the transition is magnetic dipole or electric quadrupole. It is often possible to distinguish the magnetic dipole from the electric quadrupole transitions using the detailed selection rules (Hellwege 1948), and so far only magnetic dipole transitions have been positively identified, these being present in the spectrum of trivalent europium salts. Magnetic dipole transitions can only occur subject to the selection rules,

$$\Delta J \leqslant 1, \quad (not\ 0 \rightarrow 0)$$
$$\Delta L \leqslant 1, \quad (not\ 0 \rightarrow 0).$$

On the other hand, electric dipole transitions occurring because of the lack of centre of symmetry in the crystal allow changes in J and L up to seven units, owing to the admixture of states caused by crystal field terms up to order six. A rather curious feature for some electric quadrupole transitions is that they might be present for an arbitrary light direction although absent in both transverse and axial spectra.

In view of the overwhelming majority of the transitions being electric dipole, the selection rules will be presented in tabular form for two common symmetries. Table 2 shows the selection rules for C_{3h} symmetry between states characterized by the crystal quantum number $\mu_I \equiv \mu \pm \frac{1}{2} p \Sigma_k l_k \pmod{p}$, where the sum is over the f-electrons which have $l_k = 3$ and where $p = 6$ for C_{3h} symmetry.

Table 2. Selection Rules for Electric Dipole Transitions, C_{3h} Symmetry

(*a*) Even number of electrons.

μ_I	0	±1	±2	3
0			σ	π
±1		σ	π	σ
±2	σ	π	σ	
3	π	σ		

(*b*) Odd number of electrons.

μ_I	±1/2	±3/2	±5/2
±1/2		σ	σ, π
±3/2	σ	π	σ
±5/2	σ, π	σ	

For an even number of electrons, the π and σ spectra are completely different. Satten (1957) has shown that this dichroism is preserved when vibrational interactions are included. Examples where C_{3h} symmetry applies are rare-earth impurities present in anhydrous lanthanum chloride, $LaCl_3$, and rare-earth ethylsulphates, e.g. $Nd(C_2H_5SO_4)_3 . 9H_2O$.

Another common symmetry type is C_{3v} (Judd 1955 a, c), which includes the double nitrates, e.g. $Pr_2Mg_3(NO_3)_{12} . 24H_2O$, and the bromates, e.g. $Nd(BrO_3)_3 . 9H_2O$. The selection rules are as in table 3, where the auxiliary quantum number S distinguishes those states symmetrical or anti-symmetrical with respect to reflection in the vertical reflection planes.

The corresponding table for C_3 symmetry is simply obtained by dropping the auxiliary quantum number S, and hence allowing all transitions between $\mu = 0$ states with π polarization.

Table 3. Selection Rules for Electric Dipole Transitions, C_{3v} Symmetry

(*a*) Even number of electrons.

μ		0		± 1
		$S=1$	$S=-1$	
0	$S=1$	π		σ
	$S=-1$		π	
± 1		σ		σ, π

(*b*) Odd number of electrons.

μ	$\pm 1/2$	$\pm 3/2$
$\pm 1/2$	σ, π	σ
$\pm 3/2$	σ	π

4.3. *The Zeeman Effect*

For an ion which is not in a crystal field, a magnetic field introduces a term into the Hamiltonian of the form $\beta(\mathbf{L}+2\mathbf{S}).\mathbf{H} \equiv \beta(\mathbf{J}+\mathbf{S}).\mathbf{H}$ which has eigenvalues $g\beta HM$ where β is the Bohr magneton, $\equiv eh/4\pi mc$, and M is the component of $\mathbf{J}$ in the direction of the magnetic field. The value of the Landé factor g in the Russell–Saunders scheme is independent of all quantum numbers other than S, L and J and is given by

$$g = 1+\frac{J(J+1)-L(L+1)+S(S+1)}{2J(J+1)}.$$

In the intermediate coupling approximation J is still a good quantum number, and g is simply a weighted sum of the separate Landé factors for the constituent LS states (Condon and Shortley 1935).

The original theory of the Zeeman effect in crystals (Bethe 1930) has been elaborated for all 32 point groups by Hellwege (1950 a, b). If in a uniaxial crystal the magnetic field is applied parallel to the crystal axis each doublet will be split by an amount $s_1\beta H$ where the splitting factor s_1 introduced by Dieke and Heroux (1956) is the weighted sum of the splitting factors $2gM_i$ of the constituent states, i.e.

$$s_1 = 2g(a_1^2 M_1 + a_2^2 M_2 + \ldots).$$

If the axial part of the field dominates, and the magnetic field is perpendicular to the crystal axis, then for an odd number of electrons only the $M = \pm\frac{1}{2}$ level is split and that by an amount $g(J+\frac{1}{2})\beta H$.

In general, the spectrum may be complex as the crystal field may be strong enough to mix states of different J. Such effects have been included in the theory of the magnetic splittings of the ground states which have been studied by paramagnetic resonance (Bleaney and Stevens 1953, Bowers and Owen 1955, Stevens 1952, Elliott and Stevens 1952, 1953 a, b).

4.4. *Fluorescence Spectra*

Rare-earth ions are frequently fluorescent when incorporated as impurities in crystals. An example of a fluorescence spectrum, figure 3 (*b*), illustrates the splitting of the lines into groups corresponding to different J values. The fluorescence in this solid, CaO(U, Sm) is especially brilliant because of energy transfer from the uranium to the samarium ions. Brauer (1951 a, b) has considered the possible effects of charge compensation on the spectra of rare-earth ions in alkaline-earth oxide lattices. Figure 5 (*a*, *b*) illustrates localized compensation by a vacancy and by a monovalent ion. This has been extended to fluoride lattices

by Stepanov and Feofilov (1956), and figure 5 (*c*, *d*) illustrates compensation by an oxygen ion and by an extra fluorine ion.

One of the peculiar features of the rare-earth salts is that fluorescence has only been reported for ions with from five to ten f-electrons. Promethium with four f-electrons has probably not been closely examined in this respect; but praseodymium and neodymium, and their counterparts in the upper half of the shell, i.e. thulium and erbium, might be expected to fluoresce in the visible or near infra-red.† Fluorescence has been observed for all these four elements when incorporated as impurities in various solids, e.g. $CaWO_4$.

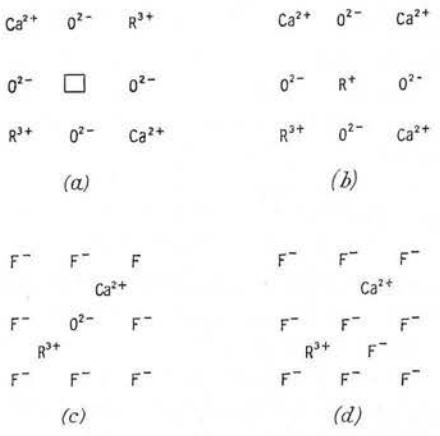

Figure 5. Charge compensation for rare-earth ions in crystal phosphors. Compensation in oxide crystals (*a*) by a vacancy and (*b*) by a monovalent ion, and in fluorite (*c*) by an oxygen ion and (*d*) by a fluorine ion. The normal fluorine ions are shown schematically and really occur in planes above and below the metal ions.

Fluorescence spectra, when they can be observed, enable information to be obtained about the different levels in the lowest multiplet of the ion. Judd (1956) has shown that a partial breakdown of Russell–Saunders coupling occurs even for the ground multiplet, and has used the spectra to obtain values of the spin–orbit splitting constant ξ for the various ions.

4.5. *Trivalent Ions*

$4f^1 : Ce^{3+}$, *ground state* $^2F_{5/2}$

The only excited state in the f configuration is $^2F_{7/2}$ at an energy of 2240 cm^{-1} (Lang 1936), which is that due to a spin–orbit splitting constant

$$\xi = 2240 \div 7/2 = 640 \text{ cm}^{-1}.$$

$4f^2 : Pr^{3+}$, *ground state* $^3H_4$

This ion has been extensively studied and recent investigations include those of Sayre, Sancier and Freed (1955) on $PrCl_3$, and of Sayre and Freed (1955) on films of PrF_3. Hellwege and Hellwege (1953) have investigated the 'crystal hyperfine structure' ($\sim$0·1 to 1 cm^{-1}) in the spectrum of praseodymium salts.

† It is significant that Dieke and Hall (1957) have found a sharp decrease in the fluorescent lifetimes as one moves away from the half-filled shell.

They attribute this structure to an exchange interaction between praseodymium ions. Brochard and Hellwege (1953) have studied the Zeeman splitting of $Pr_2Mg_3(NO_3)_{12}.24H_2O$.

There are thirteen *LSJ* levels which theory predicts will occur in the following order of increasing energy, as shown in figure 6.

$$^3H_4 \quad ^3H_5 \quad ^3H_6 \quad ^3F_2 \quad ^3F_3 \quad \overbrace{^1G_4 \quad ^3F_4} \quad ^1D_2 \quad ^1I_6 \quad ^3P_0 \quad ^3P_1 \quad ^3P_2 \quad ^1S_0.$$

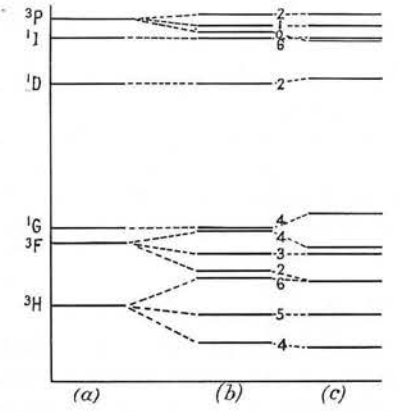

Figure 6. Energy levels for f^2. (*a*) Russell–Saunders levels, (*b*) with first-order spin–orbit interaction, (*c*) with intermediate coupling.

The $^1G_4$ and $^3F_4$ levels are bracketed as they are heavily mixed in the intermediate coupling calculations. These levels have been studied experimentally with the exception of $^3H_5$, $^3H_6$ and $^3F_2$ in the infra-red and $^1S_0$ in the ultra-violet. $^1I_6$ is a doubtful case and has probably not been observed (Jørgensen 1955 c). Figure 6 (*b*) illustrates the splitting of the levels in the Russell–Saunders approximation, whereas figure 5 (*c*) shows the importance of using the matrices of spin–orbit interaction (Spedding 1940) in the intermediate coupling approximation. Judd (1957 b) has calculated the crystal field splittings of the energy levels in $PrCl_3$ using the parameters

$$\xi = 711 \text{ cm}^{-1},$$

$$A_2{}^0\langle r^2\rangle = \quad 49{\cdot}5 \text{ cm}^{-1} \qquad A_6{}^0\langle r^6\rangle = -39{\cdot}2 \text{ cm}^{-1},$$

$$A_4{}^0\langle r^4\rangle = -39{\cdot}7 \text{ cm}^{-1} \qquad A_6{}^6\langle r^6\rangle = \quad 396{\cdot}7 \text{ cm}^{-1},$$

where $\langle r^n\rangle$ denotes the average value of r^n for a 4f electron. He has found good agreement between theory and experiment.

$4f^3 : Nd^{3+}$, *ground state* $^4I_{9/2}$

There are 41 *LSJ* levels for the ion f^3; but despite the increased complexity good progress has been made with the interpretation of the spectra. Satten (1953) obtained the absorption spectrum of $Nd(BrO_3)_3.9H_2O$ and tentatively identified about 12 of the *LSJ* levels. His interpretation has been discussed further (Jørgensen 1955 d, Satten 1955). The use of intermediate coupling calculations should enable a more positive identification to be made. Ishidzu and Obi (1950)

have calculated the matrices of spin–orbit interaction for f^3, but unfortunately not using the group-theoretical classification of the f-shell (Racah 1949). The matrices have been recalculated using this classification (Loudon, unpublished). Earlier deductions from spectroscopic and specific heat data leading to cubic symmetry for the surroundings of the rare-earth ions in the hydrated sulphates have been shown to be erroneous by Satten and Young's (1955) spectroscopic investigation of $Nd_2(SO_4)_3.8H_2O$ which suggests an orthorhombic or lower symmetry for the ion sites.

The Zeeman effect has been studied in several neodymium salts by Dieke and Heroux (1956), who have not attempted a detailed interpretation of many of the results. With these data the prospects are encouraging for a thorough understanding of the spectra of neodymium salts.

$4f^4$: Pm^{3+}, *ground state* $^5I_4$

Not much information on this ion is available because of the lack of a stable isotope. Parker and Lentz (1950) however find bands of the type expected between 12 000 and 22 000 cm^{-1}.

$4f^5$: Sm^{3+}, *ground state* $^6H_{5/2}$

Gobrecht (1937, 1938) has listed many lines in the absorption and fluorescence spectra of samarium sulphate in the visible and infra-red. By analysing the ground multiplet, Judd (1956) finds $\xi = 1180$ cm^{-1}. Jørgensen (1955 b) predicts ^4M as the lowest quartet state, and hence probably the upper state in fluorescence ; but Elliott, Judd and Runciman (1957) find the means of the lowest quartet multiplets to be, in order of increasing energy, ^4I, ^4M, ^4F and ^4G. When the spin–orbit splitting is taken into account as a first-order perturbation of the Russell–Saunders states, the lowest quartet state is predicted to be $^4F_{3/2}$. The analysis of the spectra of samarium salts is going to be difficult due to the closeness of the lowest quartet states.

The fluorescence of Sm^{3+} has been used by Oshima, Hayakawa, Nagano and Nagusa (1956) to study the phase transition in barium titanate at $-80°$c.

$4f^6$: Eu^{3+}, *ground state* $^7F_0$

Hellwege and Kahle (1951 a, b) have studied the spectra of $EuCl_3.6H_2O$ and of $Eu(BrO_3)_3.9H_2O$, and identified the lowest excited states as $^5D_0$, $^5D_1$ and $^5D_2$. Judd (1955 b) has confirmed these experimental assignments by theoretical study of the energy levels and of the crystal fine structure, and has found $\xi = 1360$ cm^{-1} (Judd 1956).

The fluorescence spectra of europic salts are unique in furnishing three examples of magnetic dipole transitions, namely $^5D_0 \rightarrow {}^7F_1$, $^5D_1 \rightarrow {}^7F_0$, $^5D_1 \rightarrow {}^7F_2$. These transitions have been studied in anhydrous europic chloride (Sayre and Freed 1956 a) and in europic ethylsulphate (Sayre and Freed 1956 b). The magnetic dipole nature of these transitions has also been verified in europic solutions using the technique of wide angle interference (Freed 1942).

$4f^7$: Gd^{3+}, *ground state* $^8S_{7/2}$

This ion has a half-filled shell of 4f electrons, and in consequence exhibits some unusual properties. The states of two highest multiplicities are the ground

state ^8S and the excited states ^6PDFGHI, all of which have zero spin–orbit and crystal field splitting in the Russell–Saunders approximation. Nutting and Spedding (1937) have examined the ultra-violet absorption spectra of many gadolinium salts, and quite appreciable spin–orbit and crystal field splittings are found which can be attributed to second-order effects. The lowest excited state is probably ^6P, although Jørgensen has predicted ^6I. The very small splitting of the ground state has been investigated by paramagnetic resonance, and discussed by Hutchison, Judd and Pope (1957). Dieke and Leopold (1957) have studied the absorption, fluorescence and Zeeman spectra of $GdCl_3.6H_2O$ at liquid helium temperatures.†

$4f^8$: Tb^{3+}, *ground state* $^7F_6$

Geisler and Hellwege (1953) have obtained the absorption and fluorescence spectra of terbium bromate. From the fluorescence data Judd (1956) deduces $\xi = 1720\ cm^{-1}$.

$4f^9$: Dy^{3+}, *ground state* $^6H_{15/2}$

Dieke and Singh (1956) have obtained the fluorescence and absorption spectra of $DyCl_3.6H_2O$ at 4·2 and 77°K. The interpretation given seems to be invalidated by the theoretical predictions for f^9 made by Elliott, Judd and Runciman (1957). For this ion Judd (1956) finds $\xi = 1920\ cm^{-1}$.

$4f^{10}$: Ho^{3+}, *ground state* $^5I_8$

Holmium is of interest because of its correspondence with the naturally missing element promethium which has four f-electrons. From an analysis of the fluorescence spectra of Gobrecht (1938) and Rosenthal (1939), Judd (1956) has deduced $\xi = 2080\ cm^{-1}$.

$4f^{11}$: Er^{3+}, *ground state* $^4I_{15/2}$

The absorption spectrum has been studied by Gobrecht (1938). The spin–orbit matrices obtained for f^3 will be applicable to this ion.

$4f^{12}$: Tm^{3+}, *ground state* $^3H_6$

The theoretical interpretation has been discussed by Bethe and Spedding (1937), who found that spin–orbit interactions produce very large corrections, up to 10 000 cm^{-1}, to the Russell–Saunders levels.

$4f^{13}$: Yb^{3+}, *ground state* $^2F_{7/2}$

The absorption spectrum of $YbCl_3.6H_2O$ consists of two sharp lines near 9700Å which are interpreted as transitions to $^2F_{5/2}$. Dieke and Crosswhite (1956) have also examined the Zeeman spectra as a function of crystal orientation.

4.6. *Divalent Ions*

Divalent europium, isoelectronic with Gd^{3+}, has been studied by Freed and Katcoff (1948), Przibram (1949) and by Gruen, Conway and McLaughlin (1956). Freed and Katcoff find the absorption is stronger, by at least a factor of 100, than that of the trivalent ions. This strong absorption is attributed to an allowed

† Cook and Dieke (1957) have now found the $^6P_{3/2}$ group as well as the $^6P_{5/2}$ and $^6P_{7/2}$ groups in gadolinium acetate, the $^6P_{7/2}$ group being lowest and the $^6P_{3/2}$ group being highest in energy.

transition, $4f^7 \rightarrow 4f^6\,5d$. Tolstoi, Tkachuk and Tkachuk (1955) find an exponential phosphorescence, $\tau \sim 6 \times 10^{-7}$ sec, which could be consistent with such an assignment. On the other hand, Butement (1948) has studied the absorption spectra of divalent samarium, europium and ytterbium and found not only the broad bands due to allowed transitions, but also narrow weak lines which he correlates with lines of the isoelectronic trivalent rare-earth ions. Feofilov (1956 b) has also studied these divalent ions when present as impurities in fluorite crystals.

§ 5. Heavy Metal Ions

This section deals with ions which have completed sub-shells of electrons in the ground state and are therefore diamagnetic. Such ions in crystals do not usually have a characteristic spectrum in the visible or near ultra-violet, i.e. for wavelengths greater than 2000 Å. However, ions with an ns^2 configuration are readily excited to $nsnp$. Examples of ions with a $6s^2$ configuration are Tl^+, Pb^{2+} and Bi^{3+}, and it is interesting to note that Prener, Hanson and Williams (1953) have used isoelectronic neutral mercury atoms as fluorescent activators. Other ions with an ns^2 configuration are $As^{3+}(4s^2)$, In^+, Sn^{2+} and $Sb^{3+}(5s^2)$, but these ions will not be discussed separately as many of their features will be similar to those of the ions with a $6s^2$ configuration.

(*a*) $6s^2$: Tl^+, *ground state* $^1S_0$

Seitz (1938) interpreted the general features of the spectra of thallium-activated alkali halides in terms of the configuration coordinate diagram. Using this model, Williams (1951) calculated the absorption and emission spectra of KCl(Tl) from the properties and wave functions of the free ions. This calculation, though open to objection on points of detail, has clarified the concept of a luminescent centre. Williams assigns the broad absorption bands at 1960 and 2490Å to the transitions $^1S_0 \rightarrow {}^1P_1$ and $^1S_0 \rightarrow {}^3P_1$ respectively, and the fluorescence band at 3050Å to $^3P_1 \rightarrow {}^1S_0$.

Runciman and Steward (1953) have verified by an x-ray investigation of KCl with up to 15% (molecular) of TlCl that the Tl^+ ions enter the lattice substitutionally, and have derived an improved value for the ionic radius. Improved wave functions have been calculated (Douglas, Hartree and Runciman 1955) by the self-consistent field method for Tl^+ in the ground state ($6s^2$) and for the first excited state (6s6p). Unfortunately these wave functions do not include the appreciable exchange and relativistic corrections. These wave functions have been used by Knox and Dexter (1956) to discuss the oscillator strengths in KCl(Tl) and only poor agreement has been obtained with the experimental values. However, Williams, Segall and Johnson (1957) obtain better agreement by including crystalline interactions.

It has been noted that Williams (1953) was mistaken in trying to remove the degeneracy of the $^3P_1$ state by orienting the 6p wave function in the cubic crystal field. It does not now seem clear whether the excited state in the fluorescent transition is the $^3P_0$ state in a field of cubic symmetry or a $^3P_1$ state in an ionic field which has undergone a Jahn–Teller distortion of the type considered by Öpik and Pryce (1957).

The absorption bands of KCl(Tl) have been measured at low temperatures by Johnson and Studer (1951) and by Johnson (1954). The emission and excitation

spectra have been studied by Patterson and Klick (1957) who suggest that the 3050Å and 4750Å emission bands may arise from different centres rather than from two excited states of the same centre as proposed by Johnson and Williams (1952).

(*b*) $6s^2$: Pb^{2+}, *ground state* $^1S_0$

Single crystals of NaCl(Pb) have been studied by Schulman, Ginther and Klick (1950). A vibrational structure has been found in the red fluorescence band in CaO(Pb) at liquid-air temperature (Runciman 1955 a).

(*c*) $6s^2$: Bi^{3+}, *ground state* $^1S_0$

Bismuth-activated oxide phosphors have a well-defined vibrational structure in their fluorescent emission (Ewles and Lee 1953). Runciman (1955 b) has found similar vibrational structure in the absorption band, and has discussed possible localized modes of vibration which are likely to be excited. The absorption and emission bands are situated in the near ultra-violet and blue regions of the spectrum, figure 3 (*c*), and are probably due to transitions between the ground state and an excited ^3P state.

§ 6. Uranium and the Transuranics

The elements from uranium onwards are of special interest because of the part played by 5f electrons in absorption and emission. This section will deal with ions analogous to rare-earth ions and with complexes of the uranyl type.

(*a*) *Uranyl*, $(UO_2)^{2+}$

Dieke and Duncan (1949) have described the known spectroscopic properties of uranyl salts, and in particular the results of isotopic substitution of one or more of the constituents. The absorption spectrum consists of several major series each of which is due to one electronic transition. Each series consists of dozens of lines due to vibrations being excited by the electronic transition. The first series is called the ' fluorescence ' series as it is almost a mirror image of the fluorescence spectrum, allowing that the vibrational frequencies are considerably altered. The symmetrical stretching frequency of the uranyl group which determines the spacing of the line groups in a series is about 880 cm^{-1} in fluorescence and 760 cm^{-1} in absorption, figure 3 (*d*, *e*). The second series in order of increasing energy is the ' magnetic ' series, all the lines of which in uniaxial crystals are split into two by a magnetic field. The ' ultra-violet ' series occurs at still shorter wavelengths.

There is at the moment no detailed theory of the energy spectrum of the uranyl ion, but it seems commonly agreed that in absorption an electron is transferred from an oxygen orbital into the 5f shell which is empty in the ground state. Many of the vibrations can be ascribed to modes characteristic of the uranyl and other groups, e.g. nitrate groups. The width of the lines may be partly due to a small Davydov splitting, as it is probable that the electronic energy is transferred from one uranyl group to another many times before fluorescence occurs. This would account for the sharpness of impurity lines, as in the case of impurities no such mechanism could occur. Further experiments on uranyl salts include a puzzling description by Samoilov (1948) of circular polarization in sodium uranyl

acetate, which is usually regarded as cubic,† and the effect of deuteration on the spectra of uranyl nitrate hydrates (Sevchenko, Vdovenko and Kovaleva 1951).

(*b*) *Hexavalent uranium.*

When many solids are activated with hexavalent uranium they show a green fluorescence at first sight similar to that of uranyl salts. However the spectrum is rather different, figure 3 (*f*), and the idea of localized charge compensation suggests that a UO_4 group is present in CaF_2(U, O), figure 7 (*a*), and a UO_6 group in CaO(U) (Runciman 1955 a). The concept of a fluorescent UO_6 group is strengthened by the existence of fluorescent alkaline earth uranates such as Ba_2CaUO_6 (Steward and Runciman 1953).

When NaF(U) is prepared under oxidizing conditions, as is necessary for it to be luminescent, then a UO_6 group, figure 7 (*b*), can be used to account for the vibrational frequencies in the fluorescence spectrum and their change with ^{18}O substitution (Runciman 1956 b). The fluorescence spectrum of NaF(U, O) changes considerably on cooling from 77 to 4·2°K (figure 8 (*a*, *b*)) indicating that the transition probability from one of the upper excited states is greater than from the lowest excited state. The absorption spectrum obtained by the reflection method, figure 8 (*c*), shows this upper excited state now in absorption.

(*c*) *Lower valence states of uranium.*‡

Uranium can readily occur in the trivalent and tetravalent states. Jørgensen (1955 a) attributes the U^{4+} spectrum to an f^2 configuration. Alexanian (1957) has described the absorption spectrum of some tetravalent uranium compounds. Galkin and Feofilov (1957) have found an infra-red luminescence of U^{3+}, and it will be interesting to see if results on U^{3+} are analogous to the rare earth ion ND^{3+}.

(*d*) *Neptunium.*‡

Freed and Leitz (1949) briefly describe the absorption spectrum of $NpCl_4$, for which the electronic configuration may be f^3.

Neptunyl salts have also been studied, and there are two bands with vibrational structure at 18 000 and 21 200 cm^{-1}. Eisenstein and Pryce (1955) suppose that the axial field in the $(NpO_2)^{2+}$ ion dominates and that the absorption spectrum is due to the one 5f electron in a non-bonding state. The ground state is $\phi_{\pm 5/2}$ and the above absorption bands are attributed to transitions to $\sigma_{\pm 3/2}$ and $\sigma_{\pm 5/2}$, where σ and ϕ stand for states with $l_z = 2, 3$ respectively.

(*e*) *Plutonium.*

Freed and Leitz (1949) have obtained the absorption spectrum of $PuCl_3$, and Cunningham, Gruen, Conway and McLaughlin (1956) have discovered and described the fluorescence of Pu^{3+} as an activator in $LaCl_3$. No analysis of these spectra is available, but the ion is probably analogous to Sm^{3+}, which has an f^5 configuration. Leontovich (1957) has obtained the absorption spectrum of tetravalent plutonium in several salts, e.g. $Pu(SO_4)_2.4H_2O$.

† Nye (1957) includes a most helpful account of optical activity in crystals. The cubic classes O and T show optical activity, and sodium acetate probably belongs to the latter class.

‡ Conway, Wallmann, Cunningham and Shalimoff (1957) have found fluorescence spectra for trivalent uranium, neptunium and curium in $LaCl_3$, and an ultra-violet absorption spectrum for curium in $LaCl_3$. The uranium fluorescence is in the range 5 400–7 000 Å and is obviously different in origin from that found by Galkin and Feofilov (1957).

Eisenstein and Pryce (1956) have extended their calculations on uranyl-type ions to plutonyl, and attribute many bands to transitions within the f^2 configuration. By comparison with the uranyl ion, Jørgensen (1957) thinks some of these bands may be due to a process in which an electron is transferred into the 5f shell.

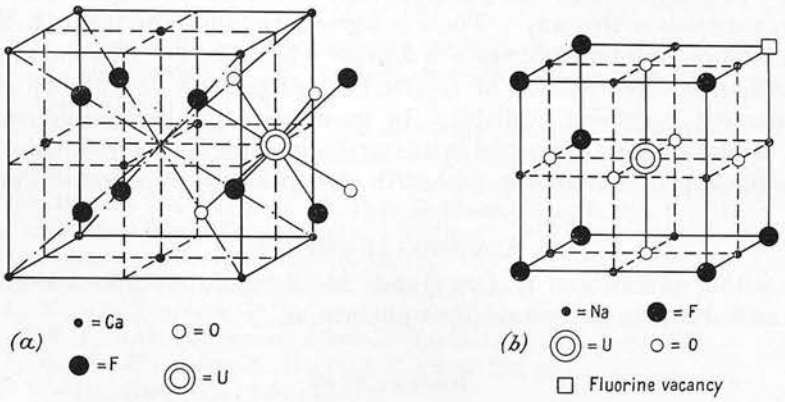

Figure 7. Charge compensation in uranium-activated fluorides. (*a*) CaF_2(U, O), (*b*) NaF(U, O).

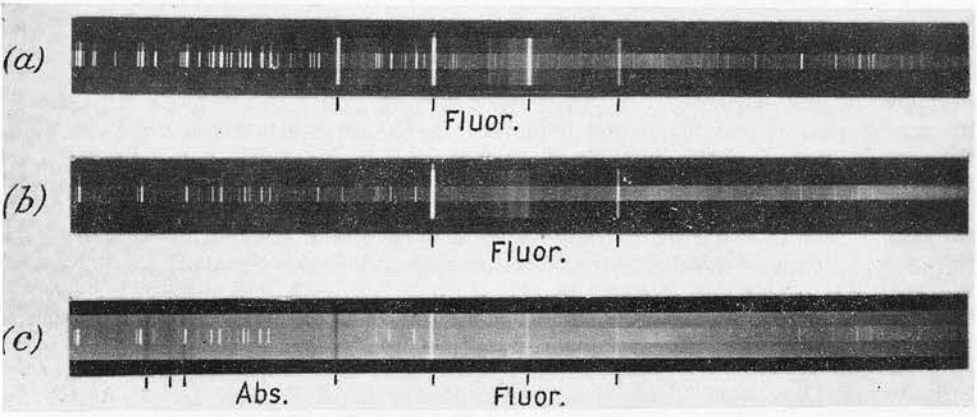

Figure 8. Crystal spectra obtained using a large glass Littrow spectrograph. For calibration purposes an iron-arc spectrum has been superimposed on the central portion of each spectrum. (*a*) Fluorescence spectrum of NaF(U, O) at 77°K. (*b*) Fluorescence spectrum of NaF(U, O) at 4·2°K. (*c*) Absorption spectrum of NaF(U, O) at 77°K.

(*f*) *Americium.*

$AmCl_3$ has a sharp line spectrum (Freed and Leitz 1949), and appears closely analogous to Eu^{3+}, f^6. The fluorescence of Am^{3+} in $LaCl_3$ has been described by Gruen, Conway, McLaughlin and Cunningham (1956), but no detailed analysis is yet available for this ion or for the americyl ion.

(*g*) *Curium.*

Trivalent curium may be expected to be similar to trivalent gadolinium f^7, and to show absorption and fluorescence in the ultra-violet. Curium does not form a stable complex of the uranyl type.

§ 7. Conclusion

The interpretation of fluorescence and absorption spectra is leading to rapid progress in our knowledge of the energy levels of ions in solids. This will extend the possible applications of spectroscopy to solid-state physics. In particular, it should be possible to study the phase changes in some ferroelectric and antiferromagnetic materials in this way. There is a great need for more research, including Zeeman studies, at liquid hydrogen or helium temperatures. On the other hand, the quantitative determination of crystal field parameters depends on improved wave functions becoming available. In most cases the wave functions of the free ion will be strongly perturbed in a crystal ; but free ion wave functions should be a useful approximation for rare-earth and possibly transuranic ions.

Acknowledgments

The author is indebted to Drs. Judd, McClure, Pappalardo and Satten for making available manuscripts prior to publication.

References

Alexanian, V. T., 1957, *Doklady Akad. Nauk. S.S.S.R.*, **115**, 333.
Ballhausen, C. J., 1954, *K. Danske Vidensk. Selsk. Mat.-fys. Medd.*, **29**, No. 4 ; 1955, *Acta Chem. Scand.*, **9**, 821.
Ballhausen, C. J., and Jørgensen, C. K., 1955, *K. Danske Vidensk. Selsk. Mat.-fys. Medd.*, **29**, No. 14.
Bethe, H., 1929, *Ann. Phys., Lpz.*, **3**, 133 ; 1930, *Z. Phys.*, **60**, 218.
Bethe, H. A., and Spedding, F. H., 1937, *Phys. Rev.*, **52**, 454.
Bjerrum, J., Ballhausen, C. J., and Jørgensen, C. K., 1954, *Acta Chem. Scand.*, **8**, 1275.
Bleaney, B., 1955, *Proc. Phys. Soc.* A, **68**, 937.
Bleaney, B., and Stevens, K. W. H., 1953, *Rep. Progr. Phys.*, **16**, 108 (London : Physical Society).
Bouriau, Y., and Lenoble, J., 1957, *C.R. Acad. Sci., Paris*, **245**, 511.
Bowen, E. J., 1946, *Chemical Aspects of Light* (Oxford : Clarendon Press).
Bowen, L. O., 1957, *J. Sci. Instrum.*, **34**, 265.
Bowers, K. D., and Owen, J., 1955, *Rep. Progr. Phys.*, **18**, 304 (London : Physical Society).
Brauer, P., 1951 a, *Z. Naturf.*, **6a**, 561 ; 1951 b, *Ibid.*, **6a**, 562.
Brochard, J., and Hellwege, K. H., 1953, *Z. Phys.*, **135**, 620.
Butement, F. D. S., 1948, *Trans. Faraday Soc.*, **44**, 617.
Condon, E. U., and Shortley, G. H., 1935, *The Theory of Atomic Spectra* (Cambridge : University Press).
Conway, J. G., Wallmann, J. C., Cunningham, B. B., and Shalimoff, G. V., 1957, *J. Chem. Phys.*, **27**, 1416.
Cook, S. P., and Dieke, G. H., 1957, *J. Chem. Phys.*, **27**, 1213.
Couture, L., 1957, *C.R. Acad. Sci., Paris*, **245**, 515.
Couture, L., Jacquinot, P., and Tsujikawa, I., 1956, *Brit. J. Appl. Phys.*, **7**, 425.
Cunningham, B. B., Gruen, D. M., Conway, J. C., and McLaughlin, R. D., 1956, *J. Chem. Phys.*, **24**, 1275.
Deutschbein, O., 1939, *Ann. Phys., Lpz.*, **36**, 183.
Deutschbein, O., Joos, G., and Teltow, J., 1942, *Naturwissenschaften*, **30**, 228.
Dexter, D. L., Klick, C. C., and Russell, G. A., 1955, *Phys. Rev.*, **100**, 603.
Dieke, G. H., and Crosswhite, H. M., 1956, *J. Opt. Soc. Amer.*, **46**, 885.
Dieke, G. H., and Duncan, A. B. F., 1949, *Spectroscopic Properties of Uranium Compounds*, National Nuclear Energy Series, III, 2 (New York : McGraw-Hill).
Dieke, G. H., and Hall, L. A., 1957, *J. Chem. Phys.*, **27**, 465.
Dieke, G. H., and Heroux, L., 1956, *Phys. Rev.*, **103**, 1227.

DIEKE, G. H., and LEOPOLD, L., 1957, *J. Opt. Soc. Amer.*, **47**, 944.
DIEKE, G. H., and SINGH, S., 1956, *J. Opt. Soc. Amer.*, **46**, 495.
DOUGLAS, A. S., HARTREE, D. R., and RUNCIMAN, W. A., 1955, *Proc. Camb. Phil. Soc.*, **51**, 486.
DREISCH, T., and KALLSCHEUER, O., 1944, *Z. Elektrochem.*, **50**, 224.
EISENSTEIN, J. C., and PRYCE, M. H. L., 1955, *Proc. Roy. Soc.* A, **229**, 20 ; 1956, *Ibid.*, **238**, 31.
ELLIOTT, J. P., JUDD, B. R., and RUNCIMAN, W. A., 1957, *Proc. Roy. Soc.* A, **240**, 509.
ELLIOTT, R. J., and STEVENS, K. W. H., 1952, *Proc. Roy. Soc.* A, **215**, 437 ; 1953 a, *Ibid.*, **218**, 553 ; 1953 b, *Ibid.*, **219**, 387.
ELLIS, J. W., and KAPLAN, J., 1935, *J. Opt. Soc. Amer.*, **25**, 357 ; 1937, *Ibid.*, **27**, 94.
EWLES, J., and LEE, N., 1953, *J. Electrochem. Soc.*, **100**, 392, 399, 402.
FEOFILOV, P. P., 1956 a, *J. Phys. Radium* (8), **17**, 656 ; 1956 b, *Optika I Spektroskopiya*, **1**, 992.
FINKELSTEIN, R., and VAN VLECK, J. H., 1940, *J. Chem. Phys.*, **8**, 790.
FREED, S., 1942, *Rev. Mod. Phys.*, **14**, 105.
FREED, S., and KATCOFF, S., 1948, *Physica*, **14**, 17.
FREED, S., and LEITZ, F. J., 1949, *J. Chem. Phys.*, **17**, 540.
GALKIN, L. N., and FEOFILOV, P. P., 1957, *Doklady Akad. Nauk. S.S.S.R.*, **114**, 745.
GARLICK, G. F. J., 1949, *Luminescent Materials* (Oxford : Clarendon Press).
GEISLER, H. F., and HELLWEGE, K. H., 1953, *Z. Phys.*, **136**, 293.
GIELESSEN, J., 1935, *Ann. Phys., Lpz.*, **22**, 537.
GOBRECHT, H., 1937, *Ann. Phys., Lpz.*, **28**, 673 ; 1938, *Ibid.*, **31**, 755.
GRECHUSHNIKOV, B. N., and FEOFILOV, P. P., 1955, *J. Exp. Theor. Phys.*, **29**, 384 (translated in *Soviet Physics JETP*, 1956, **2**, 330).
GRUEN, D. M., CONWAY, J. G., and MCLAUGHLIN, R. D., 1956, *J. Chem. Phys.*, **25**, 1102.
GRUEN, D. M., CONWAY, J. G., MCLAUGHLIN, R. D., and CUNNINGHAM, B. B., 1956, *J. Chem. Phys.*, **24**, 1115.
HAMEKA, H. F., and VLAM, C. C., 1953, *Physica*, **19**, 943.
HARTMANN, H., and SCHLÄFER, H. L., 1951 a, *Z. Phys. Chem.*, **197**, 115 ; 1951 b, *Z. Naturf.*, **6a**, 760.
HELLWEGE, A. M., 1955, LANDOLT-BÖRNSTEIN, *Zahlenwerte and Funktionen*, 6th edn, Vol. 1, Part 4, 893 (Berlin : Springer).
HELLWEGE, A. M., and HELLWEGE, K. H., 1953, *Z. Phys.*, **135**, 615.
HELLWEGE, K. H., 1948, *Ann. Phys., Lpz.*, **4**, 95, 127, 136, 143, 150 ; 1950 a, *Z. Phys.*, **127**, 513 ; 1950 b, *Ibid.*, **128**, 172.
HELLWEGE, K. H., and KAHLE, H. G., 1951 a, *Z. Phys.*, **129**, 62 ; 1951 b, *Ibid.*, **129**, 85.
HOLMES, O. G., and MCCLURE, S., 1957, *J. Chem. Phys.*, **26**, 1686.
HUSH, N. S., and PRYCE, M. H. L., 1957, *J. Chem. Phys.*, **26**, 143.
HUTCHISON, C. A., JUDD, B. R., and POPE, D. F. D., 1957, *Proc. Phys. Soc.* B, **70**, 514.
ISHIDZU, T., and OBI, S., 1950, *J. Phys. Soc. Japan*, **5**, 145.
JOHNSON, P. D., 1954, *J. Chem. Phys.*, **22**, 1143.
JOHNSON, P. D., and STUDER, F. J., 1951, *Phys. Rev.*, **82**, 976.
JOHNSON, P. D., and WILLIAMS, F. E., 1952, *J. Chem. Phys.*, **20**, 124.
JØRGENSEN, C. K., 1955 a, *K. Danske Vidensk. Selsk. Mat.-fys. Medd.*, **29**, No. 7 ; 1955 b, *Ibid.*, **29**, No. 11 ; 1955 c, *Acta Chem. Scand.*, **9**, 540 ; 1955 d, *J. Chem. Phys.*, **23**, 399 ; 1957, *Acta Chem. Scand.*, **11**, 166.
JUDD, B. R., 1955 a, *Proc. Roy. Soc.* A, **227**, 552 ; 1955 b, *Ibid.*, **228**, 120 ; 1955 c, *Ibid.*, **232**, 458 ; 1956, *Proc. Phys. Soc.* A, **69**, 157 ; 1957 a, *Proc. Roy. Soc.* A, **241**, 122 ; 1957 b, *Ibid.*, **241**, 414.
KIRK, R. D., 1954, *J. Electrochem. Soc.*, **101**, 461.
KLICK, C. C., and SCHULMAN, J. H., 1952, *J. Opt. Soc. Amer.*, **42**, 910.
KNOX, R. S., and DEXTER, D. L., 1956, *Phys. Rev.*, **104**, 1245.
KRISHNAN, R. S., 1947, *Proc. Indian Acad. Sci.*, **26A**, 450.
KRÖGER, F. A., 1948, *Some Aspects of the Luminescence of Solids* (Amsterdam : Elsevier).
LANG, R. J., 1936, *Canad. J. Res.*, **14**, 127.
LEONTOVICH, A. M., 1957, *Optika I Spektroskopiya*, **2**, 695.

LIEHR, A. D., and BALLHAUSEN, C. J., 1957, *Phys. Rev.*, **106**, 1161.
LOW, W., 1957a, *Z. Phys. Chem.*, **13**, 107 ; 1957 b, *Phys. Rev.*, **105**, 807.
MANI, A., 1942, *Proc. Indian Acad. Sci.*, **15A**, 52.
MOFFITT, W., and BALLHAUSEN, C. J., 1956, *Annual Review of Physical Chemistry*, **7**, 107 (Palo Alto : Annual Reviews).
NUTTING, G. C., and SPEDDING, F. H., 1937, *J. Chem. Phys.*, **5**, 33.
NYE, J. F., 1957, *Physical Properties of Crystals* (Oxford : Clarendon Press).
ÖPIK, U., and PRYCE, M. H. L., 1957, *Proc. Roy. Soc.* A, **238**, 425.
ORGEL, L. E., 1952, *J. Chem. Soc.*, Pt. IV, 4756 ; 1955 a, *J. Chem. Phys.*, **23**, 1004 ; 1955 b, *Ibid.*, **23**, 1819 ; 1955 c, *Ibid.*, **23**, 1824 ; 1955 d, *Ibid.*, **23**, 1958.
ORGEL, L. E., and DUNITZ, J. D., 1957, *Nature, Lond.*, **179**, 462.
OSHIMA, K., HAYAKAWA, S., NAGANO, H., and NAGUSA, M., 1956, *J. Chem. Phys.*, **24**, 903.
OWEN, J., 1955, *Proc. Roy. Soc.* A, **227**, 183.
PAPPALARDO, R., 1957 a, *Nuovo Cim.*, **6**, 392 ; 1957 b, *Phil. Mag.* (8) **2**, 1397.
PARKER, G. W., and LENTZ, P. M., 1950, *J. Amer. Chem. Soc.*, **72**, 2834.
PATTERSON, D. A., and KLICK, C. C., 1957, *Phys. Rev.*, **105**, 401.
PRENER, J. S., 1953, *J. Chem. Phys.*, **21**, 160.
PRENER, J. S., HANSON, R. E., and WILLIAMS, F. E., 1953, *J. Chem. Phys.*, **21**, 759.
PRINGSHEIM, P., 1949, *Fluorescence and Phosphorescence* (New York : Interscience Publishers).
PRZIBRAM, K., 1949, *Nature, Lond.*, **163**, 989 ; 1956, *Irradiation Colours and Luminescence* (translated by J. E. Caffyn) (London : Pergamon Press).
RACAH, G., 1949, *Phys. Rev.*, **76**, 1352.
ROSENTHAL, G., 1939, *Phys. Z.*, **40**, 508.
RUNCIMAN, W. A., 1955 a, *Brit. J. Appl. Phys.*, **6**, Suppl. No. 4, 78 ; 1955 b, *Proc. Phys. Soc.* A, **68**, 647 ; 1956 a, *Phil. Mag.* (8), **1**, 1075 ; 1956 b, *Proc. Roy. Soc.* A, **237**, 39.
RUNCIMAN, W. A., and STEWARD, E. G., 1953, *Proc. Phys. Soc.* A, **66**, 484.
SAMOILOV, B. N., 1948, *J. Exp. Theor. Phys.*, **18**, 1030.
SATTEN, R. A., 1953, *J. Chem. Phys.*, **21**, 637 ; 1955, *Ibid.*, **23**, 400 ; 1957, *Ibid.*, **27**, 286.
SATTEN, R. A., and YOUNG, D. J., 1955, *J. Chem. Phys.*, **23**, 404.
SAYRE, E. V., and FREED, S., 1955, *J. Chem. Phys.*, **23**, 2066 ; 1956 a, *Ibid.*, **24**, 1211 ; 1956 b, *Ibid.*, **24**, 1213.
SAYRE, E. V., SANCIER, K. M., and FREED, S., 1955, *J. Chem. Phys.*, **23**, 2060.
SCHULMAN, J. H., GINTHER, R. J., and KLICK, C. C., 1950, *J. Opt. Soc. Amer.*, **40**, 854.
SEITZ, F., 1938, *J. Chem. Phys.*, **6**, 150.
SEVCHENKO, A. N., VDOVENKO, V. M., and KOVALEVA, T. V., 1951, *J. Exp. Theor. Phys.*, **21**, 204.
SPEDDING, F. H., 1940, *Phys. Rev.*, **58**, 255.
SPEDDING, F. H., and NUTTING, G. C., 1934, *J. Chem. Phys.*, **2**, 421 ; 1935, *Ibid.*, **3**, 369.
STEPANOV, I. V., and FEOFILOV, P. P., 1956, *Doklady Akad. Nauk S.S.S.R.*, **108**, 615 (translated in *Soviet Physics Doklady*, **1**, 350).
STEVENS, K. W. H., 1952, *Proc. Phys. Soc.* A, **65**, 209.
STEWARD, E. G., and RUNCIMAN, W. A., 1953, *Nature, Lond.*, **172**, 75.
TANABE, Y., and SUGANO, S., 1954 a, *J. Phys. Soc. Japan*, **9**, 753 ; 1954 b, *Ibid.*, **9**, 766 ; 1957, *Ibid.*, **12**, 556.
TELTOW, J., 1938, *Z. Phys. Chem.* B, **40**, 397 ; 1939, *Ibid.*, **43**, 198.
TOLSTOI, N. A., TKACHUK, A. M., and TKACHUK, N. N., 1955, *J. Exp. Theor. Phys.* **29**, 386 (translated in *Soviet Physics JETP*, 1956, **2**, 331).
VAN VLECK, J. H., 1937, *J. Phys. Chem.*, **41**, 67 ; 1940, *J. Chem. Phys.*, **8**, 787.
WILLIAMS, F. E., 1951, *J. Chem. Phys.*, **19**, 457 ; 1953, *J. Phys. Chem.*, **57**, 780.
WILLIAMS, F. E., SEGALL, B., and JOHNSON, P. D., 1957, *Phys. Rev.*, **108**, 46.
WOLFSBERG, M., and HELMHOLZ, L., 1952, *J. Chem. Phys.*, **20**, 837.
YAMADA, S., 1951, *J. Amer. Chem. Soc.*, **73**, 1182.
YOST, D. M., RUSSELL, H., and GARNER, C. S., 1947, *The Rare-earth Elements and their Compounds* (New York : Wiley).

Offprinted from the *Faraday Society Discussions*, 1958, No. 26

THE ABSORPTION SPECTRUM OF VANADIUM CORUNDUM

THE ABSORPTION SPECTRUM OF VANADIUM CORUNDUM

By M. H. L. Pryce * and W. A. Runciman †‡

Received 14*th July*, 1958

A crystal of Al_2O_3 (V) has been studied in absorption over the wavelength range 0·4-1·2 μ. Measurements have been made at 4·2, 20 and 77°K, and polarization spectra obtained in the visible region. Two absorption bands have been resolved into finer structure than has been previously reported, and one of the components has been further split by a magnetic field. The relevant crystal field theory for two *d*-electrons in a trigonal field has been developed, using an octahedral field to provide a preliminary classification of states. The main features of the spectra are discussed in terms of this theory and possible complications due to Jahn-Teller distortions are considered.

1. Introduction

Many solids owe their colour to small quantities of impurities. For instance, ruby consists of colourless corundum, Al_2O_3, with the addition of some trivalent chromium ions which substitute in the lattice for about 1 % of the aluminium ions. In the same way, vanadium corundum contains trivalent vanadium ions, which are assumed to substitute for aluminium ions. The colouring is distinctive, being blue-grey in daylight and plum-coloured in artificial light. Unlike ruby, it is not found in nature, but it can be grown by the Verneuil process. Cut gemstones of this type are known as synthetic sapphires of the " alexandrite type ". They are recognized by their colouring and by a distinctive absorption line in the blue near 4750 Å.

Corundum is a uniaxial crystal of trigonal symmetry, with two molecules per unit cell. The aluminium ions are situated on the three-fold axis, and are coordinated to six oxygen ions which are at the corners of a deformed octahedron.

Tanabe and Sugano [1, 2] have calculated energy level diagrams for configurations d^n in an octahedral field. These results form a useful starting-point for considering the spectra due to impurities in the corundum lattice, and Tanabe and Sugano [3] have studied ruby in some detail. However, vanadium corundum is a simpler case for study, since the V^{3+} ion has only two 3*d* electrons as compared with Cr^{3+} which has a d^3 configuration. Low [4] has reported some absorption data for $Al_2O_3(V^{3+})$. The present paper includes high-resolution and polarization results together with a theoretical analysis.

Before presenting experimental results it is desirable to summarize the results of the calculations for a regular octahedron. A single *d*-electron can either occupy a triply degenerate level t_2, energy $-0{\cdot}4\,\Delta$, or a doubly degenerate level *e*, energy $0{\cdot}6\,\Delta$, where the difference in energy, Δ, is a measure of the octahedral field strength. The configuration d^2 in this notation consists of configurations t_2^2, t_2e and e^2. The states of configuration t_2^2 are $^3T_1$, $^1T_2$, ^1E and $^1A_1$ in increasing order of energy (fig. 1). The energy levels associated with t_2e are also shown in this figure; but the levels associated with e^2, namely, $^3A_2$, ^1E and $^1A_1$ are at higher energies and are not included. The states are labelled according to the representations of the cubic group, as described for instance in reviews by Moffitt and Ballhausen [5] and Runciman.[4]

* Department of Physics, University of Bristol.

† Atomic Energy Research Establishment, Harwell, Didcot, Berks.

‡ now at the Department of Physics, University of Canterbury, Christchurch, New Zealand.

A trigonal crystal field removes some of the degeneracy and splits the lowest cubic state $^3T_1$ into an upper ^3E state and the ground state $^3A_2$, now labelling states, in italics, according to point group C_{3v}. Furthermore, when the spin-orbit interaction is included, the ground state $^3A_2$ is split by a second-order effect into a doublet and singlet (fig. 2), the final degeneracy only being removed under the action of a magnetic field. This is the same situation as Abragam and Pryce [1] discussed for vanadium ammonium alum.

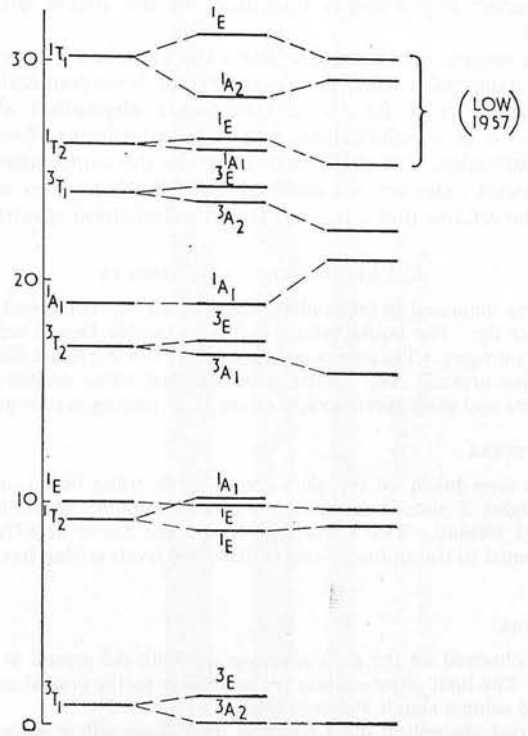

FIG. 1.—Energy levels of d^2 in a trigonal field. Energy units = 10^3 cm^{-1}.

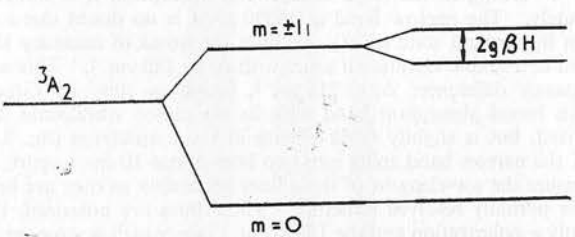

FIG. 2.—The splitting of the ground state of vanadium corundum.

The absorption spectrum in the visible and infra-red corresponds to transitions from the ground state $^3A_2$ to excited states of the configuration d^2. These transitions would be parity forbidden for the free ion, but are allowed in the crystal as the sites of the vanadium ions do not possess centres of symmetry. The site symmetry for the vanadium ions is C_3, and the pseudo-symmetry C_{3v} is used for labelling states for reasons stated in § 3. However, for a discussion of the polarization rules it will be advisable to ignore the suffixes and to label states as simply A or E, since the intensity of the transitions depends on configuration interaction

resulting from odd-parity terms in the crystal field. These odd-parity terms are not needed for the energy level calculations, where the pseudo-symmetry C_{3v} can be used. The spin prefix is dropped when allowing spin-orbit interaction to have mixed different spin states. Since the spin-orbit interaction is small, we may consider the spin states as nearly pure, and the most intense transitions are those involving no change in spin, i.e. triplet-triplet transitions. This is found experimentally and it is fortunate that in this case these transitions do not mask the weaker and sharper triplet-singlet transitions in the visible and near infra-red spectral regions.

Polarization spectra are denoted π when the electric vector is parallel to the crystal trigonal axis, and σ when the electric vector is perpendicular to the crystal axis. The selection rules for the electric-dipole absorption allow transitions $A \rightarrow A$ and $E \rightarrow E$ in π polarization, and allow transitions $A \rightarrow E$, $E \rightarrow A$ and $E \rightarrow E$ in σ polarization. In those cases in which the components of absorption from the two lowest states are not resolved it is difficult to draw any definite conclusions from the relative intensities in the two polarization spectra.

2. Experimental and results

The crystal was immersed in the cooling liquid which was contained in a glass Dewar with a transparent tip. For liquid helium (4·2°K) a double Dewar was used, the outer containing liquid nitrogen. The source used was a 6 V, 108 W ribbon filament lamp which was focused on the crystal. The spectra were obtained either on the glass optics of a Hilger large quartz and glass spectrograph or on 21 ft. grating spectrographs.

(*a*) Infra-red spectra

These spectra were taken on the glass spectrograph using liquid nitrogen (77°K) as coolant. The Kodak Z plates were sensitized in 4 % ammonia solution, and dried after a rinse in methyl alcohol. Two absorption lines were found at 8770 and 9660 cm^{-1} and can be attributed to transitions to two of the three levels arising from the cubic states $^1T_2$ and ^1E.

(*b*) Visible spectra

Spectra were obtained on the glass spectrograph with the crystal at 77°K and 4·2°K (fig. 3, plate 1). The light direction was perpendicular to the crystal axis, and polarization was obtained using a simple Polaroid filter.

There is a broad absorption band covering the orange-yellow region and at 77°K a vibrational structure is resolved. There are bands at about 15890, 16060, 16250, 16420 and 16640 cm^{-1}. Owing to the large background absorption it is difficult to find the maxima accurately. The narrow band at 15890 cm^{-1} is no doubt due to an electronic transition from the ground state to $^3T_2$. Within the limits of accuracy the other terms may be ascribed to a simple vibrational series with $\Delta\nu \approx 180$ cm^{-1}. This is rather smaller than the frequency difference, $\Delta\nu \approx 215$ cm^{-1}, found in ruby by Grechusnikov and Feofilov.[8] This broad absorption band with its associated vibrational structure is not strongly polarized, but is slightly more intense in the σ spectrum (fig. 3, plate 1). At 4·2°K or 20°K the narrow band splits into two lines about 10 cm^{-1} apart. It was found difficult to measure the wavelengths of these lines accurately as they are broad and show signs of further partially resolved structure. These lines are polarized, the 15880 cm^{-1} line being mainly π polarization and the 15890 cm^{-1} line, which is stronger, being σ polarized. This suggests that the upper state is an E state.

It has long been known that there is an absorption line in vanadium corundum near 21000 cm^{-1}. It is now found that this line is clearly resolved into two components at 77°K.

The wavelengths of these lines were accurately determined on the 21-ft. plane grating spectrograph at Harwell and found to be 4758·2 and 4756·4 Å, or as wavenumbers 21017 and 21025 cm^{-1} respectively. The line at 21017 cm^{-1} is σ polarized and only half as strong as the 21025 cm^{-1} line which is π polarized. The polarization selection rules clearly indicate that these are transitions from the two components of the $^3A_2$ ground state to the $^1A_1$ state. Both lines showed satellites spaced at 1 or 2 cm^{-1} from the central component. These did not appear to be grating " ghosts " and are not fully understood

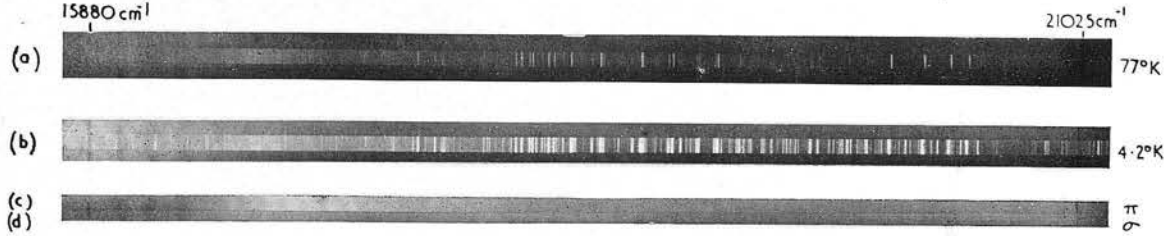

FIG. 3.—Plate 1 : absorption spectra of vanadium corundum (*a*) at 77°K, (*b*) at 4·2°K, (*c*) spectrum at 4·2°K, (*d*) spectrum at 4·2°K.

[To face page 36

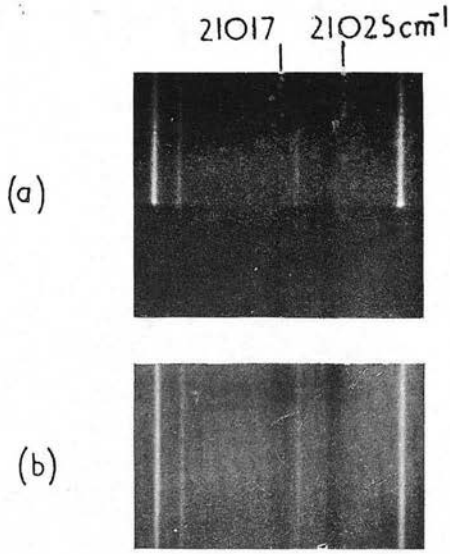

FIG. 4.—Plate 1 : (*a*) absorption lines at 21020 cm^{-1}, without magnetic field ; (*b*) with a field of 9400 gauss parallel to the crystal axis.

FIG. 3*a*, *b* and fig. 4*a*, *b* also include iron arc comparison spectra.

—they may well be due to vanadium ions which are close to another vanadium ion, for which the crystal field is slightly different.

The only other feature in the visible region is a poorly resolved vibrational structure at the long-wavelength edge of a strong broad absorption band. At 77°K the first two maxima were estimated to be at 22370 and 22570 cm^{-1}, and it is probably significant that the frequency difference $\Delta\nu \approx 200\ cm^{-1}$ is not far different from that found for the other vibrational structure in the orange-yellow. This broad blue absorption band is ascribed to transitions to the $^3T_1$ state and is stronger in π polarization.

(c) Zeeman experiment

The line at 4758·2 Å is narrow for an absorption line in a solid, having a half-width of 0·4 Å (2 cm^{-1}) at 77°K. In view of its interpretation it is expected to show a Zeeman effect, since it corresponds to a transition from a doubly degenerate lower level (see fig. 2) to a single upper level, and the degeneracy of the lower level is expected to be removed by a magnetic field. In a magnetic field H the energies of the three components of the ground triplet $^3A_2$ are given by the eigenvalues of the spin-Hamiltonian,

$$g_{\|}\beta H_z S_z + g_{\perp}\beta(H_x S_x + H_y S_y) + DS_z^2,$$

($S = 1$, $D = 8\ cm^{-1}$, $g_{\|}$ and $g_{\perp}$ roughly equal to the "spin-only" value 2, β = Bohr magneton). Formulae for $g_{\|}$, $g_{\perp}$ and D are given by Abragam and Pryce.[7] If the magnetic field is parallel to the axis, the doubly degenerate level is split by $2g_{\|}\beta H$. Hence the splitting is almost four times the "normal" Zeeman splitting. In a perpendicular field there is only a quadratic Zeeman effect. And in intermediate directions θ the linear part of the splitting is $2g_{\|}\beta H \cos\theta$.

In view of the large splitting expected, it was thought worthwhile to try to detect the effect even though the maximum field available was 9400 gauss at just over an inch gap. With $H\|C$ a splitting was detected using the 21-ft. concave grating at Imperial College (fig. 4, plate 1); but with $H \perp C$ no change in the line was found. The splitting in the former case was that expected for a g value slightly less than 2. As expected, the line at 4756·4 Å remained unsplit with the field in either direction.

3. Crystal field calculations

Only potential energy terms of even parity up to fourth order mix states within the configuration d^2. Therefore when calculating the energy levels of the configuration d^2 in a trigonal field which has symmetry C_3, only the harmonics $r^2Y_2^0$, $r^2Y_4^0$ and $r^2Y_4^{\pm 3}$ enter. By rotation about the threefold axis we can choose our axes such that the effective potential has the symmetry C_{3v}. Hence if we neglect spin-orbit interaction, states may be labelled by the total spin multiplicity, $2S + 1$, which will either be 1 or 3; and by the representations of the point group C_{3v}, which are A_1, A_2 or E (doubly degenerate). The theory of the crystal field splittings has been earlier formulated (Abragam and Pryce [7, 9]), but will be redeveloped here in a more convenient form for this problem. In particular the cubic field wave functions will be used as a basis instead of Russell-Saunders LS wave functions.

The non-cubic part of the potential energy of the crystal field can be written for a suitable orientation of axes as

$$V = A_2[yz + zx + xy] + A_4[yz(y^2 + z^2 - 6x^2) + zx(z^2 + x^2 - 6y^2) + xy(x^2 + y^2 - 6z^2)].$$

Both the terms in brackets are the sum of three functions which transform like the cubic representation T_2.

Normally one chooses as wavefunctions for a d-electron in a cubic field the functions,

$$t_x = \sqrt{15}yz,$$
$$t_y = \sqrt{15}zx,$$
$$t_z = \sqrt{15}xy,$$
$$e_1 = \tfrac{1}{2}\sqrt{5}(2z^2 - x^2 - y^2),$$
$$e_2 = \tfrac{1}{2}\sqrt{15}(x^2 - y^2).$$

TABLE 1.—REPRESENTATION PRODUCTS OF E AND T_2

	E_+	E_-	T_{2+}	T_{20}	T_{2-}
E_+	$\frac{1}{\sqrt{2}}A_1 + \frac{i}{\sqrt{2}}A_2$	$-\frac{1}{\sqrt{2}}T_{2-} - \frac{i}{\sqrt{2}}T_{1-}$	$-\frac{1}{\sqrt{2}}T_{2+} - \frac{i}{\sqrt{2}}T_{1+}$	$\frac{1}{\sqrt{2}}T_{20} + \frac{i}{\sqrt{2}}T_{10}$	
E_-	$\frac{1}{\sqrt{2}}A_1 - \frac{i}{\sqrt{2}}A_2$	$-E_+$	$\frac{1}{\sqrt{2}}T_{20} - \frac{i}{\sqrt{2}}T_{10}$	$\frac{1}{\sqrt{2}}T_{2+} + \frac{i}{\sqrt{2}}T_{1-}$	$\frac{1}{\sqrt{2}}T_{2+} - \frac{i}{\sqrt{2}}T_{1+}$
T_{2+}	$-\frac{1}{\sqrt{2}}T_{2-} + \frac{i}{\sqrt{2}}T_{1-}$	$-\frac{1}{\sqrt{2}}T_{20} - \frac{i}{\sqrt{2}}T_{10}$	$\frac{1}{\sqrt{3}}E_- + \sqrt{\frac{2}{3}}T_{2-}$	$-\frac{1}{\sqrt{3}}E_+ - \frac{1}{\sqrt{6}}T_{2+} + \frac{i}{\sqrt{2}}T_{1+}$	$-\frac{1}{\sqrt{3}}A_1 + \frac{1}{\sqrt{6}}T_{20} + \frac{i}{\sqrt{2}}T_{10}$
T_{20}	$-\frac{1}{\sqrt{2}}T_{2+} + \frac{i}{\sqrt{2}}T_{1+}$	$-\frac{1}{\sqrt{2}}T_{2-} - \frac{i}{\sqrt{2}}T_{1-}$	$-\frac{1}{\sqrt{3}}E_+ - \frac{1}{\sqrt{6}}T_{2+} - \frac{i}{\sqrt{2}}T_{1+}$	$\frac{1}{\sqrt{3}}A_1 + \sqrt{\frac{2}{3}}T_{20}$	$\frac{1}{\sqrt{3}}E_- - \frac{1}{\sqrt{6}}T_{2-} + \frac{i}{\sqrt{2}}T_{1-}$
T_{2-}	$\frac{1}{\sqrt{2}}T_{20} - \frac{i}{\sqrt{2}}T_{10}$	$\frac{1}{\sqrt{2}}T_{2+} + \frac{i}{\sqrt{2}}T_{1+}$	$-\frac{1}{\sqrt{3}}A_1 + \frac{1}{\sqrt{6}}T_{20} - \frac{i}{\sqrt{2}}T_{10}$	$\frac{1}{\sqrt{3}}E_- - \frac{1}{\sqrt{6}}T_{2-} - \frac{i}{\sqrt{2}}T_{1-}$	$\frac{1}{\sqrt{3}}E_+ - \sqrt{\frac{2}{3}}T_{2+}$

When considering a distortion acting along the (111) direction, however, it is advantageous to use the following linear combinations:

$$t_0 = -\frac{1}{\sqrt{3}}(\omega t_x + \omega^2 t_y + t_z),$$

$$t_- = \frac{1}{\sqrt{3}}(t_x + t_y + t_z),$$

$$t_0 = \frac{1}{\sqrt{3}}(\omega^2 t_x + \omega t_y + t_z),$$

$$e_+ = -\frac{1}{\sqrt{2}}(e_1 + ie_2),$$

$$e_- = \frac{1}{\sqrt{2}}(e_1 - ie_2);$$

where

$$\omega = \exp(2\pi i/3).$$

The apparently perverse signs in t_+ and e_+ are chosen for reasons of uniformity with the phase conventions for spherical harmonics,[10] and have a considerable advantage when angular momenta have to be discussed. Next we define the strength of the trigonal field by two parameters v and v' defined by the following relations between the matrix elements of the one-electron states in the crystal field:

$$\langle t_+ \mid V \mid t_+ \rangle = \langle t_- \mid V \mid t_- \rangle = -\tfrac{1}{3}v;$$
$$\langle t_0 \mid V \mid t_0 \rangle = \tfrac{2}{3}v; \qquad (1)$$

and

$$\langle t_+ \mid V \mid e_+ \rangle = \langle t_- \mid V \mid e_- \rangle = v'. \qquad (2)$$

All other matrix elements are zero.

The subscripts in t_+, t_0, t_- refer to the values + 1, 0, − 1 for the crystal quantum number μ, where $\mu \equiv M \pmod 3$ if M is the component of total angular momentum along the trigonal axis.

As a preliminary to forming two-electron states, it is useful to write down the detailed representation products of the cubic group representations E and T_2 as in table 1. The interpretation of the table is best described by an example. The product $E_+ \times T_{2+}$ is given as $-(T_{2-} + iT_{1-})/\sqrt{2}$. This means that a (normalized) two-electron wavefunction which is the product of two normalized

one-electron functions, respectively of type E_+ and T_{2+}, is the sum of two parts, belonging to the irreducible representations T_2 and T_1. The numerical factors represent the normalization and relative phases between components of a given representation. The phases are naturally to some extent arbitrary, only relative phases within a given representation having significance.

It is now possible to construct the cubic field states for d^2 out of linear combinations of determinantal two-electron states. For example one of the states of t_2^2 is

$$^1A_1 = \frac{1}{\sqrt{3}}\{-|t_+\bar{t}_-\rangle + |t_0\bar{t}_0\rangle - |t_-\bar{t}_+\rangle\}, \tag{3}$$

where a bar above the symbol denotes a spin component $m_s = -\frac{1}{2}$, whereas unbarred symbols refer to $m_s = +\frac{1}{2}$. The antisymmetric combination of the electrons is automatically formed by regarding the product as the diagonal term of a determinant formed by permutation of the states.

A more complicated example occurring in the configuration t_2e is the $^3T_{2+}$ state which has the following three-sub-states,

$$m_s = 1: \frac{1}{\sqrt{2}}\{|t_0e_+\rangle - |t_-e_-\rangle\},$$

$$m_s = 0: \frac{1}{2}\{|t_0\bar{e}_+\rangle + |e_+\bar{t}_0\rangle - |t_-\bar{e}_-\rangle - |e_-\bar{t}_-\rangle\},$$

$$m_s = -1: \frac{1}{\sqrt{2}}\{|\bar{t}_0\bar{e}_+\rangle - |\bar{t}_-\bar{e}_-\rangle\}.$$

The crystal field matrix elements are calculated by operating on the cubic field states, expressed as a linear combination of determinantal product states, with the operator of the trigonal potential field. This is accomplished using the definitions (1). This operator does not act on the spin states, which remain unchanged. For example, the calculation for the $^1A_1$ state (3) is as follows:

$$\Sigma V.\ ^1A_1 = \frac{v}{3}\left\{\frac{2}{\sqrt{3}}|t_+\bar{t}_-\rangle + \frac{4}{\sqrt{3}}|t_0\bar{t}_0\rangle + \frac{2}{\sqrt{3}}|t_-\bar{t}_+\rangle\right\} -$$

$$- \frac{v'}{\sqrt{3}}\{|e_+\bar{t}_-\rangle + |t_+\bar{e}_-\rangle + |e_-\bar{t}_+\rangle + |t_-\bar{e}_+\rangle\}$$

$$= \frac{2\sqrt{2}}{3}v\,^1T_{20a} - \frac{2}{\sqrt{3}}v'\,^1T_{20b}.$$

The subscripts a and b here refer to the configurations t_2^2 and t_2e respectively. In the following table of the trigonal field matrix elements calculated in this way the subscript a always refers to the configuration t_2^2 whereas b either refers to t_2e or e^2. There is only one state of symmetry $^3A_1$ arising from $^3T_2$ and its matrix element is

$$\langle {}^3T_{20}|\,V\,|{}^3T_{20}\rangle = -\tfrac{2}{3}v.$$

Similarly the only state of symmetry $^1A_2$ arises from $^1T_1$ and has the matrix element

$$\langle {}^1T_{10}|\,V\,|{}^1T_{10}\rangle = -\tfrac{1}{3}v.$$

The other matrices are naturally more complicated. They are given in table 2. It will be noticed that some matrix elements are imaginary. These can be made real by a trivial change of phase of the basic states $^3T_{2\pm}$ and $^1T_{1\pm}$, but we have preferred to leave them as they stand, for reference in any future work where the spin-orbit coupling matrices might be important, and where changing the phases would lead to further confusion.

TABLE 2.—TRIGONAL FIELD MATRIX ELEMENTS

$^3A_1$:

$^3T_{20}(-\frac{1}{3}v)$

$^3A_2$:

	$^3T_{10a}$	$^3T_{10b}$	$^3A_2$
$^3T_{10a}$	$-\frac{2}{3}v$	$\sqrt{2}v'$	0
$^3T_{10b}$	$\sqrt{2}v'$	$-\frac{1}{3}v$	$\sqrt{2}v'$
$^3A_2$	0	$\sqrt{2}v'$	0

^3E:

	$^3T_{1\pm a}$	$^3T_{2\pm}$	$^3T_{1b\pm}$
$^3T_{1\pm a}$	$\frac{1}{3}v$	$\pm\frac{i}{\sqrt{2}}v'$	$-\frac{1}{\sqrt{2}}v'$
$^3T_{2\pm}$	$\pm\frac{i}{\sqrt{2}}v'$	$\frac{1}{6}v$	$\mp\frac{i}{2}v$
$^3T_{1\pm b}$	$-\frac{1}{\sqrt{2}}v'$	$\pm\frac{i}{2}v$	$\frac{1}{6}v$

$^1A_1$:

	$^1T_{20a}$	$^1A_{1a}$	$^1T_{20b}$	$^1A_{1b}$
$^1T_{20a}$	$\frac{2}{3}v$	$\frac{2\sqrt{2}}{3}v$	$\sqrt{\frac{2}{3}}v'$	0
$^1A_{1a}$	$\frac{2\sqrt{2}}{3}v$	0	$-\frac{2}{\sqrt{3}}v'$	0
$^1T_{20b}$	$\sqrt{\frac{2}{3}}v'$	$-\frac{2}{\sqrt{3}}v'$	$-\frac{1}{3}v$	$\sqrt{2}v'$
$^1A_{1b}$	0	0	$\sqrt{2}v'$	0

$^1A_2$:

$^1T_{10}\left(-\frac{1}{3}v\right)$

^1E:

	$^1T_{2\pm a}$	$^1E_{\pm a}$	$^1T_{2\pm b}$	$^1T_{1\pm}$	$^1E_{\pm b}$
$^1T_{2\pm a}$	$-\frac{1}{3}v$	$-\frac{\sqrt{2}}{3}v$	$-\frac{1}{\sqrt{6}}v'$	$\pm\sqrt{\frac{3}{2}}iv'$	0
$^1E_{\pm a}$	$-\frac{\sqrt{2}}{3}v$	0	$-\frac{2}{\sqrt{3}}v'$	0	0
$^1T_{2\pm b}$	$-\frac{1}{\sqrt{6}}v'$	$-\frac{2}{\sqrt{3}}v'$	$\frac{1}{6}v$	$\pm\frac{i}{2}v$	$-v'$
$^1T_{1\pm}$	$\mp\sqrt{\frac{3}{2}}iv'$	0	$\mp\frac{i}{2}v$	$\frac{1}{6}v$	$\mp iv'$
$^1E_{\pm b}$	0	0	$-v'$	$\pm iv'$	0

The trigonal field matrix elements were then added to the corresponding matrix elements for the cubic field and the coulomb forces,[1] as given in table 3. The following trial values of the parameters were used, where B and C are the linear combinations of Slater integrals as used by Racah.[11]

$$B = 540\ \text{cm}^{-1}, \qquad C = 2600\ \text{cm}^{-1}$$

$$\Delta = 17500\ \text{cm}^{-1}, \qquad v = 1200\ \text{cm}^{-1}, v' = 0.$$

This value of v is consistent with a spin-orbit splitting constant λ of about 70 cm^{-1} when inserted in the formula of ref. (7) for the ground state splitting D, known experimentally to be 8 cm^{-1}. For the parameters assumed this formula reduces to

$$D \approx (1{\cdot}25\lambda)^2/v.$$

TABLE 3.—COULOMB AND OCTAHEDRAL CRYSTAL FIELD MATRIX ELEMENTS

$$
\begin{array}{c|cc}
 & {}^3T_{1a} & {}^3T_{1b} \\
{}^3T_{1a} & 3B & 6B \\
{}^3T_{1b} & 6B & 12B + \Delta
\end{array}
\qquad
\begin{array}{c|cc}
 & {}^3T_2 & {}^3A_2 \\
 & (\Delta), & (2\Delta),
\end{array}
$$

$$
\begin{array}{c|cc}
 & {}^1A_{1a} & {}^1A_{1b} \\
{}^1A_{1a} & 18B + 5C & -(2B + C)\sqrt{6} \\
{}^1A_{1b} & -(2B + C)\sqrt{6} & 16B + 4C + 2\Delta
\end{array}
\qquad
\begin{array}{c|cc}
 & {}^1E_a & {}^1E_b \\
{}^1E_a & 9B + 2C & +2\sqrt{3}B \\
{}^1E_b & +2\sqrt{3}B & 8B + 2C + 2\Delta
\end{array}
$$

$$
\begin{array}{c|cc}
 & {}^1T_{2a} & {}^1T_{2b} \\
{}^1T_{2a} & 9B + 2C & -2\sqrt{3}B \\
{}^1T_{2b} & -2\sqrt{3}B & 8B + 2C + \Delta
\end{array}
\qquad
\begin{array}{c|c}
 & {}^1T_1 \\
 & (12B + 2C + \Delta),
\end{array}
$$

The secular equations were solved on an electronic computer. The spin-orbit interaction was not included at this stage, since it can be treated adequately as a perturbation, being small. Its effect is to split the ^3E states into three components roughly 100 cm^{-1} apart (this is an order of magnitude figure), and the ^3A state by a much smaller amount, since the effect here operates only in second order. The energy levels relative to the ground state are in cm^{-1}:

$^3A_1$: 16,740,
$^3A_2$: 0, 23,680, 34,640,
^3E: 1,200, 17,290, 24330,
$^1A_2$: 28,420,
$^1A_1$: 10,150, 19,000, 26,480, 57,170,
^1E: 8,730, 9,970, 26,900, 29,190, 44,260.

It is not suggested that the parameters used are the best possible, and in particular v' may be considerable. However, it was not thought necessary to refine the parameters in view of uncertainties about the method, to be discussed in the next section. The tentative assignments of the observed levels are also shown in fig. 1, the three highest levels being taken from Low.[4]

4. DISCUSSION

The moderately sharp lines in the infra-red and in the visible near 21,020 cm^{-1} are precisely what one might expect from rather simple considerations. These lines are due to transitions between different states of the configuration t_2^2, and hence are unlikely to be affected very much by the crystal field, since the charge distribution is practically the same in both. Likewise one would expect broad bands for the triplet-triplet transitions, where there is a marked change in the charge distribution.

The amount of detail at the head of the band at 15,790 cm^{-1} is rather surprising and so is the existence of a well-defined vibrational series. Under the action of a trigonal field with spin-orbit interaction the $^3T_2$ state should split into six levels. No lines are found due to five of these levels; yet if the absorption lines due to these levels were sharp they should show on top of the broad absorption band associated with transitions to the lowest level coupled with the excitation of some crystal vibrations.

One possible solution of this dilemma is that Jahn-Teller distortions are very important for the position of the energy levels. The lowest level being almost a pure " spin " triplet is not affected and shows a second-order splitting due to the trigonal field plus the spin-orbit interaction. However, the excited states may be influenced by strong Jahn-Teller distortion. Such distortions will strongly couple the electronic transitions to certain asymmetric crystal vibrations which may be

partially localized near the impurity ions. This could account for the existence of a vibrational series and also for the lack of sharp lines due to the other levels as all the excited levels of the $^3T_2$ state, for example, would be mixed by the Jahn-Teller distortions. The theory of the static Jahn-Teller effect has been developed by Öpik and Pryce,[12] and for a simple case the dynamical theory has been used to calculate the energy levels resulting from the electronic vibronic interaction (Longuet-Higgins, Öpik, Pryce and Sack [13]). Independently Moffitt and Liehr [14] have tackled the same aspect of the dynamical theory with similar results. Unfortunately, detailed calculations of the type required for vanadium corundum would be of extreme complexity.

In fig. 1 a comparison is made between observed and calculated energy levels. In this figure a comparison is made with the narrow bands at the long wavelength edges of the broad absorption bands for $^3T_2$ and $^3T_1$. On the other hand, a theoretical analysis indicates that the position of the electronic energy level in the crystal field of the ground-state configuration of the lattice corresponds to the *mean* frequency of the absorption band. This mean frequency corresponds fairly closely in practice to the peak of the absorption, and it is therefore more nearly correct to compare calculated energies with peak absorption positions, as done by Low [4] and Tanabe and Sugano.[1, 2]

In view of the uncertainties here and on account of the Jahn-Teller effects it has not been felt worthwhile to complete detailed calculations of the spin-orbit interaction for all the states of d^2 in a crystal field.

On the experimental side there is the possibility of obtaining further Zeeman splittings when much higher fields of the order of 30 kilogauss are available. It would also be useful if paramagnetic resonance could be used to examine the magnetic splitting of the doublet situated 8 cm^{-1} above the ground state, as much greater accuracy would be obtained. There may be difficulties associated with the fact that this would be a magnetic quadrupole transition. Further progress may also arise from investigations on related substances, such as ruby which share some of the features here discussed.

We wish to thank Dr. E. T. Richards for help while using the 21-ft. plane grating spectrograph at Harwell and Dr. J. Anderson at Imperial College, London, for similar help with the Zeeman experiment. Also we thank Mr. P. D. Preston for assistance with the computation of the energy levels, and all those who extended the use of the facilities at their disposal.

1 Tanabe and Sugano, *J. Physic. Soc. Japan*, 1954*a*, **9**, 753.
2 Tanabe and Sugano, *J. Physic. Soc. Japan*, 1954*b*, **9**, 766.
3 Tanabe and Sugano, *J. Physic. Soc. Japan*, 1957, **12**, 556.
4 Low, *Z. physic. Chem.*, 1957, **13**, 107.
5 Moffitt and Ballhausen, *Ann. Rev. Physic. Chem.*, 1956, **7**, 107.
6 Runciman, *Rep. Prog. Physics*, 1958, **21**, 30.
7 Abragam and Pryce, *Proc. Roy. Soc. A*, 1951*a*, **205**, 135.
8 Grechushnikov and Feofilov, *J. Expt. Theor. Phys. U.S.S.R.*, 1955, **29**, 384 (trans. in *Soviet Physics JETP*, 1956, **2**, 330).
9 Abragam and Pryce, *Proc. Roy. Soc. A*, 1951*b*, **206**, 173.
10 Condon and Shortley, *The Theory of Atomic Spectra* (Cambridge Univ., 1935).
11 Racah, *Physic. Rev.*, 1942, **62**, 438.
12 Öpik and Pryce, *Proc. Roy. Soc. A*, 1957, **238**, 425.
13 Longuet-Higgins, Öpik, Pryce and Sack, *Proc. Roy. Soc. A*, 1958, **244**, 1.
14 Moffitt and Liehr, *Physic. Rev.*, 1957, **106**, 1195.

PRINTED IN GREAT BRITAIN AT
THE UNIVERSITY PRESS
ABERDEEN

Reprinted from *Acta Crystallographica*, Vol. 12, Part 9, September 1959

PRINTED IN DENMARK

Acta Cryst. (1959). **12**, 674

A Neutron-Diffraction Study of Potassium Cobalticyanide

BY N. A. CURRY AND W. A. RUNCIMAN*

Atomic Energy Research Establishment, Harwell, Berks, England

(*Received* 4 *September* 1958 *and in revised form* 19 *January* 1959)

The methods of neutron diffraction, which permit a distinction to be made between carbon and nitrogen atoms, have been used to extend the earlier X-ray studies of $K_3Co(CN)_6$. It appears that the carbon atoms are in positions adjacent to the cobalt ions. The methods of Fourier synthesis and least squares have been used to obtain improved atomic co-ordinates and values for the Debye–Waller temperature factors. The length of the C–N bonds is 1·15 Å.

Introduction

Cyanide complexes are of considerable interest, the platinocyanides showing marked dichroism and fluorescence, and iron-group cyanides having been studied by paramagnetic-resonance techniques. The structures of some cyanides have been investigated by X-rays, but these do not distinguish whether the carbon or nitrogen atoms are next to the central metal ion. However, neutron diffraction often enables one to distinguish between atoms which are neighbours in the periodic table. (Bacon, 1955, Chapter VIII). It was felt that it would be easiest to study a cyanide for which preliminary X-ray information was available, and which did not contain any water of crystallization involving additional work in the location of hydrogen atoms. Potassium cobalticyanide, $K_3Co(CN)_6$, is suitable, having been studied using X-ray methods by Barkhatov & Zhdanov (1942) and by Barkhatov (1942). Furthermore, a consideration of the scattering amplitudes, Table 1, indicates that neutron diffraction will be suitable for the determination of carbon and nitrogen positions, since the scattering amplitudes of these atoms are considerably different, and are the largest present; whereas for X-rays the heavy metal atoms are predominant.

Table 1. *Scattering amplitudes for neutrons and X-rays* (10^{-12} cm.)

		X-rays	
Atom	Neutrons	$\sin\theta/\lambda = 0$	$\sin\theta/\lambda = 0{\cdot}5$ Å^{-1}
C	0·66	1·69	0·48
N	0·94	1·97	0·53
K	0·35	5·3	2·2
Co	0·28	7·6	3·4

* Now at the Department of Physics, University of Canterbury, Christchurch, New Zealand.

Barkhatov & Zhdanov (1942) found that the true symmetry of $K_3Co(CN)_6$ is monoclinic, and not orthorhombic, as earlier supposed. They found the unit cell to be

$$a = 7{\cdot}1,\ b = 10{\cdot}4,\ c = 8{\cdot}4\ \text{Å};\ \beta = 107°\ 20',$$

with two molecules per unit cell. The space group is $P2_1/c(C_{2h}^5)$ with the cobalt and some potassium ions in special positions, as follows (Barkhatov, 1942):

$$2\ \text{Co in } 2a\ (0, 0, 0)(0, \tfrac{1}{2}, \tfrac{1}{2})$$
$$2\ \text{K}_1 \text{ in } 2c\ (0, 0, \tfrac{1}{2})(0, \tfrac{1}{2}, 0)\ .$$

The X-ray intensities indicated that a twofold symmetry axis of the octahedral $[Co(CN)_6]^{3-}$ group is directed along the *c*-axis, while the fourfold symmetry axis perpendicular to this twofold axis lies roughly perpendicular to the (130) plane. The octahedra are in two groups, those in one group being mirror images of those in the other group. This is shown in Fig. 1,

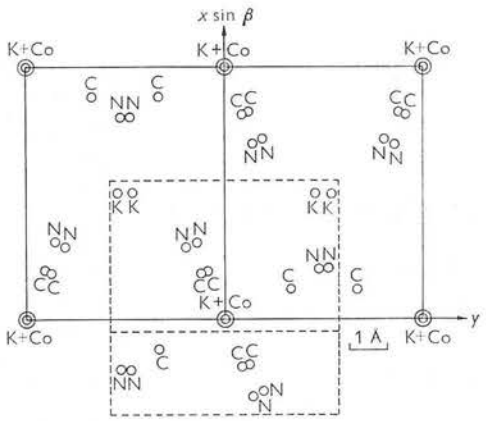

Fig. 1. The arrangement of the atoms in a projection of the structure on a plane normal to the *z* axis. The areas enclosed by dashed lines are those which appear in the Fourier projections of Fig. 2 and Fig. 3.

which is a sketch of the structure projected along the *c* axis. Barkhatov found the C–N distance to be about 1·2 Å, and the distance from the cobalt ion to the centre of the cyanide group to be about 2·5 Å. This information was used in a preliminary calculation of structure factors.

Experimental details

Crystals were readily grown from aqueous solution. The directions of the principal axes of some crystals were determined by X-ray diffraction, and we are grateful to Mr S. A. Wilson of this Establishment for carrying out this work. Most of the crystals had their largest dimension in the direction of the *c*-axis, and so it was decided to measure the intensities of the [*hk*0] zone. The crystal used in the experiment had dimensions approximately $14\times5\times3$ mm., the longest dimension being in the direction of the *c*-axis. A series of 117 *hk*0 reflexions was measured, and the observed Bragg angles for this zone were found to be consistent with $a \sin \beta = 6{\cdot}67$ Å, whereas the unit-cell dimensions earlier quoted yield $a \sin \beta = 6{\cdot}78$ Å. The value of *b* was observed as 10·4 Å, as stated by Barkhatov & Zhdanov (1942). All but two of the reflexions were measured at a neutron wavelength of 1·09 Å, using a lead crystal as monochromator. With a neutron wavelength of 0·80 Å, obtained from a copper monochromator, one additional reflexion was found in each of the main series of spectra *h*00 and 0*k*0. These were both small in intensity, and it was not considered worth while to search for additional reflexions at this wavelength. The minimum spacing for the reflexions measured was about 0·65 Å. The spectrometer used was the powder-type spectrometer described by Bacon, Smith & Whitehead (1950). The most intense reflexions were corrected for secondary extinction by the method of Bacon & Pease (1953).

Results

A preliminary calculation of structure factors was based on the information obtained from Barkhatov's work. It was assumed that the Co–C–N bond was straight, and that the carbon atom was adjacent to the cobalt ion. The values of B in the Debye factor $\exp(-B \sin^2\theta/\lambda^2)$ for correcting the structure amplitude factors for the effect of thermal vibrations, were taken as 1·0, 1·5, 2·5 and 2·5 Å^2 respectively for cobalt, potassium, carbon and nitrogen. The signs of these calculated structure factors and the experimentally observed amplitudes were used in a preliminary Fourier synthesis showing the scattering density projected on a plane perpendicular to the *c* axis. This confirmed that the main features of the assumed structure were correct, but unfortunately could not distinguish unambiguously between carbon and nitrogen atoms. This was partly because the differences in peak heights which should result from the different scattering lengths of carbon and nitrogen atoms were masked by differences in the amplitudes of their thermal vibrations. Moreover, in projection there are three pairs of overlapping atoms, one pair of carbon atoms and two pairs of nitrogen atoms. The amounts by which the atoms overlap are different in the three cases, and this further obscures the simple relationship one would expect to find between scattering length and peak height.

It was decided to examine the data further by the method of least-squares. Two trial structures were assumed, one (hereafter called the α-structure) having the carbon atom of the C–N group adjacent to the cobalt ion, and the other (hereafter called the β-structure) with the nitrogen atom next to the cobalt ion. For each structure the positions of the carbon and nitrogen atoms were re-estimated from the Fourier projection, and new values of B were estimated from the heights of the peaks. Each structure was then refined by successive cycles of least-squares, and it was

found that satisfactory results were obtained from the α-structure but not from the β-structure. For this and other reasons, which we give in detail later in the paper, we have concluded that the α-structure is the correct one.

As a result of the refinement of the α-structure, it was found that several of the calculated structure factors changed sign. A second Fourier synthesis was then carried out, using these altered signs. This is

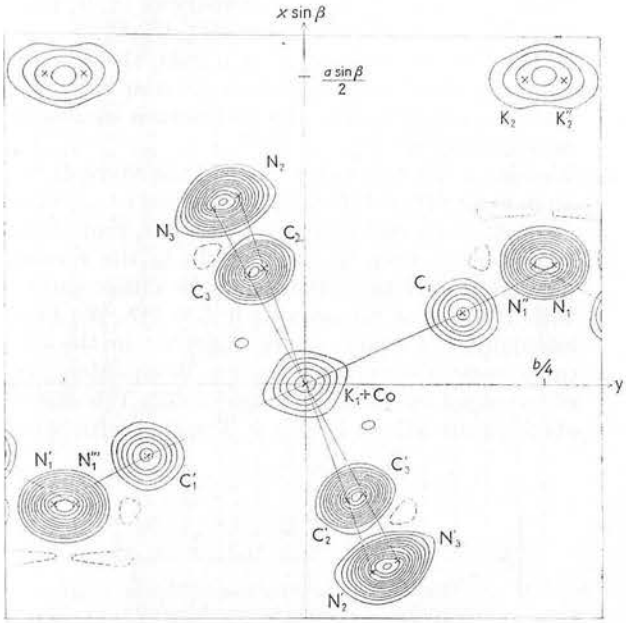

Fig. 2. Projection of the neutron scattering density on a plane normal to the z axis. Full lines are positive contours, broken lines are negative. Contours are drawn at intervals of 50 units.

shown in Fig. 2, which shows the scattering density within the region bounded by the outer dashed line in Fig. 1. The distribution of scattering density within the unit cell is quite consistent with that which would be obtained from atoms placed at the positions obtained from the least-squares analysis of the α-structure. These positions are marked by crosses in the figure.

We have also made a Fourier synthesis of the quantity (F_o-F_c), where F_o is the observed structure factor amplitude, and F_c is the structure factor calculated from the parameters obtained in the α-structure in the final cycle of least squares. This

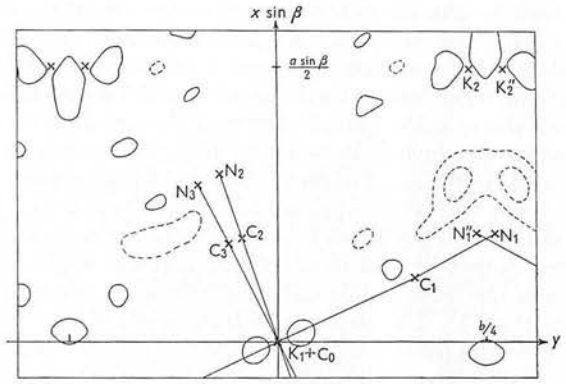

Fig. 3. The Fourier projection on a plane normal to the z axis obtained by synthesis of F_o-F_c. Contours are drawn at intervals of 25 units.

synthesis is shown in Fig. 3. The portion of the unit cell shown in this figure is the upper rectangle bounded by a dashed line in Fig. 1. Contours are drawn at intervals of 25 units, compared with intervals of 50 units for the F_o synthesis. The figure shows that there is only one region in the unit cell where the scattering density is greater than 50 units, and this is not close to any of the atoms. Only one feature of this figure appears to be due to an error in the assumptions made in calculating F_c, namely the two positive peaks on either side of the potassium and cobalt atoms which are superimposed at the origin. These peaks may be due to anisotropic vibration of either or both of these atoms, the preferred direction of vibration lying in projection along the bond Co–C_1. However we have not attempted a detailed analysis of anisotropic vibrations.

The co-ordinates, and the values of B which we have assigned to the atoms in the structure, are listed in Table 2. They are the values obtained from the least-squares analysis of the α-structure, and in the case

Table 2. *Atomic parameters and temperature factors*

	x/a		y/b		z/c^*		$B(10^{-16}$ cm.$^2)$	
Atom	Least squares	Fourier	Least squares	Fourier	Set 1	Set 2	Least squares	Fourier
Co	(0)		(0)			(0)	1·8	1·5
K_1	(0)		(0)			(0·500)		
K_2	0·499	—	0·230	—	—	—	1·8	—
C_1	0·118	0·118	0·165	0·165	0·014	0·044	1·3	1·2
C_2	0·189	—	−0·043	—	0·206	−0·113	1·5	—
C_3	0·179	—	−0·059	—	−0·114	0·203	1·1	—
N_1	0·199	—	0·261	—	0·024	0·075	2·3	—
N_2	0·306	—	−0·070	—	0·331	−0·179	2·1	—
N_3	0·286	—	−0·096	—	−0·184	0·326	1·9	—

* By geometrical calculation as described in the text.

of four parameters, a value obtained directly from the Fourier synthesis is also listed. In these four cases there is good agreement between the parameters obtained by the two methods. Because of overlapping, the remaining parameters cannot be obtained directly from the Fourier synthesis.

Our results do not yield values for the third co-ordinate z directly, as we have measured only the ($hk0$) reflexions. However, values of z for the carbon and nitrogen atoms may be obtained by assuming that the cyanide groups surround the cobalt ions in regular octahedra. It is found that the values of z can be chosen so as to make the octahedron of carbon atoms a very close approximation to a regular octahedron, with the three Co–C distances differing from one another by less than 0·01 Å, and the angles between the three bonds differing from right angles by less than 1°. The departures from regularity of the octahedron formed by the nitrogen atoms are roughly twice the corresponding values in the case of the carbon atoms. However, the values of z obtained by this method are not unambiguous. Two sets of values may be obtained, yielding two distinct octahedra. The relationship between the two is that each may be obtained from the other by reflexion across the plane through the origin perpendicular to the c axis. The two alternative sets of values for z are listed in Table 2. The bond lengths which we deduce from our data are listed in Table 3. The values obtained for the bond lengths do not depend upon which set of z-values is chosen.

Table 3. *Bond lengths*

Co–C		C–N	
Co–C_1	1·89 Å	C_1–N_1	1·14 Å
Co–C_2	1·89	C_2–N_2	1·15
Co–C_3	1·89	C_3–N_3	1·15
Mean	1·89	Mean	1·15

The standard deviation of the co-ordinates of carbon atom C_1, which does not overlap with other atoms in projection, is estimated by the method of Cruickshank (1949) to be 0·009 Å. The accuracy of the co-ordinates of the atoms which overlap in projection will obviously be less than this.

Discussion

The main interest in this substance lies in the attempt to distinguish between the α and β structures. We base our conclusion that the α-structure is the correct one upon the following evidence.

1. The least-squares refinement of the α-structure proceeded satisfactorily. In six cycles the value of the reliability index $R = \Sigma|F_o - F_c|/\Sigma|F_o|$ fell from 27·5% to 12·4% and in the final cycle the changes were small, the maximum changes being 0·0003 in a positional parameter (fractional co-ordinates) and 0·5 in a Debye factor. The reliability index for the β-structure fell in two cycles from 31·7% to 22·9%. This in itself would be satisfactory, but after the second cycle values of the Debye factor ranging from 0·5 to 6·7 had to be assigned to the carbon and nitrogen atoms. We considered these values so improbable that we did not refine this structure beyond two cycles.
2. The least-squares refinement of the α-structure yielded results which are wholly consistent with the Fourier projection shown in Fig. 2. The results for the β-structure yield inconsistencies in the positions of the overlapping atoms C_2, C_3, N_2, N_3.
3. In the Fourier 'difference' synthesis, the absence of large peaks (positive or negative) near to atomic positions suggests that the α-structure cannot be substantially wrong.
4. We have made a detailed study of the shape of the atom at (0·118, 0·165) which is the only carbon or nitrogen atom that does not overlap in projection. We calculate from its peak height in the Fourier projection that this atom could be either carbon with $B = 1{\cdot}2$ or nitrogen with $B = 2{\cdot}7$. We have calculated the shapes to be expected in the two cases, using the expression given in equation (3a) of the paper by Bacon & Pease (1953). The shapes obtained are shown in Fig. 4, together with a set of points giving the observed shape taken from the results of our Fourier synthesis. It will be seen that the observed shape is much closer to the shape calculated on the assumption that this atom is carbon with $B = 1{\cdot}2$. This is additional evidence that the α-structure is the correct one.

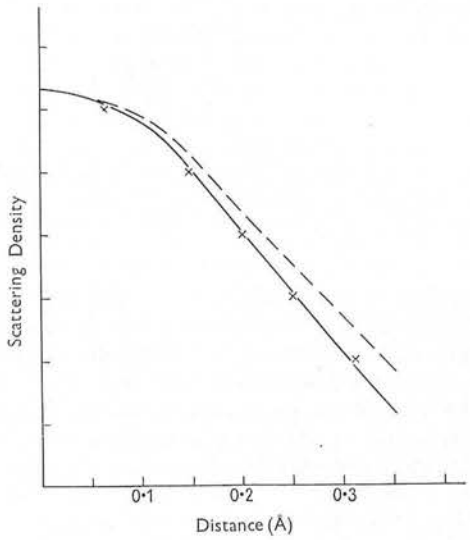

Fig. 4. The diffraction pattern of the atom at (0·118, 0·165). The full line shows the pattern expected from a carbon atom. The dashed line shows the pattern expected from a nitrogen atom. The crosses indicate points on the observed pattern. The divisions along the ordinate axis correspond to the contours in Fig. 2.

Table 4. *Observed and calculated structure factors*

h,k	F_o	F(i)	F(iii)	h,k	F_o	F(i)	F(iii)	h,k	F_o	F(i)	F(iii)
0 2	31	28	40	3 7	22	20	23	6 8	16	13	11
0 4	25	24	24	3 8	<4	4	10	6 9	19	19	19
0 6	74	75	55	3 9	25	27	26	6 10	20	24	22
0 8	33	27	34	3 10	62	67	66	6 11	<5	2	9
0 10	42	41	42	3 11	<5	11	9	6 12	<5	5	2
0 12	38	37	41	3 12	22	20	19	6 13	13	12	20
0 14	<5	4	2	3 13	<5	8	7	7 0	20	19	19
0 16	<5	4	4	3 14	16	21	24	7 1	18	20	18
0 18	21	24	8	3 15	<5	4	10	7 2	39	36	38
1 0	27	30	49	4 0	27	29	15	7 3	59	56	55
1 1	4	0	0	4 1	46	38	22	7 4	44	39	40
1 2	15	10	20	4 2	13	9	10	7 5	24	19	17
1 3	126	136	123	4 3	19	13	25	7 6	<4	5	3
1 4	20	14	8	4 4	28	25	28	7 7	39	42	38
1 5	65	58	75	4 5	12	11	2	7 8	<4	13	18
1 6	42	37	38	4 6	44	41	40	7 9	10	9	15
1 7	19	18	22	4 7	69	68	68	7 10	25	27	33
1 8	<4	2	7	4 8	33	29	29	7 11	24	24	19
1 9	51	48	43	4 9	21	21	20	7 12	19	20	18
1 10	22	19	19	4 10	24	25	24	8 0	33	37	40
1 11	<5	2	2	4 11	<5	9	15	8 1	28	29	31
1 12	<5	9	8	4 12	<5	2	8	8 2	35	31	25
1 13	28	28	23	4 13	28	30	29	8 3	24	20	20
1 14	<5	6	6	4 14	<5	4	1	8 4	11	10	8
1 15	<5	5	7	4 15	21	19	13	8 5	18	15	18
2 0	65	95	83	5 0	8	8	0	8 6	53	51	52
2 1	54	50	42	5 1	12	8	8	8 7	14	13	20
2 2	38	30	40	5 2	10	6	19	8 8	26	26	22
2 3	20	13	27	5 3	13	11	14	8 9	<5	9	12
2 4	21	14	10	5 4	73	67	64	8 10	22	23	22
2 5	25	19	42	5 5	34	31	32	8 11	11	11	10
2 6	73	80	70	5 6	<4	7	5	9 0	9	14	16
2 7	32	30	27	5 7	14	13	13	9 1	11	10	5
2 8	37	34	37	5 8	24	19	21	9 2	15	16	13
2 9	10	12	11	5 9	<4	4	4	9 3	54	50	55
2 10	32	24	25	5 10	34	31	32	9 4	<4	3	11
2 11	21	24	24	5 11	<5	5	6	9 5	21	17	11
2 12	<5	4	9	5 12	30	29	22	9 6	37	36	32
2 13	34	36	32	5 13	19	23	21	9 7	24	23	19
2 14	<5	12	12	5 14	<5	6	12	9 8	11	10	7
2 15	15	17	12	6 0	53	60	61	10 0	48	57	64
3 0	38	40	65	6 1	22	21	16	10 1	19	20	15
3 1	33	25	31	6 2	25	25	26	10 2	8	7	3
3 2	53	46	25	6 3	5	4	1	10 3	27	24	20
3 3	73	71	61	6 4	41	35	35	10 4	17	11	13
3 4	54	48	40	6 5	34	31	30	10 5	7	7	2
3 5	4	3	3	6 6	29	26	25	10 6	21	19	34
3 6	6	2	5	6 7	67	62	61	11 0	18	20	15

All structure factors are expressed as multiples of 10^{-13} cm. F(i) and F(iii) are calculated from sets of parameters (i) and (iii) as described in the text.

5. We have calculated three sets of structure factors for comparison. The parameters used were (i) those obtained from the final cycle of least-squares refinement of the α-structure, as shown in Table 2. (ii) a set of parameters obtained from (i) by interchanging carbon and nitrogen, leaving the Debye factor associated with a given *position* unaltered; (iii) parameters obtained from (ii) by adjusting the Debye factors to compensate for the changes in scattering length. The reliability indices for the three sets are 12·4%, 30·5% and 20·5% respectively. The structure factors for the α-structure (set (i)) and the more favourable variant of the β-structure (set (iii)) are listed in Table 4. It should be noted that not only does the α-structure yield the best reliability index, but several of the biggest discrepancies with the β-structure occur for low angle reflexions, for which changes in the Debye factors cannot compensate for changes in the basic structure. The (060), (100), (300), (320) and (410) reflexions are particularly noteworthy in this respect.
6. It is interesting to note that for the α-structure, the thermal vibrations of the cyanide groups increase as the distance from the central cobalt ion increases. Thus the mean Debye factors are 1·3 for the 'inner' carbon atoms, and 2·1 for the 'outer' nitrogen atoms. For the β-structure, to preserve the same peak heights, we have to assume that the 'inner' nitrogen atoms have a mean Debye factor of 2·8, and the 'outer' carbon atoms have a mean Debye factor of only 0·8. Thus in this structure the inner atoms have moderately large thermal vibrations and the outer atoms are relatively stationary. The arrangement for the α-structure seems the more plausible of the two.

These six results taken together suggest very strongly that the α-structure is the correct one, and we conclude therefore that in this compound the carbon atoms are adjacent to the cobalt ion.

The other point of interest in this structure is the C–N distance. The value of 1·15 Å which we find is not unlike that found in other molecules. For instance, using electron diffraction, Brockway (1936) and Pauling, Springall & Palmer (1939) have found a C–N distance of 1·16±0·02 Å in methyl cyanide. Similar values for the C–N distance are found in complex cyanides. For example Monfort (1942) using X-rays, finds a C–N distance of 1·16 Å in potassium sodium platinocyanide.

From our results for the α-structure, we deduce that the Co–C–N bonds are collinear in the case of the cyanide groups labelled 2 and 3, but in the case of the bond Co–C_1–N_1 we find that N_1 lies 0·08 Å from the line Co–C_1 produced. This departure from collinearity is not dependent upon the values calculated for the z co-ordinates, but may be deduced qualitatively from the observed x and y co-ordinates. However, in view of the overlapping of the atoms N_1, N_1'' it may not be significant.

We wish to thank Dr G. E. Bacon for much helpful advice and for the use of the neutron spectrometer. We are also grateful to Mr A. R. Curtis and the Atomic Energy Research Establishment Computing Section for carrying out much of the computation.

References

Bacon, G. E. (1955). 'Neutron Diffraction'. Oxford: Clarendon Press.

Bacon, G. E. & Pease, R. S. (1953). *Proc. Roy. Soc.* A, **220**, 397.

Bacon, G. E., Smith, J. A. G. & Whitehead, C. D. (1950). *J. Sci. Instrum.* **27**, 330.

Barkhatov, V. (1942). *Acta Physicochimica U.R.S.S.* **16**, 123.

Barkhatov, V. & Zhdanov, H. (1942). *Acta Physicochimica U.R.S.S.* **16**, 43.

Brockway, L. O. (1936). *J. Amer. Chem. Soc.* **58**, 2516.

Cruickshank, D. W. J. (1949). *Acta Cryst.* **2**, 65.

Monfort, F. (1942). *Bull. Soc. Roy. Sci. Liège*, **11**, 567.

Pauling, L., Springall, H. D. & Palmer, K. J. (1939). *J. Amer. Chem. Soc.* **61**, 927.

Printed in Denmark at Fr. Bagges kgl. Hofbogtrykkeri, Copenhagen

Reprinted from the JOURNAL OF CHEMICAL PHYSICS, Vol. 30, No. 6, 1632–1633, June, 1959
Printed in U. S. A.

Analysis of the Spectra of Gadolinium Salts

W. A. RUNCIMAN

Physics Department, University of Canterbury, Christchurch, New Zealand

(Received December 16, 1958)

A THEORETICAL treatment of the energy levels of rare earth ions[1] yielded Russell-Saunders energy levels and spin-orbit splitting factors for ions with the configuration f^n. The notation and procedure used here is described in that earlier account. In this approximation the spin-orbit splitting factors are all zero for the half-filled shell configuration f^7; for example, trivalent gadolinium. As there are quite substantial splittings ($\sim$1000 cm^{-1}) of the multiplets observed,[2,3] it seemed especially worthwhile in this case to proceed with more refined intermediate coupling calculations by the methods already described in outline. It is now necessary to consider the effect of the spin-orbit interaction between sextet and quartet states, and so Russell-Saunders energy levels, in units of the Slater integral F_2, were found for all the quartet states using the hydrogenic approximation for the shape of the $4f$ wave function. The basic states in Racah's classification[4] for the three highest multiplicities of f^7 are listed in Table I. They can be conveniently divided into two groups I and II. Because of special properties of a half-filled shell of electrons,[5] the Coulomb and Zeeman interactions have zero matrix elements for two states of different groups, whereas the spin-orbit and crystal field interaction have zero matrix elements for two states within one of the groups. These properties greatly reduce the amount of calculation required in a given degree of approximation; but make it all the more desirable to pursue calculations to a high degree of approximation.

The lowest excited level is the ^6P level, and there is spin-orbit interaction with ^4S levels (157.9 F_2 and 297.1 F_2) and ^4D levels (129.2 F_2, 188.0 F_2, 210.4 F_2, and 338.0 F_2). The next excited level is the ^6I which is perturbed by the ^4H levels (141.3 F_2, 184.1 F_2, and 239.4 F_2), ^4I levels (174.0 F_2 and 257.0 F_2), and ^4K levels (147.2 F_2 and 209.5 F_2). In each case perturbation is only caused by levels of the other group from that of the state concerned. The spin-orbit interaction within the octet and sextet states was completely included by diagonalizing the matrices for each J value, and the foregoing quartet interactions were included by second-order perturbation theory.

As the calculation of the matrix elements for the spin-orbit interaction Λ involves several parent states, the matrix elements are listed for reference in Table II. For brevity, the dependence on J is omitted as it only involves a single Racah function $W(JLS'1;\ SL')$. The spin-orbit splitting constant ξ for a single $4f$ electron was fixed by giving the ratio ξ/F_2 a value of 4.25. Matching the ^6P level with experiment, F_2 was found to be 404 cm^{-1}. The levels calculated in units of F_2 are given in Table III.

The ^6P levels are calculated in the order found by Cook and Dieke,[3] the differences between the levels being 1.3 and 1.7 F_2, compared with 1.5 and 1.4 F_2,

TABLE I. Classification of states of f^7 (excluding doublets).

Group I				Group II			
v	W	U	SL	v	W	U	SL
7	(000)	(00)	^8S	5	(110)	(10)	^6F
7	(200)	(20)	$^6D\ G\ I$			(11)	$^6P\ H$
7	(220)	(20)	$^4D\ G\ I$	5	(211)	(10)	^4F
		(21)	$^4D\ F\ G\ H\ K\ L$			(11)	$^4P\ H$
		(22)	$^4S\ D\ G\ H\ I\ L\ N$			(20)	$^4D\ G\ I$
3	(111)	(00)	^4S			(21)	$^4D\ F\ G\ H\ K\ L$
		(10)	^4F			(30)	$^4P\ F\ G\ H\ I\ K\ M$
		(20)	$^4D\ G\ I$				

TABLE II. Spin-orbit matrix elements.[a]

$(^8S|\Lambda|^6P) = -4(21)^{\frac{1}{2}}$
$(^6D|\Lambda|^6F) = 6(7)^{\frac{1}{2}}$
$(^6G|\Lambda|^6H) = 6(7)^{\frac{1}{2}}$
$(^6P|\Lambda|(22)^4S) = (22)^{\frac{1}{2}}/2$
$(^6P|\Lambda|(00)^4S) = (2)^{\frac{1}{2}}$
$(^6P|\Lambda|(20)^4D) = 3(14)^{\frac{1}{2}}/4$
$(^6P|\Lambda|(21)^4D) = 0$
$(^6P|\Lambda|(22)^4D) = -(4290)^{\frac{1}{2}}/4$
$(^6P|\Lambda|(20)^4D') = -6(10)^{\frac{1}{2}}$
$(^6P|\Lambda|^6D) = 3(21)^{\frac{1}{2}}$
$(^6F|\Lambda|^6G) = 3(770)^{\frac{1}{2}}/5$
$(^6H|\Lambda|^6I) = 3(455)^{\frac{1}{2}}/5$
$(^6I|\Lambda|(11)^4H) = 7(130)^{\frac{1}{2}}/10$
$(^6I|\Lambda|(21)^4H) = -4(35)^{\frac{1}{2}}$
$(^6I|\Lambda|(30)^4H) = -7(30)^{\frac{1}{2}}/2$
$(^6I|\Lambda|(20)^4I) = 3(22)^{\frac{1}{2}}$
$(^6I|\Lambda|(30)^4I) = (66)^{\frac{1}{2}}$
$(^6I|\Lambda|(21)^4K) = 4(22)^{\frac{1}{2}}$
$(^6I|\Lambda|(30)^4K) = (374)^{\frac{1}{2}}$

[a] The dash denotes the $v=3$ state.

respectively, derived from the experimental results. The agreement is considered very satisfactory in view of the neglect of configuration interaction. The $J=7/2$ level comes lowest of the ^6I levels as found by Dieke and Leopold.[2] However, the energy differences between the remaining ^6I levels are possibly too small to be significant considering the doubtful nature of the hydrogenic approximation used. More detailed analysis of the spectra of the gadolinium ion must await polarization spectra of a crystal of high symmetry, e.g., the anhydrous chloride or the ethylsulfate, in which the gadolinium ions are at sites of symmetry C_{3h}. The crystal field analysis would involve second-order crystal field interactions in addition to the interactions which are first-order in crystal field and first-order in spin-orbit coupling. These interactions have been considered briefly by Hutchison, Judd, and Pope in an analysis of the paramagnetic resonance results[6] on the ground state ^8S of the anhydrous trichloride.

TABLE III.

^6P		^6I			
$J=7/2$	79.3	$J=7/2$	85.7	$J=17/2$	88.2
$J=5/2$	80.6	$J=13/2$	86.9	$J=15/2$	88.4
$J=3/2$	82.3	$J=11/2$	87.8	$J=9/2$	88.4

[1] Elliott, Judd, and Runciman, Proc. Roy. Soc. (London) **A240**, 509 (1957).
[2] G. H. Dieke and L. Leopold, J. Opt. Soc. Am. **47**, 944 (1957).
[3] S. P. Cook and G. H. Dieke, J. Chem. Phys. **27**, 1213 (1957).
[4] G. Racah, Phys. Rev. **76**, 1352 (1949).
[5] G. Racah, Phys. Rev. **62**, 438 (1942); **63**, 367 (1943).
[6] Hutchison, Judd, and Pope, Proc. Phys. Soc. (London) **B70**, 514 (1957).

Reprinted from the JOURNAL OF CHEMICAL PHYSICS, Vol. 31, No. 4, 1149–1150, October, 1959
Printed in U. S. A.

Spectra of Trivalent Praseodymium and Thulium Ions

W. A. RUNCIMAN AND B. G. WYBOURNE

Physics Department, University of Canterbury, Christchurch, New Zealand

(Received December 22, 1958)

DIEKE and Sarup[1] have found all the multiplet components of the ^3H and ^3F levels in an investigation of the absorption and fluorescence spectra of $PrCl_3$, and have also reported absorption lines due to the previously undetected $^1I_6$ state. Calculations of the energy-level scheme for the praseodymium ion[2,3] have allowed a clear assignment of most levels but have not given their positions very precisely.

The matrix elements of the spin-orbit interaction for the $4f^2$ and $4f^{12}$ configurations have been given by Spedding[4], and the coulombic contributions in terms of the Slater integrals F_k by Condon and Shortley.[5]

(The spin-orbit coupling constant used in this paper is twice that defined in Spedding's paper). Previous calculations of the matrix elements have involved the knowledge of four independent parameters, the Slater integrals F_2, F_4, and F_6 together with the spin-orbit coupling constant ξ. Judd[3] has used the Slater integral ratios F_4/F_2 and F_6/F_2 calculated from the $4f$ hydrogenic wave function and calculated the F_2 and ξ values from spectral data. More recently, Ridley[6] has calculated the Slater integral ratios for the Pr^{3+} and Tm^{3+} free ions from wave functions calculated by the method of self-consistent fields without exchange.

Dieke and Sarup[1] have found the $^1I_6$ level in $PrCl_3$ to be approximately 290 cm^{-1} above the $^3P_1$ level. All previously calculated energy-level schemes, considering only the coulombic and spin-orbit interaction, have given the position of the $^1I_6$ level below the $^3P_1$ level.

Trees[7] has introduced an empirical term $\alpha L(L+1)$, where L is the total angular momentum of the energy level and α is assumed constant for the configuration, and found a greatly improved fit for the configuration $3d^54s$. The nature of this orbit-orbit interaction of the type $\Sigma 1_i \cdot 1_j$ has been discussed by Ufford and Callen.[8]

A least-squares method[9] has been used to derive new values of the five parameters F_2, F_4, F_6, ξ, and α for the energy levels of the Pr^{3+} and Tm^{3+} ions by using the experimental results of Dieke and Sarup,[1] Gobrecht,[10,11] and Johnsen.[12] The experimental data for the Tm^{3+} ion is incomplete with the $^1I_6$, $^1S_0$ and $^3H_4$ levels unobserved. The parameters obtained with and without the inclusion of the orbit-orbit interaction parameter are given in Table I.

TABLE I.

(a) Parameters for energy calculations for Pr^{3+}

Parameter	Jørgensen[2]	Judd[3]	Ridley[6]	With α	Without α
F_2 cm^{-1}		305		306.7	306.6
F_4/F_2	0.2	0.138	0.1287	0.1615	0.1680
F_6/F_2	0.02	0.151	0.01366	0.01647	0.01724
ζ cm^{-1}	800	711		781	737
α cm^{-1}				11.6	

(b) Parameters for energy calculations for Tm^{3+}

F_2 cm^{-1}	450			441.2	447.5
F_4/F_2	0.2		0.1290	0.1400	0.1354
F_6/F_2	0.02		0.01370	0.01597	0.01541
ζ cm^{-1}	2800			2709	2575
α cm^{-1}				−18.0	